Dissertation zur Erlangung des Doktorgrades

der Fakultät für Chemie und Pharmazie

der Ludwig-Maximilians-Universität München

Generation of universal recipient cells for the testing and characterization of transgenic TCRs

Nadja Sailer

aus

Starnberg, Deutschland

2018

Table of content

Table of figures

List of tables

Summary

Utilizing adoptive transfer of autologous T cells engineered to express a transgenic tumor-reactive T cell receptor (TCR) is a promising immunotherapeutic approach to treat cancer (Restifo, Dudley and Rosenberg, 2012). However, severe side-effects observed in clinical trials due to on-target/off-tumor or off-target reactivity emphasize the need for extensive safety testing of transgenic TCRs before clinical application (Cameron *et al.*, 2013; Morgan *et al.*, 2013). In addition to excluding toxicities in patients, the tumor antigen-specific TCR has to be proven fully functional in a transgenic setting to ensure efficient anti-tumor responses of patient-derived peripheral blood lymphocytes (PBL) displaying the transgenic TCR. A large number of cells expressing the transgenic TCR are required for this elaborate efficacy and safety evaluation. While bulk PBL can be isolated in sufficient numbers and carry all effector functions essential for a physiological read-out, the presence of endogenous TCRs with unknown specificities could severely affect or alter the function of the transgenic TCR by dominant negative effects of the endogenous TCRs or TCR mispairing. Therefore, appropriate recipient cells are needed that can serve as a stable and reproducible test system for the thorough characterization of transgenic TCRs without the constraints of endogenous TCR expression. However, the generation of TCR-negative recipient cells is complicated by the fact that once the endogenous TCR of a T cell is absent, physiological T cell activation is impeded and the possibility to subsequently expand the T cell to sufficient numbers is lost. To circumvent this classical T cell activation via the TCR complex, chimeric antigen receptors (CARs) were tested for their potential to induce proliferation in isolated T cell clones for long-term *in vitro* expansion. While CARs are generally introduced into bulk PBL to redirect T cells to eliminate tumor cells, prolonged persistence of CAR-expressing T cells in patients months after treatment indicates that re-activation of these T cells could be attributed to the introduced CAR (Porter *et al.*, 2011). Using two well-characterized CAR constructs recognizing the CEA antigen, optimal *in vitro* expansion conditions for isolated T cell clones could be determined. In T cell clones showing TCR-independent, high proliferative capacity, the endogenous TCR was targeted for knockout using the TALEN technology. Initial poor survival of the resulting TCR-negative recipient cells could be overcome by the introduction of a CAR recognizing the CD19 antigen on B cells, which also provide co-stimulatory molecules for T cell activation. Additionally, a CD3 fusion protein, termed CD3-Chimera, was generated that should mimic physiological activation of T cells in the absence of TCR expression via binding of mitotic antibodies. Using these chimeric constructs, a new high-throughput strategy could be developed that allowed the generation and immediate identification of TCR-deficient T cell clones that could be expanded via engagement of CD19-CAR or CD3-Chimera, respectively. These well-defined universal recipient cells retained their effector functions and served as a stable and reproducible *in vitro* test system for the characterization and direct comparison of

different transgenic TCRs. Besides constituting an *in vitro* tool for the safety and efficacy testing of transgenic TCRs, the generated universal recipient cells represent the first step towards a universal approach to provide off-the-shelf T cell products for cellular therapies.

1   Introduction

1.1   T cell biology

The human immune system comprises powerful weapons to defend our body against various viral and microbial invaders. While the innate immune system efficiently detects and eradicates pathogens carrying conserved components that can be recognized by invariant pattern recognition receptors, the adaptive immune system evolved to recognize specific antigens derived from any invader it encounters and to establish immunological memory that will protect from re-infection (Ahmed and Gray, 1996). Key players in this adaptive immunity are B cells and T cells, that both generate receptors of unique specificity by somatic recombination of germline variable (V), diversity (D) and joining (J) gene segments during lymphocyte development (Bassing, Swat and Alt, 2002). The B cell receptor (BCR) is composed of immunoglobulin light (IgL) and heavy (IgH) chains created by VJ- or VDJ-recombination, respectively, and will be secreted as antibody once the B cell is activated by specific binding of the BCR to cognate antigen (Dal Porto *et al.*, 2004). Two types of T cell receptors (TCRs) have been identified that are either generated by combination of α and β chains ($\alpha\beta$TCR) or γ and δ chains ($\gamma\delta$TCR). While both types of TCRs use the CD3 complex for signaling, they differ in the way they recognize antigen (Love and Hayes, 2010). The much more prevalent $\alpha\beta$ T cells bind to peptide presented by major histocompatibility complex (MHC) molecules on antigen presenting cells (APCs). In contrast, $\gamma\delta$ T cells, which make up about 5% of peripheral blood T cells, are thought to bind directly to antigens, like proteins, phosphorylated ligands or lipids, independent of the classical MHC molecules (Allison and Garboczi, 2002). In the following, the focus lies on $\alpha\beta$ T cells, which will be simply referred to as T cells, and their role in adaptive immunity.

The TCR α and β chains are encoded by different loci on chromosome 14 and 7, respectively. The *TRA* locus contains V and J gene segments as well as a constant region segment (C), while the *TRBC* locus comprises V, D and J gene segments and 2 constant region gene segments (C1 and C2). To enable expression of the TCR on the cell surface, irreversible V(D)J recombination of the germline DNA has to occur to join the respective gene segments into one open-reading frame. V(D)J recombination is mediated by a complex comprising lymphocyte-specific proteins encoded by *recombination activating genes 1* and *2* (RAG1 and RAG2), which bind recombination signal sequences (RSS) flanking the gene segments to introduce single-strand nicks at the 3' end of the gene segments resulting in closed hairpin structures (Bassing, Swat and Alt, 2002; Jung and Alt, 2004; Abbey and O'Neill, 2008). Subsequently, double strand breaks (DSB) are repaired by error-prone non-homologous end-joining (NHEJ), which in concert with terminal deoxynucleotidyl transferase (TdT) results in modification of the cut

region creating highly variable junctions (Schatz and Ji, 2011). Random selection of joined gene segments in combination with these imprecise junctions generates unique and highly variable sequences coding for the variable regions of the TCR chains. The rearranged V(D)J segments are joined to the respective constant regions by mRNA splicing to generate mature TCR α and β chain transcripts. Pairing of unique TCR α and β chains in the endoplasmic reticulum (ER) results in formation of the TCR molecule. Pairing of different TCR α and β chains to generate a functional TCR together with genetic recombination events creates a unique antigen specificity and contributes to the high diversity of TCR repertoire (reviewed in Bassing, Swat and Alt, 2002; Jung and Alt, 2004; Abbey and O'Neill, 2008; Schatz and Ji, 2011).

To ensure that only one functional TCR will be expressed in each diploid T cell, a process known as allelic exclusion regulates the silencing of the second allele during lymphocyte development (Malissen *et al.*, 1992). TCR β chain rearrangements initially start on both alleles and occur prior to recombination events in the *TRA* locus (Raulet *et al.*, 1985). Once a functional pre-TCR complex comprising an invariant pre-TCR α chain and a productive TCR β chain can be expressed, feedback inhibition mechanisms stop rearrangements of the *TRB* locus on the second allele and prevent transcription (Fehling and Boehmer, 1997; Carpenter and Bosselut, 2010). After β-selection, the T cells express one productive TCR β chain and initiate CD4 and CD8 expression as well as rearrangements of the *TRA* locus (Borgulya *et al.*, 1992; Carpenter and Bosselut, 2010). VJ recombination is thought to occur simultaneously on both alleles encoding the TCR α chains, while successful interaction of a functional TCR with self-peptide-MHC complexes in the thymus results in positive selection of the T cell and stops recombinase activity (Borgulya *et al.*, 1992; Malissen *et al.*, 1992; Petrie *et al.*, 1993). In general, this results in expression of one functional TCR α chain that pairs with the corresponding TCR β chain. However, in up to 20% of circulating T cells two TCR α chains can be detected on mRNA level (Malissen *et al.*, 1992). While usually one of these TCR α chains comprises unproductive rearrangements resulting in the expression of only one functional TCR on the surface, in rare cases two productive TCR α chains can give rise to two TCRs with different specificities (Malissen *et al.*, 1988; Padovan *et al.*, 1993). Overall, more than 90% of the T cells will not pass positive selection in the thymus due to the expression of "non-functional" TCRs, which are not able to interact properly with self-peptide-MHC complexes on antigen-presenting cells, termed cortical thymic epithelial cells (cTECs) (Klein *et al.*, 2014). In the subsequent negative selection, auto-reactive cells strongly recognizing self-peptide presented by self-MHC molecules will undergo apoptosis and are eliminated from the T cell repertoire (Starr, Jameson and Hogquist, 2003). T cells expressing functional TCRs while not recognizing self-peptide, will undergo a lineage choice between CD4-expressing T

cells (CD4⁺ T cells) or CD8-expressing T cells (CD8⁺ T cells), that includes the termination of either CD8 or CD4 expression, respectively. These co-receptors interact with MHC molecules on APCs and enhance signaling via the TCR complex by recruiting Lck kinase associated with their cytoplasmic tail to the immunological synapse (Veillette *et al.*, 1989). While CD4⁺ T cells recognize antigen presented by MHC class II molecules, CD8⁺ T cells interact with peptide on MHC class I molecules. However, it is thought that lineage choice depends on signaling strength mediated by presence of Lck kinase, where strong signals promote CD4-lineage choice and weak signals promote CD8-lineage choice (Singer, Adoro and Park, 2008).

MHC class I molecules, corresponding to human leukocyte antigens (HLA) A, B and C, are expressed by most cells of the human body and present peptides derived from intracellular proteins (Germain, 1994). This allows the efficient detection of virus-infected cells as well as cancerous cells displaying mutated or aberrantly expressed self-peptides (Boon *et al.*, 1994; Coulie *et al.*, 2014). In contrast, MHC class II molecules are usually found on specialized APCs and predominantly present extracellularly-derived peptides that have been internalized by phagocytosis or endocytosis (Germain, 1994). Naïve T cells that underwent thymic selection have to be activated in order to survive and mediate an immune response, which requires 3 signals: (I) interaction of the TCR complex with specific antigen presented by MHC molecules on APCs, (II) interaction of co-stimulatory molecules on APCs and naïve T cells, like CD28-CD80/CD86 ligation, and (III) cytokine secretion by APCs to control T cell differentiation into different T cell subsets (Curtsinger *et al.*, 1999). Guided by cytokine secretion, CD4⁺ T cells differentiate into functionally distinct T helper subsets, Th1, Th2 and Th17, and regulatory T cells (Treg) that exhibit different effector functions (Zhu and Paul, 2010). Th1 cells secret the signature cytokines IFN-γ and IL-2 and support activation of macrophages, B cells and CD8⁺ T cells to defend against viral pathogens, while Th2 cells are characterized by the secretion of IL-4 and IL-5, which is required for antibody isotype switch to IgE in B cells and recruitment of eosinophils and mast cells to fight parasite infection. Th17 cells play critical roles in protection against extracellular bacteria and fungi by mediating neutrophil responses. Treg in turn, help to suppress immune responses to prevent autoimmunity (Zhu and Paul, 2010). While CD4⁺ T cells predominantly help to mediate the adaptive immune response, CD8⁺ T cells are characterized as cytotoxic lymphocytes, which efficiently kill virus-infected or cancerous cells by inducing apoptosis via release of perforin, granzymes and granulysin or engagement of Fas death receptors (Harty, Tvinnereim and White, 2000). Upon antigen encounter, naïve T cells progressively differentiate into central-memory (Tcm), effector memory (Tem) and finally, effector (Teff) T cells, accompanied by changes in metabolism, cell surface molecules and acquisition of effector functions, eventually resulting in senescence (Restifo and Gattinoni, 2013). Multipotent, self-renewing memory stem cells (Tscm) that exhibit increased proliferative

capacity and superior anti-tumor responses were identified as an efficacious T cell subset for the use in adoptive T cell therapy (Gattinoni *et al.*, 2011).

The first signal required for activation of a T cell is the specific recognition of peptide-MHC complexes on APCs via the TCR. The TCR α and β chains form a heterodimer that binds the target via the extracellular variable domain assuming a barrel-shaped structure of two anti-parallel β-strands that contact antigen via hypervariable complementary-determining regions (CDRs) (Garcia *et al.*, 1996). However, the constant region of the TCR comprises hydrophobic transmembrane domains that anchor the TCR in the cell membrane but lack any signaling function. Therefore, to enable signal transduction upon antigen recognition, the TCR has to associate with invariant accessory proteins, which are termed the CD3 complex. The CD3 complex comprises six subunits, which form three signaling dimers, CD3$\delta\epsilon$ CD3$\gamma\epsilon$ and CD3$\zeta\zeta$ that assemble with the TCR α and β chains in the ER (Exley, Terhorst and Wileman, 1991). Correct assembly of the TCR complex is thought to occur via polar interactions in the transmembrane regions of the respective dimers resulting in association of the TCR α chain with the CD3$\gamma\epsilon$ the CD3$\zeta\zeta$ dimer, while the CD3$\delta\epsilon$ dimer interacts with the TCR β chain (Call *et al.*, 2002). Additional interactions of the extracellular domains comprising conserved CxxCxE motif in CD3 stalk regions and loops in the TCR α and β constant immunoglobulin domains contacting CD3 ectodomains are thought to contribute to the correct assembly of the TCR complex (Call and Wucherpfennig, 2007; Natarajan *et al.*, 2016). Conformational changes in the TCR complex upon antigen contact resulting in rearrangements of the respective subunits are thought to trigger signal transduction possibly amplified by TCR dimerization or clustering (Call and Wucherpfennig, 2007; Birnbaum *et al.*, 2014; Pryshchep *et al.*, 2014; Natarajan *et al.*, 2016) However, recent studies showed that exclusively monomeric TCR-CD3 complexes drive the recognition of peptide-MHC complexes via the immunological synapse without the requirement of ligand-induced multimerization of TCRs (Brameshuber *et al.*, 2018).

While the exact mechanism by which TCR-peptide-MHC interaction is transmitted across the membrane is still a topic of active research, downstream signal transduction has been well elucidated. Signal transduction is initiated by phosphorylation of tyrosine-based activation motifs (ITAMs) present in the cytoplasmic domain of the CD3 subunits by Scr family kinase Lck associated with the co-receptors CD4 and CD8. This results in the recruitment and activation of tyrosine kinase ZAP-70, which binds to the phosphorylated ITAMs via SH2 domains. ZAP-70 in turn phosphorylates the scaffold proteins LAT and SLP-76, which, together with another adaptor protein (Gads), form a membrane-proximal complex with phospholipase C-γ (PLC-γ). PLC-γ activation is mediated by Itk tyrosine kinase and represents the key event in downstream signaling mediated through the generation of the second messengers diacylglycerol (DAG) and inositol-1,4,5-triphosphate (IP3). Downstream signaling

events result in the activation of the transcription factors NFκB, NFAT and AP-1, which coordinate transcription of specific genes resulting in T cell activation, proliferation and differentiation. (Smith-Garvin, Koretzky and Jordan, 2009; Kannan *et al.*, 2012; Malissen and Bongrand, 2015)

1.2   TCR-based cancer immunotherapy

While T cells have the ability to recognize various viral and microbial invaders mediated by the high variability of their TCRs recognizing specific antigens, recognition of self-antigens is usually prevented by thymic selection of T cells to avoid autoimmunity (Klein *et al.*, 2014). However, in the last century the theory that cancerous cells displaying altered or aberrantly expressed self-antigens could be detected and efficiently eradicated by the immune system was proposed by Burnet in 1957 (Burnet, 1957). Over the past decades, extensive research utilizing immunocompromised mouse models led to the acceptance of the principle of cancer immune surveillance and immunoediting, which consists of three phases: (I) elimination of developing tumors by the immune system, (II) equilibrium state, in which the tumor growth is restrained, and (III) escape of tumor variants that are no longer recognizabled by the immune system (Dunn *et al.*, 2004; Schreiber, Old and Smyth, 2011). The effector functions required for tumor eradication include IFN-γ secretion and cytotoxicity, both characteristics of antigen-specific T cell responses (Dunn *et al.*, 2004). This led to a new focus in cancer therapy, that included the administration of tumor-specific T cells to patients with the aim of targeting cancerous cells utilizing the immune system, termed adoptive T cell transfer (ACT) therapy (Dudley and Rosenberg, 2003). First proof of concept in humans was provided by Rosenberg *et al.*, who observed cancer regression in patients suffering from metastatic melanoma after re-infusion of *ex vivo* expanded autologous tumor-infiltrating lymphocytes (TILs) (Rosenberg, Spiess and Lafreniere, 1986; Dudley *et al.*, 2005; Rosenberg *et al.*, 2011). While the presence of TILs in human tumors simultaneously demonstrated the involvement of the immune system in protection from cancerous cells, this approach is dependent on the pre-existence of tumor-reactive cells in the patient and might therefore not be applicable to all patients nor indications other than melanoma (Morgan *et al.*, 2006; Restifo, Dudley and Rosenberg, 2012; Miller and Sadelain, 2015). Utilizing autologous T cells engineered to express tumor-specific TCRs can circumvent this limitation and has been shown to induce anti-tumor responses in melanoma patients (Morgan *et al.*, 2006; Johnson *et al.*, 2009). Currently, various clinical trials utilizing ACT of genetically engineered T cells have been registered to target tumors other than melanoma, including synovial cell sarcoma, neuroblastoma, colorectal cancer and leukemia (Duong *et al.*, 2015; Ping, Liu and Zhang, 2017). Production procedures for this kind of therapy usually comprise the isolation of patient-derived autologous T cells, which are subsequently

transduced with the tumor-specific TCR utilizing retroviral vectors, and re-infusion of the expanded cells into the patient (Restifo, Dudley and Rosenberg, 2012). A key prerequisite of TCR immunotherapy is the identification of tumor-specific TCRs that efficiently recognize cancerous cells without showing off-target recognition. Different methods have been developed for the isolation of these TCRs, which can be derived from TILs of cancer patients, humanized mice or *in vitro* priming methods, that utilize autologous or allogenic peptide-specific stimulation of T cells from healthy donors (Ho *et al.*, 2006; Wilde *et al.*, 2009; Dössinger *et al.*, 2013; Blankenstein *et al.*, 2015; Obenaus *et al.*, 2015). After identification of T cell clones exhibiting the desired effector functions and specificity, the sequence of the endogenous TCR has to be isolated by polymerase chain reaction (PCR)-based methods, like rapid amplification of cDNA-ends (RACE)-PCR, and subsequently evaluated for safety and efficacy in a transgenic setting (Wilde, Sommermeyer, *et al.*, 2012; Dössinger *et al.*, 2013; Simon *et al.*, 2014; Rosati *et al.*, 2017). However, the basis for obtaining tumor-specific TCRs that can be used in a clinical setting is the selection of appropriate target antigens. Two classes of non-viral antigens can be distinguished: tumor-associated antigens (TAAs) and tumor-specific antigens (TSAs). TAAs are aberrantly- or over-expressed self-antigens also present on healthy tissues, which include cancer-testis antigens, like the MAGE family, tissue differentiation antigens, like Melan-A, and overexpressed self-proteins, like Her-2/Neu. In contrast, TSA are neoantigens that arise as a consequence of somatic mutations in tumors, which would make them ideal targets for immunotherapy. However, while neoantigens are mostly patient-specific, TAA are usually shared between patients making them more suitable for the development of widely applicable therapies (Heemskerk, Kvistborg and Schumacher, 2013; Blankenstein *et al.*, 2015). Moreover, toxicities due to on-target recognition of TAAs in tissues other than tumor is a major concern and has already been proven fatal in the case of the MAGE-A3 antigen (Morgan *et al.*, 2013). One strategy to improve the safety of adoptive T cell therapy is the inclusion of so-called suicide genes, like the genes encoding herpes simplex virus-1 thymidine kinase (HSV-TK) or inducible caspase 9 (iCasp9), which can be activated by prodrugs or small molecules, respectively, and result in the rapid elimination of the infused T cells (Bonini and Mondino, 2015). Another way to reduce the risk of off-target toxicity is to prevent mispairing of endogenous and exogenous transgenic TCR chains, which can result in unpredictable new TCR specificities possibly causing autoimmunity (Bendle *et al.*, 2010; Yang, 2015). Strategies to achieve preferential pairing of the transgenic TCR chains include minimal amino acid exchanges or addition of cysteines into the TCR constant regions, as well as generation of hybrid molecules comprising the extracellular part of the TCR chains fused to the intracellular CD3ζ domain (Kuball *et al.*, 2007; Sebestyen *et al.*, 2008; Sommermeyer and Uckert, 2010). However, in order to completely abolish the risk of TCR mispairing and ensure high surface expression of the tumor-specific TCR, the endogenous TCR chains have to be

suppressed. This can be achieved by TCR knockout mediated by gene editing tools, like TALEN or CRISPR/Cas9 (Knipping *et al.*, 2017).

1.3   Chimeric antigen receptors (CARs) and cancer immunotherapy

The first *in vitro* experiments of chimeric T cell receptors, which comprised an extracellular antibody-derived immunoglobulin domain and could redirect T cells to target tumor cells with an antibody-type specificity, were published in 1989 by Gross *et al.* (Gross, Waks and Eshhar, 1989). Since then, extensive research on these chimeric antigen receptors (CARs) has resulted in clinical application of CAR T cells for various indications with a present focus on B cell malignancies (Gill, Maus and Porter, 2016). CARs are modularly assembled proteins that link the extracellular ligand recognition domain, comprised typically of an antibody-derived single chain variable fragment (scFv), to an intracellular signaling domain containing the CD3ζ chain to mimic signal transduction via the TCR complex and induce T cell activation (Srivastava and Riddell, 2015). The scFv is coupled to the intracellular signaling moiety via a hinge domain and a transmembrane domain. However, these first generation CARs failed to provide necessary T cell stimulation to achieve tumor cell lysis and persistence, probably due to the lack of co-stimulation required for proper T cell activation (Gong *et al.*, 1999; Sadelain, Brentjens and Rivière, 2009). The development of second generation CARs targeting CD19 that comprised additional intracellular co-stimulatory domains, including CD28, 4-1BB, and OX40, dramatically improved efficacy in clinical trials even obtaining complete remissions in some patients (Ramos, Savoldo and Dotti, 2014; Maus and June, 2016). Third generation CARs containing a combination of two co-stimulatory domains, like CD28/4-1BB or CD28/OX40, targeting CD20 and CD19, respectively, show promising results in mouse models and are currently evaluated in clinical settings (Till *et al.*, 2012; Tang *et al.*, 2016). However, severe fatal toxicities and cytokine storm syndrome were reported for a patient treated with a third generation ERBB2-specific CAR (Morgan *et al.*, 2010). This demonstrates the importance of thorough target evaluation equivalent to TCR-based adoptive T cell transfer. While TCRs recognize intracellularly processed protein in an MHC-dependent manner, CARs utilize the specificity of monoclonal antibodies to bind directly to target structures present on the tumor cell surface (Harris and Kranz, 2016). Both TCRs and antibodies are generated by hypervariable V(D)J recombination enabling the recognition of a vast variety of antigens, however, determining the required affinity suitable for T cell activation and tumor cell eradication is still challenging due to factors like antigen density and receptor expression levels affecting activity (Turatti *et al.*, 2007; Harris and Kranz, 2016). Spatial constraints between CAR T cells and target epitopes on APCs, influencing formation of the immunological synapse, might additionally impact tumor cell recognition (Srivastava and Riddell, 2015). The

dependency on the nature and length of the extracellular spacer domain for *in vivo* anti-tumor activity demonstrated the influence of this spatial interaction, which in turn can vary based on structure and density of the target molecule (Hudecek *et al.*, 2015). While it could be assumed that the higher the affinity of the receptor the better the activation of the T cell, recent studies demonstrated an affinity threshold for both TCRs and CARs that did not further increase activation, but rather contributed to decreased sensitivity (Zhong *et al.*, 2013; Chmielewski *et al.*, 2004; Caruso *et al.*, 2015). Especially when targeting overexpressed TAAs in immunotherapy, discrimination between tumor and healthy tissue is imperative to avoid on-target off-tumor toxicity. Another factor affecting CAR T cell efficacy in eradicating tumors is proliferation and persistence of the adoptively transferred T cells. While this can be negatively influenced by a suppressive tumor microenvironment, proliferative capacity is largely dependent on the co-stimulatory signaling domains incorporated in the CAR construct (Lim and June, 2017). Most of the CARs tested in recent clinical trials utilize CD28 or 4-1BB for co-stimulation to enhance efficacy *in vivo*. While CD28-containing CARs seem to exhibit a higher initial anti-tumor activity, CARs comprising the 4-1BB signaling domain show better persistence and overall tumor control (Milone *et al.*, 2009; Lim and June, 2017). This was impressively demonstrated by sustained remission in CLL patients months after infusion of 4-1BB-containing CD19-CAR T cells, which simultaneously showed that immunological memory can be established using adoptively transferred receptor-engineered T cells (Kalos *et al.*, 2011; Porter *et al.*, 2011).

1.4 TCR knockout – TALEN & CRISPR/Cas9 in immunotherapy

Transcription activator-like effectors (TALEs) is a class of specific DNA binding proteins derived from plant pathogenic bacteria *Xanthomonas spp.*, which contribute to disease by mimicking eukaryotic transcription factors (Kay *et al.*, 2007; Boch and Bonas, 2010). The DNA binding domain of TALEs is characterized by a central repeat domain of variable length, each repeat typically consisting of 24 amino acids (Herbers, Conrads-Strauch and Bonas, 1992). While the number of repeats can vary between 1.5 and 33.5, 17.5 repeats followed by a half repeat are most frequently observed (Boch and Bonas, 2010). Binding specificity is mediated by an adjacent pair of hypervariable amino acids, termed repeat-variable di-residues, (RVDs), at positions 12 and 13 in each repeat, which independently bind one base of the DNA. The 4 most frequent RVDs (NG, HD, NI, NN) preferentially associate with one of the four bases of the DNA (T, C, A, G) resulting in a remarkably simple code that governs sequence specificity (Boch *et al.*, 2009; Moscou and Bogdanove, 2009). Each RVD consists of two α-helices connected by a short RVD loop that contacts the major groove of the DNA. While residue 12 stabilizes the RVD loop, the 13th residue mediates the base-specific contact and serves as

the structural basis of the sequence-specific interaction (Deng *et al.*, 2012). In contrast to other DNA binding proteins, like zinc fingers, which can be challenging to design due to difficult target prediction, the straightforward sequence relationship of TALEs allows the easy identification of TALE binding sites. Additionally, the modular repeat structure in combination with the simple DNA binding code enables the easy assembly of TALE repeat arrays that can function as highly specific DNA binding domains (Boch, 2011; Bogdanove and Voytas, 2011). Combining the customized DNA binding domain of TALEs with catalytic domains of nucleases or transcription activation or repressor domains to generate TALE nucleases (TALENs) or TALE transcription factors (TALE-TFs), respectively, opened the possibility to create sequence-specific gene editing tools that could be used for gene knockout or for modulation of gene expression (Bogdanove and Voytas, 2011). While the modular repeat structure facilitates TALE design, assembly can be challenging due to the highly repetitive nature of these RVD-containing repeats (Cermak *et al.*, 2011). Several groups developed different protocols for the generation of TALEN and TALE-TF that are predominately based on Golden Gate cloning strategy enabling the simultaneous assembly of multiple DNA fragments in an ordered fashion (Cermak *et al.*, 2011; Li *et al.*, 2011; Morbitzer *et al.*, 2011; Zhang *et al.*, 2011; Sanjana *et al.*, 2012). Golden Gate cloning is based on type IIS restriction enzymes characterized by their property of cleaving outside the recognition site to create unique 4 bp overhangs. When utilized for molecular cloning, correct ligation of DNA fragments is guided by pairing of the unique overhangs, which simultaneously eliminates restriction enzyme recognition site upon correct assembly (Engler *et al.*, 2009). Based on the described protocols TALENs and TALE-TF can be customized to target any gene in different organisms, which has been already demonstrated *in vitro* and *in vivo* (Christian *et al.*, 2010; Cermak *et al.*, 2011; Zhang *et al.*, 2011; Huang *et al.*, 2011; Li *et al.*, 2011; Miller *et al.*, 2011; Mussolino *et al.*, 2011; Sander *et al.*, 2011; Tesson *et al.*, 2011; Wood *et al.*, 2011; Haute *et al.*, 2013).

To improve target specificity and reduce the risk of off-target cleavage, TALENs are designed as pairs that bind different target sites, which are separated by a 10 – 30 base pair spacer (Bogdanove and Voytas, 2011). Since the commonly used FokI endonuclease functions as a dimer, each TALEN can be fused to a monomeric catalytic domain (Bitinaite *et al.*, 1998). Only upon specific binding of both TALENs to the respective target site in inverse orientation, dimerization of the monomeric FokI domains in the spacer region can occur and nuclease activity will generate a non-specific DNA double strand break (DSB) (Pingoud and Wende, 2011). For the identification of suitable TALEN target sites in any gene of interest, which are usually preceded by a T or C, prediction tools have been developed that scan the input sequence according to custom set parameters, like number of repeats and spacer length, and allow identification of potential off-target sites (Doyle *et al.*, 2012)

In addition to TALENs, another gene editing system has recently been developed that is based on clustered regularly interspaced short palindromic repeats (CRISPR) RNAs that guide CRISPR-associated (Cas) proteins to mediate DNA cleavage (Cong *et al.*, 2013; Mali *et al.*, 2013). The CRISPR/Cas system functions as a nucleic acid-based adaptive immune system in prokaryotes for protection against invading viral and plasmid DNA (Wiedenheft, Sternberg and Doudna, 2012; Barrangou and Marraffini, 2014). CRISPR loci comprise short palindromic DNA repeats (CRISPR repeats) separated by unique spacer sequences (CRISPR spacers) homologous to exogenous genetic elements. It has been shown in *S. thermophilus* that new short virus-derived sequences will be preferentially integrated at the leader end of the CRISPR locus upon phage-challenge, thereby demonstrating how protective immunity is acquired in prokaryotes (Barrangou *et al.*, 2007). Proto-spacer adjacent motifs (PAMs) have been identified in exogenous donor DNA, termed proto-spacer, that mediate both immunization by identifying spacer sequences for incorporation and target selection for foreign DNA cleavage (Mojica *et al.*, 2009; Gasiunas *et al.*, 2012; Jiang *et al.*, 2013; Paez-Espino *et al.*, 2013). The mechanism of spacer integration involves the conserved Cas1 and Cas2 proteins that form an integrase complex, which catalyzes a nucleophilic attack of prespacer 3'OH ends on the leader-proximal repeat thereby mediating integration of the spacer sequence into the CRISPR loci (Jackson *et al.*, 2017; Xiao *et al.*, 2017). The CRISPR/Cas system functions in three steps: (I) Acquisition of new spacers into the CRISPR locus, (II) CRISPR RNA (crRNA) biogenesis to generate small interfering RNAs, and (III) targeting of foreign homologous sequences with Cas nucleases guided by crRNAs (Barrangou and Marraffini, 2014). Three types of CRISPR/Cas systems can be distinguished that differ in the mechanism of crRNA processing and the protein machinery involved in target recognition and cleavage. In contrast to type I and III CRISPR/Cas systems utilizing large multimeric nucleoprotein complexes, type II CRISPR/Cas system requires only Cas9 nuclease to mediate DNA cleavage via intrinsic RuvC and NHN domains. Due to its simplified nature, this system predominately serves as the basis for the use of CRRISPR/Cas as a gene editing tool (Barrangou and Marraffini, 2014). Cas9 endonuclease is guided to the PAM-containing target sequence by crRNA, which is processed and loaded onto Cas 9 with the help of RNaseIII and trans-encoded CRISPR RNA (tracRNA), comprising a complementary region of 24 nucleotides to the repeat region of the crRNA precursor transcript (Deltcheva *et al.*, 2011). By generating a chimeric fusion RNA of tracRNA and crRNA, termed single-guide RNA (sgRNA) that retains secondary structures required for Cas9 cleavage activity, the CRISPR/Cas9 system was further simplified for the use as an RNA-directed gene editing tool (Jinek *et al.*, 2012). Therefore, in order to target a specific gene for disruption by Cas9 nuclease, only the crRNA moiety that mediates specific DNA binding has to be adapted to show homology to the DNA target region. Several structural studies in the recent years revealed that the CRISP/Cas9-mediated DNA cleavage mechanism requires sgRNA

accommodation in Cas9 to induce conformational changes that convert the ribonucleoprotein complex into an active form. The Cas9 protein comprises six domains responsible for sgRNA binding (RecI), initiation of binding to target DNA (PAM interacting domain) and cleavage of single-stranded DNA (RuvC and HNH). Upon recognition of the PAM-containing target sequence, the DNA duplex is unwound to allow specific pairing of target DNA and homologous crRNA, which triggers DNA cleavage by RuvC and HNH nuclease domains, each targeting separate DNA strands. An arginine-rich bridge helix is critical for sgRNA and ssDNA interaction, which form a heteroduplex via Watson-Crick base pairs that is accommodated in a central channel in the Cas9 protein between two lobes (Jinek *et al.*, 2014; Nishimasu *et al.*, 2014; Jiang and Doudna, 2017; Nishimasu and Nureki, 2017). Cleavage activity of both nuclease domains is regulated by HNH conformational changes into the active form, which is prevented by mismatches between target DNA and sgRNA, thereby serving as a conformational checkpoint to prevent off-target cleavage (Dagdas *et al.*, 2017).

While TALENs mediate target recognition via amino acid residues interacting with the DNA, the CRISPR/Cas9 system utilizes Watson-Crick base pairing of an RNA-DNA-heteroduplex to identify homologous target regions. However, both systems utilize non-specific nuclease domains that are guided by the DNA binding moiety to create a sequence-specific DNA double strand break (DSB) in the host genome. The introduced DSB activates endogenous DNA repair mechanisms, which attempt to restore the integrity of the genome. Two highly conserved mechanisms are predominately used in eukaryotes for repair of DSB: (I) non- homologous end joining (NHEJ), which mostly results in small deletions or insertions at the break site that can disrupt gene function and lead to gene knockout, and (II) homologous recombination (HR), which restores the break site without introducing mutations by utilizing the sister chromatid or homologous chromosome as a repair template (Jackson, 2002). HR can be exploited for directed genome editing to introduce a gene of interest or correct a mutated gene by providing repair templates comprising homologous sequences to the DNA target site (Pingoud and Wende, 2011; Sander and Joung, 2014).

The simple design and production process of both TALEN and CRISPR/Cas system revolutionized gene editing in the scientific community and opened the possibility for therapeutic applications (Gaj, Gersbach and Barbas, 2013; Hsu, Lander and Zhang, 2014; Sander and Joung, 2014; Mojica and Montoliu, 2016). Several clinical trials have been registered at *clinicaltrials.gov* (Table 2.16) in the recent years that comprise *ex vivo* and *in vivo* gene therapy (Shim *et al.*, 2017; Dunbar *et al.*, 2018). As of today, *in vivo* approaches mainly focus on the delivery of wildtype-genes to replace a mutated or missing gene in patients predominantly utilizing randomly integrating viral vectors or adeno-associated virus (AAV) vectors. However, first genome editing trials in patients using zinc finger nucleases (ZFNs) to

replace defective genes in the albumin locus for the treatment of mucopolisaccharidosis (MPS) I and II were launched in 2017 (Dunbar *et al.*, 2018). Despite rapid technological advances in TALEN- and CRISPR/Cas-mediated gene editing *in vitro*, application and safety hurdles that include potential off-target mutations and immunogenicity will first have to be overcome before these therapies will be approved for clinical testing in patients (Shim *et al.*, 2017). In contrast, TALEN and CRISPR/Cas system are currently already applied in *ex vivo* modification of autologous cells before re-infusion into the patient. This includes the disruption of the CCR5 gene in T cells and hematopoietic stem and progenitor cells (HSPC) of patients infected with HIV using CRISPR, however ZFN are more often used in this indication based on extensive pre-clinical studies (Gu, 2015). TALENs targeting the TCR α chain of T cells are predominately used in the production of universal CD19-CAR T cells for treatment of B cell malignancies to prevent off-target recognition mediated by the endogenous TCR. Treatment of two infants suffering from acute lymphoblastic leukemia (ALL) with genetically engineered cells resulted in sustained molecular remission and currently more patients are being recruited (Qasim *et al.*, 2017). Clinical studies utilizing the CRISPR/Cas9 system involve primarily the knockout of inhibitory PD-1 (programmed cell death protein 1) to prevent T cell dysfunction and exhaustion mediated by interaction with PD-1 ligands (Xu-Monette *et al.*, 2017; Dunbar *et al.*, 2018). Recently, the first phase I CRISPR gene editing trial was initiated in the United States that uses autologous T cells redirected with a NY-ESO-1-specific TCR and genetically engineered to eliminate endogenous TCR as well as PD-1 expression for the treatment of melanoma, synovial sarcoma, and multiple myeloma (Baylis and McLeod, 2017). The knockout of the endogenous TCR in this setting prevents mispairing with transgenic TCR chains and the possible generation of unintended neo-reactivities (Heemskerk, 2010). Another approach is currently investigated in pre-clinical studies, which comprises the directed knockin of a CD19-CAR into the *TRAC* locus utilizing the CRISP/Cas9 system to generate a sequence-specific DSB and an AAV vector coding for the CAR to mediate integration into the target loci (Eyquem *et al.*, 2017). This enables the expression of the CD19-CAR under natural regulatory elements and simultaneously prevents possible off-target recognition through the endogenous TCR.

1.5   Aim of this thesis

Various high-throughput platforms have been developed for the isolation of tumor antigen-specific TCRs for the use in adoptive immunotherapy for cancer (Montagna *et al.*, 2001; Ho *et al.*, 2006; Wilde, Geiger, *et al.*, 2012). For clinical application, tumor antigen-specific TCRs are introduced into patient lymphocytes followed by adoptive transfer of the *ex vivo* engineered T cells. To facilitate efficient anti-tumor reactivity of the transferred lymphocytes, the introduced TCR has to be fully functional in the transgenic setting. That means the TCR has to confer the

antigen specificity and effector functions of the original T cell clone to the recipient T cell population. Additionally, extensive evaluation of potential toxicities has to be performed prior to the clinical use of the respective TCR to ensure safe administration of the genetically modified T cells to patients. Common TCR-induced toxicities can be divided into on-target and off-target toxicities. On-target toxicities occur by antigen expression in tissues other than the targeted tumor, while common off-target toxicities are caused by cross-recognition of alternative epitopes by the transgenic receptor or newly formed specificities of mispaired heterodimers of endogenous and transgenic TCR α and β chains, i.e. TCR mispairing (Bendle *et al.*, 2010; Yang, 2015). Both toxicity scenarios have to be excluded by elaborate safety testing of the TCR against healthy tissue samples and peptide libraries before the initiation of clinical trials. However, a large number of cells expressing the transgenic TCR are required for thorough efficacy and safety evaluation. Hence, appropriate TCR recipient cells are needed that allow efficient testing of isolated candidate TCRs. To date, bulk peripheral blood lymphocytes (PBL), which can be isolated from donor blood in sufficient numbers, are commonly used as TCR recipient cells. Even though these cells carry all signaling and effector functions required for a physiological read-out of transgenic TCR function and reactivity, they also comprise a diverse mixture of different lymphocyte subsets with heterogenous reactivity profiles that introduce unknown variables into experiments. In addition, the resulting recipient cells express the introduced antigen-specific TCRs as well as the endogenous TCRs of unknown specificity, which could severely affect or alter the function of the transgenic TCR by dominant effects of the endogenous TCR or TCR mispairing.

To prevent interference of endogenously expressed TCRs with experimental procedures and read-outs, the endogenous TCR chains would have to be eliminated in recipient cells. The generation of a suitable TCR-negative universal recipient cell that efficiently proliferates *in vitro* and retains all necessary effector functions for efficacy and safety testing would allow the creation of a stable test system, in which transgenic TCRs could be introduced without the constraints of endogenous TCR expression (Figure 1.1).
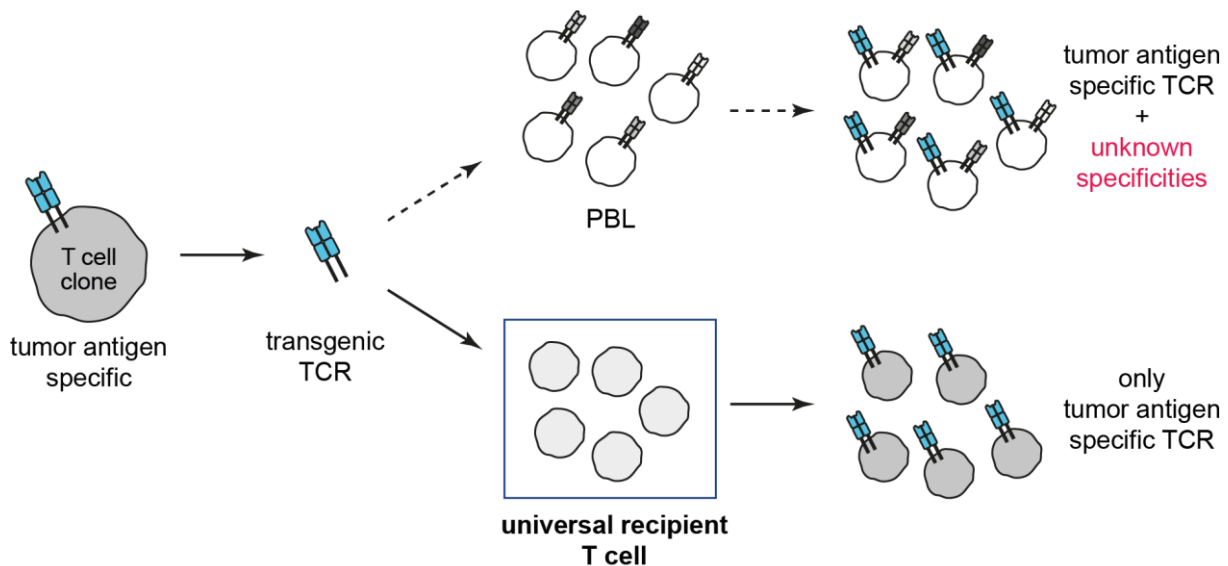
Figure 1.1: Recipient cells for the characterization of transgenic TCRs. A tumor antigen-specific TCR is isolated from the original T cell clone exhibiting the desired reactivity patterns. To test whether effector functions and specificity can be conferred to recipient cells, the transgenic TCR is introduced either in PBL or universal recipient cells, respectively. PBL express the introduced tumor antigen-specific TCR as well as endogenous TCRs of unknown specificity. In contrast, universal recipient cells lacking an endogenous TCR will only express the transgenic TCR specific for the desired tumor antigen, thereby abolishing the risk of TCR mispairing and dominant effects of endogenously expressed TCRs.

However, the generation of TCR-negative recipient cells is complicated by the fact that physiological activation and proliferation of T cells is mediated through the specific interaction of the TCR with peptide-bound MHC molecules on antigen presenting cells (Figure 1.2). Once the endogenous TCR of a T cell is absent, the possibility to activate and expand the cell to sufficient numbers is lost. Therefore, in order to generate a stable test system for the characterization of multiple transgenic TCRs, continuous T cell growth has to be achieved independent of TCR signaling prior to TCR knockout. Ideally, the desired test system would utilize an alternative route for expansion – other than the TCR itself – without introducing adverse modifications into the inherent T cell signal transduction cascade.

A promising alternative to classical activation of T cells via the endogenous TCR is the stimulation of T cells through the engagement of an introduced CAR. Although the exact signaling events following specific antigen binding via the scFv of CARs are still a topic of active investigation, various studies have demonstrated the feasibility of TCR-independent activation of T cells via these chimeric receptors (Maher *et al.*, 2002; Finney, Akbar and Alastair, 2004; Sommermeyer *et al.*, 2015). Observed long persistence of these CAR T cells in patients, months after treatment, could be attributed to re-activation of these cells *in vivo* mediated through the introduced CAR (Porter *et al.*, 2011). However, it is unknown whether long-term continuous T cell expansion can be achieved via CAR engagement in T cells lacking endogenous TCR expression.

The ability of a selected CAR to promote T cell expansion can be influenced by various factors, including the combination of the incorporated signaling domains as well as the respective target antigen. Since CAR constructs are generally designed to mediate tumor cell killing, rather than to enhance proliferative capacity of recipient T cells, the CAR domain structure best suited for physiological T cell expansion is not yet fully resolved.

The aim of this thesis was the generation of universal recipient cells for testing and characterization of transgenic TCRs that can be expanded independently of the endogenous TCR (Figure 1.2). TCR-independent activation of T cells was achieved through an introduced CAR that can mediate T cell proliferation upon specific binding of antigen. CAR constructs comprising different combinations of signaling domains were evaluated for their ability to promote T cell growth. Once the modified T cells expanded sufficiently via CAR engagement, the endogenous TCR was knocked out utilizing state-of-the-art gene editing tools, like TALEN and CRISPR/Cas9, to generate recipient cells that lack the endogenous TCR. The resulting TCR-negative universal recipient cells that proliferated upon CAR-specific activation subsequently served as recipients for transgenic TCRs to validate their suitability as a stable and reproducible test system for direct comparison of individual TCRs.
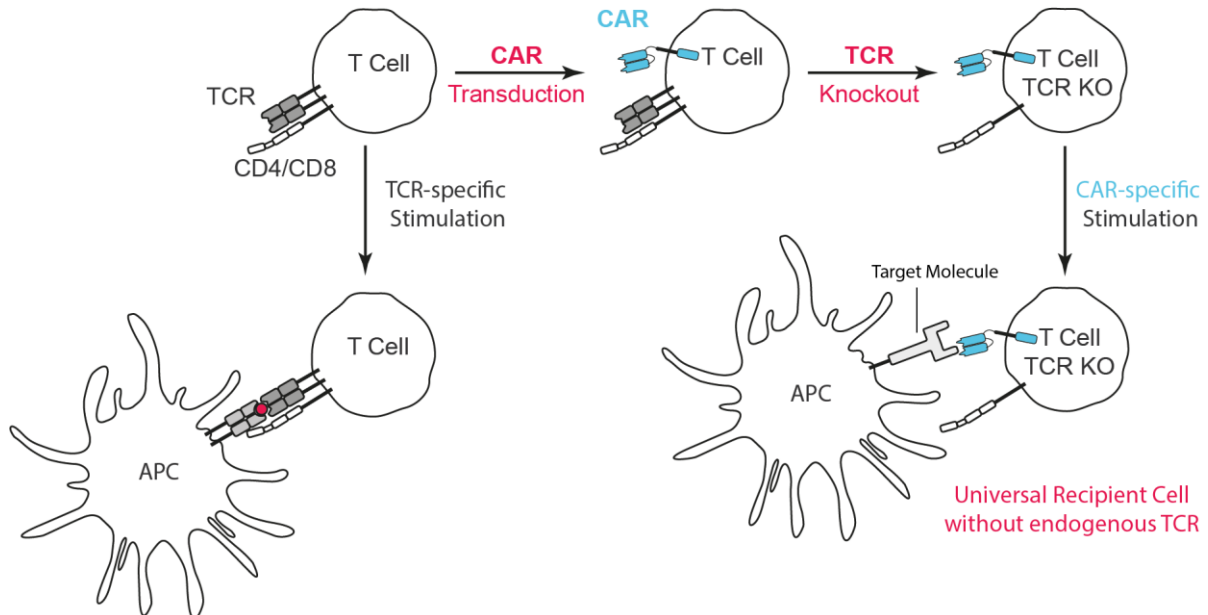
Figure 1.2: Strategy for generation of universal recipient cells for testing of transgenic TCRs. Physiological antigen-specific activation of T cells is mediated through the interaction of the TCR and peptide-bound MHC molecules on antigen presenting cells (APCs). CD4 or CD8 co-receptors support this interaction and distinguish CD4+ and CD8+ T cells, respectively. Once the TCR is absent, the ability to expand T cells is lost. By introducing a CAR into T cells, TCR-independent stimulation can be achieved. The knockout of the endogenous TCR creates universal recipient cells that lack an endogenous TCR but can be expanded via CAR engagement.

2 Materials

2.1 Equipment and consumables

Table 2.1: Equipment and consumables

Product Name	Manufacturer
Accu-jet® pro	Brand, Wertheim, Germany
BD™ High Throughput Sampler (HTS)	BD Bioscience, Heidelberg, Germany
BD Plastipak™ Wund- und Blasenspritze, 100 ml	BD Bioscience, Heidelberg, Germany
C-Chip, Neubauer improved	NanoEnTek, Seoul, Korea
Cell culture flasks (25, 75 and 150 cm2) Cellstar ®	Greiner Bio-One, Munich, Germany
Cell culture plates (6, 12, 24, 48, 96 well)	Corning, New York,USA
Cell culture plates (6, 12, 24, 48, 96 well)	TPP, Trasadingen, Switzerland
Cell Sorter FACSAria™ Fusion	BD Bioscience, Heidelberg, Germany
Centrifuge 1-16K	Sigma, Osterode am Harz, Germany
ChemiDoc™ XRS+ Gel Documentation System	Bio-Rad Loboratories, Munich, Germany
Counting chamber according to Neubauer	Neo-Lab, München, Germany
Cryopreservation vials (1 and 2 mL)	Nunc, Wiesbaden, Grmany
Cryopreservation vials (1.8 mL)	Corning, New York, USA
DNA LoBind Tubes (0.5 and 1.5 mL)	Eppendorf, Hamburg, Germany
DynaMag™-2/5 Magnet	Thermo Fisher Scientific, Waltham, MA, USA
ECOSHIELD™ ECO NITRILE PF 250	Shield Scientific, Bennekom, Netherlands
Electrophoresis chambers	Bio-Rad Laboratories, Munich, Germany
Electroporation cuvettes (0.4/0.1cm)	Bio-Rad Laboratories, Munich, Germany
Electroporator Gene Pulse Xcell™	Bio-Rad Laboratories, Munich, Germany
Elix® Advantage 15 Water Purification System	Merck, Darmstadt, Germany
Falcon® tubes (15 and 50 mL)	Corning, New York, USA
Falcon® round bottom test tubes sterile (5 mL)	Corning, New York, USA
Finnpette™ F2 Pipette 8/12-channel	Thermo Fisher Scientific, Waltham, MA, USA
Flow cytometer, LSR Fortessa	BD Bioscience, Heidelberg, Germany
Freezer -150 °C	Panasonic, Kadoma, Osaka, Japan
Freezer -20 °C	Liebherr, Bulle, Sitzerland
Freezer -80 °C	Panasonic, Kadoma, Osaka, Japan
Freezing container, Nalgene ® Mr. Frosty	Nalgene, Hereford, UK
Glass beads	Carl Roth, Karlsruhe, Germany
GRIPTIPS (sterile) 300 µL, 1250 µL	Integra Biosciences AG, Zizers, Switzerland
Heracell™ 150i CO2 incubator	Thermo Fisher Scientific, Waltham, MA, USA
Heraeus™ Multifuge™ X3R Universalzentrifuge	Thermo Fisher Scientific, Waltham, MA, USA
Herasafe HSP 12, laminar flow	Heraeus, Hanau, Germany

Product Name	Manufacturer
ImmunoSpot® S6 ULTIMATE	CTL, Cleveland, OH, USA
IncuCyte® ZOOM System	Essen Bioscience, Ann Arbor, Michigan, USA
Laboratory balance	Satorius, Goettingen, Germany
Magnet DynaMag™	Thermo Fisher Scientific, Waltham, MA, USA
Mastercycler® nexus	Eppendorf, Hamburg, Germany
MC6® chemical hood	Waldner, Wangen, Germany
Microcentrifuge tubes (0.5, 1.5 and 2 mL)	Eppendorf, Hamburg, Germany
Microwave	Bosch, Stuttgart, Germany
Mikroskop Primovert	Zeiss, Göttingen, Germany
Multiskan™ FC Mikrotiterplatten-Photometer	Thermo Fisher Scientific, Waltham, MA, USA
NanoDrop™ 2000c	Thermo Fisher Scientific, Waltham, MA, USA
Nunc Immuno Washer 8/12-channel	Nunc, Wiesbaden, Grmany
Nunc-Immuno™ 96 Well Plate	Thermo Fisher Scientific, Waltham, MA, USA
Parafilm	Pechiney, Menasha, USA
Pasteur pipettes	Peske OHG, Munich, Germany
Petri dishes 10 cm	Thermo Fisher Scientific, Waltham, MA, USA
Pipette tips (2, 20, 200, 1000 μL)	Mettler Toledo, Giessen, Germany
Pipette tips filtered (2, 20, 100, 200, 1000 μL)	Starlab, Hamburg, Germany
Pipettes	Eppendorf, Hamburg, Germany
PMC-60 Tomy Capsulefuge	Tomy, Tokyo, Japan
Power supply PowerPac™	Bio-Rad Laboratories, Munich, Germany
Radiation facility Xstrahl RS225	Xstrahl Limited, Camberly, Surrey, UK
Refrigerator 4 °C	Liebherr, Bulle, Sitzerland
RNase-free Microfuge Tubes (1.5 mL); Ambion	Thermo Fisher Scientific, Waltham, MA, USA
Round bottom tubes 5 ml	Corning, New York, USA
Round bottom tubes with cell strainer cap 5 ml	Corning, New York, USA
Scotsman AF103 Ice Flaker	Hubbard Systems, Ipswich, UK
SONY SH800S Cell Sorter	SONY Biotechnology, San Jose, CA, USA
Sterile plastic pipettes (5, 10, 25 mL)	Corning, New York, USA
Surflo® winged infusion sets	Terumo, Eschborn, Germany
Thermomixer comfort	Eppendorf, Hamburg, Germany
Tritec® Cooling Incubator with orbital shaker	Tritec, Hannover, Germany
UV transilluminator (366 nm)	Bachofer, Reutlngen, Germany
VIAFLO II 12-channel, 1250 μl	Integra Biosciences AG, Zizers, Switzerland
Vortex-Genie 2	Scientific Industries, Inc., Bohemia, NY, USA
VOYAGER II 6-channel, 1250 μl	Integra Biosciences AG, Zizers, Switzerland
VWB 12 waterbath	VWR International, Darmstadt, Germany
WTW inolab 720 pH meter	WTW, Weilheim, Germany

2.2   Chemicals and reagents

Table 2.2: Chemicals and reagents

Product Name	Manufacturer
Agarose, Ultra Pure	Thermo Fisher Scientific, Waltham, MA, USA
Ampicillin	Merck, Darmstadt, Germany
Aqua ad iniectabilia	Braun, Kronberg im Taunus, Germany
Bacillol AF	Bode science center, Hamburg, Germany
Biocoll	Biochrom, Berlin, Germany
BSA (bovine serum albumin)	Sigma-Aldrich, St. Louis, MO, USA
DEPC (diethylpyrocarbonate)	Sigma-Aldrich, St. Louis, MO, USA
Dismozon® plus	Bode science center, Hamburg, Germany
DMSO (dimethyl sulfoxide)	Merck, Darmstadt, Germany
EDTA	Sigma-Aldrich, St. Louis, MO, USA
EDTA (0.5 M)	Thermo Fisher Scientific, Waltham, MA, USA
Ethanol absolute	Carl Roth, Karlsruhe, Germany
Ethidium bromide 0,025 %	Carl Roth, Karlsruhe, Germany
FACS^{TM} Flow and Rinse	BD Bioscience, Heidelberg, Germany
FcR Blocking Reagent, human	Milteny Biotec, Bergisch Gladbach, Germany
Glycerol	Sigma-Aldrich, St. Louis, MO, USA
Heparin-Natrium	Braun, Kronberg im Taunus, Germany
IncuCyte® NucLight Red Lentivirus Reagent	Essen Bioscience, Ann Arbor, Michigan, USA
Ionomycin	Sigma-Aldrich, St. Louis, MO, USA
Isopropanol	Carl Roth, Karlsruhe, Germany
Luria Broth Base powder	Thermo Fisher Scientific, Waltham, MA, USA
Nuclease-free water	Thermo Fisher Scientific, Waltham, MA, USA
Paraformaldehyde 4% in PBS	Thermo Fisher Scientific, Waltham, MA, USA
PBS Dubelco w/o Ca2$^+$	Merck, Darmstadt, Germany
Phenol-chloroform-isoamylalcohol	Carl Roth, Karlsruhe, Germany
Phosphoric acid 85%	Carl Roth, Karlsruhe, Germany
PMA (phorbol 12-myristate 13-acetate)	Sigma-Aldrich, St. Louis, MO, USA
Remel™ Phytohaemagglutinin (PHA)	Thermo Fisher Scientific, Waltham, MA, USA
Retronectin®	Takara Bio, Montain View, CA, USA
RNaseZap™	Thermo Fisher Scientific, Waltham, MA, USA
Select agar	Thermo Fisher Scientific, Waltham, MA, USA
Skim milk powder	Sigma-Aldrich, St. Louis, MO, USA
SOC medium	Thermo Fisher Scientific, Waltham, MA, USA
Sodium acetate (3M)	Thermo Fisher Scientific, Waltham, MA, USA
Sodium carbonate (Na_2CO_3)	Sigma-Aldrich, St. Louis, MO, USA

Product Name	Manufacturer
Sodium hydrogen carbonate (NaHCO$_3$)	Sigma-Aldrich, St. Louis, MO, USA
TAE 50X buffer (Tris Acetate EDTA)	Thermo Fisher Scientific, Waltham, MA, USA
TRI-Reagent®	Sigma-Aldrich, St. Louis, MO, USA
Tween® 20	Sigma-Aldrich, St. Louis, MO, USA
UltraComp eBeads®	Thermo Fisher Scientific, Waltham, MA, USA

2.3   Solutions and buffer systems

Table 2.3: Solutions and buffer systems

Buffer	Components
Blocking Buffer	2% (v/v) BSA in PBS
Cell Fixation Solution	1% (v/v) PFA in PBS
DEPC-treated water	0.1% (v/v) DEPC in Elix® H$_2$O
ELISA Blocking Buffer	1% (w/v) skim milk powder in PBS
ELISA Coating Buffer	8.4 g/L NaHCO$_3$, 3.56 g/L Na$_2$CO$_3$ in Elix® H$_2$O (pH 9.5)
ELISA Washing Buffer	0.05% (v/v) Tween® 20 in PBS
FACS Buffer	1% (v/v) FBS in PBS
Isolation Buffer	0.1% (v/v) BSA, 2 mM EDTA in PBS (pH 7.4)
TAE Buffer (RNA) 1X	1x TAE (50X Thermo Fisher Scientific) in DEPC-treated water
TEA Buffer (DNA) 1X	1x (50X Thermo Fisher Scientific) TAE in Elix® H$_2$O

2.4   Kits

Table 2.4: Kits

Product Name	Manufacturer
OptEIA™ Human IFN-γ ELISA Set	BD Bioscience, Heidelberg, Germany
Dynabeads® Human T-Activator CD3/CD28	Thermo Fisher Scientific, Waltham, MA, USA
Dynabeads® FlowCompTM Human CD3	Thermo Fisher Scientific, Waltham, MA, USA
Golden Gate TALEN and TAL Effector Kit 2.0	Addgene, Cambridge, USA
RNeasy® Mini Kit	Qiagen, Hilden, Germany
JetStarTM Plasmid Purification Kit (mini, maxi)	Genomed, Löhne, Germany
QIAquick Gel Extraction Kit (250)	Qiagen, Hilden, Germany
mMessage mMachinTM T7 Transcription Kit	Thermo Fisher Scientific, Waltham, MA, USA
Poly(A) Tailing Kit	Thermo Fisher Scientific, Waltham, MA, USA
CTL-LDC™ Live/Dead Cell Counting Kit	CTL, Cleveland, OH, USA
TMB Substrate Reagent Set	BD Bioscience, Heidelberg, Germany
SMARTer® RACE 5'/3' Kit	Takara Bio, Montain View, CA, USA

Product Name	Manufacturer
First Strand cDNA Synthesis Kit for RT-PCR	Roche Diagnostics, Mannheim, Germany
PCR Master Mix	Promega, Madison, WI, USA
CellTrace™ Violet Cell Proliferation Kit	Thermo Fisher Scientific, Waltham, MA, USA
Dynabeads™ CD3	Thermo Fisher Scientific, Waltham, MA, USA
GeneArt™ CRISPR Nuclease mRNA and CRISPR T7 Strings	Thermo Fisher Scientific, Waltham, MA, USA
TransIT®-LT1 Transfection Reagent	Mirus Bio, Madison, WI, USA

2.5 Enzymes

Table 2.5: Enzymes

Enzymes	Buffers	Manufacturer
Restriction Endonucleases	10x NEB Buffer1-4, CutSmart Buffer, BSA	New England Biolabs, Frankfurt, Germany
T4 DNA Ligase	10x T4 DNA Ligase Buffer	New England Biolabs, Frankfurt, Germany

2.6 Plasmids

Table 2.6: Description vector backbones

Vector backbone	Description
pMA	Vector for molecular cloning and amplification in bacteria purchased from Geneart® (Thermo Fisher Scientific); *AmpR*
pGEM	Vector for synthesis of ivt-RNA containing T7 promoter and polyA$_{120}$-tail; *AmpR* (S. Milošević)
pES-12.6	Retroviral self-inactivating (SIN) vector for transduction (BioNTech IMFS); EF1A internal promoter, CMV enhancer, 5' LTR of MoMuLV, psi/psi+ packaging signal of MoMuLV, MCS, WPRE element of Woodchuck Hepatitis Virus 8, self-inactivating (SIN) 3' LTR of MoMuLV, *AmpR*
pMP71	Retroviral vector for transduction; (Engels *et al.*, 2003) Myeloproliferative sarcoma virus (MPSV)-LTR promoter-enhancer sequences and improved UTR derived from the murine embryonic stem cell virus (MESV), PRE element of woodchuck hepatitis virus in 3' UTR, *AmpR*

Table 2.7: Plasmids

Plasmid	Description	Source
pGEM_eGFP_A120	Vector for generation of eGFP ivt-RNA	S. Milošević*
pES.12-6-MIT	Retroviral SIN vector backbone without insert	C. Ellinger*
pMP71-MIT	Retroviral vector backbone without insert	C. Ellinger*
pMA_CD3-Chimera_FCS_P2A_RS_eGFP	Cloning vector encoding CD3-Chimera coding sequence coupled to eGFP via P2A element; Furin cleavage site (FCS) and additional restriction sites (RS)	this work[#]
pGEM_CD3-Chimera_P2A_GFP_wm-A120	Vector for ivt-RNA synthesis encoding CD3-Chimera coding sequence coupled to eGFP via P2A element	this work
pES.12-6_CD3-Chimera_P2A_GFP_EF1a_MIT	Retroviral SIN-vector encoding CD3-Chimera coding sequence coupled to eGFP via P2A element	this work
pMP71_CD3-Chimera_P2A_GFP_MIT	Retroviral vector encoding CD3-Chimera coding sequence coupled to eGFP via P2A element	this work
pMA_CD19-CAR_P2A_GFP	Cloning vector encoding CD19-CAR coding sequence coupled to eGFP via P2A element	this work[#]
pGEM_CD19-CAR_P2A_GFP_wm-A120	Vector for ivt-RNA synthesis encoding CD19-CAR coding sequence coupled to eGFP via P2A element	this work
pES.12-6_CD19-CAR_P2A_GFP_EF1a_MIT	Retroviral SIN-vector encoding CD19-CAR coding sequence coupled to eGFP via P2A element	this work
pMP71_CD19CAR_P2A_GFP_MIT	Retroviral vector encoding CD19-CAR coding sequence coupled to eGFP via P2A element	this work
pBullet_CAR#607	Retroviral vector encoding CAR#607, termed "CEA-CAR_CD8" in this work	H. Abken[$]
pBullet_CAR#908	Retroviral vector encoding CAR#908, termed "CEA-CAR_CD4" in this work	H. Abken[$]
ptruncTAL3_13.3_TCRa_L (TALEN_TCRα_left)	Vector for ivt-RNA synthesis encoding TALEN coding sequence targeting the *TRAC* locus	N. Sailer[$]
ptruncTAL3_14.1_TCRa_R (TALEN_TCRα_right)	Vector for ivt-RNA synthesis encoding TALEN coding sequence targeting the *TRAC* locus	N. Sailer[$]
ptruncTAL3_15.2_TCRb_L (TALEN_TCRβ_left)	Vector for ivt-RNA synthesis encoding TALEN coding sequence targeting the *TRBC* locus	N. Sailer[$]
ptruncTAL3_16.2_TCRb_R (TALEN_TCRβ_right)	Vector for ivt-RNA synthesis encoding TALEN coding sequence targeting the *TRBC* locus	N. Sailer[$]
TRAC Crispr String	String DNA fragment for ivt-RNA synthesis of CRISPR gRNA for targeting of *TRAC* locus	this work[#]
TRBC Crispr String	String DNA fragment for ivt-RNA synthesis of CRISPR gRNA for targeting of *TRBC* locus	this work[#]
pcDNA3.1(+) (gag/pol)	Expression vector encoding retroviral structural proteins (gag) and reverse transcriptase (pol); for generation of viral particles in mammalian cells (HEK293FT)	S. Milošević*
K83-hCMV-GALV	Expression vector encoding gibbon ape leukemia virus (GALV) envelope protein (Env); for generation of viral particles in mammalian cells (HEK293FT)	S. Milošević*
pMP71-T58-b-P2A-a muco	Retroviral vector encoding coding sequence of TCR T58 β and α chain coupled via P2A element; murine constant region	S. Wilde* (Wilde *et al.*, 2009)

Plasmid	Description	Source
pMP71-D115-b-P2A-a muco	Retroviral vector encoding coding sequence of TCR D115 β and α chain coupled via P2A element; murine constant region	S. Wilde* (Wilde *et al.*, 2009)
pES.12-6_mmcys _NY-ESO_ab	Retroviral SIN vector encoding coding sequence of NY-ESO TCR β and α chain coupled via P2A element; minimal murinized constant region with additional cysteine bridge	G. Longinotti*

*Medigene Immunotherapies GmbH, Martinsried, Germany

#Synthesized by Thermo Fisher Scientific, Waltham, MA, USA

$Hinrich Abken, Center for Molecular Medicine Cologne, University of Cologne, and Department I of Internal Medicine, University Hospital Cologne, Cologne, Germany

§Generated in a previous work: Master thesis "Targeting the Human T Cell Receptor with TAL Effector Nucleases in Herpesvirus saimiri Transformed T Cells", 2013 (Sailer, 2013).

2.7 Primer and oligonucleotides

Table 2.8: Primer

Primer	Sequence	Manufacturer
3'AST	CTTGCCTCTGCCGTGAATGT	Sigma-Aldrich*
3'BST	GAGGTAAAGCCACAGTTGCT	Sigma-Aldrich*
CD3-CAR_P1_for	AGAATATCGGCTCCGATGAGG	Sigma-Aldrich*
CD3-CAR_P2_for	ATGAAGGGCGAGCGGAGAAG	Sigma-Aldrich*
CD3-CAR_P3_for	GGCCACAAGCTGGAGTACAAC	Sigma-Aldrich*
pGEM_for	ACAGGAAACAGCTATGACCATG	Sigma-Aldrich*
pGEM_rev	CGTGATTCACTCGTTCTCACC	Sigma-Aldrich*
pGEM_wm_rev	GAATTACGTGATTCACTCGTTCT	Sigma-Aldrich*
pES.12-6_for	CGCAACGGGTTTGCCGCCA	Sigma-Aldrich*
pMP71_for	GCTCCGCCACTGTCCGAG	Sigma-Aldrich*
pMP71_rev	AATGGCGGTAAGATGCTC	Sigma-Aldrich*
TCRab_P2A	GCAGCGGCGCCACCAACTT	Sigma-Aldrich*
pMA_for (M13 uni (-21));	TGTAAAACGACGGCCAGT	Eurofins Genomics#
pMA_rev (M13 rev (-29));	CAGGAAACAGCTATGACC	Eurofins Genomics#
PCR1_3pAC_IUP	GTCTCGTGGGCTCGGAGATGTGTATAAGAG ACAGAATCAAAATCGGTGAATAGGCAG	Sigma-Aldrich*
PCR1_3pBC_IUP	GTCTCGTGGGCTCGGAGATGTGTATAAGAG ACAGGGCACACCAGTGTGGCCTT	Sigma-Aldrich*
TRAC_RACE_PCR	CGGCCACTTTCAGGAGGAGGATTCGGAAC	Sigma-Aldrich*
TRBC_RACE_PCR	CCGTAGAACTGGACTTGACAGCGGAAGTGG	Sigma-Aldrich*

* Sigma-Aldrich, St. Louis, MO, USA

#Eurofins Genomics, Ebersberg, Germany oder Brussels, Belgium

2.8 Molecular weight markers and loading dyes

Table 2.9: Molecular weight markers and loading dyes

Name	Manufacturer
100 bp DNA Ladder	Thermo Fisher Scientific, Waltham, MA, USA
1 kb DNA Ladder	Thermo Fisher Scientific, Waltham, MA, USA
2X RNA Loading Dye	Thermo Fisher Scientific, Waltham, MA, USA
DNA Gel Loading Dye (6X)	Thermo Fisher Scientific, Waltham, MA, USA
RiboRulerTM High Range RNA Ladder	Thermo Fisher Scientific, Waltham, MA, USA
RNA Loading Dye, (2X)	Thermo Fisher Scientific, Waltham, MA, USA

2.9 Antibodies

Table 2.10: Antibodies

Antibody	Clone	Isotype	Species	Conjugation	Manufacturer
CCR7	3D12	IgG2a	rat	PE	Thermo Fisher Scientific
CD16	3G8	IgG1	mouse	Alexa700	Thermo Fisher Scientific
CD19	HIB19	IgG1	mouse	Hz450	BD Biosciences
CD19	HIB19	IgG1	mouse	PE-Cy7	Thermo Fisher Scientific
CD19	SJ25C1	IgG1	mouse	PE-Cy7	BD Biosciences
CD3	UCHT1	IgG1	mouse	BUV395	BD Biosciences
CD3	UCHT1	IgG1	mouse	FITC	BD Biosciences
CD3	UCHT1	IgG1	mouse	PB	BD Biosciences
CD3	SK7	IgG1	mouse	PE-Cy7	BD Biosciences
CD3	SK7	IgG1	mouse	PerCP	BD Biosciences
CD3delta	MEM-57	IgG2a	mouse	FITC	antikörper-online
CD3gamma	MEM-57	IgG2a	mouse	PE	antikörper-online
CD4	RPA-T4	IgG1	mouse	APC	BD Biosciences
CD4	RPA-T4	IgG1	mouse	APC-Cy7	BD Biosciences
CD4	SK3	IgG1	mouse	FITC	BD Biosciences
CD4	RPA-T4	IgG1	mouse	PB	BD Biosciences
CD4	RPA-T4	IgG1	mouse	PE	BD Biosciences
CD4	VIT4	IgG2a	mouse	PerCP	Miltenyi Biotec
CD45RA	HI100	IgG2b	mouse	APC	BD Biosciences
CD45RA	T6D11	IgG2b	mouse	FITC	Miltenyi Biotec
CD45RA	HI100	IgG2b	mouse	PerCP-Cy5.5	Thermo Fisher Scientific
CD45RO	UCHL1	IgG2a	mouse	PE	BD Biosciences*
CD56	B159	IgG1	mouse	Alexa700	BD Biosciences*

Antibody	Clone	Isotype	Species	Conjugation	Manufacturer
CD56	B159	IgG1	mouse	V450	BD Biosciences*
CD62L	145/15	IgG1	mouse	APC	Miltenyi Biotec#
CD62L	DREG-56	IgG1	mouse	APC-Cy7	Thermo Fisher Scientific§
CD62L	SK11	IgG2a	mouse	FITC	BD Biosciences*
CD62L	DREG-56	IgG1	mouse	PE	BD Biosciences*
CD8	RPA-T8	IgG1	mouse	Alexa700	BD Biosciences*
CD8	HIT8a	IgG1	mouse	FITC	BD Biosciences*
CD8	RPA-T8	IgG1	mouse	Horizon V500	BD Biosciences*
CD8	RPA-T8	IgG1	mouse	PB	BD Biosciences*
CD8	RPA-T8	IgG1	mouse	PE	BD Biosciences*
CD8	RPA-T8	IgG1	mouse	V450	BD Biosciences*
CD80	L307.4	IgG1	mouse	APC-Cy7	BD Biosciences*
CD86	2331 (FUN-1)	IgG1	mouse	APC	BD Biosciences*
CD95	DX2	IgG1	mouse	APC	BD Biosciences*
CEACAM-5	487609	IgG2a	mouse	PE	R&D Systems**
F(ab')2 Anti-Human IgG	polyclonal	Goat F(ab')2 IgG	goat	R-PE	Southern Biotech***
HLA-A2	BB7.2	IgG2b	mouse	FITC	BD Biosciences*
mTCRβ	H57-597	IgG2a	hamster	APC	BD Biosciences*
mTCRβ	H57-597	IgG2a	hamster	PE	BD Biosciences*
panTCR a/β	IP26A	IgG1	mouse	PE	Beckman Coulter$
panTCR a/β	IP26A	IgG1	mouse	PC5	Beckman Coulter$
panTCR γ/δ	B1.1	IgG1	mouse	FITC	Thermo Fisher Scientific§
panTCR γ/δ	IMMU510	IgG1	mouse	PE	Beckman Coulter$
TCR-Vβ1	BL37.2	IgG1	Rat	PE	Beckman Coulter$
TCR-Vβ23	AF23	IgG1	mouse	PE	Beckman Coulter$
TCR-Vβ8	56C5.2	IgG2a	mouse	PE	Beckman Coulter$
FcR Blocking reagent	-	-	-	-	Miltenyi Biotec

*BD Biosciences, Heidelberg, Germany

#Milentyi Biotec, Bergisch Gladbach, Germany

§Thermo Fisher Scientific, Waltham, MA, USA

**R&S Systems, Minneapolis, MN, USA

***Southern Biotech, Birmingham, AL, USA

$Beckman Coulter, Brea, CA, USA

Table 2.11: Tetramer and peptides

Compound	Peptide	HLA	Conjugation	Manufacturer
Tetramer	YMDGTMSQV	HLA-A2	PE	immunAware*
Peptide	YMDGTMSQV	-	-	Peps4LS GmbH#
Peptide	SLLMWITQC	-	-	ProteoGenix§

*immunAware, Copenhagen, Denmark

#Peps4LS GmbH, Heidelberg, Germany

§ProteoGenix, Schiltigheim, France

2.10   Bacteria culture

2.10.1   Bacterial strains

Table 2.12: Bacterial strains

Bacterial Strain	Genotype	Source
XL1-Blue Competent Cells (*E. coli*)	*recA1 endA1 gyrA96 thi-1 hsdR17 supE44 relA1 lac* [F´ *proAB lacIqZΔM15 Tn10* (Tetr)]	Aligent Technologies, Santa Clara, CA, USA
NEB Turbo Competent *E. coli*	F´ *proA+ B+ lacIq Δ lacZ M15/ fhuA2 Δ(lac-proAB) glnV gal R(zgb210::Tn10)*Tet^S *endA1 thi-1 Δ(hsdS-mcrB)5*	New England Biolabs, Frankfurt, Germany

2.11 Cell culture

2.11.1 Cells

Table 2.13: Cells

Cells	Description	Source/Reference
HEK293FT	Human embryonic kidney 293 cells, transformed with SV40 Large T antigen	Thermo Fisher Scientific*
Jurkat-76-IVB10	TCR α and β chain deficient T cell lymphoma cell line	M. Heemskerk[#] and M. Bürdek**
K562	Chronic myelogenous leukemia (CML) cell line	ATCC® CCL-243™, ATCC[§] (Lozzio and Lozzio, 1975)
K562_A2	K562 CML cell line transduced with vector coding for HLA-A*02:01	G. Longinotti**
K562_A2_CD86	K562_A2 transduced with vector coding for CD86	G. Longinotti**
Mel624.38	Melanoma cell line	M. Panelli*** (Rivoltini *et al.*, 1995)
MelA375	Melanoma cell line	ATCC® CRL-1619™, ATCC[§]
647-V	Urothelial bladder carcinoma cell line	ACC 414, DSMZ[$]
LS174T	Dukes' type B colorectal adenocarcinoma cell line	ATCC® CL-188™, ATCC[§]
Clone 234	CD4^{+} T cell clone, HLA-A24-restricted	isolated by D.J. Schendel**
LCL_BW	Lymphoblastoid cell line, B cells transformed with EBV	isolated by D.J. Schendel**
mLCL_ME	Lymphoblastoid cell line, B cells transformed with Mini-EBV	C. Ellinger**
LCL_Eva1	Lymphoblastoid cell line, B cells transformed with EBV	C. Wehner**
PBMC	Peripheral blood mononuclear cells (PBMC). Derived from human peripheral blood of healthy donors by density gradient centrifugation (Biocoll)	this work
PBL	Peripheral bool lymphocytes (PBL). Derived from human peripheral blood of healthy donors by density gradient centrifugation (Biocoll) and subsequent plate adherence	this work

* Thermo Fisher Scientific, Waltham, MA, USA

[#] Hematology, Leiden University Medical Center

[§] ATCC, Manassas, VA, USA

** Medigene Immunotherapies GmbH, Planegg, Germany

*** National Cancer Institute, Bethesda, MD, USA

[$] DSZM, Braunschweig, Germany

2.11.2 Media, solutions and supplements

Table 2.14: Media, solutions and supplements for cultivation of cells

Product Name	Manufacturer
Dulbecco's Modified Eagle Medium (DMEM)	Thermo Fisher Scientific, Waltham, MA, USA
Dulbecco's phosphate buffer saline (PBS)	Thermo Fisher Scientific, Waltham, MA, USA
Endotoxin-Free Dulbecco's PBS (1X)	Sigmal-Adrich, St. Louis, MO, USA
Fetal bovine serum (FBS)	Thermo Fisher Scientific, Waltham, MA, USA
HEPES (1M)	Thermo Fisher Scientific, Waltham, MA, USA
Human Serum MDG (HS_MDG)	Medigene Imuunotherapies, Planegg, Germany
Ibidi Freezing medium	Ibidi, Planegg, Germany
L-Glutamin 200 mM	Thermo Fisher Scientific, Waltham, MA, USA
MEM Non-essential amino acids (NEAA) 100X	Thermo Fisher Scientific, Waltham, MA, USA
Penicillin-Streptomycin (10,000 U/mL)	Thermo Fisher Scientific, Waltham, MA, USA
Pool Human Serum (PHS)	ZKT Tübingen, Tübingen, Germany
Proleukin ® S (IL-2)	Novartis, Basel, Switzerland
Puromycin	Invivogen, San Diego, CA, USA
RPMI Medium 1640	Thermo Fisher Scientific, Waltham, MA, USA
Sodium pyruvate (100 mM)	Thermo Fisher Scientific, Waltham, MA, USA
Trypan blue stain 0.4%	Thermo Fisher Scientific, Waltham, MA, USA
Trypsin-EDTA (0.05%), phenol red	Thermo Fisher Scientific, Waltham, MA, USA

Table 2.15: Composition of cell culture media

Medium	Composition
Freezing medium	10% (v/v) FBS (inactive) in DMSO
DMEM_IV	2mM L-Glutamine, 1 mM Sodium Pyruvate, 1% (v/v) MEM NEAA and 10% (v/v) inactive FBS in DMEM medium
RPMI_IV	2mM L-Glutamine, 1 mM Sodium Pyruvate, 1% (v/v) MEM NEAA and 10% (v/v) inactive FBS in RPMI 1640 medium
T cell medium (TCM)	2mM L-Glutamine, 1 mM Sodium Pyruvate, 1% (v/v) MEM NEAA, 10 mM HEPES, 1% (v/v) Penicillin-Streptomycin and 10% (v/v) inactive PHS or HS_MDG in RPMI 1640 medium
Clone234 medium	2mM L-Glutamine, 1 mM Sodium Pyruvate, 1% (v/v) MEM NEAA, 10% (v/v) inactive FBS and 6% (v/v) inactive HS_MDG in RPMI 1640 medium
647-V medium	2 mM L-Glutamine, 15% (v/v) inactive FBS in DMEM medium

2.12 Software and Databases

Table 2.16: Software and databases

Software or Database	Manufacturer or Website
Adobe Illustrator® CC	Adobe Systems, San Jose, USA
Adobe Reader XI	Adobe Systems, San Jose, USA
BD FACSDiva™ Software	BD Biosciences, Franklin Lakes, NJ, USA
Chromas Lite	Technelysium, South Brisbane, Australia
ClinicalTrials.gov	ClinicalTrials.gov [Internet] Bethesda (MD): National Library of Medicine (US) at the National Institutes of Health (NIH); [2002] – [cited 2018 Sep 12]. Available from: https://clinicaltrials.gov/
Clone Select Imager	Molecular Devices, Sunnyvale, CA, USA
Clone Manager Basic 9	Scientific & Educational Software, Denver, USA
Clustal Omega	EMBL-EBI, Hixton, UK (Sievers *et al.*, 2011)
FlowJo v10	Tree Star, Ashland, OR, USA
Geneart™ CRISPR Search and Design Tool	Geneart™ CRISPR Search and Design Tool [Internet] Thermo Fisher Scientific, Waltham, MA, USA; [cited 2018 Sep 12]. Available from: http://www.thermofisher.com/de/de/home/life-science/genome-editing/geneart-crispr/geneart-crispr-search-and-design-tool.html
GraphPad Prism 6	GraphPad Software, La Jolla, CA, USA
Image Lab™ Software	Bio-Rad Laboratories, Munich, Germany
IMGT® (THE INTERNATIONAL IMMUNOGENETICS INFORMATION SYSTEM®)	Laboratoire d'ImmunoGénétique Moléculaire Institut de Génétique Humaine, IGH, UMR9002 CNRS-UM, Montpellier Cedex 5, France http://www.imgt.org/ (Lefranc *et al.*, 2015)
IncuCyte® ZOOM Software 2016B	Essen Bioscience, Ann Arbor, Michigan, USA
Mendeley Reference Manager	Mendeley, London, UK
Microsoft Office 2010/2016	Microsoft Corporation, Redmond, WA, USA
National Center of Biotechnology Information (NCBI) Databases	National Center for Biotechnology Information (NCBI)[Internet]. Bethesda (MD): National Library of Medicine (US), National Center for Biotechnology Information; [1988] – [cited 2018 Apr 12]. Available from: https://www.ncbi.nlm.nih.gov/ (Agarwala *et al.*, 2016)
NEB Tm Calculator	NEB Tm Calculator [Internet] New England Biolabs, Frankfurt, Germany; [cited 2018 Sep 12]. Available from: http://tmcalculator.neb.com/#!/main
NEBcloner®	NEBcloner® [Internet] New England Biolabs, Frankfurt, Germany; [cited 2018 Sep 12]. Available from: https://nebcloner.neb.com/#!/redigest

3   Methods

3.1   Molecular biology methods

3.1.1   Cryopreservation of bacteria

For cryopreservation of bacteria 500 µL of an overnight culture were thoroughly mixed with 500 µL of sterile 99% glycerol. The mixture was immediately frozen and stored at - 80 °C. These glycerol stocks can be used to inoculate a new bacteria culture for plasmid preparations.

3.1.2   Transformation of bacteria

Transformation describes the uptake of exogenous genetic material into bacteria. To enable this uptake, it is required to permeabilize the bacterial cell wall and plasma membrane. One method to achieve this is electroporation. By applying an exogenous electrical field, transient pores are generated in the membrane that allow hydrophilic molecules to enter the bacterial cell (Tieleman, 2004).

To efficiently transform electrocompetent *E. coli* (XL1-Blue) with exogenous plasmid DNA an aliquot of bacteria suspension was first thawed on ice. After addition of 1 - 5 µL of purified ligation (3.1.8) or plasmid DNA, the suspension was transferred into a pre-cooled electroporation cuvette (0.1 cm, Gene Pulser, Bio-Rad). Using the electroporator Gene Pulser Xcell™ (Bio-Rad), an electric pulse of 1.8 kV was applied. For recovery, bacteria were immediately transferred into 1 mL SOC medium (Thermo Fisher Scientific) and incubated under 220 rpm agitation for 45 min at 37 °C. Afterwards, 20 µL - 200 µL of the bacterial suspension were plated onto LB agar plates (Select Agar™, Thermo Fisher Scientific) that contained the appropriate antibiotic for selection and incubated at 37 °C overnight.

3.1.3   Cultivation of bacteria

The transformed bacteria (3.1.2) were cultivated overnight at 37 °C on LB agar plates that contained the appropriate antibiotic for selection. If not used directly for plasmid preparation, bacteria were stored at 4 °C for up to 1 week.

For small-scale plasmid isolation 4 mL LB medium containing the appropriate antibiotic for selection were inoculated with a single bacteria colony from the LB agar plates. The 4-mL-culture was incubated overnight at 37 °C in an orbital shaker (220 rpm). This pre-culture could subsequently be used for the inoculation of a large-scale bacteria culture.

For the isolation of larger amounts of plasmid DNA 400 mL LB medium containing the appropriate antibiotic for selection were inoculated with 1 - 2 mL of the 4-mL-pre-culture or 10 µL of a glycerol stock (3.1.1). The 400-mL-culture was also incubated overnight at 37 °C in an orbital shaker (220 rpm).

3.1.4   Plasmid DNA isolation from bacteria

For small-scale plasmid isolation 4 mL overnight cultures (3.1.3) were centrifuged at 825 x g at 4 °C for 10 min. The plasmid DNA was isolated from the bacteria pellet using the JetStar^{TM} Plasmid Purification Kit (Genomed) according to the manufacturer's instructions. The pelleted plasmid DNA was resuspended in the appropriate amount of ddH$_2$O (typically 60 µL).

For large-scale plasmid isolation 400 mL bacteria cultures (3.1.3) were pelleted at 5000 x g for 15 min at 4 °C. Isolation of the plasmid DNA was performed using the JetStar^{TM} Plasmid Purification Kit (Genomed) according to the manufacturer's instructions. The dried DNA pellet was resuspended in 200 - 800 µL sterile ddH2O.

3.1.5   Agarose gel electrophoresis

Linearized plasmid DNA, ivt-RNA or DNA fragments were separated according to their sizes by agarose gel electrophoresis. To prepare a 1% agarose gel, 1% (w/v) agarose was dissolved in 1 x TEA buffer (Table 2.3) by boiling using a microwave. After letting the solution cool down to approximately 60 °C, it was poured into a gel rack and 0.2 µg/mL ethidium bromide were added. Prior to loading the DNA samples onto the solid 1% gel, they were mixed with DNA Gel Loading Dye 6X (Thermo Fisher Scientific). To determine the respective DNA fragment sizes 8 µL of GeneRuler 1 kb or 100 bp DNA Ladder (Thermo Fisher Scientific) were loaded separately onto the agarose gel. The DNA was separated by electrophoresis at a voltage of 100 - 120 V for 45 - 120 min. Ethidium bromide – intercalated into the DNA – was visualized under UV light using the ChemiDoc™ XRS+ Gel Documentation System (Bio-Rad) or an UV transilluminator (Bachhofer). Documentation and analysis of the agarose gel was performed using the Image Lab^{TM} Software (Bio-Rad).

For the visualization of ivt-RNA, DEPC-treated water was used for the generation of the agarose gel as well as the running buffer. The ivt-RNA samples were denatured by incubation at 70 °C for 10 min in the presence of 2X RNA Gel Loading Dye (Thermo Fisher Scientific). RiboRuler High Range RNA Ladder (Thermo Fisher Scientific) was treated the same way and used for length determination of ivt-RNA.

3.1.6 DNA extraction from agarose gels

DNA fragments that were separated by agarose gel electrophoresis (3.1.5), were purified utilizing the QIAquick Gel Extraction Kit (Qiagen). After visualizing the DNA fragments under UV light, they were cut out of the agarose gel. DNA fragments were then extracted by proceeding according to the manufacturer's instructions. Generally, DNA was eluted from the spin column by adding 25 - 30 μL ddH$_2$O.

3.1.7 Restriction digest of plasmid DNA

Restriction digest of plasmid DNA can either be performed for preparative or analytical purposes. The preparative digest is part of the cloning procedure for a given plasmid in which two DNA molecules are cut with the same combination of restriction enzymes. This allows the ligation (3.1.8) of two chosen DNA fragments to generate a new plasmid.

An analytical restriction digest can be performed to check the quality of newly generated DNA plasmids. The corresponding DNA fragment pattern can be analyzed by agarose gel electrophoresis (3.1.5).

For the restriction digest, 1 - 4 units (U) of restriction enzyme were used according to the manufacturer's instructions. Plasmid DNA or PCR product was incubated for 1 - 2 h with the restriction enzyme at the recommended temperature using appropriate buffer conditions.

Whenever preparative restriction digest was performed, the digest was followed by purification of the extracted DNA fragments as described in 3.1.6. The purification allows the removal of excess nucleotides, proteins or buffer agents that could interfere with downstream applications.

3.1.8 Ligation of DNA fragments

The purpose of a ligation reaction is to generate a new vector plasmid from two DNA fragments that have been digested with the same restriction enzymes (3.1.7). With the help of DNA ligases, the complementary ends of the DNA molecules can be joined to generate a recombinant DNA molecule. For this T4 DNA ligase (NEB) and the appropriate buffer was used according to the manufacturer's instructions. The ligation reaction was performed in a total volume of 20 μl with DNA fragments in a vector to insert ratio of 1:3. After incubation over night at 16 °C, the ligation reaction was directly used for the transformation of bacteria (3.1.2) in order to allow the selection of newly generated plasmids with the correct nucleotide sequence.

3.1.9 Isolation of messenger RNA (mRNA)

In order to determine the coding sequence of a specific gene or to verify its expression, mRNA was isolated from T cell clones using TRI-Reagent® (Sigma-Aldrich). For this, up to 1 x 10^6 cells were resuspended in 200 µL TRI-Reagent® and mRNA was isolated according to the manufacturer's instructions. The mRNA pellet was resuspended in 20 µl nuclease-free H$_2$O and the concentration was determined (3.1.17).

3.1.10 Complementary DNA (cDNA) synthesis

Reverse transcription of 0.5 - 1 µg isolated mRNA (3.1.9) was performed using the First Strand cDNA Synthesis Kit for RT-PCR (Roche Diagnostics) according to the manufacturer's instructions. The generated cDNA was directly used for PCR (3.1.11) without further purification.

3.1.11 Polymerase chain reaction (PCR)

PCR allows the selective amplification of a particular DNA sequence for sequencing (3.1.13) or molecular cloning. Using a heat-stable DNA polymerase, the DNA template is exponentially amplified during thermal cycling. One reaction cycle is characterized by heat-induced de-hybridization of the DNA double strand (melting), annealing of specific primers to single-stranded DNA and DNA synthesis by a DNA Polymerase (Mullis *et al.*, 1986).

For the amplification of a specific DNA sequence the 2X PCR Master Mix (Promega) was used, that includes *Taq* DNA Polymerase, dNTPs, MgCl$_2$ and the appropriate reaction buffer. Depending on the target sequence, specific primers were used (Table 2.8) that show complementarity with the target gene's 3' and 5' end, respectively. Based on the primer composition, a unique melting temperature for each reaction was calculated with the help of the online-tool "NEB Tm Calculator" (Table 2.16). Table 3.1 shows the typical composition of a PCR.

Table 3.1: PCR composition

Components	Concentration
2X PCR Master Mix	50% (v/v) total volume
3' Primer (10 µM)	0.1 – 1 µM
5' Primer (10 µM)	0.1 – 1 µM
DNA template	<250 ng
Nuclease-free H$_2$O	add to total volume

3.1.12   Rapid amplification of cDNA ends (RACE)-PCR

The determination of TCR sequences by classical PCR amplification is impeded by the large number of possible 5' variable TCR α and β variable gene segments, which have to be covered using unique specific primers. RACE-PCR allows the amplification of the full-length sequence of an RNA transcript independent of a known 5' template sequence (Chenchik *et al.*, 1996). For the TCR complex, the known sequence is represented by the constant regions of the TCR α and β chain. Starting from the constant region, every TCR sequence – irrespective of the variable regions – can be amplified using 5' RACE-PCR. For this, the SMARTer® RACE 5'/3' Kit was used according to the manufacturer's instructions. 1 - 10 µg isolated mRNA (3.1.9) was used as a template to generate RACE-ready cDNA. 5' RACE-PCR was subsequently performed utilizing 2.5 - 5 µL RACE-ready cDNA and the gene specific primers for TCR α (TRAC_RACE_PCR) and β (TRBC_RACE_PCR) chain, respectively (see Table 2.8). RACE-PCR reactions were analyzed using agarose gel electrophoresis (3.1.5). After extraction from the agarose gel (3.1.6) the isolated PCR products were sent for DNA sequencing (3.1.13) to allow the determination of the full-length DNA sequence of the respective TCR chains.

3.1.13   DNA sequencing

To verify the correct DNA sequence of isolated plasmid DNA (3.1.4) or PCR products (3.1.11, 3.1.12), DNA samples were sent for sequencing by Eurofins MWG (Ebersberg, Germany) according to the provider's instructions. The sequencing results were reviewed using the software Clone Manager 9 (Scientific & Educational Software), Chromas Lite (Technelysium) and the online tools Clustal Omega (EMBL-EBI) or IMGT® databases (Lefranc *et al.*, 2015).

3.1.14   Molecular cloning of vector constructs

For molecular cloning of CD19-CAR and CD3-Chimera the respective constructs were ordered from GeneArt Gene Synthesis (Thermo Fisher Scientific) in the backbone vector pMA comprising ampicillin resistance (Table 2.7). The vector plasmids were transformed into electrocompetent *E. coli* (XL1-Blue) by utilizing a 1/1000 dilution as described in 3.1.2. Large-scale plasmid DNA was isolated with JetStar™ Plasmid Purification Kit (Genomed) as described in 3.1.4. 20 µg of plasmid was digested with the restriction enzymes NotI-HF and EcoRI-HF (New England Biolabs) (3.1.7). To allow isolation of the desired insert fragment coding for the respective construct, agarose gel electrophoresis was performed with the digested DNA (3.1.5). The insert was excised from the gel and subsequently purified using the QIAquick Gel Extraction Kit (Qiagen) as described in 3.1.6. To allow ligation of the insert with the desired backbone vector, the vectors pGEM_eGFP_A120, pES.12-6-MIT and pMP71-MIT

(Table 2.7) were cut with the same restriction enzymes and processed as described for the CD19-CAR and CD3-Chimera constructs, except for isolation of the backbone fragment instead of the insert. The isolated insert coding for CD19-CAR or CD3-Chimera, respectively, were ligated with the respective backbone vector fragments comprising complementary ends (3.1.8). The ligation reaction was transformed into bacteria (3.1.2) to allow identification of colonies carrying ampicillin resistance. Selected colonies were picked for inoculation of small-scale cultures (3.1.3). After isolation of plasmid DNA (3.1.4), the vectors were sent for sequencing (3.1.13) utilizing the respective primers CD3-CAR_P1_for, CD3-CAR_P2_for, CD3-CAR_P3_for, pGEM_for, pGEM_wm_rev, pES.12-6_for, TCRab_P2A, pMP71_for and pMP71_rev (Table 2.8). Bacteria cultures comprising the plasmid with the correct DNA sequences were used to inoculate large-scale cultures (3.1.3) to allow the isolation of large amounts of plasmid DNA (3.1.4). The correctness of the isolated DNA sequence was again verified by DNA sequencing (3.1.13) with the same primers described above. The generated vectors could now be used for transduction of T cells with the CD19-CAR or CD3-Chimera construct (3.2.9).

Tyrosinase-specific TCRs T58 and D115 in pMP71 backbone vectors were provided by S. Wilde (Wilde *et al.*, 2009). NY-ESO-1-specific TCR in pES-12.6 backbone vector was provided by G. Longinotti (Longinotti, 2018).

The CD3-Chimera construct comprised CD8α leader sequence (NCBI database M12828.1) followed by a CD3δ subunit without the stalk region (NCBI database BC039035.1) and CD3ϵ subunit without the stalk region (NBCI database X03884.1) separated by (Gly$_4$Ser)$_3$ linker. The extracellular domain is coupled to the CD28 transmembrane domain (NCBI database J02988.1) and the intracellular CD3ζ signaling domain (NCBI database J04132.1) via a CD8α hinge region (NCBI database M12828.1). The construct was codon-optimized before synthesis by GeneArt (Thermo Fisher Scientific).

The CD19-CAR construct was designed as described by Hudecek *et al.* (Hudecek *et al.*, 2015).

The CAR constructs CEA-CAR_CD4 (CAR#908) and CEA-CAR_CD8 (CAR#607) were kindly provided by H. Abken (Hombach *et al.*, 2001).

TALEN pairs targeting the TCR α and β chains, respectively, were developed in a previous work (Sailer, 2013). TALEN pairs were designed and generated according to Cermak *et al.* (Cermak *et al.*, 2011) utilizing Golden Gate cloning method. TALEN were designed as pairs to target either the *TRAC* locus (TALEN_TCRα_left, TALEN_TCRα_right) or the *TRBC* locus (TALEN_TCRβ_left, TALEN_TCRβ_right), respectively (Table 3.2).

Table 3.2: TALEN RVD sequences and corresponding target sequences in *TRAC* and *TRBC* loci

TALEN	TALEN RVD sequence and corresponding target sequence (5' → 3')
TALEN_TCRα_left	C C A G A A C C C T G A C C C | | | | | | | | | | | | | | | HD HD NI NN NI NI HD HD HD NG NN NI HD HD HD *
TALEN_TCRα_right	C A C T G G A T T T A G A G T | | | | | | | | | | | | | | | HD NI HD NG NN NN NI NG NG NG NI NN NI NN NG *
TALEN_TCRβ_left	C C C A C C G A G G T C G C | | | | | | | | | | | | | | HD HD HD NI HD HD HD NN NI NN NN NG HD NN HD *
TALEN_TCRβ_right	G G G A G A T C T C T G C T T | | | | | | | | | | | | | | | NN NN NN NI NN NI NG HD NG HD NG NN HD NG NG *

*target DNA sequence indicated by the 4 bases cytosine (C), guanine (G), adenine (A) and thymine (T); corresponding TALEN RVDs indicated by the amino acids asparagine (N), isoleucine (I), glycine (G) histidine (H) and aspartic acid (D).

The Geneart™ CRISPR Search and Design Tool (Thermo Fisher Scientific) was used for design and generation of CRISPR gRNA. CRISPR gRNAs was designed to target either the *TRAC* locus (TRAC_CRISPR) or *TRBC* locus (TRBC_CRISPR), respectively (Table 3.3).

Table 3.3: CRISPR gRNA target sequence in *TRAC* and *TRBC* loci

TALEN	CRISPR gRNA target sequence (5' → 3')
TRAC_CRISPR	TCTCTCAGCTGGTACACGGC
TRBC_CRISPR	TCAAACACAGCGACCTCGGG

3.1.15 Next generation sequencing (NGS)

To determine mutations in the *TRAC* and *TRBC* genes introduced by TALEN-induced double strand breaks, mRNA of selected clones was isolated utilizing the Dynabeads® mRNA DIRECT™ Kit (Thermo Fisher Scientific) according to the manufacturer's instructions. Isolation of mRNA was performed in FrameStar® Break-A-Way PCR Plates (4titude) using the DynaMag 96 Slide Magnet (Life Technologies). Supernatant containing mRNA was transferred to Eppendorf® twin-tec PCR plates 96 (Eppendorf) after incubation at 70°C for 2 min in Thermocycler Nexus (Eppendorf). Reverse transcription was performed using the SMARTScribe™ reverse transcriptase (Clontech) according to the manufacturer's instructions. Specific 3' primers binding either the TCR α or β constant region, respectively, were combined with 5' Switch oligos comprising a unique barcode to synthesize cDNA coding for the respective TCR chains. Subsequent PCR steps utilizing KAPA HiFi Hot Start Ready Mix (KAPA Biosystems), according to the manufacturer's instructions, allowed amplification of the target sequence and addition of specific sequences to the PCR product required for NGS. In PCR I Illumina universal oligos (IUO) was added to the 5' and 3' ends, whereas 2 new primers, PCR1_3pAC_IUP and PCR1_3pBC_IUP, were used to attach IUO to the 3' end of TCR α or

β chain sequences, respectively. PCR products were purified utilizing CleanPCR kit (CleanNA) and used as templates for PCR II that included addition of Nextera oligos to the ends of the PCR product using Nextera® Index Kit v2 (Illumina). The prepared DNA library was concentrated by phenol-chloroform-isoamylalcohol (Roth) extraction and QIAquick spin columns (Qiagen) and subsequently purified using the BluePippin pulsed-field electrophoresis device (sage science) according to the manufacturer's instructions. Purification of the PCR products was verified utilizing High Sensitivity NGS Fragment Analysis Kit (Advanced Analytica) and Fragment Analyzer (Advanced Analytica) according to the manufacturer's instructions. NGS was performed on MiSeq System (Illumina) with MiSeq V3 Kit (Illumina) according to the manufacturer's instructions. Irrelevant DNA Library, PhiX control v3 (Illumina), is mixed with the sample DNA library to enable reliable cluster formation by MiSeq System.

Bioinformatic analysis of NGS data was performed by A. Moesch (Medigene Immunotherapies GmbH). For this, raw FASTQ reads were searched for both flanking TALEN target sites and the target sequence in between was aligned to the wildtype sequence [NCBI Database X02883.1, M12887.1, M14157.1]. Reads containing the same mismatches, deletions, insertions or the wildtype sequences were grouped, and average read quality was calculated. To unambiguously identify whether a T cell clone contained wildtype or mutated sequences, a high number of reads was required comprising an average read quality of at least 30.

3.1.16   Generation of *in vitro* transcribed RNA (ivt-RNA)

For the *in vitro* transcription of plasmid DNA into capped ivt-RNA the mMessage mMachine™ T7 Transcription Kit (Thermo Fisher Scientific) was used according to the manufacturer's instructions. The required plasmid DNA was linearized using the appropriate restriction enzyme (3.1.7) and subsequently purified via precipitation with 0.25 M EDTA, 0.3 M sodium acetate in the presence of 70% ethanol at – 20 °C for 30 min. After centrifugation with 15500 x g at 4 °C for 15 min, the DNA pellet was resuspended in the appropriate amount of ddH$_2$O to a final concentration of 0.5 µg/µL. 2 – 5 µg of the purified, linearized plasmid DNA was used as template for the *in vitro* transcription reaction. The reaction mixture was incubated for 3 h at 37 °C using the Mastercyler® nexus (Eppendorf). After adding 1 µL of TURBO DNase supplied with the kit, the mixture was incubated for another 30 min at 37 °C. For the purification of the generated ivt-RNA the RNeasy Mini Kit (Qiagen) was used according to the manufacturer's instructions. After eluting the RNA in 50 µL nuclease-free H$_2$O, the concentration was determined (3.1.17) and the ivt-RNA was stored at - 20 °C until it was used for electroporation (3.2.8). If the template vector did not contain a poly(A) tail in the sequence, the ivt-RNA was polyadenylated prior to purification. For this the Poly(A) Tailing Kit (Thermo Fisher Scientific) was used according to the manufacturer's instructions. Samples were taken

before and after polyadenylation and loaded onto a denaturing agarose gel (3.1.5) in order to verify a successful addition of a poly(A) tail and to check for the correct length of the generated ivt-RNA. For generation of ivt-RNA for CRISPR/Cas9 approach, TRAC and TRBC string fragments (Table 2.7) were used as templates for *in vitro* transcription utilizing either mMessage mMachin[TM] T7 Transcription Kit as described above or TranscriptAid T7 High Yield Transcription Kit (Thermo Fisher Scientific).

3.1.17 Determination of nucleic acid concentration

The concentration of nucleic acids can be determined using spectrometric quantification by exposing DNA and RNA to UV light of a wavelength of 260 nm. The extinction is measured by a spectrophotometer. This method is based on the Beer-Lambert law, where the amount of light absorbed by the substance relates to the concentration of the absorbing molecule.

The concentration of plasmid DNA and ivt-RNA was determined using the NanoDrop[TM] 2000c spectralphotometer (Thermo Fisher Scientific) according to the manufacturer's instructions.

3.2 Cell biology methods

3.2.1 Culture and passaging of human cells

To avoid contaminations, all cell culture work was performed under sterile conditions with sterile media, solutions and materials. All cells were incubated in Heracell[TM] 150i CO_2 incubators (Heraeus) at 37.5 °C with 6% CO_2 and 95% humidity. If not indicated otherwise, all centrifugations were performed at 350 g for 5 min in Centrifuge 1-16K (Sigma).

3.2.1.1 PBL, PBMC and T cell clones

Isolated PBL or PBMC (Table 2.13) were cultured in T cell medium (Table 2.15) in the presence of 100 U/ml IL-2. Depending on cell density, the cells were either split in the appropriate ratio or half of the culture medium was exchanged with fresh T cell medium every other day. The same culture conditions were used for isolated T cell clones derived from PBL or PBMC. Depending on cell numbers, T cell clones were cultured in 96-well, 48-well, 24-well, or 6-well plates. For cell numbers above 5×10^6, the cells were generally cultured in 25 or 75 cm^2 cell culture flasks. Clone 234 (Table 2.13) was cultured in Clone234 medium (Table 2.15) in the presence of 50 – 100 U/IL-2. Depending on cell expansion rate, the cells were either split in

the appropriate ratio or half of the culture medium was exchanged with fresh Clone234 medium every other day. Clone234 cells were cultured exclusively in 24-well plates.

3.2.1.2 Lymphoblastoid cell lines (LCL)

LCL and mLCL (Table 2.13) were cultured in RPMI_IV medium (Table 2.15) in 75 cm^2 cell culture flasks. Depending on cell density, the cells were split in the appropriate ratio or half of the culture medium was exchanged with fresh RPMI IV medium every 3 – 4 days.

3.2.1.3 Tumor cells

The tumor cell lines Jurkat-76-IVB10, K562, K562_A2, K562_A2_CD86, Mel624.38 and MelA375 (Table 2.13) were cultured in RPMI_IV medium (Table 2.15) in either 75 or 150 cm^2 cell culture flasks depending on cell numbers. HEK293FT cells and LS174T cells (Table 2.13) were cultured in DMEM_IV medium (Table 2.15), while 647-V cells (Table 2.13) were cultured in 647-V medium (Table 2.15) in either 75 or 150 cm^2 cell culture flasks. Suspension cells, like Jurkat-76-IVB10 and the K562 derivatives, were split in the appropriate ratio every 3 – 4 days. Adherent tumor cells, including HEK293FT, LS174T, 647-V, Mel624.38 and MelA375, were grown to 80 – 100% confluence and then passaged as follows. For detachment of adherent cells, the cells were washed with 10 mL PBS and subsequently incubated with 3 – 5 mL Trysin-EDTA (Table 2.14) at 37.5 °C until all cells were released from the flask surface. By adding 7 mL pre-warmed culture medium Trypsin was inactivated. After centrifugation, the cells were resuspended in 30 mL of fresh culture medium and seeded into new cell culture flasks.

3.2.2 Thawing and freezing of human cells

The cryopreserved cells were thawed in a 37 °C water bath until only a small pellet of ice remained in the cryopreservation vial. The cells were immediately transferred into 10 mL of RPMI_IV medium (Table 2.14) to dilute the DMSO that is present in the freezing medium. After the cells were centrifuged at 350 g for 5 min, the supernatant was discarded and the cell pellet was resuspended in 2 – 10 mL of appropriate medium. The cell count was determined using a counting chamber according to Neubauer (3.2.3) and the cells were seeded in the appropriate cell culture flask at the desired cell density.

For cryopreservation the desired number of cells was first pelleted at 350 g for 5 min and then resuspended in 1 mL Freezing medium (Table 2.15) or Ibidi Freezing medium (Table 2.14). The cryopreservation vial was immediately transferred into a Mr. Frosty Freezing Container (Nalgene) and stored at – 80 °C for at least 24 h. The cells were stored afterwards in -150 °C freezers for long-term cryopreservation.

3.2.3 Determination of cell count

For the determination of cell count, a counting chamber according to Neubauer (C-Chip, NanoEnTek) was used. 10 µL sample was taken after the cell suspension had been mixed thoroughly. Depending on cell density, the sample was diluted in an appropriate amount of trypan blue (Table 2.14) to establish a representative and countable cell concentration. The mixture was applied to the edge of the coverslip so that it would be drawn into the void between the two glass surfaces by capillarity. The living cells in the 4 large squares of the counting chamber were counted using a light microscope (Zeiss). The discrimination between live and dead cells was aided by the use of the azo compound that traverses only the porous cell membrane of dead cells and stains them dark blue. From the number of cells counted in the chamber, the number of cells in 1 mL cell suspension can be calculated using the following equation:

$$cell\ concentration\ \left[\frac{cells}{mL}\right] = \frac{number\ of\ cells\ counted}{number\ of\ large\ squares\ counted}\ x\ dulition\ factor\ x\ 10^4$$

3.2.4 Isolation and stimulation of PBMC and PBL

PBMC and PBL were isolated from donor blood by density gradient separation using Biocoll (Biochrom) according to the manufacturer's instructions. To prevent coagulation 100 µL Heparin-Natrium (Braun) was added per 50 mL of donor blood. Donor blood was subsequently diluted with PBS (Biochrom) at a ratio of 1:1 or 1:2, respectively. Approximately 35 mL of diluted blood per 50 mL Falcon tube was carefully layered over 15 mL Biocoll solution and subsequently centrifuged at 840 g for 20 min without brakes. The PBMC layer was carefully removed and transferred to a new 50 mL tube. Up to 3 PBMC layers from different tubes were pooled and PBS was added to a total volume of 50 mL. The PBMC layers were washed by centrifugation at 470 g for 10 min. After pooling the cell pellets of 2 tubes, the cells were washed again with PBS as described above. All cell pellets from one donor were pooled and resuspended in 20 mL PBS and the cell count was determined (3.2.3). After centrifuging the cells at 470 g for 10 min, the PBMC were resuspended in the appropriate amount of T cell medium (Table 2.15) and seeded for activation utilizing Dynabeads® Human T-Activator CD3/CD28 (Thermo Fisher Scientific) according to the manufacturer's instructions. Alternatively, for isolation of PBL from PBMC, plate adherence was used for removal of monocytes from the isolated PBMC. For plate adherence, 75 x 10^6 PBMC were resuspended in 10 mL DC medium and plated in 80 cm^2 Nunclon™ ∆Surface flasks. After incubating the cells for 60 min at 37.5 °C and 6% CO_2 at 95% humidity and occasional tilting, the supernatant containing PBL was collected. Isolated PBL were activated as described for PBMC above.

3.2.5 Stimulation of T cell clones

Isolated T cell clones were activated to induce proliferation using one of the stimulation methods described below.

Stimulation of Clone 234:

Clone 234 was activated by co-culturing 1×10^6 T cells per 24-well with 0.3×10^6 irradiated LCL_BW in the presence of 100 U/mL IL-2 in a total of 2 mL Clone234 medium.

Stimulation of T cell clones with PHA:

For activation utilizing the mitogen PHA, 1×10^6 T cells were co-cultured with 0.1×10^6 irradiated LCL_Pia1 and 1×10^6 feeder cells in 2 mL T cell medium in 24-well plates. Stimulation-mix was completed with 250 ng/mL PHA and 100 U/mL IL-2. For activation of single cell clones in 96-well plates, 30×10^3 irradiated feeder cells and 2×10^3 LCL were used in combination with 250 ng/mL PHA and 100 U/mL IL-2.

Stimulation of T cell clones with OKT-3 antibody:

Isolated T cell clones were stimulated with 32 ng/mL OKT-3 crosslinking antibody and varying amounts of co-stimulatory cells dependent on number of T cells to be activated. Generally, the conditions depicted in Table 3.4 were used, however cell numbers could vary based on experimental layout.

Table 3.4: Conditions for T cell stimulation via OKT-3 antibody.

Components	96-well	24-well	6-well – 25 cm^2 flask
T cells	Up to 0.2×10^6	$0.05 – 0.5 \times 10^6$	$0.05 – 2 \times 10^6$
Feeder cells	Up to 0.2×10^6	2×10^6	$5 – 10 \times 10^6$
LCL	Up to 0.02×10^6	1×10^6	$1 - 2 \times 10^6$
Medium	200 µL	2 mL	6 – 10 mL
IL-2	100 U/mL	100 U/mL	100 U/mL

Co-stimulatory cells were always irradiated using Radiation facility Xstrahl RS225 (Xstrahl limited). LCL were irradiated at 100 Gy, while feeder cells were irradiated at 50 Gy. IL-2 was generally added 5 – 24 hours after co-culturing the cells

CAR-specific stimulation of T cell clones:

T cell clones transduced with CEA-CARs were stimulated utilizing irradiated LS174T cells (250 Gy). Generally, effector to target ratios of 1:4 – 1:6 were used. In 24-well plates $0.5 – 1 \times 10^6$ T cells were activated with CAR target cells in the presence of 100 U/mL IL-2.

T cell clones transduced with CD19-CAR were activated with CD19-positive LCL_Eva1 utilizing the conditions described in Table 3.4 without addition of OKT-3 antibody. CD3-Chimera-transduced T cells were activated utilizing OKT-3 antibody and stimulation mix as described in Table 3.4.

3.2.6   Magnetic cell separation

Magnetic cell separation was used to isolate CD3-negative T cells after introduction of TALEN pairs. For this purpose, Dynabeads® CD3 (Thermo Fisher Scientfic) were used according to the manufacturer's instructions. For the separation of up to 2.5×10^6 cells, 50 – 75 µL beads were washed twice with 1 mL isolation buffer (Table 2.3) and then resuspended in the initial volume in isolation buffer. Following the procedure, bead-captured CD3-positive cells were depleted from the cell suspension. The supernatant that was now enriched with CD3-negative cells was transferred into a new 1.5 mL tube and the procedure was repeated twice. The repeated depletion of the bead-bound CD3-positive cells was critical to obtain a high purity of the CD3-negative cell population. After the cell count was determined (3.2.3), the isolated CD3-negative cells were centrifuged and seeded in 24-well plates in the appropriate culture medium.

3.2.7   Transfection of HEK293FT cells

HEK293FT cells were transfected with plasmids coding for retroviral packaging vectors Gag-Pol and GALV (Table 2.7) and respective CAR or TCR constructs included in retroviral backbone vectors pES-12.6, pMP71 or pBullet (Table 2.7) for generation of viral particles that were used for transduction of T cells. For this, $1.5 – 2 \times 10^6$ HEK293FT cells were seeded per 10 cm petri dish in 10 mL DMEM_IV medium (Table 2.15) on day prior to transfection. Cells that reached a confluency of 50 – 60% after 24 h were transfected utilizing TransIT®-LT1 Transfection Reagent (Mirus Bio) according to the manufacturer's instructions. Per approach, 30 µL TransIT®-LT1 Transfection Reagent was diluted in 470 µL DMEM medium without any supplements. After incubation at room temperature for 5 min, a total of 12.5 µg DNA was added and gently mixed by pipetting. The mixture was incubated for 15 min at room temperature and subsequently added drop-wise to the seeded HEK293FT cells. Transfection-mix contained 3.1 µg GALV plasmid, 4.7 µg Gag-Pol plasmid and 4.7 µg retroviral vector containing the respective construct. HEK293FT cells were cultured for 3 – 4 days at 37 °C with 5% CO_2 and 95% humidity before viral particles were harvested from the cell culture supernatant. Virus-containing supernatant was centrifuged at 300 g for 10 min to remove any

cell debris and either used directly for transduction or stored at -80 °C and thawed when required for transduction.

3.2.8   Transfection of T cells (with TALEN & Cas9/gRNA)

T cells were transfected with ivt-RNA coding for TALENs by electroporation to allow transient expression of the constructs for targeting of the respective TCR chains. For this, TALEN ivt-RNA was generated as described in 3.1.16, which included polyadenylation. Five days prior to electroporation, the cells were activated (3.2.4, 3.2.5) to achieve maximal T cell proliferation. To prepare T cells for the electroporation, they were washed twice with 10 mL serum-free RPMI medium and stored on ice. For one electroporation approach $2.5 - 3 \times 10^6$ cells were resuspended in $200 - 250$ µL RPMI medium and then transferred into a pre-cooled electroporation cuvette (0.4 cm, BioRad). To slow down metabolism and make cells more resistant to overheating, they were incubated on ice for 5 min. TALEN ivt-RNA was thawed on ice and added to the cell suspension in the appropriate amount (Table 3.5). After mixing the solution thoroughly, the cuvette was placed in the Electroporator Gene Pulse Xcell^{TM} (Bio-Rad) and pulsed at 400 V for 5 ms utilizing the time constant protocol. After pulsing, the cells were immediately transferred into 4 mL pre-warmed growth medium in a 6 well culture vessel and incubated at 37.5 °C with 6.5% CO_2 and 95% humidity until further application. For CRISPR/Cas9 approach ivt-RNA coding for CRISPR gRNA was generated from TRAC or TRBC Crispr strings (Table 2.8) as described in 3.1.16. RNA coding for Cas9 protein was purchased from Thermo Fisher Scientific and used together with produced gRNA for CRISPR/Cas9 approach (Table 3.5). Preparation of cells and electroporation was performed as described above.

Table 3.5: Transfection-mix for TALEN or CRISPR/Cas9 approach.

Approach	Target	Ivt-RNA	Amount [µg]
TALEN	TCR α chain	ptruncTAL3_13.3_TCRa_L ptruncTAL3_14.1_TCRa_R	15 µg each
TALEN	TCR β chain	ptruncTAL3_15.2_TCRb_L ptruncTAL3_16.2_TCRb_R	15 µg each
TALEN	TCR α and β chain	ptruncTAL3_13.3_TCRa_L ptruncTAL3_14.1_TCRa_R ptruncTAL3_15.2_TCRb_L ptruncTAL3_16.2_TCRb_R	10 – 15 µg each
CRISPR/Cas9	TCR α chain	CRISPR Cas9 mRNA TRAC String ivt-RNA	7.5 µg 5.0 µg
CRISPR/Cas9	TCR β chain	CRISPR Cas9 mRNA TRBC String ivt-RNA	7.5 µg 5.0 µg

3.2.9   Transduction of T cells and PBL

Transduction of T cells with retroviral vectors results the incorporation of DNA sequences coding for the respective CAR or TCR construct into the host genome and allowed stable

expression. To achieve maximal transduction rates, T cells were activated 4 – 5 days prior to transduction as described in 3.2.4 or 3.2.5. Not-treated 24-well plates (Corning) were coated with 1 mL Retronectin® (Takara Bio) at a concentration of 10 µg/mL and incubated over night at 4 °C. After removal of Retronectin® solution, the plates were blocked with PBS containing 2% bovine serum albumin (BSA) for 30 min at room temperature. 1 – 2 mL supernatant containing viral particles, which was generated as described in 3.2.7, was subsequently added to the blocked 24-well plates. The plates were centrifuged at 1000 g for 1.5 hours at 32 °C to allow binding of viral particles to Retronectin®. After supernatant was removed 0.5 – 1 x 10^6 T cells were added per well in 1 mL appropriate culture medium and incubated at 37.5 °C with 6.5% CO_2 and 95% humidity. If required, the procedure was repeated the following day to increase transduction rates.

3.2.10   Automated workflow platform for T cell clone imaging and picking

After single cell sorting (3.3.3) expanded T cell clones were identified in 96-well plates using the software Clone Select Imager (Molecular Devices) in combination with the automated workflow platform EVO200 (Tecan). Designated T cell clones were then picked using the Hit Selector Software (Tecan) to guide the liquid handling arm LiHa (Tecan), which transferred selected T cell clones into new 96-well plates for further analysis and expansion.

3.3   Flow Cytometry

All flow cytometric analyses were performed using the BD LSRFortessa™ cell analyzer (BD Bioscience), depending on sample count in combination with High Throughput Sampler (HTS, BD Bioscience). Flourescence-activated cell sorting (FACS) was performed utilizing either BD FACSAria™ Fusion (BD Bioscience) or SONY SH800S Cell Sorter (SONY Biotechnolgy) according to the manufacturer's instructions. Acquired flow cytometric data were analyzed with the software FlowJo v10 (Tree Star).

3.3.1   Staining of cell surface markers

For staining of cell surface markers in tubes up to 1 x 10^6 cells were harvested, centrifuged and washed with 500 µL FACS buffer (Table 2.3). The cell pellet was resuspended in 50 µL FACS buffer and the desired antibody conjugated with a fluorescent dye was added. The optimal amount of a specific antibody for the staining was tested in preceding experiments and was in the range of 2 – 6 µL per 50 µL. The cell suspension was mixed thoroughly and incubated at 4 °C for 30 – 45 min in the dark. To remove unbound antibody, the cells were

washed with 500 µL FACS buffer and then fixed in 100 – 150 µL cell fixation solution (Table 2.3) or resuspended in FACS buffer. The fixed cells were stored at 4 °C in the dark until they were analyzed in a flow cytometer. For plate staining and subsequent analysis using HTS, the cells were washed with 200 µL FACS buffer. Staining with F(ab')2 anti-human IgG (α-IgG antibody, Southern Biotech) was always performed prior to staining with other antibodies included in the staining panel to exclude unspecific binding. For this, harvested cells were washed 3-times with PBS before and after incubation at 4 °C for 30 min. Subsequent staining of other cell surface markers was performed as described above. Tetramer staining was performed according to the manufacturer's instructions, which included incubation of washed cells for 20 min at room temperature with 10 µL tetramer per approach before subsequent staining of other surface markers, as described above. When cell samples still containing LCL were analyzed by flow cytometry, FcR Blocking Reagent (Miltenyi Biotec) was used prior to cell staining as recommended by the manufacturer.

3.3.2 Labeling of T cells with dyes

To track cell divisions and therefore proliferation of T cells, the cells were labeled with CellTrace^{TM} Violet Cell Proliferation Kit (Thermo Fisher Scientific) according to the manufacturer's instructions. For cell preparation in 96-well plates, a final concentration of 5 µM CellTrace^{TM} Violet in 100 µL was used for labeling of the cells. The cells were washed twice with 200 µL of appropriate culture medium before adding them to the stimulation-mix to induced proliferation. Alternatively, the cells were labeled 4 days after activation as described above. Subsequent staining of cell surface markers was performed as described in 3.3.1.

3.3.3 Sorting of T cells

For FACS, T cells were stained for cell surface markers as described in 3.3.1. Antibody amount as well as staining and washing volumes were increased proportionally to cell numbers used for staining. After the last washing step, cells were resuspended in 0.5 – 2 mL PBS or FACS buffer and strained using round bottom tubes with cell strainer cap (Corning) to generate a uniform single-cell suspension. Cells were stored at 4 °C until FACS. Bulk sorted cells were collected in 15 mL Falcon® tubes (Corning) and subsequently centrifuged and resuspended in appropriate cell culture medium for further cultivation (3.2.1.1) or activation (3.2.4 ,3.2.5). For single cell cloning, individual T cell clones were sorted into 96-well plates comprising the respective stimulation-mix (3.2.4, 3.2.5). IL-2 and PHA or OKT-3, respectively, were added after FACS to complete the stimulation-mix.

3.4   Immunological methods

3.4.1   ELISA

Enzyme-linked immunosorbent assay (ELISA) was performed using the OptEIA™ Human IFN-γ ELISA Set (BD Bioscience) according to the manufacturer's instructions. Co-culture was set up 16 – 24 h prior to ELISA as descried individually for each experiment. If not indicated otherwise, 5×10^4 T cells were used per 96-well in a total volume of 200 µL appropriate culture medium without addition of IL-2. Target cells were added in the respective effector to target ratios as specified for each approach. For ELISA, 50 µL co-culture supernatant per well was transferred to pre-coated and blocked Nunc-Immuno™ 96 Well Plates (Thermo Fisher Scientific). Coating was performed overnight at 4 °C utilizing 50 µL ELISA Coating Buffer (Table 2.3) and 0.2 µL Capture Antibody. Before and after blocking the plates with 300 µL ELISA Blocking Buffer (Table 2.3) per well for 30 min at room temperature, the plates were washed 3 times with ELISA Washing Buffer (Table 2.3). IFN-γ standard doublets were included to allow calculation of standard curves for each plate. After incubating co-culture supernatants for 1 h at room temperature the plates were washed 4 times before addition of detection-mix, which included 0.25 µL Detection Antibody and Enzyme Reagent in 50 µL ELISA Blocking Buffer per well. Upon incubation for 30 min in the dark, the plates were washed 4 times and 50 µL substrate reagent derived from TMB Substrate Reagent Set (BD Bioscience) was added. After 3 – 5 min 100 µL 1 M H_3PO_4 was added per well to stop the enzymatic reaction. The plates were imaged using Multiskan™ FC Mikrotiterplatten-Photometer (Thermo Fisher Scientific) to detect absorbance at 450 nm and 570 nm to allow wavelength correction.

3.4.2   IncuCyte® Immune Cell Killing Assay

To observe real-time killing mediated by T cells targeting the respective tumor cells the IncuCyte® ZOOM System (Essen Bioscience) was used in combination with IncuCyte® ZOOM Software 2016B (Essen Bioscience) according to the manufacturer's instructions. For this, tumor cells were labeled with IncuCyte® NucLight Red Lentivirus Reagent (Essen Bioscience) according to the manufacturer's instructions to allow cell count based on fluorescence detected in cell nuclei. If not indicated otherwise, 4×10^4 T cells were co-cultured with NucLight Red-labeled tumor cells at described effector to target ratios in 200 µL appropriate culture medium without addition of IL-2. Images of quadruplicates per approach were taken every 2 h and the data were analyzed utilizing masks created to specifically detect the cell count of the respective tumor cell lines.

4 Results

The proposed strategy for the generation of universal recipient T cells comprised the knockout of the endogenous TCR to enable testing of transgenic TCRs in these recipient cells without the risk of TCR mispairing. To generate a stable test system for the characterization of multiple transgenic TCRs, expansion of these universal recipient T cells has to be consequently achieved independent of the endogenous TCR. TCR-independent activation and proliferation of T cells should be mediated through an introduced chimeric antigen receptor (CAR) as soon as the endogenous TCR is absent after the directed knockout. Therefore, first experiments were performed to investigate whether selected CAR constructs can generally support TCR-independent expansion of T cells to an extent comparable to physiological T cell proliferation. Once T cell expansion via CAR engagement could be demonstrated in a selected T cell clone, the endogenous TCR was targeted for knockout using gene editing tools, including transcription activator-like effector nucleases (TALENs). Subsequently, the strategy for generating universal recipient cells was further improved to allow the selection of various T cell clones that show superior proliferative capacity upon CAR engagement. Based on poor survival of the generated TCR-negative T cells, new chimeric constructs were generated that should improve TCR-independent proliferation of universal recipient cells. Using these chimeric constructs, a new high-throughput strategy for the generation of universal recipient cells could be developed that enabled the isolation of several promising candidate T cell clones, which exhibited high proliferative capacity in the absence of the endogenous TCR via engagement of the introduced chimeric construct. The generated universal recipient cells were subsequently characterized for suitability as a reproducible test system for transgenic TCRs.

4.1 T cell stimulation via chimeric antigen receptors (CARs)

To investigate whether CARs can support TCR-independent expansion of T cells in a manner comparable to physiological T cell activation via the TCR, an established and well-characterized CD4+ T cell clone, termed Clone 234 (HLA-A*24:01-restricted), was used as a first test system. Clone 234 recognizes antigen presented by the HLA-A*24:01-positive lymphoblastiod cell line BW (LCL_BW). Co-culture of Clone 234 with LCL_BW results in high expansion of the T cells accompanied by specific IFN-γ release. It has been shown previously that bulk populations of primary human T cells can be expanded *in vitro* through CAR engagement, yielding cell numbers comparable to physiological TCR stimulation (Maher *et al.*, 2002; Finney, Akbar and Alastair, 2004). However, this has never been investigated for isolated T cell clones that show a lower proliferative capacity compared to mixed lymphocyte populations. Even though these populations expand more rapidly, they consist of different T

cell subsets comprising various effector functions and unknown TCR specificities. In contrast, the use of a defined T cell clone, like Clone 234, of known target specificity and proliferative capacity allows a direct comparison of the effects of TCR and CAR engagement on T cell expansion.

To enable monitoring of proliferation induced by CAR engagement, it was important to use CAR constructs that have been shown to promote expansion of T cells. For this reason, two well validated CAR constructs, CEA-CAR_CD8 and CEA-CAR_CD4, that both recognize the human carcinoembryonic antigen (CEA), were used for these experiments (Hombach *et al.*, 2001; courtesy Hinrich Abken). While the CEA-CAR_CD8 comprises a CD28 transmembrane and a co-stimulatory signaling domain, the CEA-CAR_CD4 contains a CD4 transmembrane domain followed by a 4-1BB (CD137) signaling domain (Figure 4.1). Due to the respective arrangements of signaling domains, CEA-CAR_CD8 is predicted to induce proliferation preferably in CD8$^+$ T cells, while CEA-CAR_CD4 should be favorable when introduced into CD4$^+$ T cells.
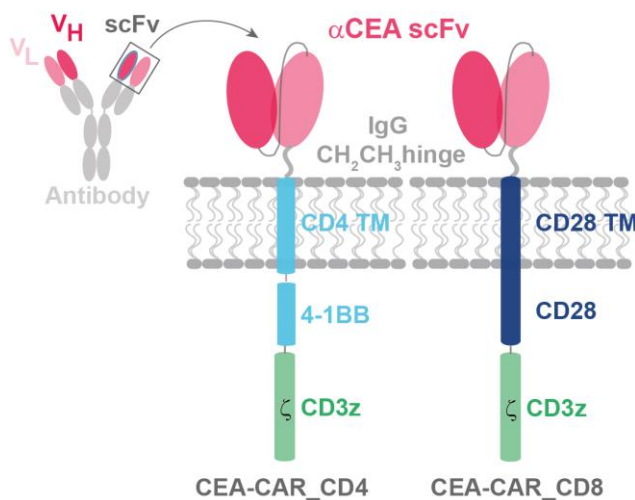
Figure 4.1: Schematic representation of CEA-CAR constructs provided by Hinrich Abken. The single chain variable fragment (scFv) is derived from the variable light and heavy chains (V$_L$, V$_H$) of a monoclonal antibody recognizing CEA protein. Specificity of this antibody is conferred to T cells via the expression of the CAR on the cell surface. CEA-CAR_CD8 comprises the CD28 transmembrane and intracellular signaling domains, while CEA-CAR_CD4 contains a CD4-derived transmembrane domain followed by a 4-1BB (CD137) signaling domain. Both constructs carry the same α-CEA scFv coupled to the respective transmembrane domains via an IgG CH$_2$CH$_3$ hinge domain as well as a terminal CD3ζ signaling domain. For transduction of T cells both constructs are embedded in the retroviral backbone vector pBullet.

4.1.1 Enrichment and expansion of CAR-expressing T cells

To enable the comparison between TCR- and CAR-specific activation of T cells, the two CEA-CAR constructs (CEA-CAR_CD8; CEA-CAR_CD4) were transduced into the defined CD4$^+$ T cell clone, Clone 234. On day 10 post transduction, the T cells were stained for CAR expression using a F(ab')$_2$ goat anti-human IgG antibody (α-IgG antibody) directed against the CH$_2$CH$_3$ hinge domain of the CARs and sorted by FACS. Cell preparations with initial transduction rates of 12.7% and 22% for CEA-CAR_CD8 and CEA-CAR_CD4, respectively, could be enriched to nearly 100% purity (Figure 4.2a).
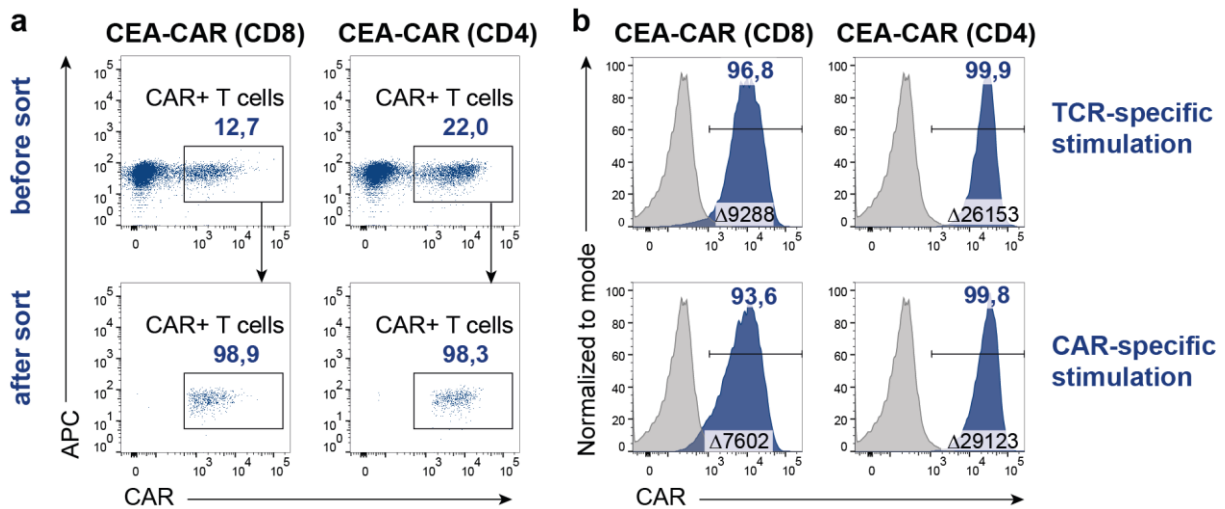
Figure 4.2: Flow cytometric analysis and sorting of CAR-transduced Clone 234. a) FACS of Clone 234 transduced with the CAR constructs CEA-CAR_CD8 and CEA-CAR_CD4. FACS staining was performed 10 days after transduction using an α-IgG antibody. Untransduced cells of Clone 234 were used as negative control. **b)** Representative flow cytometric analysis of CAR expression in enriched CEA-CAR_CD8 and CEA-CAR_CD4-positive cells 12 days after TCR- or CAR-specific stimulation. For activation, 1×10^6 CAR-positive cells were stimulated with 0.3×10^6 irradiated TCR (LCL_BW) or CAR (LS174T) target cells. Enriched (blue) and untransduced control cells (gray) were stained with α-IgG antibody and analyzed by flow cytometry. Median fluorescence intensity (FI) values of enriched and untransduced cells were used for calculation of Δmedian FI for each approach to demonstrate CAR expression levels.

To exclude an influence of antigen-specific activation on CAR expression levels in transgenic T cells, CAR-enriched cells were activated either by TCR- or CAR-specific stimulation and analyzed for CAR expression after the expansion period. For this, CEA-CAR_CD8- and CEA-CAR_CD4-positive cells were activated utilizing irradiated target cells that express the respective TCR or CAR target molecule (TCR: LCL_BW, HLA-A24*01-positive; CAR: LS174T, CEA-positive). Twelve days after activation, the expanded cells were analyzed for CAR expression in comparison with untransduced cells (Figure 4.2b). More than 93% CAR-positive cells could be detected for all approaches indicating that CAR expression was stable for both CAR constructs independent of TCR or CAR engagement. Distinct populations, reflected by large Δmedian FI values between CAR-transduced and untransduced control cells, suggested no downregulation of CAR expression. CEA-CAR_CD4 showed 2-fold higher Δmedian FI values compared to CEA-CAR_CD8, which indicated a higher surface expression of CEA-CAR_CD4 in the CD4+ T cell clone. This stable CAR surface expression was observed over more than 42 days, while CAR-transduced T cells were repeatedly activated every 14 days via CAR or TCR engagement, respectively. Even though CAR expression was comparable, independent of TCR- or CAR-specific activation, proliferation rates of cells stimulated via CAR engagement were diminished three-fold or more compared to cells activated via the TCR (Figure 4.3). Untransduced Clone 234 was stimulated via the TCR in presence of LCL_BW target cell line and used as a control to monitor the proliferation rate. These untransduced control cells did not expand when co-cultured with CAR target cells (data not shown). The low expansion rate of cells stimulated via CAR engagement indicated that optimization of the

activation conditions was required in order to achieve expansion comparable to physiological TCR-specific stimulation. It is important to note that CAR-transduced cells stimulated via the endogenous TCR seemed to proliferate even better than untransduced control cells.
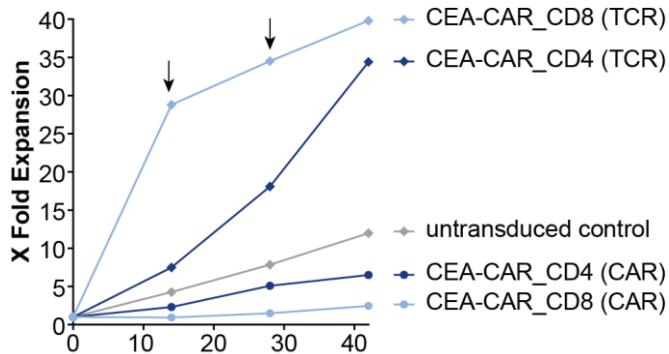
Figure 4.3: Fold expansion of CAR-transduced T cells over 42 days. *In vitro* expansion of 1 x 10^6 CAR-transduced T cells either via CAR or TCR engagement, respectively. 1x 10^3 irradiated LS174T cells (CAR) or LCL_BW (TCR) were used for CAR- or TCR-specific activation, respectively. Black arrows indicate timepoints of re-stimulation. Untransduced Clone 234 was stimulated via TCR by addition of their natural target cells (LCL_BW). Total number of cells was determined after each 14-day expansion period.

4.1.2   Proliferation of CAR-transduced Clone 234

Low expansion rates of T cells activated via CAR rather than the endogenous TCR demonstrated differences in activation thresholds when identical conditions were used for stimulation. The differential activation of the cells might be attributed to differences in antigen recognition mediated through the respective receptors and subsequent signal transduction. While the TCR recognizes its target antigen in the context of MHC molecules, CARs interact with their target antigen directly via the antibody-derived scFv domain. Even though the mechanism by which binding of the scFv to cognate antigen propagates signals across the plasma membrane through this artificially assembled receptor is still poorly understood, T cell activation can be influenced by various factors, including CAR affinity, antigen density and CAR surface expression (Turatti *et al.*, 2007). Therefore, enhancing antigen density by increasing the number of CAR target cells was used as a first attempt to positively influence T cell activation and proliferation mediated by CAR engagement.

To evaluate the effect on proliferative capacity when the amount of antigen was increased, enriched CAR-transduced Clone 234 was co-cultured with graded numbers of irradiated CEA-expressing target cells (Figure 4.4). Activation status of the cells was determined after 24 hours by IFN-γ ELISA (Figure 4.4a). The impact of increased antigen availability on proliferation of the cells was evaluated by CellTrace staining four days after initial co-culture and subsequent flow cytometric analysis on day seven (Figure 4.4b). To ensure exclusive evaluation of proliferation of CAR-positive effector cells, the cell preparations were additionally stained with α-CD3 and α-IgG antibody prior to flow cytometric analysis. While the same co-culture was used for both experiments, IL-2 was added to support T cell survival only after analysis of the co-culture supernatant in ELISA. As controls, untransduced Clone 234, which only express the

endogenous TCR, as well as irrelevant LCL target cells, that express neither the TCR nor the CAR antigen, were used.
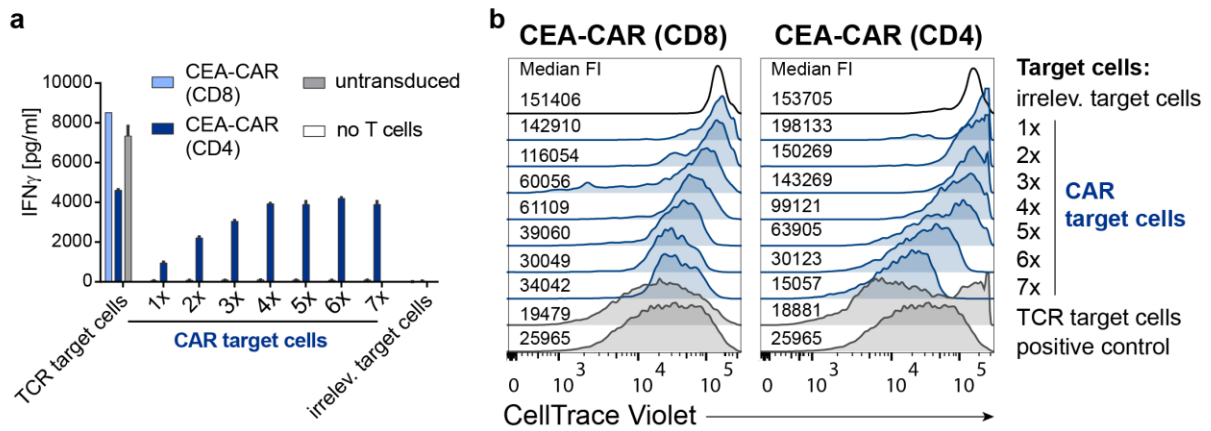
Figure 4.4: Target cell titration for CAR-transduced Clone 234. a) IFN-γ release of CAR-transduced T cells with increasing amounts of target cells. IFN-γ ELISA 24 h after co-culture of 2.5 x 10^4 CAR-positive effector cells with irradiated target cells at a ratio of 1:1. Increasing numbers of CAR target cells (LS174T) are indicated as 2x – 7x. TCR target cells (LCL_BW) were used as positive control for TCR activation and irrelevant target cells (mLCL_ME) as negative control for both TCR and CAR engagement. **b**) Proliferation of CAR-transduced T cells with increasing numbers of target cells. Expansion of CAR-transduced Clone 234 was assessed by CellTrace staining 4 days after co-culture and subsequent flow cytometric analysis 7 days after activation. Cells were additionally stained with α-CD3 and α-IgG antibody to enable the selection of CAR-transduced T cells for analysis. Decreasing median FI of CellTrace Violet indicates higher numbers of cell divisions and therefore proliferation. Positive control represented by untransduced Clone 234 activated with TCR target cells.

TCR-specific activation of CAR-expressing T cells utilizing TCR target cells served as a positive control for maximal T cell activation, as determined by IFN-γ release and proliferative capacity. CEA-CAR-transduced Clone 234 and untransduced Clone 234 released comparable amounts of IFN-γ when incubated with TCR target cells, even though IFN-γ release of CEA-CAR_CD4-transduced cells was slightly lower (Figure 4.4a). Co-culture with the same amount of CAR target cells led to an at least four-fold lower IFN-γ release for CEA-CAR_CD4-transduced cells compared to TCR target cells. Increasing the number of CEA-expressing target cells led to proportionally increased IFN-γ release. Beyond the effector to target (E:T) ratio of 1:4, the quantity of IFN-γ was comparable to maximal activation via the TCR and did not increase further when more CEA target cells were present. This showed that for maximal activation of T cells via CEA-CAR constructs four-fold as much antigen was required compared to physiological activation via the TCR. Untransduced control cells did not release IFN-γ when incubated with CAR target cells, which indicated that activation of CEA-CAR_CD4-transduced cells in the presence of CEA antigen was triggered following specific antigen recognition mediated through the expressed CAR. This was further supported by the fact that CEA-CAR_CD4-transduced cells did not release IFN-γ when co-cultured with CEA-negative irrelevant target cells. For CEA-CAR_CD8-transduced cells, IFN-γ levels did not exceed background-levels when co-cultured with CEA target cells, indicating that activation via the

CEA-CAR_CD8 construct could not induce IFN-γ release in CD4$^+$ T cells. However, when the same cells were analyzed for proliferation after co-culture with increasing amounts of CEA target cells, a decrease in median CellTrace Violet FI could be observed, which indicated multiple cycles of cell division (Figure 4.4b). Hence, even though CEA-CAR_CD8 engagement did not result in IFN-γ release, antigen recognition mediated by the CAR was able to induce proliferation of the T cells. A median CellTrace Violet FI of nearly 30 000 was detected when E:T ratios were higher than 1:5, compared to more than 150 000 when T cells were incubated with irrelevant target cells that did not induce proliferation. As also indicated by IFN-γ release, activation of the CEA-CAR-transduced cells via TCR engagement resulted in even higher proliferation rates reflected by median FI values of nearly 19 000. For CEA-CAR_CD4-transduced cells, expansion increased gradually with increasing numbers of CAR target cells, which reflected the observed increase in IFN-γ secretion. The high median FI values for E:T ratios of 1:1 to 1:3, that exceeded the median FI value of the negative control, hindered a quantitative interpretation of the results. In summary, these experiments showed that increasing the numbers of CAR target cells improves CAR-induced proliferation of T cells. At E:T ratios of 1:5, proliferation rates could be induced that were comparable to physiological activation via the endogenous TCR. Based on these results, E:T ratios of 1:5 or higher were used for CAR-specific activation of T cells in subsequent experiments.

4.2 Knockout of the endogenous TCR in CAR-transduced T cells

Increasing the number of CAR target cells in co-culture with CAR-transduced T cells resulted in comparable proliferation rates for CAR- or TCR-specific activation, respectively. Since sufficient numbers of T cells could be expanded via CAR engagement, the next step for generating a universal recipient cell comprised the knockout of the endogenous TCR in these T cells. For the directed knockout of the human TCR in CAR-expressing T cells, TALENs as well as CRISPR gRNAs were designed to target the TCR α (*TRA*) and TCR β (*TRB*) locus, respectively.

4.2.1 TALEN and CRISPR/Cas9 design

TALENs as well as the CRISPR/Cas9 system have proven effective for the knockout of the human TCR α and β chains in primary human T cells (Osborn *et al.*, 2016; Knipping *et al.*, 2017). However, whether these gene editing tools could be also utilized for targeted TCR knockout in isolated T cell clones exhibiting lower proliferation rates compared to bulk T cell populations, has not been investigated yet. To evaluate the knockout of the human TCR in T

cell clones, TALEN pairs and CRISPR/Cas9 guide RNAs were designed to target the human TCR α and β chains, respectively (Figure 4.5). In order to allow the knockout of any TCR, independent of antigen specificity, the gene segments coding for the constant regions of the respective TCR chains (*TRAC* and *TRBC*) were chosen as target sites. Since the human TCR β chain can comprise either constant region 1 or 2, a homologous region that is present in both *TRBC* gene segments, *TRBC1 and TRBC2,* was chosen to allow targeting of both variants. To knockout the TCR α and β chains, sequences in exon 1 of both the *TRAC* and *TRBC2* gene (homologous to *TRBC1*) segments were selected as target sites, since gene disruption early in the coding region would most likely result in a non-functional protein.
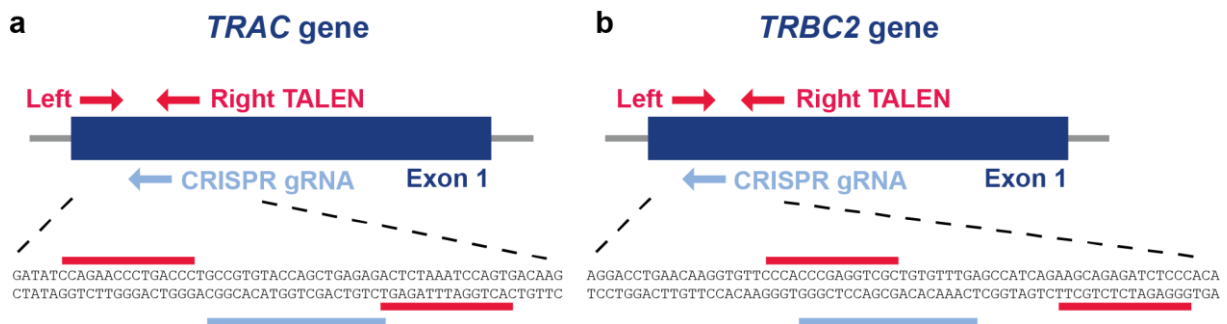
Figure 4.5: Target sites for TCR knockout. TALEN pair (red) and CRISPR gRNA (light blue) recognition sites overlap within exon 1 of *TRAC* or *TRBC2* gene (dark blue), respectively. Black lower-case letters represent DNA sequences of the TALEN target sites. **a)** TALEN and CRISPR gRNA binding sites in *TRAC* gene to target the TCR α constant region. **b)** TALEN and CRISPR gRNA binding sites in the *TRBC2* gene to knockout the TCR β chain.

TALENs were designed and generated in a previous work (Sailer, 2013) according to Cermak *et al.* utilizing the Golden Gate cloning method (Cermak *et al.*, 2011). The assembled TALEN constructs encoded in ptruncTAL3 vectors (Table 2.7) were transcribed to ivt-RNA before transfection into T cell clones. CRISPR gRNAs were designed using the Geneart™ CRISPR Search and Design Tool (Thermo Fisher Scientific) and ordered as GeneArt Strings DNA fragments from Thermo Fisher Scientific (Table 2.7). DNA fragments encoding for CRISPR gRNA were *in vitro* transcribed and transfected into T cells together with mRNA coding for the Cas9 protein (Thermo Fisher Scientific).

4.2.2   Knockout of the human TCR using TALEN and CRISPR/Cas9

Before performing the TCR knockout in CAR-transduced T cells, the TALEN and CRISPR/Cas9 approach was evaluated for efficiency in untransduced Clone 234. Ivt-RNA coding for the designed TALEN pairs as well as CRISPR gRNA in combination with mRNA coding for Cas9 were introduced into T cells using electroporation. The resulting knockout efficiency was evaluated 7 days after transfection by flow cytometric analysis (Figure 4.6a). All components of the TCR complex, comprising the TCR α and β chains as well as the CD3 complex, are required for correct assembly in the ER and cell surface expression (Davis and

Bjorkman, 1988; Exley, Terhorst and Wileman, 1991). Therefore, the successful knockout of the TCR by targeting either one of the TCR chains could be monitored by the downregulation of CD3 expression on the cell surface. Additionally, using CD3 as a marker allowed a fast and simple isolation of TCR knockout cells from a mixed population by using magnetic beads coated with α-CD3 antibody (Sailer, 2013). Utilizing α-CD3-coated magnetic beads, CD3-positive T cells that do not comprise a TCR knockout are retained in the magnet, while CD3-negative T cells containing the desired TCR knockout can be collected from the supernatant medium, a process termed negative isolation.

Targeting the TCR α or β chain using the generated TALEN pairs resulted in a knockout efficiency of up to 20% in Clone 234, as indicated by the presence of a CD3-negative cell population (Figure 4.6a). In contrast, knockout of both TCR chains utilizing the CRISPR/Cas9 system was not successful, since no CD3-negative cell population could be detected. Based on these results, the TALEN technology was used for all further knockout experiments.
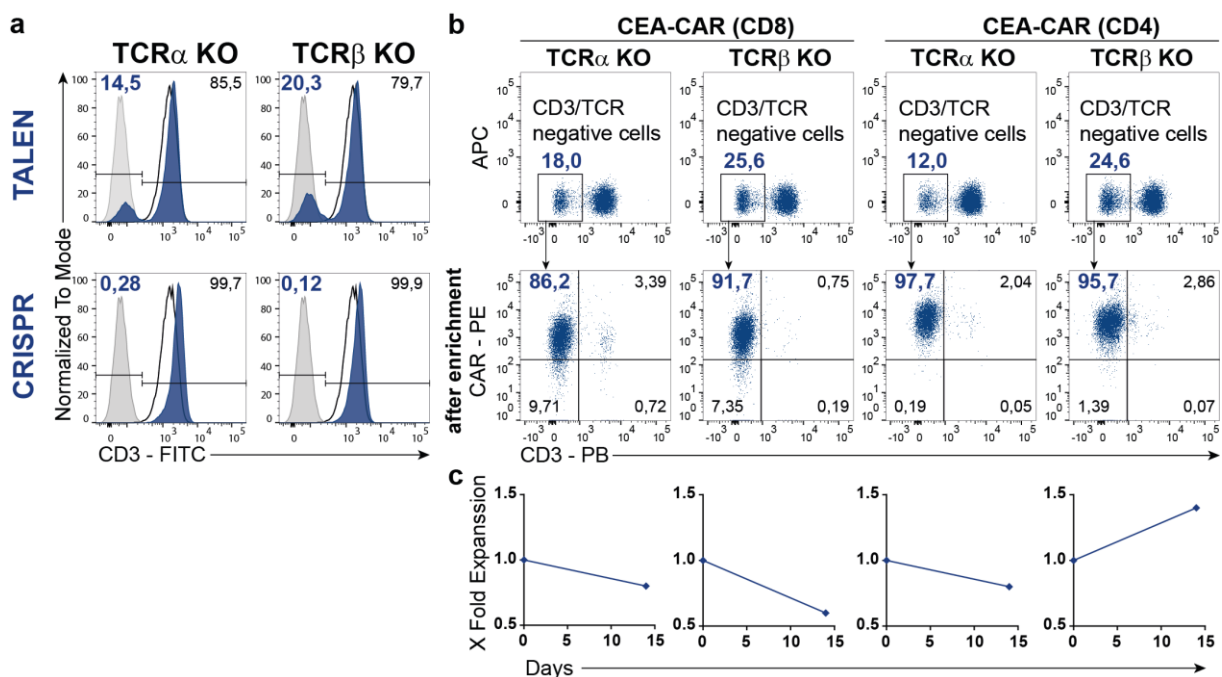
Figure 4.6: Knockout of the human TCR in Clone 234 and CAR-transduced cells. a) Flow cytometric analysis using α-CD3 antibody for detection of successful TCR knockout 7 days after transfection of Clone 234 (blue) with ivt-RNA coding for TALEN pairs (TALEN) or CRISPR gRNA and Cas9 mRNA (CRISPR). TCR α and β chains were targeted separately. Unstained cells served as negative control (gray) and untransfected Clone 234 as positive control (black). **b)** Flow cytometric analysis of CEA-CAR_CD4- and CEA-CAR_CD8-transduced Clone 234 7 days after TALEN transfection. For detection of TCR α or β chain knockout, the cells were stained with α-CD3 antibody. After enrichment of CD3-negative cells using α-CD3-coated magnetic beads, separation efficiency was determined by antibody staining with α-CD3 and α-IgG antibody. Untransfected cells served as control (not shown) **c)** Fold expansion of isolated CD3-negative populations of CEA-CAR_CD4- and CEA-CAR_CD8-transduced cells after activation via CAR. 1 x 10^6 TCR knockout cells were incubated with irradiated CAR target cells (LS174T) at a ratio of 1:6 in the presence of IL-2 for 14 days. Cell count was determined after expansion period at day 14.

Clone 234 transduced with CEA-CAR_CD4 or CEA-CAR_CD8 could be expanded solely via CAR engagement reaching a proliferation rate comparable to physiological activation. To perform the knockout of the endogenous TCR in these CAR-transduced cells, CEA-CAR_CD4- and CEA-CAR_CD8-expressing Clone234 cells were transfected with TALEN pairs targeting either the TCR α or β chain, respectively. Knockout efficiency was determined by staining with α-CD3 antibody 3 days after introduction of the TALENs (Figure 4.6b). In both CEA-CAR_CD8- and CEA-CAR_CD4-transduced cells, the knockout of the TCR α or β chain could be achieved in up to 25% of the cells. The knockout efficiency of the TCR α chain was slightly lower, reflected by only 12 – 18% CD3-negative cells. However, for all approaches CD3-negative cells could be successfully enriched by negative isolation utilizing magnetic beads coated with α-CD3 antibody 4 days after TALEN electroporation (Figure 4.6b). To evaluate the efficiency of the enrichment, the isolated cells were stained with α-CD3 and α-IgG antibody, which allowed the simultaneous verification of CAR expression in TCR- and CD3-negative cells. Flow cytometric analysis revealed a successful enrichment of CD3-negative cells with almost all TCR knockout cells expressing the transgenic CAR construct (Figure 4.6b). As observed before, CEA-CAR_CD8 expression levels were lower compared to CEA-CAR_CD4, which explained the slightly lower percentage of CD3-negative and CAR-positive cells in CEA-CAR_CD8-transduced cells compared to CEA-CAR_CD4-expressing Clone 234 (CEA-CAR_CD8: 86.2% and 91.7%; CEA-CAR_CD4: 97.7% and 95.7%). However, the negative isolation strategy enabled the enrichment of TCR knockout cells to a purity of up to 97% with only negligible numbers of CD3-positive cells still present in the cell preparation.

Two days after enrichment, CAR-expressing TCR-negative cells were stimulated for expansion via CAR by incubation with CAR target cells at a ratio of 1:6. However, proliferation of the TCR knockout cells via CAR engagement was not observed (Figure 4.6c). Fourteen days after stimulation the cell numbers declined for 3 of the 4 approaches, indicating that the culture conditions could not promote survival of the cells. For CEA-CAR_CD4-transduced cells comprising TCR β chain knockout, the cell numbers increased slightly, but the proliferation rate was not comparable to previous activation of CAR-transduced Clone 234 via CAR engagement.

4.3 Improved strategy for selection of CAR⁺ T cell clones

To exclude the possibility that failed cell expansion via CAR in TCR knockout cells was an isolated effect based on the nature and proliferative capacity of the selected CD4⁺ T cell clone (Clone 234), the procedure was modified to allow the evaluation of various T cell clones (Figure 4.7). For this, instead of transducing a single isolated T cell clone, a mixture of different T cell

clones with individual characteristics and proliferative capacities present in bulk PBL were transduced with the two CAR constructs introduced earlier. The CAR-expressing PBL were subsequently single cell cloned to enable the identification of T cell clones that show superior proliferation upon CAR engagement while retaining their physiological functionality. Once suitable candidates were identified the knockout of the TCR was performed using TALENs as described for Clone 234 above. The generated universal recipient cells should then be expanded via CAR engagement enabling the production of sufficient cell numbers for extensive evaluation of transgenic TCRs.
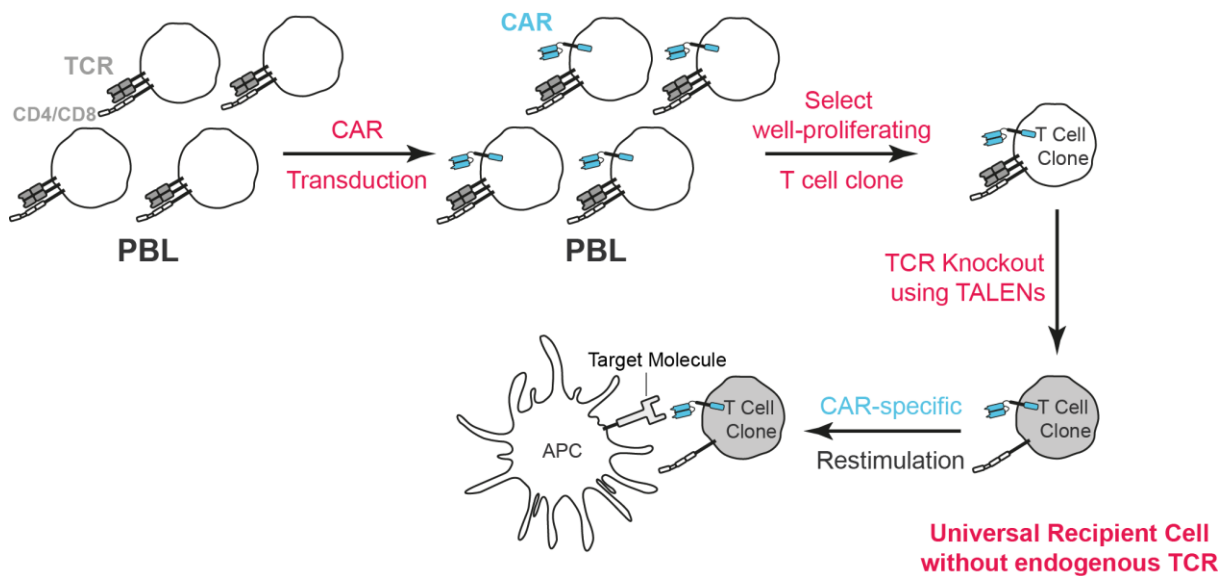
Figure 4.7: Improved strategy for identification of CAR-positive T cell clones suitable for generating universal recipient cells. PBL isolated from healthy donors were transduced with CAR constructs. Single cell clones were generated from CAR-expressing T cells. After identification of suitable candidates exhibiting superior proliferative capacity upon CAR engagement while retaining functionality, the endogenous TCR was knocked out utilizing the TALEN technology. The generated TCR-negative universal recipient cells could then be expanded via CAR engagement.

4.3.1 CAR transduction and expression

For the generation of various T cell clones that express the desired CAR construct, PBL comprising T cell clones of different origin were transduced with either CEA-CAR_CD8 or CAE-CAR_CD4, respectively. Following transduction, CD4$^+$ or CD8$^+$ single cell clones were generated from CEA-CAR-positive T cells using FACS (Figure 4.8).
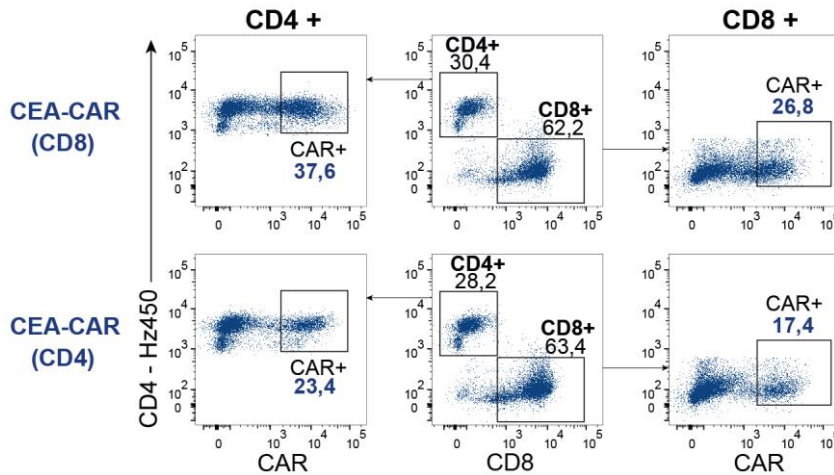
Figure 4.8: Single cell sorting of CAR-transduced PBL by FACS. Prior to FACS CAR-transduced PBL were stained with α-CD4, α-CD8 and α-IgG antibodies. Untransduced PBL were used as negative control and to set the electronic sorting gates. CAR-expressing CD4⁺ or CD8⁺ T cells, were single-cell-sorted into 96-well plates and subsequently activated utilizing irradiated feeder cells and LCL in combination with PHA and IL-2.

The ratio of CD8⁺ to CD4⁺ T cells in PBL used for transduction of the CAR constructs was nearly 2:1 (Figure 4.8). Both cell populations were further screened for expression of CEA-CAR_CD8 or CEA-CAR_CD4, respectively. CEA-CAR_CD8 transduction rate was slightly higher than for the CEA-CAR_CD4 construct in both CD4⁺ and CD8⁺ T cells. Even though CD4⁺ T cells represented the smaller fraction in PBL, the percentage of CAR-expressing cells was higher than for CD8⁺ T cells transduced with the same construct (CEA-CAR_CD8: 37.6% CD4⁺, 26.8% CD8⁺; CEA-CAR_CD4: 23.4% CD4⁺, 17.4% CD8⁺). Independent of transduction rate, sufficient numbers of CAR-expressing single cell clones could be generated from all approaches.

4.3.2 Selection of well-proliferating CAR⁺ T cell clones

Using the improved strategy for the generation of multiple CAR-expressing T cell clones, various CD4⁺ and CD8⁺ T cell clones could be isolated. To evaluate the suitability of the generated single cell clones as universal recipient cells that are able to proliferate independent of the endogenous TCR, they first had to be characterized for proliferative capacity upon CAR engagement. For this, 178 selected T cell clones were expanded from 96-well plates by repeated stimulation using phytohaemagglutinin (PHA) every two weeks for a period of 41 days. While this expansion period allowed the accumulation of sufficient cell numbers for further evaluation of the selected T cell clones, it also enabled a pre-selection of clones that showed superior proliferative capacity. In a first experiment following the expansion period, 40 well-expanding T cell clones were analyzed regarding CAR expression and functionality after the expansion period (Figure 4.9). This early evaluation of CAR reactivity allowed further discrimination of suitable T cell clones that expressed the respective CAR construct and showed the desired reactivity pattern, which included no recognition of CEA-negative cells.

CAR-specific activation of selected T cell clones was evaluated by specific IFN-γ release upon co-culture with irradiated target cells, either positive or negative for the CEA antigen.
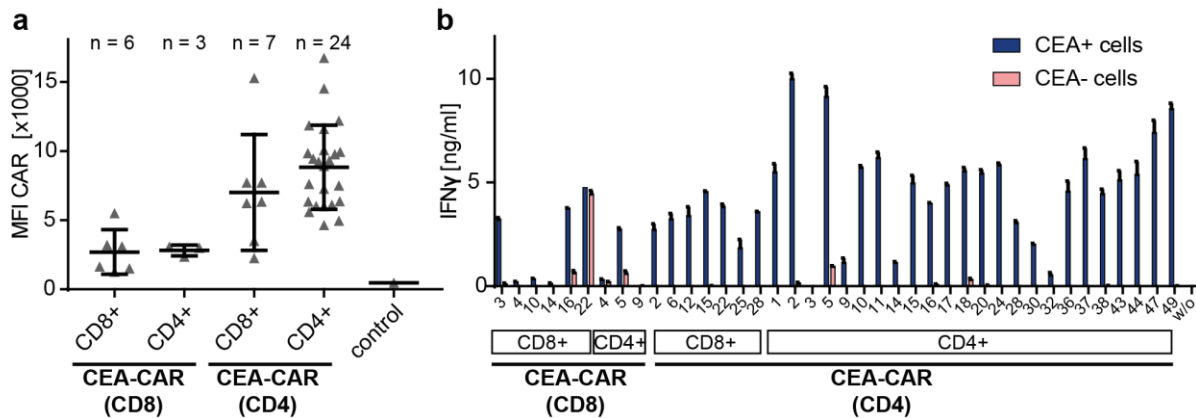
Figure 4.9: Evaluation of CAR expression and functionality of selected single cell clones. a) CAR (CEA-CAR_CD8, CEA-CAR_CD4) expression of 40 individual CD4$^+$ or CD8$^+$ T cell clones analyzed by α-IgG antibody staining and subsequent flow cytometric analysis. Level of CAR expression is shown as median FI (MFI). Untransduced T cell clones served as negative control. **b)** CAR functionality determined by IFN-γ ELISA 20 h after co-culturing selected T cell clones with irradiated target cells either positive (blue) or negative (pink) for the CEA antigen. LS174T served as CEA$^+$ target cells and Jurkat-76 as CEA- target cells. 2 x 10^5 target cells were seeded per well and 50 μL of the respective T cell culture was added.

As observed before, expression levels of CEA-CAR_CD8 were lower compared to CEA-CAR_CD4 reflected by the detected median FI (MFI) values for α-IgG antibody bound to CAR-transduced single cell clones (Figure 4.9a). This was true for CD4$^+$ as well as CD8$^+$ T cell clones, demonstrating that CAR expression was not dependent on either co-receptor. However, MFI values of all 40 selected clones exceeded those of the negative control represented by untransduced T cell clones, showing that all clones expressed the transduced CAR construct. The qualitative assessment of CAR reactivity by ELISA showed that almost all T cell clones were able to produce IFN-γ when exposed to CEA antigen, while no or only little IFN-γ was released in the absence of antigen (Figure 4.9b). The CEA-CAR_CD8-expressing T cell clones 22 (CD8$^+$) and 4 (CD4$^+$) exhibited undesired reactivity in the absence of CEA antigen and were therefore not used in further experiments. As already reflected by the number of T cell clones isolated from each approach, CEA-CAR_CD4-expressing T cells seemed to expand better upon stimulation with PHA than cells transduced with CEA-CAR_CD8. However, whether these T cell clones would be able to proliferate upon CAR engagement independent of the endogenous TCR, had to be determined in subsequent experiments.

To evaluate the proliferative capacity of selected T cell clones following stimulation via CAR engagement, the CAR-expressing T cell clones were exposed to CAR target cells (LS174T). To be able to quantify the observed expansion rates upon CAR stimulation, the same T cell clones were simultaneously activated by addition of phytohaemagglutinin (PHA) mimicking the engagement of the TCR. PHA is a plant-derived lectin that serves as a mitogen to trigger T cell division by binding carbohydrates on cell surface receptors, including the TCR, resulting

in TCR crosslinking (Chilson, Boylston and Crumpton, 1984). This mitogen-mediated activation of T cells was used since TCR specificities of the isolated T cell clones were unknown, rendering antigen-specific activation via the TCR impossible. For further evaluations, four representative T cell clones derived from each approach were selected. The proliferative capacity of the T cell clones when activated via CAR in comparison to TCR engagement was first assessed using CellTrace staining and subsequent flow cytometric analysis (Figure 4.10). For this, resting T cells were stained with Cell Trace Violet prior to co-culture with irradiated CAR target cells (CAR-specific activation) or PHA stimulation-mix (TCR-specific activation), respectively. The proliferation status of the individual T cell clones was determined on day 3 and 7 after activation by analyzing CellTrace Violet median FI values using flow cytometry.
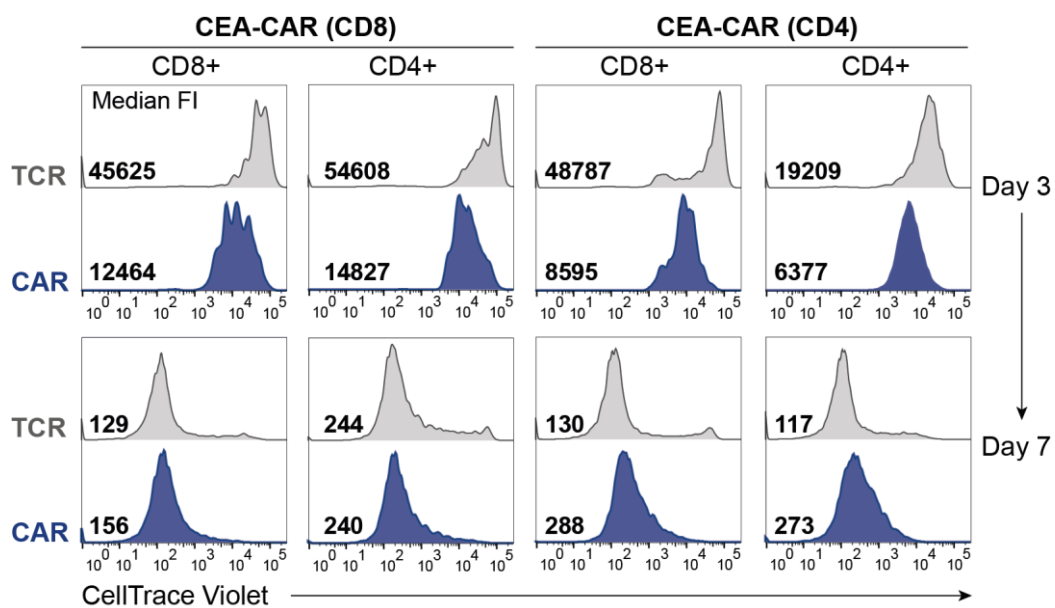
Figure 4.10: Proliferation of CAR-transduced T cell clones induced either by TCR or CAR engagement. Expansion of T cell clones transduced with CEA-CAR_CD4 or CEA-CAR_CD8, respectively, was monitored 3 and 7 days after activation by flow cytometric analysis of CellTrace Violet-stained T cells. CAR-specific stimulation (blue) was performed in 96-well utilizing 1×10^5 T cells and 4×10^5 irradiated CAR target cells (LS174T). TCR-specific activation (gray) of 1×10^5 T cells was mimicked using PHA stimulation-mix comprising 2×10^5 irradiated feeder cells and 2×10^4 irradiated LCL in the presence of PHA. Decreasing median FI values for CellTrace Violet indicated higher numbers of cell divisions reflecting proliferation. Unstimulated T cells served as a negative control (not shown).

Proliferative capacity of each T cell clone could be estimated by decreasing CellTrace Violet median FI values following TCR- or CAR-specific activation (Figure 4.10). When comparing median FI values of T cells that were activated via TCR with those stimulated via CAR three days after initial co-culture, it became apparent that CAR-stimulated cells initially proliferated stronger. Higher proliferation rate was indicated by lower median FI values of approximately 10 000 for T cell clones stimulated via CAR compared to median FI values ranging from 19 000 to over 50 000 for TCR-stimulated T cells. However, seven days after activation median FI values as well as population shifts visible in the respective histograms were comparable both for cells stimulated via TCR or CAR, respectively. This demonstrated comparable proliferation rates seven days after stimulation for both approaches. Based on these results it could be

assumed that CAR-specific stimulation of the T cell clones would be sufficient to expand T cell clones once endogenous TCRs are absent after the knockout.

To further quantify the proliferative capacity of T cells activated via CAR, the cell count was determined eleven days after CAR-specific activation of the same T cell clones using irradiated CAR target cells (LS174T) (Figure 4.11a). Expansion rates of the respective T cell clones following CAR engagement was compared to proliferation rates upon activation with PHA (TCR-specific stimulation). After the expansion period, the T cells clones that were either activated via CAR or TCR engagement, were subsequently analyzed for responsiveness to CAR target cells (Figure 4.11b). Since the selected T cell clones were previously able to specifically secrete IFN-γ upon encounter of CAR target cells, this method was used to ensure that only CAR-expressing T cells specifically recognizing the CEA antigen expanded after activation.
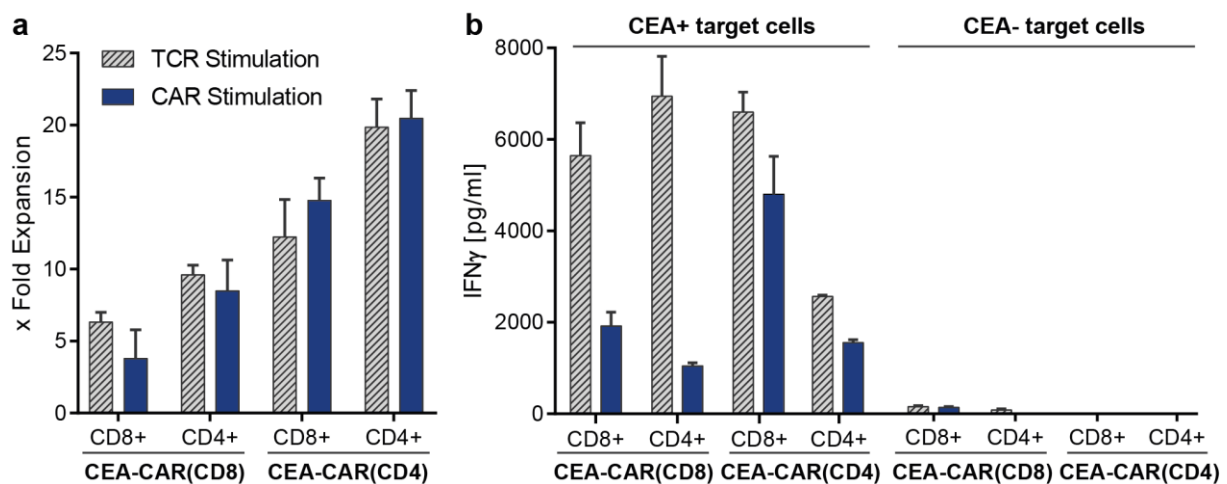
Figure 4.11: Fold expansion and IFN-γ release of CAR-expressing T cell clones activated either via CAR or TCR, respectively. a) Fold expansion of 5 x 10^5 CAR-expressing T cells in 24-well plates was determined 11 days after co-culture with either 2 x 10^6 irradiated LS174T cells (CAR stimulation) or PHA stimulation mix (TCR stimulation). Representative expansion rates of CD8$^+$ and CD4$^+$ T cell clones either transduced with CEA-CAR_CD4 or CEA-CAR_CD8, respectively, are depicted. **b)** After expansion period IFN-γ release of the same cells was determined in ELISA 20 h after co-cultivation with either CEA$^+$ target cells (LS174T) or CEA$^-$ target cells (mLCL_ME). Co-culture was set up using 5 x 10^4 CAR-positive T cells at an E:T ratio of 1:4.

For each CAR-expressing T cell clone, the expansion rates were comparable when stimulated either TCR- or CAR-specific (Figure 4.11a). These observations are in accordance with results obtained from CellTrace Violet staining upon activation of the same T cell clones (Figure 4.10). However, when comparing the fold expansion of the individual clones with each other, differences in proliferation rates could be observed (Figure 4.11a). T cell clones transduced with CEA-CAR_CD4 showed a higher proliferation rate compared to CEA-CAR_CD8-expressing T cell clones. While CEA-CAR_CD8-transduced cells reached a maximal expansion rate of 10-fold, T cells expressing CEA-CAR_CD4 showed up to 20-fold expansion 11 days after activation. Additionally, CD4$^+$ T cell clones proliferated slightly stronger compared to CD8$^+$ T cells transduced with the same CAR construct. Interestingly, this did not correlate

with IFN-γ release when exposed to the same CAR target cells (Figure 4.11b). T cell clones that were activated via TCR expressed much higher IFN-γ levels than CAR-stimulated T cells, even though proliferation rates were comparable. Additionally, CD4$^+$ T cell clones initially activated via CAR secreted less INF-γ than the respective CD8$^+$ T cell clones. However, none of the T cell clones reacted with CEA-negative control target cells, indicating that IFN-γ release observed with CEA-positive target cells represented specific recognition mediated through the transduced CAR. In summary, while all T cell clones could be expanded via CAR engagement, proliferation rates of CEA-CAR_CD4 transduced cells were slightly higher than for CEA-CAR_CD8-expressing cells. At the same time, the amount of IFN-γ released in response to CAR target cells did not correlate with proliferative capacity. However, all T cell clones independent of activation approach specifically recognized the CAR target cells, which indicated specific expansion of CAR-expressing cells.

4.3.3   Knockout of the endogenous TCR using TALENs

Various CAR-expressing CD4$^+$ and CD8$^+$ T cell clones could be generated that could be successfully expanded via CAR engagement. The next step in the generation of universal recipient cells comprised the subsequent knockout of the endogenous TCR in these expanded T cell clones. For the specific knockout of either the TCR α or β chain, the TALEN technology introduced earlier was utilized. Knockout efficiency rate was determined by loss of CD3 on the cell surface 5 days after introduction of TALEN pairs (Figure 4.12a). While the knockout efficiency rate was comparable for targeting of TCR α and β chain, respectively, only TCR β chain knockout is depicted in Figure 4.12a. TCR-negative T cell cells were subsequently isolated using magnetic beads coated with α-CD3 antibody by extraction of TCR-positive cells that did not comprise a knockout of the endogenous TCR. The isolated TCR-negative cells that expressed the introduced CAR construct were then stimulated via CAR engagement that should allow expansion of the cells independent of the endogenous TCR (Figure 4.12b).
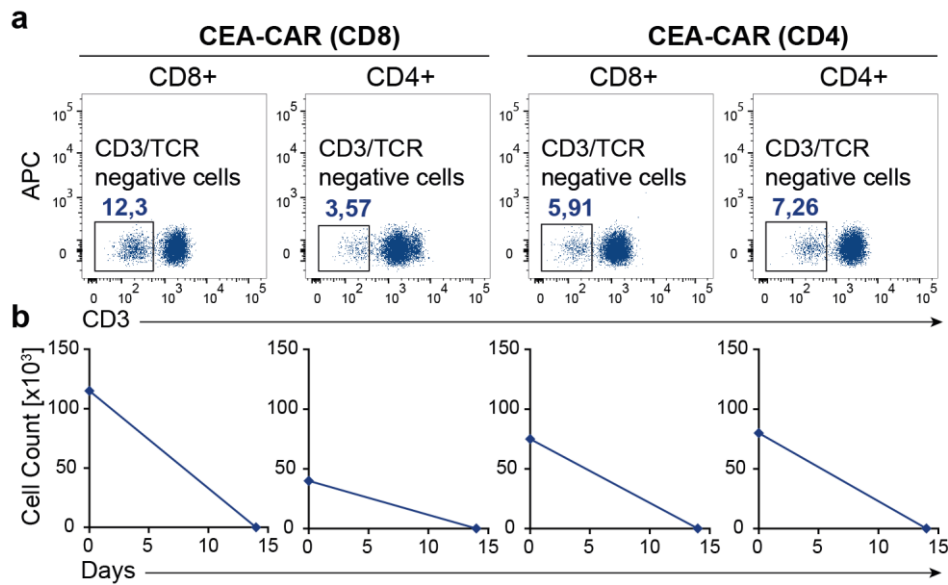
Figure 4.12: Knockout of the endogenous TCR β chain in CAR-transduced T cell clones. a) Flow cytometric analysis of CAR-transduced CD8+ and CD4+ T cell clones (CEA-CAR_CD4 or CEA-CAR_CD8) using α-CD3 antibody for detection of successful TCR knockout 5 days after transfection with TALEN pairs targeting the TCR β chain. Untransfected cells served as negative controls. **b)** Total cell count of CD3-negative cells after magnetic bead-based isolation and 14 days after subsequent stimulation of TCR-negative cells via CAR. TCR-negative T cells were isolated 7 days after incubation with 2.5×10^5 irradiated CAR target cells (LS174T) in the presence of IL-2 for 14 days. Cell count was determined after expansion period at day 14. Data are representative for two independent experiments.

While in all four T cell clones the TCR β chain could be targeted using TALEN pairs, knockout efficiency was relatively low compared to previous experiments using Clone 234. Only 3 – 12% of the cells exhibited a knockout of the TCR β chain indicated by the loss of CD3 on the cell surface (Figure 4.12a). Consequently, the number of TCR-negative T cells that could be isolated utilizing α-CD3 coated beads was also very low for all four approaches (CEA-CAR_CD8: CD8+ = 115×10^3, CD4+ = 40×10^3; CEA-CAR_CD4: CD8+ = 75×10^3, CD4+ = 80×10^3) (Figure 4.12b). Stimulation of these low numbers of cells via CAR engagement did not result in TCR-independent proliferation of T cells and the cells did not survive the 14-day expansion period.

Independent of the nature or origin of the selected T cell clones, TCR-deficient T cells could not be stimulated to proliferate via the transduced CEA-CAR. While other mechanisms connected to regulation and signaling of the respective CAR construct could be responsible for the failed expansion, another possible explanation roots in the nature of the CAR target cells (LS174T). These fast-expanding, adherent tumor cell lines might not create an optimal environment for T cell expansion compared to a standard stimulation mix, which contains feeder cells and LCL providing co-stimulatory signals that promote T cell activation. Especially low numbers of T cells, as was the case after TCR knockout by TALENs, might be affected more drastically by this hostile environment. For this reason, one measure to improve the strategy for generating universal recipient cells for TCR-independent expansion comprised the expansion of the molecular toolbox (see 4.4).

4.4 Process improvements

Because proliferation via CAR engagement could not be induced in TCR-deficient T cell clones, a re-evaluation of the process was performed. This comprised the expansion of the molecular toolbox by generating two new chimeric constructs that should improve T cell survival of TCR-knockout T cell clones. Additionally, different T cell subsets were investigated for their proliferative capacity and survival *in vitro* to determine whether CAR-T cell clones derived from a specific T cell compartment would be better suited as universal recipient cells. Based on results obtained with the two new chimeric constructs, a new strategy for the generation of universal recipient cells was developed that would allow a faster selection process of T cell clones comprising a TCR knockout that could be expanded simultaneously via CAR engagement.

4.4.1 Expansion of molecular toolbox

To improve the process of generating universal recipient cells, two new CAR constructs were generated and tested for their feasibility to promote T cell expansion. While the CEA-CARs mediated optimal proliferative capacity, the unsuccessful expansion of TCR knockout T cell clones from small cell numbers could possibly originate in the nature of the CEA positive target cells creating an unfavorable environment for T cell proliferation. To circumvent this, new CAR constructs were generated that could activate T cells in the presence of B cell-derived LCL providing various co-stimulatory signals to T cells during activation.

4.4.1.1 CD19-CAR

CD19 has proven to be a suitable target for CAR T cell therapy in patience with B cell malignancies. While CD19-CAR-transduced T cells effectively eradicate cancer cells, they have also been shown to persist in patience months after initial therapy (Porter *et al.*, 2011). Since the CD19 antigen is highly expressed on malignant as well as healthy B cells, LCL included in the standard stimulation-mix of T cells could be utilized as target cells. Compared to tumor cells, these natural antigen-presenting cells would serve as ideal stimulation cells for T cell expansion since they express co-stimulatory molecules required for T cell activation and generally no inhibitory molecules, such as PD-L1 that would counteract T cell proliferation. While the ideal combination of co-stimulatory molecules in CAR constructs is still a subject of extensive debate, 4-1BB containing CD19-CARs showed more than 1000-fold expansion and long persistence in B cell chronic lymphocytic leukemia (CLL) patients (Kalos *et al.*, 2011; Porter *et al.*, 2011). Since the introduced CAR should be utilized for T cell expansion rather than tumor cell killing, survival of CAR-expressing T cells is the predominant focus for the

selection of a suitable construct. CD19-CARs comprising the 4-1BB signaling domain compared to CD28 mediated enhanced T cell survival *in vivo*, although the length and nature of the spacer region is decisive for CAR activity (Milone *et al.*, 2009; Hudecek *et al.*, 2015). Based on these data a CD19-CAR construct was generated that comprised the domain structure published by Hudecek *et al.*, which included the α-CD19 antibody FMC63 scFv coupled to a CD28 transmembrane domain and 4-1BB and CD3ζ signaling domains via an IgG4 hinge extracellular spacer (Hudecek *et al.*, 2015). Instead of using EGFRt as a transduction marker, eGFP was coupled to the CD19-CAR construct via a P2A element (Figure 4.13). To ensure co-translational localization to the ER for correct folding and surface expression, the GM-CSF receptor α chain signal peptide was added 5' of the CAR coding sequence (Wang *et al.*, 2011). Molecular cloning of the CD19-CAR construct is described in 3.1.14.
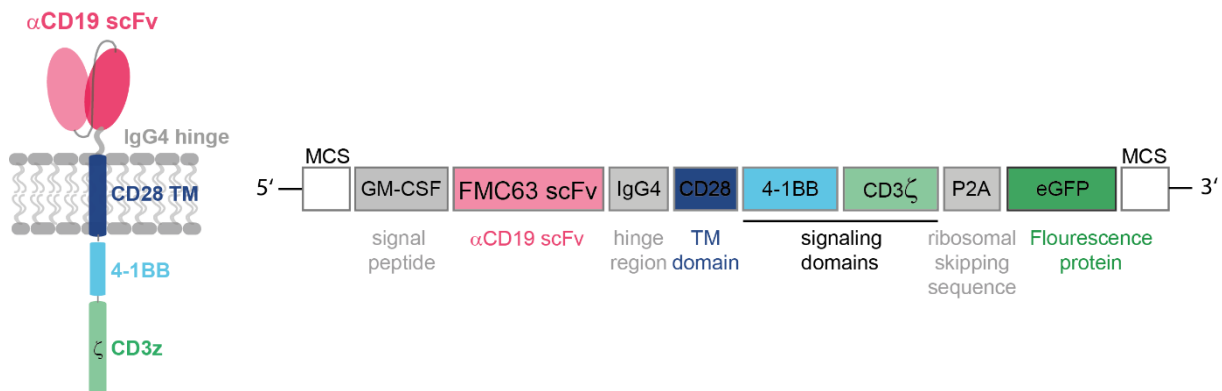
Figure 4.13: Schematic representation of the CD19-CAR construct. α-CD19 scFv is coupled to CD28 transmembrane domain and intracellular signaling domains (4-1BB and CD3ζ) via an IgG4 hinge region. GM-CSF signal peptide preceding the coding sequence for the CAR ensures translation on the ER membrane. CAR construct is coupled to eGFP via P2A element to allow tracking of transduction rate in T cells.

In order to verify correct expression and functionality of the newly generated construct, PBL were transduced with the CD19-CAR construct. Transduction rate and expression of the CD19-CAR construct was evaluated by analyzing eGFP expression in the transduced T cells (Figure 4.14a). Specificity and functionality of the CD19-CAR was evaluated by IFN-γ ELISA after co-culture of transduced PBL with CD19$^+$ (LCL_Eva1) and CD19$^-$ (Jurkat-76) target cell, respectively (Figure 4.14b). CD19-CAR-expressing single cell clones were generated, as described before for CEA-CAR constructs, by sorting transduced PBL into 96-well plates using FACS. However, due to the nature of the CAR target cells, the generated single cell clones could be directly activated via CAR by co-culturing them with irradiated CD19-positive LCL without addition of PHA or OKT-3 antibody that would deliver activation signals through the TCR. This allowed the pre-selection of clones that can be expanded via CAR engagement, since only those that could be activated sufficiently were able to survive the stimulation period for 14 days. After further expansion of the generated single cell clones, selected T cell clones

were analyzed for their proliferative capacity via CAR engagement and compared to physiological activation via the TCR utilizing a stimulation-mix comprising PHA (Figure 4.14c).
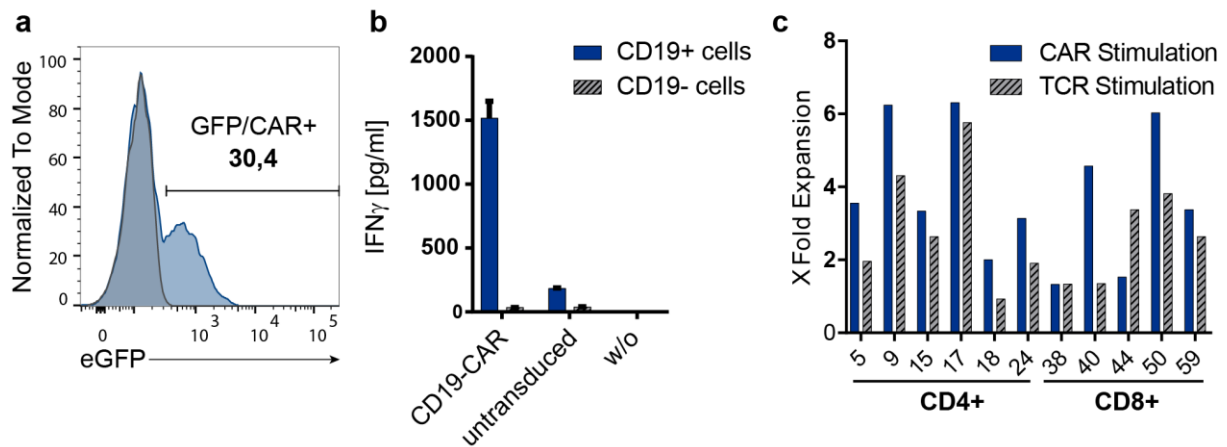
Figure 4.14: CD19-CAR expression and functionality in PBL. a) Isolated PBL were transduced with the CD19-CAR construct 4 days after activation. Successful transduction was confirmed 7 days after transduction utilizing eGFP expression as an indicator (blue). Untransduced cells served as negative controls (gray). **b)** Specificity and functionality of the CD19-CAR construct was evaluated by IFN-γ ELISA 20 h after co-culturing transduced PBL with target cells at an E:T ratio of 1:1. CD19-positive (LCL_Eva1) and CD19-negative (Jurkat-76) cells were used as target cells. **c)** Proliferative capacity of CD19-CAR-expressing single cell clones was evaluated by fold expansion over 14 days. Cell count was determined before and after the expansion period. 1 x 10^5 T cells per 96-well were either activated via CAR stimulation (4 x 10^5 irradiated CD19-positive LCL and 1 x 10^5 irradiated feeder cells) or TCR stimulation (stimulation-mix comprising 2 x 10^4 irradiated CD19-negative K562_A2_CD86, 2 x 10^5 irradiated feeder cells and PHA).

The new CD19-CAR construct could be successfully expressed in PBL indicated by 30% eGFP positive cells (Figure 4.14a). Functionality and specificity of the transduced CAR construct was confirmed by IFN-γ ELISA (Figure 4.14b). Only CD19-CAR transduced cells showed significant IFN-γ release in the presence of CD19 antigen and did not react to antigen-negative cells. Untransduced cells served as control to estimate the amount of unspecific IFN-γ release of PBL in the presence of CD19-CAR target cells. This functional read-out showed that the CD19-CAR construct was correctly assembled and expressed on the cell surface of transduced T cells. After single cell clones were generated from the transduced PBL, they could be individually analyzed for their expansion rate when activated via the CAR or TCR, respectively (Figure 4.14c). A selection of representative clones shows that CD4^{+} as well as CD8^{+} T cell clones could proliferate upon CAR engagement. While individual clones achieved a 6-fold expansion over 14 days, others could only increase their cell count about 2-fold. However, the generated CD19-CAR construct could support T cell proliferation in individual T cell clones comparable to proliferation rates observed for TCR-specific activation.

4.4.1.2 CD3-Chimera

To mimic physiological T cell activation via the TCR complex as closely as possible, an additional construct was designed that should promote T cell proliferation in the absence of

the endogenous TCR. For this, the modular domain structure of CAR constructs was combined with an extracellular domain of a CD3$\delta\epsilon$ dimer derived from the CD3 complex (Figure 4.16). In contrast to regular CAR constructs, this chimeric protein is not equipped with an antibody-derived scFv that recognizes antigen. Instead, the single chain fragment (scF) is generated from the extracellular domains of the CD3δ and ϵ subunits, respectively, which naturally are expressed as two individual proteins. However, the Ig-fold ectodomains of CD3 δ and ϵ form, via non-covalent interactions, one of the heterodimers of the CD3 complex, which supports signaling through the TCR (Arnett, Harrison and Wiley, 2004). It has been shown that T cell activation can be mediated by binding of antibodies, like OKT-3, to the ϵ subunit of the CD3-complex, thereby mimicking the physiological activation via TCR and MHC-peptide interaction (Van Wauwe, De Mey and Goossens, 1980). Therefore, binding of an α-CD3ϵ antibody to the CD3-Chimera should theoretically lead to an activation of the transduced T cell when intracellular signaling domains are present that can mediate signal transduction. In order to mimic the natural structure and signal transduction of the CD3-complex as closely as possible, only the intracellular domain of CD3ζ was chosen as a signaling domain, similar to first generation CARs. Complex interactions mediated by polar contacts in the transmembrane region and conserved motifs in the stalk domains of CD3 and TCR subunits are responsible for the correct assembly of the TCR-complex in the ER (Call *et al.*, 2002). Therefore, none of the transmembrane domains derived from the multi-subunit TCR-complex seemed suitable for the expression of an unpaired monomeric protein like the CD3-Chimera. Instead, the single-pass transmembrane domain of CD28 as well as the hinge domain of CD8α were chosen, both of which have been used and evaluated in various CAR constructs (Imai *et al.*, 2004; Milone *et al.*, 2009). Molecular cloning of the CD3-Chimera construct is described in 3.1.14.
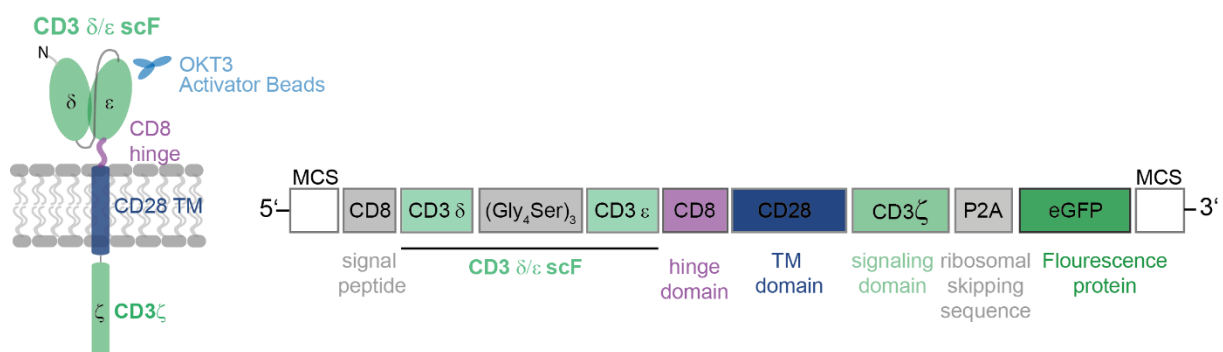
Figure 4.15: Domain structure of CD3-Chimera construct. The extracellular single chain fragment of CD3$\delta\epsilon$ separated by a flexible (Gly$_4$Ser)$_3$ linker is coupled to the CD28 transmembrane domain and CD3ζ signaling domain via a CD8 hinge domain. The single chain CD3$\delta\epsilon$ dimer should retain the epitope for α-CD3 antibody OKT-3 upon native folding. The coding sequence for the CD3-Chimera is preceded by a CD8 signal peptide to ensure co-translational localization to the ER membrane. EGFP coupled via the P2A element can be used to monitor successful transduction in CD3-positive cells. Multiple cloning sites (MCS) allow easy cloning into different backbone vectors.

The extracellular domain of the CD3-Chimera construct was designed as a single-chain fragment consisting of the ectodomains of the CD3ε and CD3δ subunit. The native folding of soluble ectodomain CD3$\delta\varepsilon$ dimers in combination with α-CD3 antibody UCHT1 scFv has been demonstrated in a 1.9-Å crystal structure by Arnett *et al.* (Arnett, Harrison and Wiley, 2004). Simultaneously, the crystal structure of the CD3$\gamma\varepsilon$ dimer based on a soluble single chain fragment in complex with OKT-3 Fab' fragment has been shown (Kjer-Nielsen *et al.*, 2004). These findings proved that binding of the respective α-CD3 antibodies was mediated via the CD3 ε subunit, which could be stably expressed together with the CD3 γ or δ subunit, respectively, to achieve native folding of the soluble, isolated heterodimers. However, a study by Law *et al.* demonstrated a higher binding affinity of α-CD3 antibodies to CD3$\delta\varepsilon$ compared to CD3$\gamma\varepsilon$ fusion proteins (Law *et al.*, 2002). While the soluble CD3$\delta\varepsilon$ dimer could be stably expressed from a single polypeptide separated by a flexible $(Gly_4Ser)_3$ linker to comprise α-CD3 antibody epitopes, oligomerization probably due to unpaired cysteine residues in the CxxCxE motif comprising stalk domain could be observed (Law *et al.*, 2002). This disulfide scrambling of the CD3 stalk domains was also observed by Kim *et al.* and led to the conclusion that the stalk domain was not necessary for native association of the respective CD3 subunits in a single chain fragment, but rather supported correct assembly of the TCR-complex in the ER (Kim *et al.*, 2000; Sun *et al.*, 2001). Based on these observations the extracellular domain of the CD3-Chimera was designed as a single chain CD3$\delta\varepsilon$ dimer separated by a flexible $(Gly_4Ser)_3$ linker often used in scFv of CARs without the CxxCxE motif comprising stalk regions of the respective CD3 subunits. Utilizing this domain structure should ensure correct folding and binding of α-CD3 crosslinking antibodies that mediate T cell activation. The proposed mode of action would then include the activation of TCR-complex-deficient cells via OKT-3 binding to the CD3-Chimera in the presence of CD28 co-stimulation (Figure 4.16). This should resemble the natural activation via the TCR-complex and lead to cell proliferation in the absence of an endogenous TCR. Compared to regular CAR constructs comprising antibody-derived scFv recognizing a target antigen, the CD3-Chimera construct does not bind any target and should therefore abolish the risk of off-target recognition.
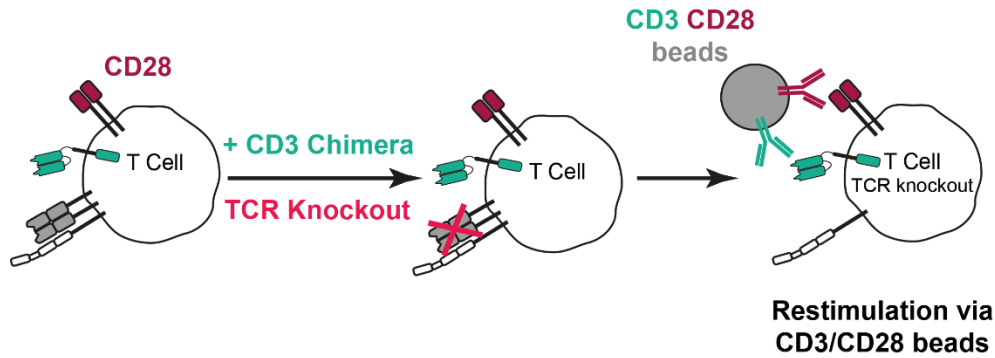
Figure 4.16: Strategy for universal recipient cell utilizing CD3-Chimera. CD3-Chimera-transduced T cells can be activated by α-CD3 and α-CD28 antibodies to deliver signal 1 and 2 in the absence of the endogenous TCR after knockout. Antibodies binding CD3-Chimera can be soluble in the presence of feeder cells or bead-bound in combination with α-CD28 antibody.

In order to investigate correct expression and folding of the CD3-Chimera, TCR-deficient Jurkat-76 cells were used as a first test system. While this T cell lymphoma cell line serves as appropriate recipient cells to evaluate TCR or CAR expression, the cells have lost their ability to provide basic T cell effector functions, like cytokine secretion, rendering them unsuitable for functional read-outs (Heemskerk *et al.*, 2003; Bürdek, 2009). However, due to lack of TCR expression, CD3 is also not present on the cell surface, which allows the detection of the CD3-Chimera construct using α-CD3 antibodies without interference from endogenous CD3. To evaluate expression, Jurkat-76 cells were transduced with the CD3-Chimera construct and expression of the CD3-Chimera was verified by staining with α-CD3 antibody (Figure 4.17). To detect possible differences in CD3-Chimera surface expression in individual clones, single cell clones were generated by FACS and subsequently analyzed for expression of CD3-Chimera construct. Since the P2A element present in the vector construct allows bicistronic expression of CD3-Chimera and eGFP, which should ensure equimolar expression levels, eGFP expression was compared to staining with α-CD3 antibody (Osborn *et al.*, 2005).
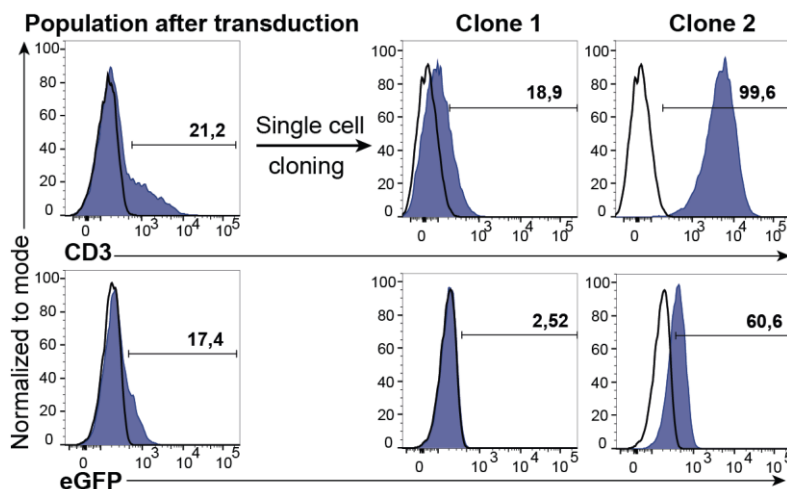
Figure 4.17: CD3-Chimera expression in TCR-deficient Jurkat-76 cells. Transduced Jurkat-76 cells were analyzed for CD3-Chimera and eGFP expression 7 days after transduction by staining with α-CD3 antibody and subsequent flow cytometric analysis. Generated single cell clones were again evaluated for CD3-Chimera and eGFP expression by α-CD3 antibody staining followed by flow cytometric analysis 2 weeks after FACS. Shown here are results of 2 representative clones. Transduced cells are shown in blue. Untransduced Jurkat-76 cells served as negative controls (black line).

CD3-Chimera expression indicated by α-CD3 staining was present in 21% of Jurkat-76 cells 7 days after transduction (Figure 4.17). In comparison, only 17% of the transduced cells showed eGFP expression exceeding the negative control. Neither α-CD3 staining nor eGFP expression resulted in distinct positive populations in bulk-transduced Jurkat-76. Therefore, single cell clones were generated to allow visualization of differences in expression levels in individual clones. Two representative clones are shown in Figure 4.17 that expressed the CD3-Chimera construct at different levels. While clone 1 exhibited low expression levels of the construct, Clone 2 expressed the CD3-Chimera at high levels, indicated by the shift of the positive population compared to the negative control. The same was true for eGFP expression, which was, however, lower compared to α-CD3 staining for clone 2. Clone 1 did not show any positive population, while low CD3 expression could be observed. This demonstrated that expression of eGFP from the bicistronic construct did not yield equimolar expression levels compared to the CD3-Chimera construct. However, the marker could still be used to detect CD3-Chimera high-expressing cells. When comparing the single cell clones with the transduced population before sorting, it became apparent that expression levels varied greatly in individual clones, which explains the lack of a distinct positive population when a bulk mixture of transduced clones was present. Nevertheless, these results still demonstrated that the designed CD3-Chimera construct could be correctly folded and expressed on the cell surface, which was indicated by binding of the α-CD3 antibody recognizing an epitope on natively folded CD3ε subunits.

4.4.2   Phenotypic evaluation of CAR-transduced T cells

Besides generating new chimeric constructs to improve T cell expansion after the TCR knockout, another measure to prolong survival of T cell clones *in vitro* would comprise the selection of a defined T cell subset exhibiting superior proliferative capacity. Recent publications have shown the benefit of utilizing transgenic TCR- or CAR-transduced T cells derived from the central memory compartment to improve efficacy of adoptive T cell transfer in patients (Berger *et al.*, 2008; Gattinoni *et al.*, 2011; Graef *et al.*, 2014; Sommermeyer *et al.*, 2015). These studies demonstrated better proliferative capacity, effector function and persistence of central-memory derived T cell populations compared to cells derived from the effector compartment *in vivo*. All these traits would be also favorable for universal recipient cells for *in vitro* testing of transgenic TCRs in order to generate an effective and stable test system. However, whether isolated T cell clones originating from the central-memory subset show superior T cell expansion and prolonged survival in *in vitro* culture has not been investigated.

In order to evaluate whether a certain T cell subset exhibited a proliferative advantage, previously isolated CEA-CAR_CD4-expressing T cell clones were stained with common T cell markers to characterize their phenotype (Figure 4.18). To be able to identify differences in phenotype linked to proliferative capacity, four CEA-CAR_CD4-transduced T cell clones were chosen that showed either high or low proliferation rates and either expressed CD4$^+$ or CD8$^+$, respectively. Even though various markers were identified to distinguish different T cell subsets, the four most prominent T cell subsets can be identified utilizing two markers, CD62L and CD45RA (Seder and Ahmed, 2003; Golubovskaya and Wu, 2016). Utilizing these markers naive (CD45RA$^+$ CD62L$^+$), central memory (CD45RA$^-$ CD62L$^+$), effector memory (CD45$^-$ CD62L$^-$) and effector (CD45RA$^+$ CD62L$^-$) T cell subsets can be discriminated. By adding the memory marker CD95, naive T cells (CD45RA$^+$ CD62L$^+$ CD95$^-$) can be distinguished from stem cell memory cells (CD45RA$^+$ CD62L$^+$ CD95$^+$) (Lugli et $al.$, 2012).
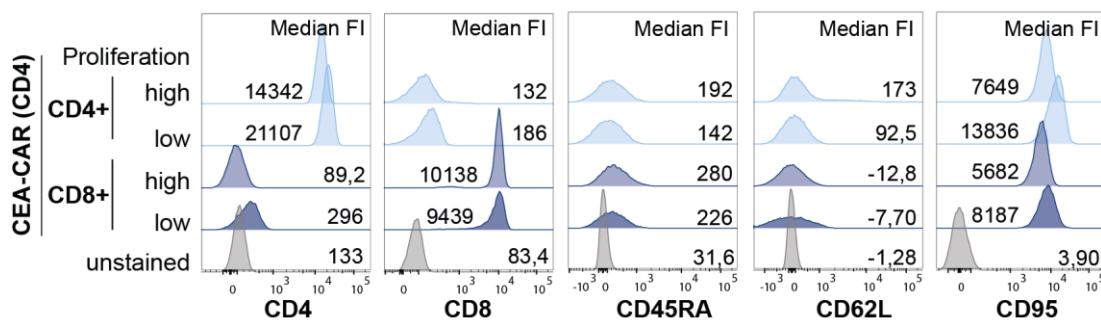
Figure 4.18: Phenotypical characterization of high and low proliferating CAR-transduced T cell clones. CEA-CAR_CD4-transduced T cell clones showing differences in proliferation rates (high or low) and co-receptor expression (CD8$^+$ or CD4$^+$) were stained with α-CD4, α-CD8, α-CD45RA, α-CD62L, α-CD95 and analyzed by flow cytometry. Unstained CEA-CAR_CD4-transduced cells served as a negative control. Median FI indicates population shift compared to unstained control (gray).

All CAR-transduced T cell clones, independent of their proliferative capacity or co-receptor expression, exhibited the same phenotype (Figure 4.18). Based on the combination of cell surface markers, they could be characterized as effector memory T cells (T$_{EM}$, CD4$^+$/CD8$^+$ CD45RA$^-$ CD62L$^-$ CD95$^+$). This indicated that T cells all exhibit the same phenotype after several weeks in in $vitro$ culture. Therefore, these cell surface markers could not be utilized to allow distinction between isolated T cell clones showing either high or low proliferation rates.

Even though no correlation could be observed linking a distinct phenotype to proliferative capacity of T cell clones expanded in in $vitro$ culture, differences could possibly still be rooted in the origin of the T cell clones. Therefore, it was investigated whether T cell clones derived from a specific T cell subset would show higher expansion rates. For this, freshly isolated PBL were transduced with the CD19-CAR construct and subsequently sorted into 96-well plates to

generate single cell clones. Prior to FACS the cells were stained for common T cell surface markers using α-CD8, α-CD45RA and α-CD62L antibodies that would allow their classification into different T cell subsets. The sorting strategy comprised FACS of CAR-positive T cells, indicated by eGFP expression, that expressed either the CD4 or CD8 co-receptor. For sorting, the CD45RA and CD62L expression was neglected to allow the expansion of any CAR-transduced T cell clone independent of subset origin. However, these markers could be later used to determine from which T cell subset the expanded T cell clones were derived. This could be achieved by analyzing index sort data of these markers that were collected during sorting using the BD FACSDiva™ Software (BD Bioscience) (Figure 4.19a). After single cell sorting, the cells were activated in the presence of OKT-3 antibody and expanded for 10 days before 142 growing T cell clones were identified and transferred into new 96-well plates using the automated workflow platform EVO200 (Tecan). Subsequently the picked T cell clones were activated using a modified rapid expansion protocol in 24-well plates (Riddell and Greenberg, 1990; Hudecek *et al.*, 2013). The proliferative capacity of 48 selected T cell clones was determined after the expansion period and could be subsequently connected to T cell subset descent (Figure 4.19b).
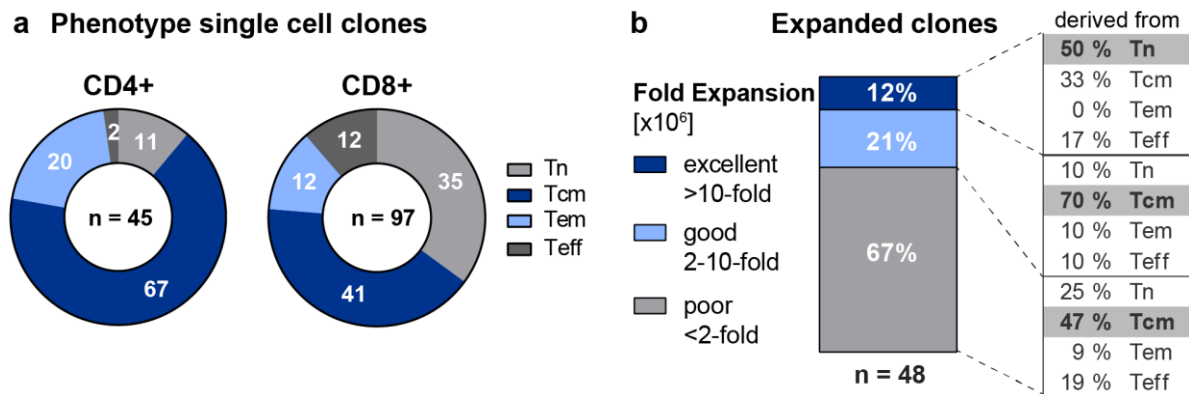
Figure 4.19: Phenotypic characterization of CD19-CAR-transduced single cell clones. a) Analysis of index sort data using BD FACSDiva™ Software. Re-analysis of CD4+ or CD8+ single cell clones, respectively, for expression of CD45RA and CD62L at day of sort. Cells were derived either from naïve (Tn), central memory (Tcm), effector memory (Tem) or effector (Teff) compartment. **b)** Fold expansion of 48 selected single cell clones 28 days after sorting. After identification of single cell clones 10 days after sorting, the cells were stimulated via CAR engagement (without addition of OKT-3) using 2 x 10^6 irradiated feeder cells and 1 x 10^6 irradiated LCL_Eva1 that served as CAR target cells. Cell count was determined on day 14 after activation. Expansion rate was categorized as excellent (>10 x 10^6 cells), good (2-10 x 10^6 cells) or poor (<2 x 10^6 cells), respectively. Analysis of index sort data using BD FACSDiva™ Software allowed determination from which T cell subset single cell clones were derived. Data represent the mean of 2 donors.

The CAR-transduced T cell clones that expanded after single cell sorting were derived from all four T cell subsets, however the majority of of the cells originated from the naïve (Tn) or central-memory (Tcm) compartment (Figure 4.19a). While 67% of CD4+ T cells expressed marker that characterized them as Tcm cells at the time of sorting, only 41% of CD8+ T cells were derived from this compartment. However, 35% of the CD8+ T cells that expanded after sorting originated from native T cells. Whereas, a higher percentage of effector-memory (Teff) cells

compared to Tn cells proliferated in the CD4$^+$ T cell compartment. When analyzing the proliferative capacity of 48 selected single cell clones 28 days after sorting, the majority of the cells were again derived either from Tcm or Tn cells, respectively, independent of expansion rate (Figure 4.19b). However, also T cell clones derived from Tem od Teff cells showed good or excellent expansion rate, respectively, at percentages comparable to poor proliferating clones. Therefore, the T cell compartment from which the T cell clones derived did not allow a prediction of their proliferative capacity *in vitro*. The distribution of certain T cell subset origins in the different expansion categories rather simply mirrored the percentages already observed at the time of sorting (Figure 4.19a). However, Figure 4.19b demonstrated that the majority of the isolated single cell clones exhibited a poor proliferation rate renderinging them unsuitable as an *in vitro* test system. Only 12% of the T cell clones could be expanded to more than 1 x 10^7 cells four weeks after single cell sorting, which indicated that only a small fraction of isolated lymphocytes had the capacity to proliferate to sufficient cell numbers for use in *in vitro* experiments. However, based on the phenotype, this superior expanding cell population could not be identified. Therefore, to avoid exclusion of potentially suitable T cell clones for the generation of universal recipient cells, mixed PBL populations were used in subsequent experiments without restricting the starting material to a specific T cell subset.

4.4.3   New strategy for generation of universal recipient cells

The improved strategy introduced in 4.3 allowed the generation of various CAR-transduced T cell clones that exhibited a high proliferative capacity via CAR engagement. However, while the knockout of the endogenous TCR could be performed, the resulting TCR-deficient T cells failed to expand upon activation via the transduced CAR. One reason for this might have been the nature of the CEA-CAR target cells used, which might have constituted an unfavorable environment for T cell expansion from small cell numbers. This low expansion after TCR knockout should be circumvented when the newly generated constructs, CD19-CAR and CD3-Chimera, are used for TCR-independent T cell activation. In contrast to CEA-CARs, the CD19-CAR construct mediates T cell proliferation by binding the antigen on LCL, which constitute natural antigen presenting cells displaying various co-stimulatory molecules that should support proper T cell activation. The requirement of target cells for T cell stimulation has been bypassed when utilizing the CD3-Chimera construct by antibody-based activation via OKT-3, while LCL are only included in the stimulation-mix to provide co-stimulation to T cells. However, the poor expansion rate of the TCR-deficient cells revealed another complication that might occur even when the new constructs would be used. In order to generate a universal recipient cell after the knockout of the endogenous TCR, the cells need to be expanded again from single cell clones to allow the determination of the knockout status of the respective TCR

chains at the mRNA level. In a complex mixture of cells that all comprise different insertions or deletions in either one or both of the TCR chains, respectively, this would not be feasible. Therefore, the generated CAR-expressing TCR-deficient cells would have to go through an additional round of clonal expansion, which might drastically shorten their life span. To circumvent this, a new strategy was developed that allowed the simultaneous knockout of the endogenous TCR and the introduction of the CD19-CAR or CD3-Chimera construct, respectively, in a single step to promote T cell expansion in the absence of the TCR (Figure 4.20). The resulting CAR-expressing TCR-deficient T cell clones would then only need to be expanded from a single T cell clone once, thereby shortening the *in vitro* expansion period considerably. Additionally, performing the TCR knockout and CAR transduction in one step before generating single cell clones would allow the immediate pre-selection of suitable T cell clones that are able to proliferate via engagement of the chimeric construct in the absence of the endogenous TCR. With the TCR no longer available to mediate T cell activation in these T cell clones, only T cell clones that can expand sufficiently via CD19-CAR or CD3-Chimera engagement would be detected after the expansion period, thereby accomplishing the prerequisite to generate desired universal recipient cells. Since any proliferating T cell clone would be derived from an individual single cell, the expanding cells would all comprise identical modifications in the *TRAC* and *TRBC* loci, allowing an easy determination of the knockout status of the respective TCR chains.
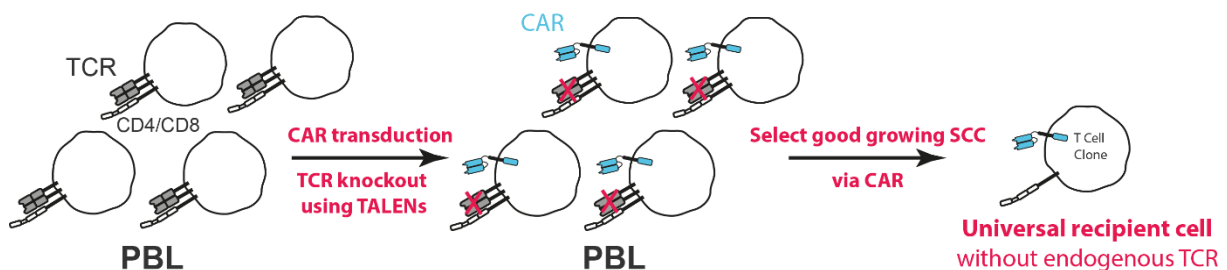
Figure 4.20: Schematic representation of the new strategy for the generation of universal recipient cells. Simultaneous knockout of the endogenous TCR via TALEN technology and introduction of either the CD19-CAR or CD3-Chimera construct, respectively, generates TCR-deficient CAR-expressing T cells. Subsequent generation of single cell clones allows immediate pre-selection of T cell clones that are able to expand via the introduced constructs independent of the TCR.

To perform and evaluate the new strategy for the generation and identification of suitable universal recipient cells, a high-throughput workflow was designed (Figure 4.21). While the example is shown for the CD19-CAR, it was also applied for the CD3-Chimera construct. After isolation of PBMC from donor blood, $\alpha\beta$ T cells were enriched by FACS and subsequently activated. This enrichment step ensured that no other cell types, like $\gamma\delta$ T cells, would be present in the starting material. On day 4 after activation, the cells were first electroporated with the respective TALEN pairs targeting the TCR α and β chain. After resting the cells for

approximately 4 h, the cells were transduced with the CD19-CAR construct. The successful transduction and simultaneous TCR knockout was determined 8 days later by flow cytometric analysis following a test staining for CAR and TCR expression. Two days later, the cells were sorted by FACS and the resulting single cell clones were subsequently activated via the transduced CAR. Following an expansion period of 11 days, emerging T cell clones were imaged and transferred into new 96-well plates for analysis and expansion using the automated workflow platform EVO200 (Tecan). One day later, the selected T cell clones were screened for lack of TCR expression and simultaneous presence of the transduced CAR construct utilizing the BD™ High Throughput Sampler (HTS) in combination with flow cytometric analysis on the BD LSRFortessa™. This step enabled the selection of well-expanding T cell clones that exhibited the desired phenotype and simultaneously identified T cell clones that were falsely sorted by FACS. T cell clones lacking TCR expression while showing successful transduction with CD19-CAR and promising expansion rates, were subsequently selected for NGS analysis to verify the knockout of the endogenous TCR at the mRNA level. The same clones were again activated and further expanded to investigate their proliferative capacity mediated via the CD19-CAR. At this point, data from NGS analysis was available, which allowed the merging of expansion rate with the corresponding TCR knockout status. Alternatively, T cells were frozen until NGS data could be analyzed. T cell clones that exhibited sufficient proliferative capacity and comprised frameshift mutations in *TRAC* and *TRBC* loci, respectively, could then be tested for their potential to serve as universal recipient cells for transgenic TCRs by evaluating their functional characteristics.
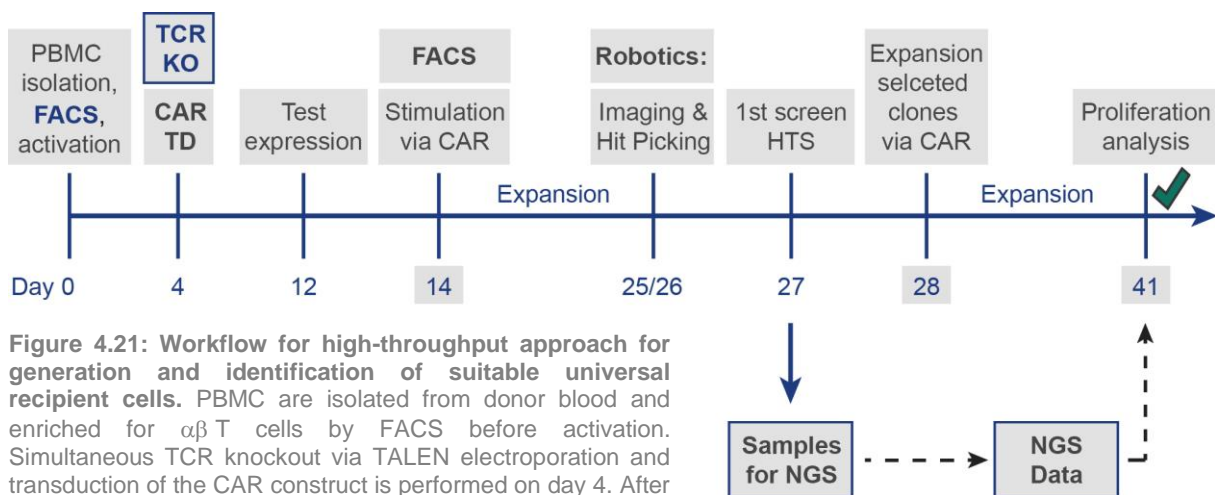
Figure 4.21: Workflow for high-throughput approach for generation and identification of suitable universal recipient cells. PBMC are isolated from donor blood and enriched for $\alpha\beta$ T cells by FACS before activation. Simultaneous TCR knockout via TALEN electroporation and transduction of the CAR construct is performed on day 4. After successful TCR knockout and CAR transduction is verified on day 12, the TCR-deficient cells are sorted by FACS and subsequently stimulated via CAR. Only the cells that can be activated via CAR engagement will proliferate and will be selected for further analysis after the expansion period. Cell imaging and transfer is performed by Clone Select Imager (Molecular Devices) in combination with the automated workflow platform EVO200 (Tecan). The transferred cells will then be screened for the desired phenotype utilizing HTS in combination with flow cytometry one day later. Well-expanding T cell clones lacking TCR expression while expressing the transduced CAR are selected for NGS analysis and further expansion. After another expansion period the proliferative capacity of individual T cell clones can be analyzed. These data can then be combined with the knockout status of the cell determined by NGS, which allows the selection of candidates suitable as universal recipient cells for testing of transgenic TCRs.

4.4.3.1   Enrichment of αβ T cells by FACS

To ensure that only αβ T cells would be used as starting material for the generation of universal recipient cells, freshly isolated PBMC were stained with α-TCRαβ and α-CD3 antibody and subsequently sorted by FACS (Figure 4.22). This enrichment step allowed the exclusion of other cell populations present in isolated PBMC, like γd T cells, that might interfere with subsequent sorting procedures. Instead of an αβTCR these T cells express γδTCRs that also form a TCR-complex together with the CD3 subunits. Therefore, γδ T cells would theoretically exhibit the same phenotype as TCR-deficient CD3-Chimera-expressing cells (αβTCR⁻ CD3⁺) that would be generated subsequently by TCR knockout and transduction of the chimeric α-CD3 antibody-binding construct. To circumvent the unintended selection of these γδ T cells in successive FACS procedures, αβ T cells were enriched and subsequently evaluated for purity utilizing α-TCRαβ and α-TCRγδ antibody staining (Figure 4.22).
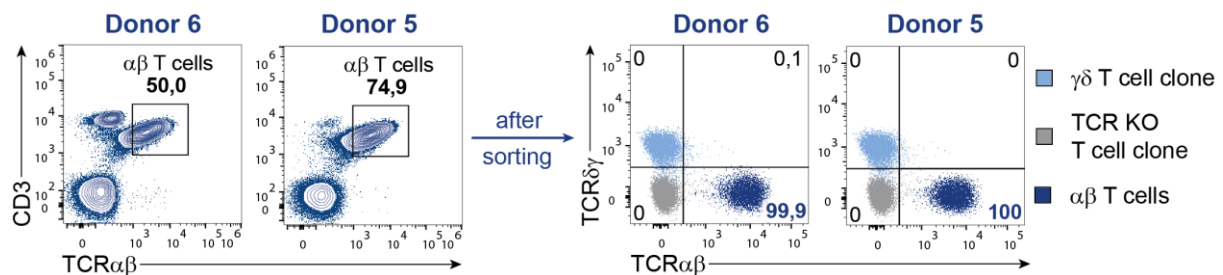
Figure 4.22: Enrichment of αβ T cells from PBMC. Isolated PBMC from 2 donors were stained with α-CD3 and α-TCRαβ antibodies for subsequent FACS. Only cells expressing both markers were sorted. After sorting the enriched αβ T cells were stained with α-TCRαβ and α-TCRγδ antibodies to evaluate purity of the sorted cells. Stained cells were analyzed by flow cytometry. A γδ T cell clone and TCR-deficient T cells were used as controls.

Isolated PBMC from donor blood contained various cell populations (Figure 4.22). Besides TCRαβ- and CD3-negative cells, that include B cells, NK cells and monocytes, γδ T cells were also present that express CD3 but not αβTCRs. These γδ T cells would also be activated by a standard stimulation mix comprising OKT-3 antibody that binds CD3. As demonstrated in Figure 4.22, the number of γδ T cells in the blood can vary greatly in different donors. While donor 6 cells comprised a quite dominant γδ T cell population, donor 5 cells only exhibited a small population of these cells. Accordingly, the number of αβ T cells can also vary between donors, with donor 6 sample comprising 50% and donor 5 sample comprising roughly 75% of this cell population. Analysis of the sorted cells clearly demonstrated a successful high-purity enrichment of αβ T cells. While no γδ T cells could be detected in the enriched cell population, the γδ T cell clone served as a positive control verifying successful staining with the α-TCRγδ antibody. TCR-deficient T cells were not bound by either α-TCRγδ or α-TCRαβ antibody, confirming specificity and lack of background staining.

4.4.3.2   Refined sorting strategy

The enriched $\alpha\beta$ T cells served as starting material for the next step in the new workflow for generating universal recipient cells comprising the knockout of the endogenous TCR and simultaneous introduction of the chimeric constructs. For this, the enriched $\alpha\beta$ T cells were first simultaneously electroporated with ivt-RNA coding for the TALEN pairs targeting the TCR α and β chain 4 days after activation. After a short resting period, the electroporated cells were transduced with either the CD19-CAR or the CD3-Chimera construct. A new sorting strategy was developed to subsequently identify and sort T cell clones exhibiting the desired phenotype that was characterized by lack of TCR expression and presence of the transduced CD19-CAR or CD3-Chimera, respectively (Figure 4.23). For this, the cells were stained with α-CD3, α-TCR$\alpha\beta$ and α-CD8 antibody. While the lack of CD3 and TCR$\alpha\beta$ expression indicated a successful knockout of the TCR, the expression of eGFP proved the transduction of the CD19-CAR or CD3-Chimera, respectively. The α-CD8 antibody staining allowed the distinction between CD8$^+$ and CD8$^-$ T cells. For CD19-CAR-transduced cells, CD3- and TCR-negative T cells were pre-gated and subsequently divided into CD8-positive or -negative cells that expressed eGFP (Figure 4.23a). In case of the CD3-Chimera-transduced cells, CD8$^-$ or CD8$^+$ cells exhibiting eGFP expression were selected from TCR-negative cells that could still bind α-CD3 antibody recognizing the CD3-Chimera construct (Figure 4.23b).
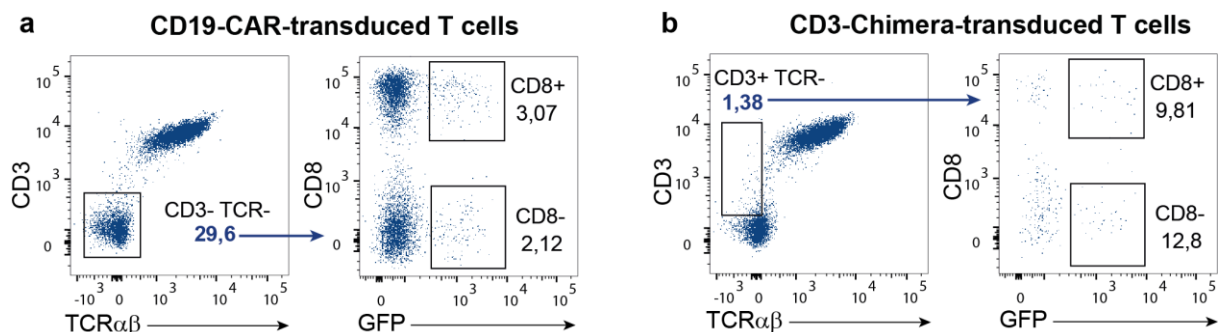
Figure 4.23: New sorting strategy for isolation of TCR-deficient cells transduced with CD19-CAR or CD3-Chimera, respectively. a) Sorting strategy for CD19-CAR-transduced cells for FACS. The cells were stained with α-CD3 and α-TCR$\alpha\beta$ antibodies to allow gating of CD3- and TCR-negative cells indicating successful knockout of the TCR. Staining with α-CD8 antibody could distinguish CD4$^+$ and CD8$^+$ T cells expressing eGFP, which served as a marker for successful transduction. **b)** Sorting strategy for CD3-Chimera-transduced cells for FACS. The cells were stained with α-CD3 and α-TCR$\alpha\beta$ antibodies to allow gating of TCR-negative cells that are CD3-positive indicating successful knockout of the TCR and simultaneous expression of CD3-Chimera. By staining with α-CD8 antibody, CD8$^+$ and CD4$^+$ T cell could be distinguished that showed successful transduction indicated by eGFP. Untransduced $\alpha\beta$ T cells served as controls (not shown). Results are representative for 3 donors.

For CD19-CAR-transduced cells, 30% of the cells comprised a knockout of the endogenous TCR indicated by the lack of CD3 and TCR$\alpha\beta$ expression (Figure 4.23a). Gating of these cells allowed the further distinction of CD8$^+$ and CD8$^-$ T cells that exhibited successful transduction with CD19-CAR, reflected by eGFP expression. Only 2 – 3% of the TCR-deficient cells were positive for eGFP revealing a relatively low transduction rate of the cells that were successfully

transfected with TALEN pairs. Cells that were transduced with the CD3-Chimera construct displayed the same TCR knockout rate as CD19-CAR-transduced cells since transduction was performed using cells derived from the same knockout experiment (Figure 4.23b). However, the number of cells that were successfully transduced with CD3-Chimera was relatively low, with only 1.38% of the cells able to bind α-CD3 antibody. After gating on this low number of cells and dividing them into CD8$^-$ and CD8$^+$ T cells, successful transduction could only be confirmed in 10% and 13% of the cells, respectively, which was indicated by eGFP expression. However, even if transduction rates of the TALEN-transfected cells were relatively low, single cell clones could still be generated from these few cells that exhibited the desired phenotype. The subsequent successful expansion of the sorted TCR-negative single cells clones mediated through the transduced chimeric construct, would then unambiguously demonstrate correct expression and functionality of the introduced CD19-CAR and CD3-Chimera constructs.

4.4.3.3 Improved expansion strategy

Expansion of TCR-deficient T cell clones via engagement of the respective transduced chimeric construct allowed the pre-selection of T cell clones with the ability to proliferate independent of TCR signaling. Due to the absence of the TCR on the cell surface of these T cell clones, activation could only be induced through the CD19-CAR or CD3-Chimera construct, respectively. For both approaches 5×10^3 irradiated LCL and 5×10^4 feeder cells were added per 96-well in the presence of IL-2. CD19-expressing LCL served simultaneously as target and co-stimulatory cells for activation of T cell clones expressing the CD19-CAR. For CD3-Chimera-transduced cells, LCL present in the stimulation-mix merely provided co-stimulation and OKT-3 antibody was added additionally to achieve activation via engagement of the chimeric construct. After an expansion period of 11 days the 96-well plates were screened for expanded single cell clones by utilizing Clone Select Imager (Molecular Devices) in combination with an automated workflow platform EVO200 (Tecan). T cell clones that were able to proliferate upon engagement of the chimeric construct were selected and transferred into a new 96-well plate to allow further analysis and expansion. Picking of the T cell clones was performed with Hit Selector Software (Tecan) to guide the liquid handling arm LiHa (Tecan). In total 369 CD19-CAR- and only 8 CD3-Chimera-transduced single cell clones were picked, demonstrating that utilizing the new strategy resulted in the successful isolation of T cell clones that were able to proliferate in the absence of the endogenous TCR. The low number of CD3-Chimera-expressing T cell clones might be the result of the very low transduction rate observed in Figure 4.23b. Alternatively, the low number of expanded CD3-Chimera-expressing T cell clones might indicate that the designed construct could not sufficiently support T cell expansion. Since the construct was previously only tested in

Jurkat-76 cells that proliferate independent of activation, the expression in TCR-deficient T cell clones represented the first functional evaluation of the CD3-Chimera construct.

4.4.3.4 New screening process

After the T cell clones exhibiting TCR-independent proliferation were identified, they were screened for the desired phenotype, which comprised the lack of TCR expression and detection of the transduced CD19-CAR or CD3-Chimera construct, respectively. This screening step allowed the identification of T cell clones that were falsely sorted by FACS and did not exhibit the desired phenotype as shown exemplarily for Clone 2 in Figure 4.24a. The further analyses focused on CD19-CAR-transduced cells since cells transduced with CD3-Chimera should exhibit a different phenotype, which will be discussed later in 4.5.2. All 369 picked CD19-CAR-transdcued T cell clones were evaluated for their phenotype and summarized as percentage of TCR- and CD3-nagtive cells (%TCR/CD3 negative) and percentage of CAR-positive cells (%CAR-positive) reflected by eGFP expression (Figure 4.24b). The detected phenotype allowed prediction of the TCR knockout status for each T cell clone. Dependent on TCR and CD3 expression levels the screened cells were categorized into 3 groups: "TCR KO", "TCR KO unconfirmed" and "No TCR KO" (Figure 4.24c). Subsequently, cells that were categorized as "TCR KO" were further analyzed for high, moderate and low CAR expression to determine whether TCR-negative cells expressed the transduced CAR sufficiently to allow activation.
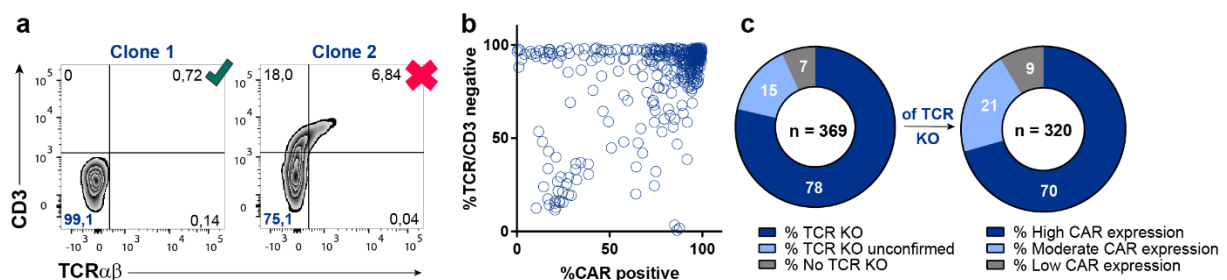
Figure 4.24: Screening for TCR-negative CAR-positive T cell clones by flow cytometric analysis. Cells were stained with α-CD3 α-TCR$\alpha\beta$ antibodies and subsequently analyzed utilizing BD® HTS in combination with flow cytometric analysis. **a)** Exemplary depiction of 2 T cell clones exhibiting different phenotypes. While Clone 1 exhibits unambiguously a knockout of the endogenous TCR, Clone 2 does not, depicted by low expression of CD3 and TCR$\alpha\beta$. **b)** Phenotype of all 369 CD19-CAR-transduced clones summarized as %TCR/CD3-negative and %CAR-positive cells. Gates for analysis were set as shown in a) based on negative and positive controls. **c)** Translation of phenotype determined by cytometric analysis to TCR knockout status. Categories comprised TCR KO (>80% TCR-/CD3-), TCR KO unconfirmed (>30%; <80% TCR-/CD3-) and No TCR KO (<30% TCR-/CD3-). Cell categorized as TCR KO were further analyzed for high (>80%), moderate (>30%; <80%) and low (<30%) CAR expression reflected by eGFP detection. Cutoffs were set as described based on background detected in staining of positive and negative controls.

Figure 4.24a shows examples of FACS blots of two representative T cell clones that were screened for CD3 and TCR$\alpha\beta$ expression. Clone 1 exhibited the desired phenotype with 99% CD3- and TCR$\alpha\beta$-negative cells and was subsequently selected for NGS analysis and further

expansion. In contrast, Clone 2 still expressed low amounts of CD3 and TCR$\alpha\beta$ indicating incomplete TCR knockout as interpreted by flow cytometric analysis. The phenotypic analysis of all 369 CD19-CAR-transduced T cell clones presented as %TCR/CD3-negative and %CAR-positive cells showed that the majority of the isolated clones highly expressed the transduced CAR while lacking the expression of CD3 and TCR$\alpha\beta$ (Figure 4.24b). While most of the cells exhibited the desired phenotype, clusters of cells could be detected that still did express the TCR-complex and showed either low or moderate CAR expression. Some T cell clones did not express the TCR-complex while CAR expression was nearly undetectable. The collected flow cytometry data served to predict the TCR knockout status of the individual T cell clones (Figure 4.24c). According to the defined categories, over 78% of the T cell clones exhibited a knockout of the endogenous TCR, whereas the TCR knockout could not be confirmed based on the phenotype for 15% of the T cell clones. No TCR knockout was detected in 7% of the T cell clones. This showed that by using the new sorting strategy described in Figure 4.23, the yield of T cell clones with the desired phenotype is very high with only a few outliers that represented technical contaminants. Accordingly, the majority of the cells that exhibited the TCR knockout also expressed the transduced CAR construct at high or moderate levels, with only 9% of the cells showing low CAR expression. T cell clones categorized as TCR KO with high CAR expression levels and promising expansion rates, that were determined by analyzing the data from Clone Select Imager (Molecular Devices), were selected for NGS analysis and further expansion (Figure 4.25). In order to validate the newly developed protocol for NGS sample preparation and analysis described in 4.4.3.5, clones that were categorized as not having a TCR knockout phenotype were also included. For these T cell clones, wildtype sequences in the *TRAC* and *TRBC* genes would be expected.

	%TCR/CD3 -	%CAR +	Proliferation	Select for expansion	
Clone 1	98.7	95.9	+++	yes	→
Clone 2	99.1	96.5	-	no	NGS
Clone 3	99.0	78.1	+++	yes	→
Clone 4	75.1	58.9	-	no	

Figure 4.25: Exemplary strategy for selection of T cell clones for NGS analysis. T cell clones showing a high percentage of TCR⁻/CD3⁻ and CAR⁺ cells while exhibiting high proliferation rates were selected for expansion and NGS analysis. Clones that did exhibit the same phenotype, but did not proliferate were not selected. Clones with high proliferative capacity and high percentages of TCR⁻/CD3⁻ cells, but lower percentages of CAR+ cells were also selected for NGS and further expansion. Clones exhibiting low percentages of TCR⁻CD3⁻ cells as well as CAR+ cells combined with low expansion rates were not selected. In total 161 T cell clones were selected for NGS analysis.

4.4.3.5 Development of a NGS protocol for identification of TCR knockout clones

NGS analysis of the TCR repertoire usually focuses on the hypervariable complementary-determining regions (CDRs) in the variable region of the TCR α and β chains, which mediate specific MHC- and peptide-binding (Bolotin *et al.*, 2012). However, for determination of the knockout status of individual single cell clones, the TALEN target sites in the respective TCR α and β constant regions need to be analyzed (Figure 4.26a). Therefore, primers were designed that bind to a region 3' of the respective TALEN target sites (Table 2.8). For amplification of all TCR β chain sequences a primer binding site was chosen that is homologous in the *TRBC1* and *TRBC2* genes. The preparation of DNA libraries for NGS analysis included two PCR reactions based on cDNA templates derived from mRNA isolated from each T cell clone. Since the recombined V(D)J segments defining the variable region of the respective TCR chains are joined to the constant regions by splicing to generate a mature transcript, mRNA rather than gDNA is used for sequence determination (Figure 4.26a). In the first PCR reaction (PCR I) Illumina universal oligos (IUO) were attached to the 5' and 3' ends of the cDNA templates. Reverse primers were designed, that would bind downstream of the TALEN target region in both TCR α and β chain cDNA, respectively (Figure 4.26b). The 3' primers comprised the IUO to allow addition of Nextera® indices (Illumina) in the subsequent PCR II reaction, which in turn were required for cluster generation by bridge amplification in Illumina NGS analysis.
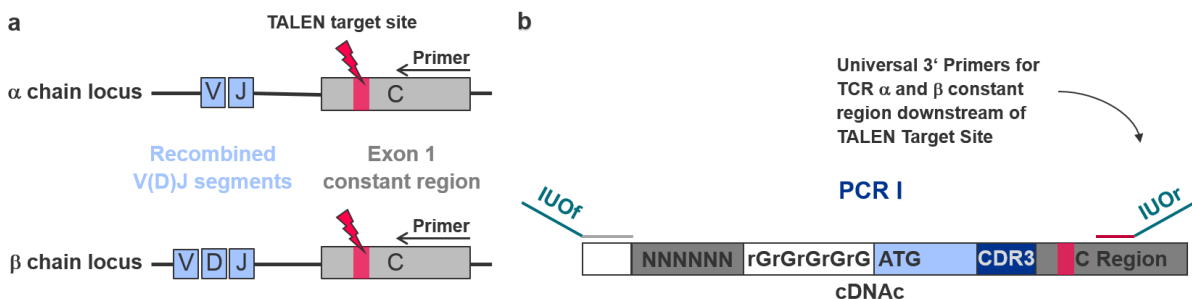
Figure 4.26: NGS library preparation to include TALEN target sites. a) TALEN target sites schematically depicted in TCR α or β locus, respectively. Both target sites reside within exon 1 of the respective constant regions. 3' primers were designed to bind downstream of the TALEN target sites to allow detection of mutations introduced by TALEN-induced double strand breaks. Recombined V(D)J segments are joined to the constant regions by splicing after transcription. **b)** Universal 3' primers for PCR I bind downstream of TALEN target sites in cDNA template and contain IUO sequences. cDNA contains spliced coding sequence of the respective TCR chain as well as barcoded (NNNNNN) switch oligo sequence that was ligated via (rG)$_5$ added by SMARTScribe^{TM} reverse transcriptase (Clonetech). An IUO sequence is required for addition of Nextera® (Illumina) indices in subsequent PCR II reaction.

Once the DNA library was prepared using the new primer set, NGS utilizing MiSeq System (Illumina) was performed to identify T cell clones carrying a knockout of the endogenous TCR chains.

After adapting sample preparation for NGS analysis, the next step included the modification of the analysis tool for generated NGS data. For this, bioinformatic analysis was perfomed by A.

Moesch that identified the TALEN target sites in sequences obtained from NGS and subsequently align the sequences in between two TALEN target sites with the wildtype sequences of the *TRAC* and *TRBC* genes (Figure 4.27). Raw FASTQ reads were searched for both flanking TALEN target sites and the target sequence in between was aligned to the wildtype sequence. Reads containing the same mismatches, deletions, insertions or the wildtype sequences were grouped, and average read quality was calculated. To unambiguously identify whether a T cell clone contained wildtype or mutated sequences, a high number of reads was required, comprising an average read quality of at least 30.

Figure 4.27: Functional principle of the software for NGS data analysis. The software generated by A. Moesch identified TALEN target sites in sequences obtained from NGS and aligned the sequence in between two TALEN target sites with the wildtype sequence of the *TRAC* and *TRBC* genes, respectively. Clustering of reads comprising the same sequence allowed the hierarchical ordering of the resulting sequences to identify the sequence supported by the largest number of reads.

Shown in Figure 4.28 is an exemplary output file summary for the different possible results for the knockout status of individual T cell clones. If no mutation could be detected in the TALEN target region, the results were homologous to the wildtype sequence indicated as "WT". When mutations have been introduced, the modified sequence was displayed. This allowed the deeper analysis of the type of mutation that occurred as a consequence of base deletions or insertions, respectively, since only frame-shift mutations would most definitely result in non-functional proteins. The translation of these frame-shift mutations generates aberrant amino acid sequences that frequently result in the introduction of premature stop codons preventing the expression of a functional protein, hence knocking out the respective gene. While T cell clones usually only express one rearranged TCR β chain, they can carry two TCR α chains due to simultaneous rearrangements of the TCR α locus on both alleles (Petrie *et al.*, 1993). Allelic exclusion of a functional TCR α chain is thought to occur only after positive selection in the thymus (Borgulya *et al.,* 1992; Malissen *et al.,* 1992). This normally results in the expression of one functional TCR α chain that pairs with the corresponding TCR β chain. However, unproductive TCR α chains originating from the second silenced TCR α locus can

sometimes be detected at the mRNA level (Malissen *et al.*, 1992). In rare cases even two productive TCR α chains can be found in one cell giving rise to two independent TCRs (Padovan *et al.*, 1993). When two TCR α chains were detected in one sample, the variable region of the TCR sequence that was also amplified during the NGS sample preparation was analyzed utilizing the software MiTCR (Bolotin *et al.*, 2013). The output sequence could then be evaluated for productive or unproductive TCR α chain rearrangements using the IMGT® tool IMGT/V-QUEST (Lefranc *et al.*, 2015).

Example output:

	β chain	α chain 1	α chain 2	Status
Clone 1	WT	unproductive	TGCCGTGT**A**ACCAGCTGAGAG	α KO
Clone 3	TGTG---GAGAGCCATCAG	WT	–	β KO
Clone 4	WT	WT	–	no KO
Clone 5	TGTGTTTG--CCATCAG	TGCCGTGT-CCA-CTGAGAG	unproductive	α/β KO

Figure 4.28: Exemplary output file for determination of TCR knockout status based on NGS data. Results of sequence alignments of the TALEN target sites with wildtype sequences of *TRAC* and *TRBC* genes for individual T cell clones. WT indicates no modification of the sequence. Dash (-) indicates base deletion and letters marked in red indicate base insertions. Knockout of either TCR chain only occurs when mutations in the TALEN target site result in frame-shift mutations. Unproductive TCR chains were identified by analysis of the NGS data utilizing MiTCR software and IMGT/V-Quest tool. Dependent on mutations in the TCR α or β constant regions, the cells exhibited either α, β, $\alpha\beta$ or no knockout (KO).

A total of 161 T cell clones were selected for NGS and subsequently analyzed for TCR knockout status as described above. Three positive controls were included, that comprised T cell clones not exhibiting a TCR knockout based on the phenotype. Based on NGS data, nine T cell clones could be identified that unambiguously contained a knockout of both the TCR α and β chain (6%; Figure 4.29). 38% of the analyzed T cell clones comprised cells with a knockout of either the TCR α or β chain, while 14% did only contain wildtype sequences of both TCR chains. A relatively large fraction of T cell clones (42%) could either not be analyzed due to low NGS data quality or comprised cells with two TCR α chains, with only one of the α chains containing mutations in the constant region. Since for universal recipient

% TCR α and β KO
% TCR α or β KO
% To be determined
% No TCR KO

Figure 4.29: Summary TCR knockout status based on NGS analysis. 158 T cell clones were analyzed. Description see text.

cells a knockout of both TCR chains would be preferable, further experiments focused on T cell clones comprising a knockout of both the TCR α and β chains. As controls, selected T cell clones comprising an unambiguous knockout of either the TCR α or β chain were also included in subsequent experiments.

4.5 Characterization of TCR-deficient T cell clones

The new strategy for generation of universal recipient cells resulted in a large number of T cell clones that lost expression of the endogenous TCR while being successfully transduced with the CAR construct, according to flow cytometric data. Selected T cell clones that showed the desired phenotype, in combination with promising proliferative capacity, were evaluated for their TCR knockout status at the mRNA level by NGS analysis. T cell clones whose TCR knockout could be confirmed in NGS analysis were selected for further characterization to investigate their suitability as universal recipient cells. Certain criteria have to be met by a T cell clone in order to qualify as a suitable test system for the characterization of transgenic TCRs. First, the cells have to exhibit high proliferative capacity in order to allow the expansion of sufficient numbers of cells for *in vitro* experiments. Second, TCR knockout has to be achieved in the cells to enable expression of the transgenic TCR without dominant effects of the endogenous TCR, while the cells should otherwise retain their natural phenotype. And third, the TCR-deficient cells have to exhibit all effector functions required for a physiological read-out of transgenic TCR specificity, killing capacity and functional avidity. This extensive evaluation was performed with either CD19-CAR or CD3-Chimera-expressing T cell clones, respectively.

4.5.1   CD19-CAR-transduced universal recipient cells

4.5.1.1 Proliferative capacity

For univeral recipient cells to be of value as an *in vitro* test system, they need to exhibit high proliferation rates over multiple *in vitro* restimulation cycles. Therefore, 21 selected TCR-deficient T cell clones were expanded over a period of 56 days, while CAR-specific stimulation of the cells was performed every 14 days utilizing $1 - 2 \times 10^6$ irradiated LCL and $5 - 8 \times 10^6$ feeder cells in the presence of IL-2 (Figure 4.30). All of the selected clones carried the knockout of the endogenous TCR as verified by NGS analysis. Clone CD4$^+$_50, which still expressed the endogenous TCR, served as a positive control for proliferation in the presence of the TCR-complex.
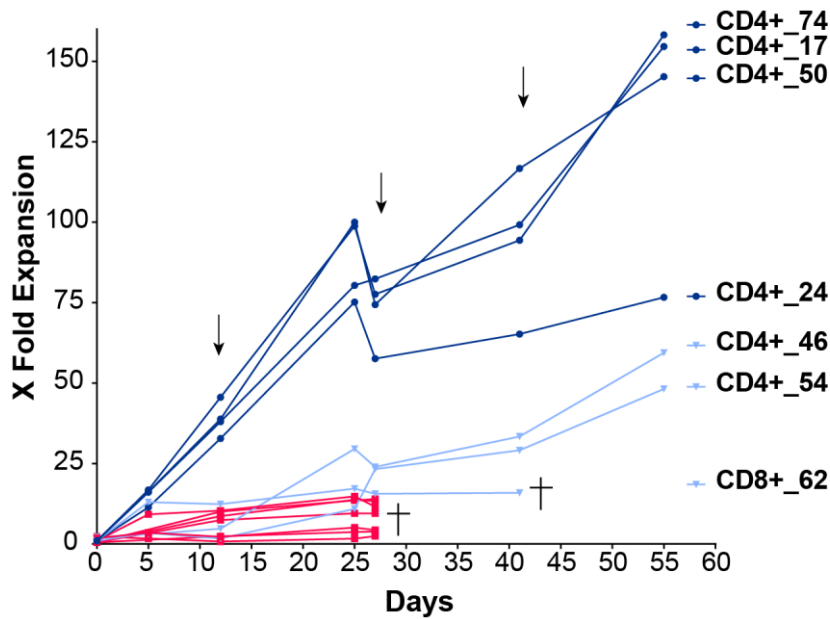
Figure 4.30: Fold expansion of selected TCR-deficient CD19-CAR expressing T cell clones over a period of 56 days. 21 selected T cell clones were expanded by repeated CAR-specific stimulation every 14 days indicated by arrows. Cell count was determined after each expansion period and calculated to total fold expansion. Clone CD4+_50 that still expressed the endogenous TCR serves as control to evaluate proliferative capacity. Crosses indicate that T cell clones could not be expanded further and were categorized as dead. 21 T cell clones categorized as exhibiting high (dark blue), moderate (light blue) and low (red) proliferation rates.

Of the 21 selected T cell clones that were initially activated on day 0, only seven could be expanded longer than 28 days (Figure 4.30). While 10 CD8+ T cell clones and 11 CD4+ T cell clones, including control Clone CD4+_50, were chosen based on NGS analysis and phenotype, only CD4+ T cell clones could be expanded over the entire 56-day period. All CD8+ T cell clones, except for Clone CD8+_62, went into apoptosis after the second expansion period. Clone CD8+_62 could be stimulated again on day 28, but failed to proliferate after the second stimulation. In contrast, the T cell clones exhibiting high proliferation rates, CD4+_74, CD4+_17, CD4+_50 and CD4+_17, continued to expand at comparable levels even after repeated stimulation. The moderately expanding T cell clones, CD4+_46 and CD4+_54, did not expand well after the first stimulation, but increased their proliferation rates upon repeated stimulation. In summary, only TCR-deficient CD4+ T cell clones could be expanded to sufficient cell numbers via engagement of the transduced CD19-CAR. The drop in the expansion rate after day 25 showed that cell numbers decline after day 11 following activation, which indicated that in order to achieve maximal proliferation rates, the cells would have to be activated every 11 days instead of every 2 weeks. This 11-day stimulation cycle was used for further cultivation of the cells.

4.5.1.2 NGS results and phenotype

The NGS results and knockout (KO) status for the six TCR-deficient T cell clones that could be expanded longer than 28 days are summarized in Table 4.1. Based on NGS results the KO status of the individual T cell clones was categorized as comprising a knockout of both TCR chains (α + β) or only of the TCR β chain (β). CD19-CAR-positive Clone CD4+_50 still expressing the endogenous TCR, served as a positive control to validate the integrity of the

performed data analysis. The NGS data were analyzed as described before and the results were additionally confirmed by RACE PCR.

Table 4.1: NGS results for TCR-deficient CD19-CAR-transduced T cell clones.

Clone	β chain	α chain 1	α chain 2	KO status
74	TG--------CTTCAG*	TG-------------AGAG	TGCCGTG-ACCAGCTGAGAG	α (+ β)
24	TGTGTTTGA--CATCAG	WT	unproductive	β
17	TGTGTTT**T**GAGCCATCAG	unproductive	TGCCGTGTA**A**CCAGCTGAGAG	α + β
54	TGTG-TTGAGCCATCAG	TGCCGTGTA**A**CCAGCTGAGAG	–	α + β
46	TGTG-TTGAGCCATCAG	unproductive	WT	β
62	TGTGTTTGA-CCATCAG	unproductive	TGCCGTGTA**A**CCAGCTGAGAG	α + β
50	WT	WT	unproductive	**No KO**

*in-frame mutation

All mutations detected in NGS led to frame-shift mutations that resulted in a premature stop codon rendering the protein non-functional, except for Clone CD4$^+$_74 in which an in-frame mutation was introduced by the TALEN pairs targeting the TCR β chain. Therefore, the KO status was indicated as "α (+ β) KO", since the effect of this mutation on the functionality of the TCR β chain could not be predicted. For most of the T cell clones a second rearranged TCR α chain was detected by NGS and the identification of the productive chain was performed by MiTCR analysis in combination with the IMGT/V-Quest tool as described before.

After a 42-day expansion period, the phenotype of the TCR-deficient T cell clones was re-examined by flow cytometry to ensure that the expanded cells still expressed the respective co-receptor while lacking TCR expression (Figure 4.31). Clone CD4$^+$_50 served again as a positive control to ensure proper binding of the antibody.

Co-receptor	CD4+	CD4+	CD4+	CD4+	CD4+	CD8+
KO status	α (+ β)	β	α + β	α + β	β	α + β
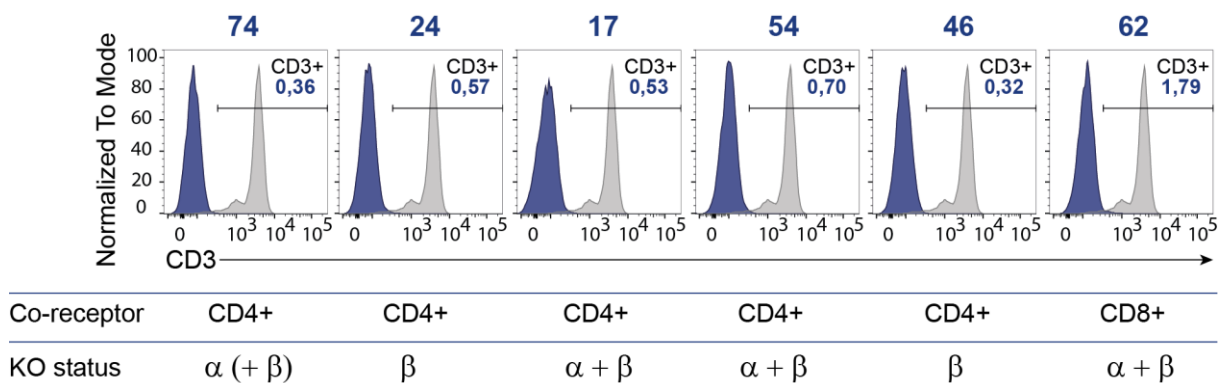
Figure 4.31: Combination of phenotype and knockout status of the CD19-CAR-transduced T cell clones. Phenotype of TCR-deficient T cell clones (blue) was determined after 42-day expansion period by staining with α-CD3, α-CD4 and α-CD8 antibodies and subsequent flow cytometric analysis. TCR-positive Clone CD4$^+$_50 served as positive control (gray). Co-receptor expression was also determined by flow cytometry and results are indicated below the histograms. Knockout status was determined by NGS analysis and is shown below histograms for each T cell clone.

All of the selected T cell clones did not express the TCR complex on the cell surface indicating the knockout of the endogenous TCR, which was additionally verified by NGS analysis (Figure 4.31). While some of the clones exhibited mutations in both TCR chains, some clones only contained mutations in the *TRBC* locus. However, independent of knockout status, the TCR could not be expressed on the cell surface when one or both TCR chains, respectively, exhibited frame-shift mutations. Additionally, even in the absence of the endogenous TCR, all T cell clones still expressed the CD4 or CD8 co-receptor, respectively.

In order to verify that the knockout of the endogenous TCR complex did not have any impact on the phenotype of the expanded T cell clones, they were stained with antibodies for common T cell markers defining the T cell subset affiliation (Figure 4.32).
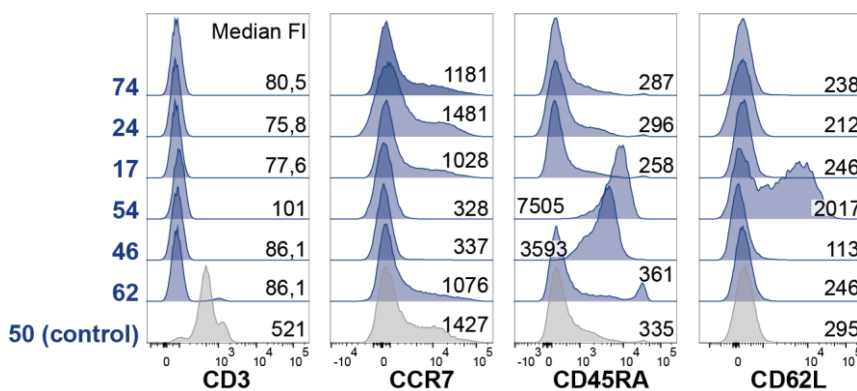
Figure 4.32: Phenotype of TCR-deficient T cell clones. The selected T cell clones exhibiting a knockout of the endogenous TCR (blue) were stained with α-CD3, α-CCR7, α-CD45RA and α-CD62L antibodies and analyzed by flow cytometry. Endogenous TCR-expressing T cell clone, Clone CD4+_50, served as control (gray). Noted median FI indicated levels of cell surface expression of the respective phenotypic marker.

The phenotype of the T cell clones 74, 24, 17 and 62 was comparable to the control and resembled a CCR7- CD45RA- CD62L- effector-memory phenotype as observed before for other T cell clones from *in vitro* cultures (Figure 4.32). Clones 54 and 46 exhibited expression of CD45RA, characterizing them as more terminally differentiated effector T cells. However, a large fraction of clone 54 cells additionally expressed CD62L, which is normally expressed on naïve or central-memory T cell subsets (Golubovskaya and Wu, 2016).

4.5.1.3 Functional experiments

To validate effector functions of the TCR-deficient T cell clones, a well-characterized TCR recognizing the NY-ESO-1 antigen was transduced into each T cell clone. This HLA-A2-restricted TCR, termed NY-ESO TCR, recognizes the peptide SLLMWITQC corresponding to the residues 157 to 165 of NY-ESO-1 (NY-ESO-1$_{157-165}$) (Longinotti, 2018). Successful transduction of the respective TCR-deficient T cell clones with the transgenic NY-ESO TCR could be easily monitored by re-expression of endogenous CD3 together with the introduced transgenic TCR on the cell surface. Expression of the transgenic TCR was verified by binding of α-TCRVβ1 antibody recognizing the TCR β chain of the NY-ESO TCR. Using these cell surface markers, the NY-ESO TCR-transduced cells were enriched by FACS (Figure 4.33c).

High purity of transduced cells could be achieved by FACS enrichment, which was indicated by over 95% double-positive cells. The lack of CD3 and TCR β chain expression in untransduced TCR-deficient cells demonstrated that endogenous CD3 will only be present on the cell surface when a functional TCR is translated, thereby proving the knockout of the endogenous TCR in the isolated T cell clones (Figure 4.33c). The enriched NY-ESO TCR-positive T cell clones were expanded, using a rapid expansion protocol utilizing OKT-3 antibody, before they were used in subsequent functional experiments.

To investigate the killing capacity of the NY-ESO TCR-expressing T cell clones, tumor cell killing mediated by the enriched cells was monitored utilizing the IncuCyte® ZOOM System (Essen Bioscience). The cytotoxic capacity of T cell clones expressing the NY-ESO-1-specific TCR was visualized by the disappearance of IncuCyte® NucLight Red-labeled antigen-positive tumor cell line Mel624.38 (Figure 4.33a). To assess the specificity mediated by the introduced TCR the targeting of IncuCyte® NucLight Red-labeled NY-ESO-1-negative 647-V cells was monitored as a control. Specific activation of the TCR-transduced T cell clones was additionally assessed by IFN-γ release 20 hours after co-culture with the respective tumor cells (Figure 4.33b). The supernatants utilized in IFN-γ ELISA were derived from the same co-culture used in the killing assay described above. Additional controls were used for ELISA co-culture that included CD19-positive LCL to determine activation of the respective T cell clones via the transduced CAR and the T cell clones alone to detect any background IFN-γ release when no target cells were present.

Simultaneous expression of CD3 and the transgenic TCR in transduced cells allowed the assumption that a functional TCR-complex was present in these cells (Figure 4.33c). This could be proven by high levels of IFN-γ release of TCR-transduced cells after co-culture with NY-ESO-1-expressing Mel624.38 cells (Figure 4.33b). The transduced T cell clones did not produce any IFN-γ in the presence of NY-ESO-1-negative 647-V tumor cells, indicating that the activation of the cells was mediated specifically via the introduced NY-ESO TCR. IFN-γ release upon interaction with CD19-positive LCL served as a positive control that demonstrated the functionality of the expressed CD19-CAR and the general ability of the isolated T cell clones to produce this cytokine. This could be nicely observed for the T cell clones 74, 46 and 54. However, clone 17 failed to produce IFN-γ upon CAR engagement. No detection of IFN-γ in the absence of any target cells demonstrated that the isolated TCR-deficient T cell clones did not spontaneously release IFN-γ and that the specificity was mediated through the transduced TCR or CAR, respectively. While IFN-γ release indicated specific recognition of the target antigen, it did not necessarily demonstrate specific killing. As shown in Figure 4.33a, specific lysis of the NY-ESO-1-expressing Mel624.38 tumor cells could only be achieved by the T cell clones 74 and 17, indicated by decreasing tumor cell numbers,

even though IFN-γ release was comparable for all T cell clones after co-culture with this target cell line (Figure 4.33b). While the specificity of all TCR-deficient T cell clones could be redirected via introduction of the transgenic TCR, not all of them exhibited the capacity to kill target cells. Proliferation of NY-ESO-1-negative 647-V cells was not influenced by the presence of the transduced T cell clones, which again demonstrated the specificity mediated by the introduced NY-ESO TCR (Figure 4.33a).
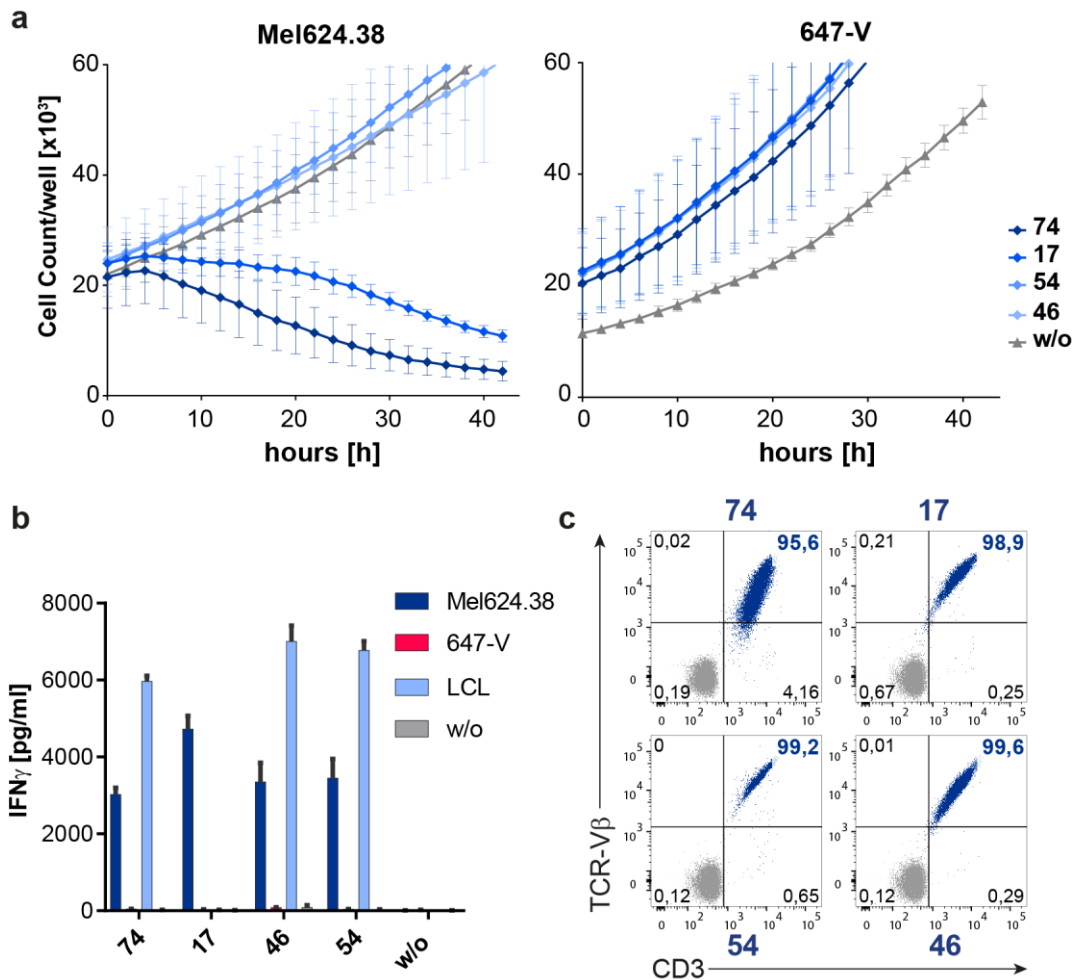
Figure 4.33: Effector functions of isolated T cell clones after introduction of transgenic NY-ESO-1-specific TCR. a) Killing assay utilizing the IncuCyte® ZOOM System to monitor killing of NY-ESO-1-positive (Mel624.38) and -negative (647-V) tumor cells labeled with IncuCyte® NucLight Red dye over 42 hours with E:T ratio of 2:1. Respective tumor cells alone (grey) served as control for proliferation in the absence of effector cells. Cell count/well was determined by using IncuCyte® ZOOM Software 2016B to analyze quadruplicates of each approach. **b)** IFN-γ ELISA of supernatants derived from the same co-culture after 20 h of incubation. Co-culture with LCL (CD19-positive, light blue) served as positive control for the transduced CD19-CAR. T cell clones without any target cells (w/o, gray) were used as negative control to assess background activation of the transduced T cells. **c)** Flow cytometric analysis of NY-ESO TCR-expressing T cell clones after enrichment by FACS. NY-ESO TCR-transduced T cell clones (blue) were stained with α-CD3 and α-TCR-Vβ1 antibody specific for the TCR β chain of the NY-ESO TCR. The same antibodies were used for FACS enrichment of the cells 10 days after transduction. The respective untransduced T cell clones served as negative control (gray) to determine purity of the sorted cells expressing the transgenic TCR.

4.5.2 CD3-Chimera-transduced universal recipient cells

4.5.2.1 Proliferation

In contrast to T cell clones transduced with the CD19-CAR, which mediates activation via CD19 antigen recognition, cells expressing the CD3-Chimera construct have to be stimulated in an antigen-independent manner. As described in 4.4.1.2, the proposed mode of action includes the activation of the transduced TCR-deficient T cell clones via engagement of the CD3-Chimera construct by binding of α-CD3 OKT-3 antibody that exhibits mitogenic properties (Van Wauwe, De Mey and Goossens, 1980). To deliver the required co-stimulation for proper activation, α-CD28 antibodies or CD28-interacting molecules, like CD80 or CD86 can be used. To assess the proliferative capacity, CD80- and CD86-expressing LCL were chosen to generate a more natural co-stimulatory signal in activated T cell clones. In contrast to the CD19-CAR approach, where 369 T cell clones could be isolated after the first stimulation period, only eight CD3-Chimera-transduced T cell clones could be detected. Four T cell clones exhibiting initial promising proliferative capacity, were further analyzed for their expansion over 56 days (Figure 4.34a). For repeated stimulation via the transduced CD3-Chimera construct, the isolated T cell clones were co-cultured with $1 - 2 \times 10^6$ irradiated LCL and $5 - 8 \times 10^6$ feeder cells in the presence of IL-2 and OKT-3 antibody. Clone CD4$^+$_50, which expressed the CD19-CAR and did not comprise a TCR knockout, was used as a control to compare expansion via CD3-Chimera engagement to physiological activation via the TCR. To ensure that activation of the TCR-deficient T cell clones was mediated through the CD3-Chimera construct, two promising T cell clones, CD8$^+$_001 and CD8$^+$_002, were stimulated with and without OKT-3 antibody (Figure 4.34b).
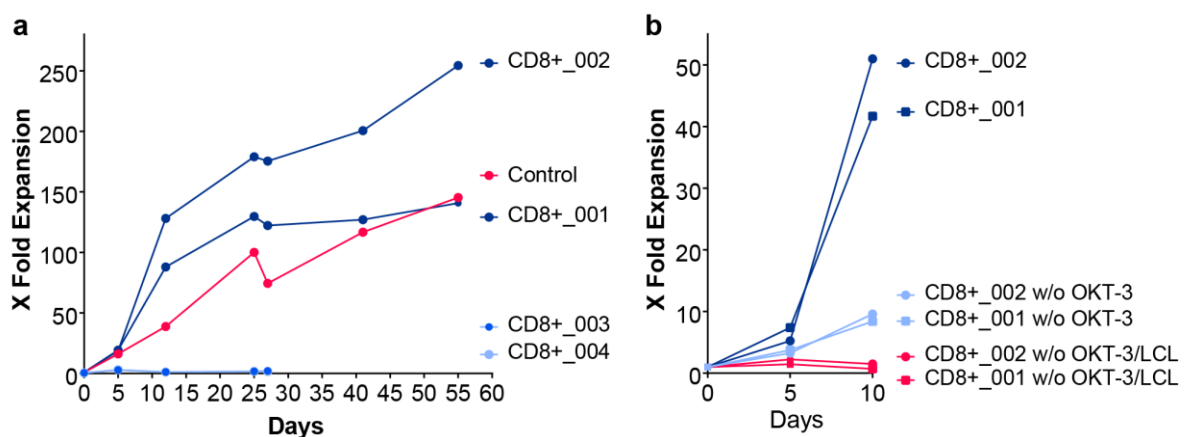
Figure 4.34: Fold expansion of TCR-deficient T cell clones transduced with CD3-Chimera construct. a) Fold expansion of 4 T cell clones, CD8$^+$_001, CD8$^+$_002, CD8$^+$_003 and CD8$^+$_004, over 56 days by repeated stimulation every 14 days. Cell count was determined at least after each expansion period. Clone CD4$^+$_50 served as a control (red) to compare proliferative capacity. **b)** Fold expansion of 2 selected T cell clones over 1 stimulation cycle under different activation conditions. Cells were either stimulated with complete stimulations mix (dark blue) comprising LCL, feeder cells, IL-2 and OKT-3 antibody, or with stimulation mix lacking OKT-3 (light blue) or OKT-3 and LCL (red), respectively. Cell count was determined on day 5 and 10.

While two of the TCR-deficient T cell clones died after two rounds of stimulation, Clone CD8$^+$_001 und CD8$^+$_002 showed exceptional proliferative capacity (Figure 4.34a). With more than 100-fold expansion after 56 days, Clone CD8$^+$_001 exhibited comparable proliferation rates to the control. Clone CD8$^+$_002 even reached 250-fold expansion after 56 days of *in vitro* culture. The observed high proliferation rates of the two TCR-deficient T cell clones were induced by binding of OKT-3 antibody, since cells that were activated in the absence of OKT-3 failed to expand (Figure 4.34b). CD3-Chimera-expressing T cell clones that were activated without OKT-3 antibody or LCL went into apoptosis, while cells that still received co-stimulatory signals via LCL survived, but expanded only about 9-fold. In contrast, cells that were activated in the presence of OKT-3 antibody and co-stimulatory cells expanded 40 – 50-fold, indicating that OKT-3 antibody is required to achieve maximal stimulation.

4.5.2.2   NGS results and phenotype

Based on proliferative capacity, only the T cell clones CD8$^+$_001 and CD8$^+$_002 were further characterized for suitability as universal recipient cells. For this, the NGS data were analyzed to determine the TCR knockout status of these cells as described above. Table 4.2 summarizes the results of the NGS analysis demonstrating that Clone CD8$^+$_001 carried mutations in the *TRAC* gene, while CD8$^+$_002 exhibited base deletions in the *TRBC* gene. Both resulted in frame-shift mutations that introduced a pre-mature stop codon in the amino acid sequence of the constant regions, thereby preventing cell surface expression of the TCR-complex.

Table 4.2: NGS results for TCR-deficient CD3-Chimera-transduced T cell clones.

Clone	β chain	α chain 1	α chain 2	KO status
001	WT	unproductive	TGCC-------AGCTGAGAG	α
002	TGTG----AG—ATCAG	WT	–	β

While the knockout of the endogenous TCR could also be visualized by flow cytometric analysis, the expression of the transduced CD3-Chimera construct could not be detected by α-CD3 antibody staining (Figure 4.35a, b). Since most of the CD3 antibodies used were derived from the clone UCHT-1, the cells were additionally stained with α-CD3 antibody OKT-3 conjugated to eFluor 450 dye (Figure 4.35b). In this way the same antibody used for activation of the cells was also used for detection, even though both antibodies should be able to bind the CD3ε subunit present in the CD3-Chimera construct (Arnett, Harrison and Wiley, 2004; Kjer-Nielsen *et al.*, 2004). To exclude that the antibody concentrations used were not sufficient to detect the CD3-Chimera construct on the cell surface, 5-fold higher amounts of α-CD3

antibody were used (Figure 4.35c). TCR complex-expressing T cell clone CD4$^+$_50 was used as a positive control, while TCR-deficient T cell clone CD4$^+$_74 transduced with CD19-CAR was utilized as a negative control for antibody staining.
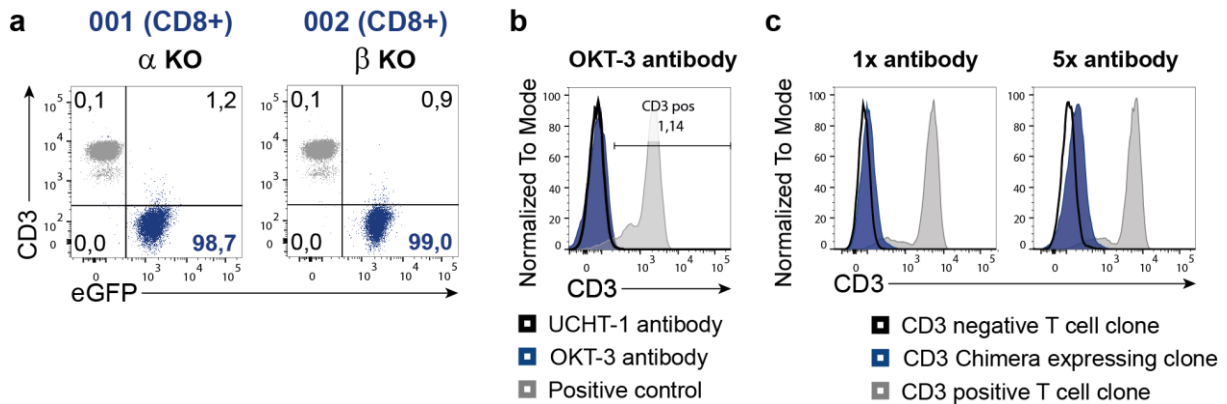
Figure 4.35: CD3 staining of CD3-Chimera-transduced TCR-deficient T cell clones. a) Staining of TCR-deficient T cell clones CD8$^+$_001 and CD8$^+$_002 (blue) with α-CD3 antibody and subsequent analysis by flow cytometry. Expression of eGFP indicated successful transduction with CD3-Chimera construct. **b)** Staining of Clone CD8$^+$_002 with α-CD3 antibody either derived from clone UCHT-1 (black) or OKT-3 (blue) and subsequent flow cytometric analysis. **c)** Staining of Clone CD8$^+$_002 (blue) with α-CD3 antibody using normal antibody concentration (1x antibody) or 5-times the usual concentration (5x antibody), respectively, followed by analysis by flow cytometry. TCR-deficient T cell clone CD4$^+$_74 was used as a negative control (black). For all approaches (a-c) TCR-complex-expressing T cell clone CD4$^+$_50 was used as a positive control (gray).

The two CD3-Chimera-transduced T cell clones that either comprised a knockout of the TCR α or β chain, respectively, exhibited the same phenotype as TCR-deficient T cell clones transduced with CD19-CAR (Figure 4.35a). The lack of CD3 or TCR$\alpha\beta$ expression indicated the successful knockout of the endogenous TCR, while expression of eGFP demonstrated a successful transduction with the CD3-Chimera construct. However, in contrast to the CD19-CAR, the CD3-Chimera construct should have been detected by α-CD3 antibody staining thereby resulting in a TCR$^-$ CD3$^+$ phenotype. Even staining with high amounts of α-CD3 OKT-3 antibody, which was also used for activation of the cells, did not result in a positive staining of CD3-Chimera-transduced cells, while TCR-complex-positive cells could be nicely detected with both antibodies (Figure 4.35b). Direct comparison of CD3 staining of CD3-Chimera-transduced T cell clone CD8$^+$_002 with the negative control clone CD4$^+$_74 (CD19-CAR-positive, CD3-negative) revealed a slight positive shift of the clone CD8$^+$_002 population compared to the negative control (Figure 4.35c). When the antibody concentration was increased 5-fold, the detected positive shift of α-CD3-stained clone CD8$^+$_002 could be slightly increased compared to the negative control. While the positive control was also stained at both antibody concentrations, the 5-fold higher antibody concentration also resulted in a comparable positive shift of the CD3-positive population. In summary, no distinct CD3-positive population could be detected for T cell clones transduced with CD3-Chimera, independent of

antibody clone or concentration. In contrast to the proliferation experiments, which demonstrated the mitotic properties and functionality of OKT-3 antibody (Figure 4.34b), OKT-3 was not able to detect the chimeric construct in the flow cytometric analysis.

To verify that the isolated TCR-deficient T cell clones, that exhibited high proliferation rates, still maintained the characteristic phenotype of *in vitro* cultured T cells, the cells were stained for common T cell markers (Figure 4.36). Clone CD4+_50 served as a control to compare the expression levels of selected cell surface markers.
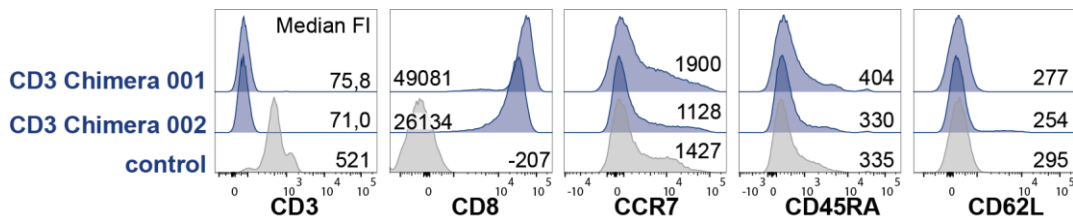
Figure 4.36: Phenotype of TCR-deficient T cell clones transduced with CD3-Chimera. The two CD8+ T cell clones 001 and 002 (blue) were stained with α-CD3, α-CCR7, α-CD45RA and α-CD62L antibodies and analyzed by flow cytometry. Endogenous TCR-expressing T cell clone, Clone CD4+_50, served as control (gray). Noted median FI indicated levels of cell surface expression of the respective phenotypic marker.

The CD3-Chimera-transduced T cell clones exhibited a CCR7-CD45RA-CD62L- effector-memory phenotype resembling the control (Figure 4.36). In contrast to Clone CD4+_50 they expressed the co-receptor CD8 and lacked CD3 expression, as observed before. Therefore, the isolated T cell clones showed a normal phenotype for *in vitro* cultured T cells.

4.5.2.3 Functional experiments

As mentioned before, high proliferative capacity and TCR knockout are two prerequisites for suitable universal recipient cells, which are met by the two isolated T cell clones. However, the third characteristic these cells need to display is retention of effector functions required for physiological read-outs after transgenic TCRs have been introduced. In order to evaluate the killing capacity, the two TCR-deficient T cell clones, CD8+_001 and CD8+_002, were transduced with two well-characterized TCRs recognizing the antigen tyrosinase. These TCRs, T58 and D115, bind the same tyrosinase$_{369-377}$ peptide (YMDGTMSQV) presented by HLA-A2 in a CD8-dependent manner. However, while T58 is characterized as a TCR conferring high functional avidity in a transgenic setting, T cells expressing transgenic D115 TCRs show lower functional avidity to the same target (Wilde *et al.*, 2009). Utilizing these two TCRs allowed a detailed evaluation of the functionality as well as sensitivity of the CD3-Chimera-transduced T cell clones when transgenic TCRs were introduced. To use high-purity cell preparations in further experiments, the transduced cells were enriched by FACS after staining with α-CD3 and specific TCR-Vβ antibodies (T58: α-TCR-Vβ23; D115: α-TCR-Vβ8) (Figure 4.38a). To allow a direct comparison with PBL, which have served as the standard test system for

transgenic TCRs up to date, freshly isolated PBL were also transduced with the two tyrosinase-specific TCRs and prepared in the same manner as described for the isolated T cell clones.

In order to assess the killing capacity of the enriched TCR-transduced T cell clones, clone CD8$^+$_001 and CD8$^+$_002 as well as transgenic TCR-expressing PBL were co-cultured with tyrosinase-positive Mel624.38 or tyrosinase-negative A375 cells, respectively (Figure 4.37). Outgrowth of the IncuCyte® NucLight Red-labeled tumor cells was monitored utilizing the IncuCyte® ZOOM System (Essen Bioscience) over a period of 72 hours. The tumor cell killing mediated by the T cell clones CD8$^+$_001 and CD8$^+$_002 expressing either TCR T58 or D115, was compared to tumor cell lysis induced by PBL transduced with the same TCRs. As an additional control, tumor cells were co-cultured under the same conditions with the respective untransduced T cell clones, which should not exhibit any activity due to lack of an endogenous TCR. Untransduced PBL served as a control to estimate the background killing mediated by various endogenous TCRs present in this complex mixture of different T cells.
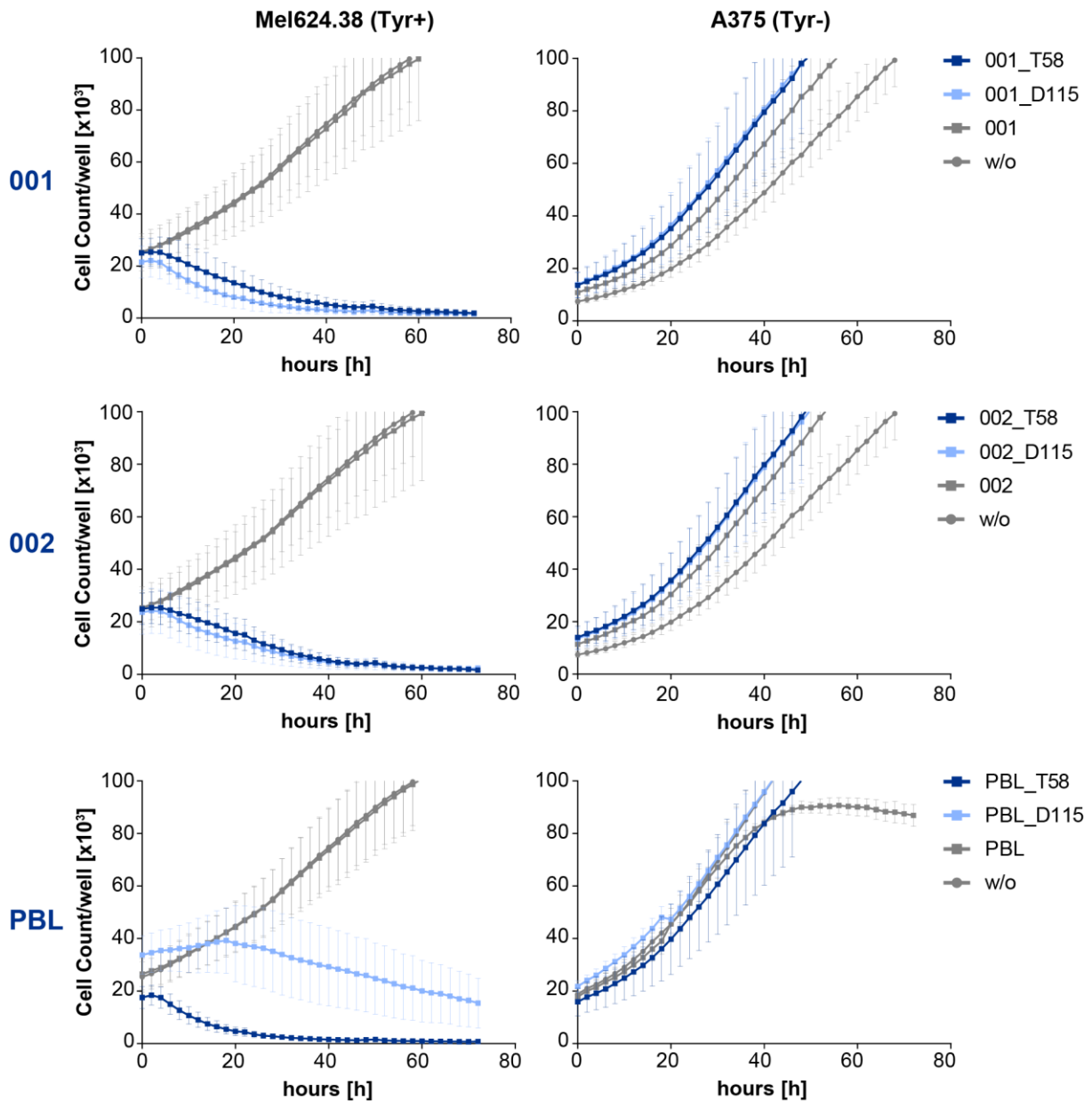
Figure 4.37: Killing capacity of isolated CD3-Chimera-expressing T cell clones after introduction of transgenic tyrosinase-specific TCRs T58 and D115. Killing assay utilizing the IncuCyte® ZOOM System to monitor killing of tyrosinase-positive (Mel624.38) and -negative (A375) tumor cells labeled with IncuCyte® NucLight Red dye over 72 hours with E:T ratio of 2:1. Respective tumor cells alone (grey dots) served as control for proliferation in the absence of effector cells. Untransduced effector cells (gray squares) served as control to estimate background killing in the absence of transgenic TCRs. Cell count/well was determined by using the IncuCyte® ZOOM Software 2016B to analyze quadruplicates of each approach.

The two T cell clones (CD8^{+}_001 and CD8^{+}_002) expressing either TCR T58 or D115, killed the tyrosinase-positive tumor cells, while tyrosinase-negative A375 cells were not targeted by the same effectors (Figure 4.37). Untransduced T cell clones CD8^{+}_001 and CD8^{+}_002 did not influence outgrowth of the respective target cells, indicating that the target specificity was mediated via the introduced transgenic TCR. PBL transduced with the transgenic TCRs could also eradicate tyrosinase-expressing Mel624.38 cells, while tyrosinase-negative cells were not affected by the same cells. However, PBL expressing the D115 transgenic TCR could not control tumor growth as efficiently as PBL transduced with T58, which exhibited higher

functional avidity. This difference in killing capacity was not observed in the isolated T cell clones CD8⁺_001 and CD8⁺_002 that lack an endogenous TCR. While transduced PBL did not kill A375 cells, untransduced control PBL seemed to target the tyrosinase-negative cells after 40 hours of co-culture. This indicated a background activity mediated by the mixture of different lymphocytes that was independent of the transgenic TCRs. In summary, the isolated TCR-deficient T cell clones exhibited the capacity to effectively kill tumor cells directed by the specificity of the introduced transgenic TCRs. However, different levels of killing capacity based on distinct functional avidities of the transgenic TCRs, T58 and D115, could only be observed in transduced PBL and were not detected in the TCR-deficient T cell clones CD8⁺_001 and CD8⁺_002.

IFN-γ release upon specific recognition of target cells by TCR-transduced effector cells was determined in order to evaluate the capacity to produce cytokines (Figure 4.38b). For this, the supernatants of the same cells used in the killing assay were collected 20 hours after co-culture and analyzed by IFN-γ ELISA. Additional positive controls to determine maximal IFN-γ release included activation of the isolated T cell clones and PBL with the mitogens phorbol 12-myristate 13-acetate (PMA) and ionomycin (Hashimoto *et al.*, 1991). Successful enrichment of TCR-transduced cells used in the co-culture experiments was determined by staining with α-CD3 and the respective α-TCR-Vβ-specific antibodies and subsequent flow cytometric analysis. Additionally, the cells were stained with α-CD3 antibody and a tetramer comprising the tyrosinase-derived peptide YMDGTMSQV (YMD) bound to *in vitro* synthesized HLA-A2 molecules coupled to a fluorescent dye (Figure 4.38a). These tetramers mimic the presentation of peptide via HLA-A2 molecules by antigen presenting cells and allows the estimation of expression of functional transgenic TCRs binding the peptide-MHC complexes by the transduced effector cells (Altman *et al.*, 1996). Since the TCR T58 and D115 recognize the same tyrosinase peptide bound to HLA-A2, cells transduced with both TCRs can be stained with the same tetramer.
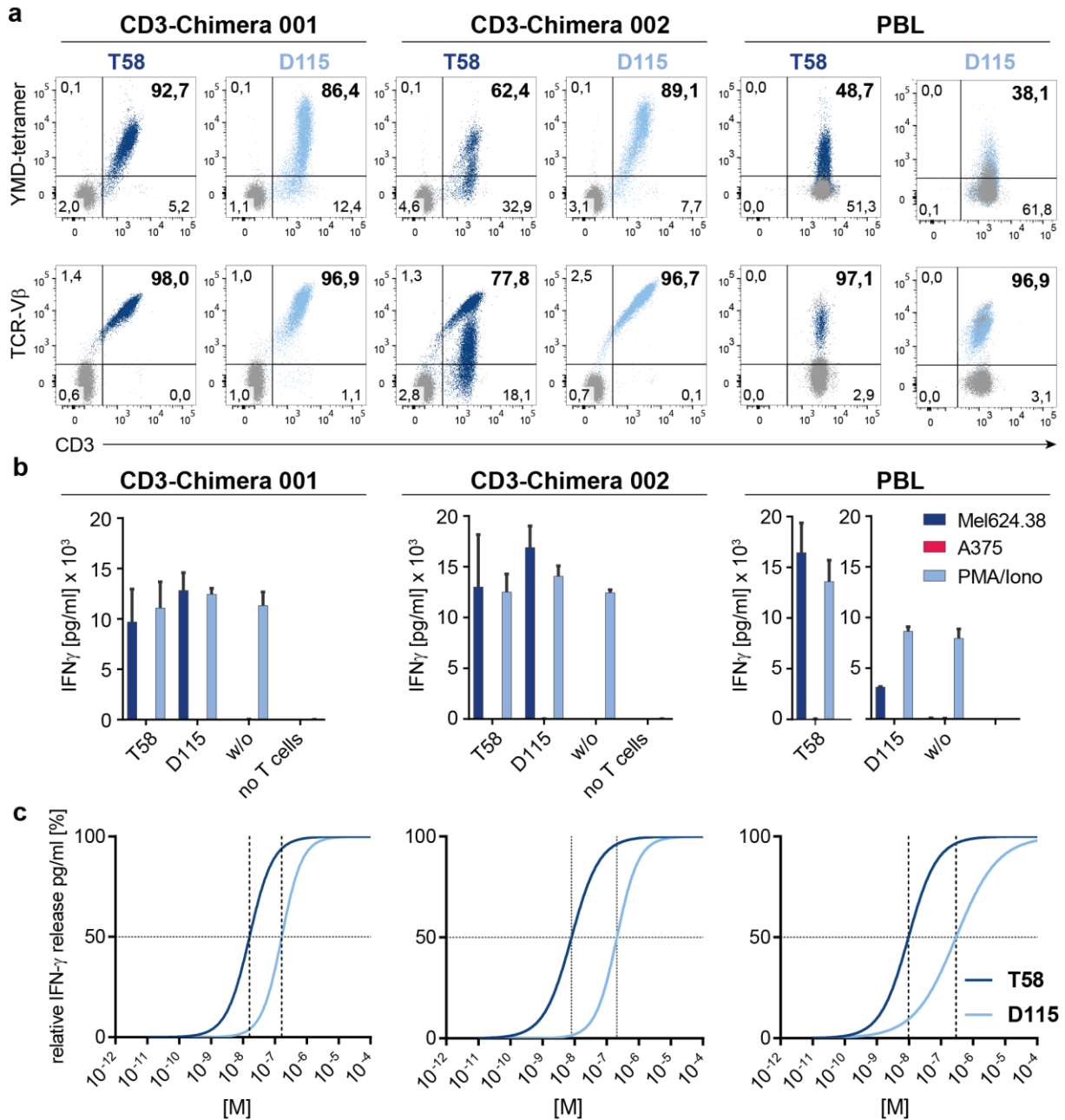
Figure 4.38: Effector function of CD3-Chimera-transduced T cell clones after introduction of tyrosinase-specific TCRs T58 and D115. a) Staining of isolated T cell clones (CD8+_001 and CD8+_002) and PBL transduced either with T58 (dark blue) or D115 (light blue), respectively, with α-CD3 and α-TCR-Vβ antibodies specific for the respective transgenic TCR β chain and tretramer comprising the YMDGTMSQV (YMD) peptide. After enrichment by FACS, cells were subsequently analyzed by flow cytometric analysis. Untransduced CD8+_001 and CD8+_002 T cell clones and untreated PBL were used as respective negative controls (gray). **b)** IFN-γ ELISA of supernatants derived from the same co-cultures used in the killing assay 20 hours after incubation of transduced T cells (CD8+_001, CD8+_002 or PBL) with target cells at an E:T ratio of 2:1. Positive control comprised effector cells activated with 750 ng/mL PMA and 5 ng/mL ionomycin (PMA/Iono). IFN-γ release of transduced PBL was determined in two independent experiments. Untransduced cells (w/o) served as negative control. Target cells comprised tyrosinase-positive (Mel624.38) and tyrosinase-negative tumor cells (A273). **c)** Functional avidity of TCR-transduced T cell clones (CD8+_001, CD8+_002) and PBL plotted as relative IFN-γ release to decreasing peptide concentrations. K562_A2_CD86 cells were loaded with decreasing amounts of peptide (10^{-4} to 10^{-12} M) and co-cultured with T58 or D115-expressing T cells, respectively, at fixed E:T ratio of 2:1. IFN-γ release was determined 20 hours later by IFN-γ ELISA and relative IFN-γ release was calculated by setting maximal IFN-γ release to the reference value of 100%. Lower values were calculated according to this reference. Values were derived from biological duplicates. Dashed lines indicate calculated EC50 values. K652_A2_CD86 cells loaded with 10^{-4} M irrelevant SLLMWITQC peptide served as negative controls.

IFN-γ release, determined 20 h after co-culturing TCR-transduced cells with the respective target cells, mirrored the observations made in the killing assay (Figure 4.37). Isolated T cell clones transduced with either T58 or D115, specifically recognized tyrosinase-positive Mel634.38 cells while showing no recognition of tyrosinase-negative A375 cells (Figure 4.38b). The amount of IFN-γ secreted by the T cell clones CD8$^+$_001 and CD8$^+$_002 was comparable when target cells were recognized via TCR T58 and D115, respectively. The amount of IFN-γ released upon specific activation was comparable to stimulation via the mitogens PMA and Ionomycin that trigger maximal cell activation. Untransduced T cell clones secreted the same amounts of IFN-γ as transduced clone CD8$^+$_001 and CD8$^+$_002 upon activation with PMA and ionomycin. However, untransduced T cell clones did not release IFN-γ when co-cultured with tumor cells. PBL transduced with TCR D115 secreted approximately 3-times lower amounts of IFN-γ when co-cultured with tyrosinase-positive target cells than T58-transduced PBL. This is in accordance with observations made in the killing assay, where D115-transduced PBL could not control tumor cell growth as efficiently as PBL expressing TCR T58, that confers higher functional avidity. However, the positive control comprising mitogen-based activation via PMA and ionomycin indicated that maximal IFN-γ release of D115-transduced cells was also lower compared to T58-transduced PBL. Unlike in the killing assay, no unspecific IFN-γ release of untransduced PBL upon incubation with tyrosinase-negative A375 cells could be observed. Staining with α-CD3 and α-TCR-Vβ antibodies indicated that enrichment of the transduced cells via FACS yielded TCR-Vβ$^+$CD3$^+$ cell populations exhibiting a purity of up to 98% (Figure 4.38a). For both T cell clones, CD8$^+$_001 and CD8$^+$_002, expression of the respective transgenic TCR β chains correlated with binding to the YMD-tetramer complex. Specific binding of the YMD-tetramer indicated the presence of functional transgenic TCRs on the cell surface, which was confirmed by IFN-γ ELISA and specific tumor cell killing (Figure 4.37b, Figure 4.38). T cell clone CD8$^+$_002 transduced with TCR T58 exhibited two distinct CD3-positive cell populations that bound the YMD-tetramer as well as the specific TCR-Vβ antibody to varying degrees. Nearly 97% of the TCR-transduced PBL showed expression of the respective transgenic TCR β chain. However, in contrast to isolated T cell clones, transgenic TCR β chain expression did not correlate with specific binding to the YMD-tetramer. Less than half of the enriched TCR-transduced PBL bound the YMD-tetramer, which indicated that PBL comprising various endogenous TCRs expressed lower amounts of functional transgenic TCR on the cell surface. This reduced transgenic TCR expression did not affect specific killing capacity or IFN-γ secretion of T58-transduced PBL exhibiting high functional avidity (Figure 4.37b, Figure 4.38). However, D115-expressing PBL, which exhibit a lower functional avidity, also showed reduced IFN-γ secretion and killing capacity when co-cultured with tyrosinase-positive tumor cells compared to T58-transdcued PBL.

Functional avidity is a biological measure to determine the sensitivity of T cell clones to varying concentrations of antigen *in vitro* and can therefore be considered the activation threshold of a given T cell clone (Viganò *et al.*, 2012). Therefore, T cell clones exhibiting high functional avidity require lower amounts of antigen to be activated compared to T cell clones of lower functional avidity. It has been shown that the sensitivity to antigen can be conferred to recipient cells via the introduced transgenic TCR (Wilde *et al.*, 2009). To investigate the functional avidity of the isolated T cell clones expressing the transgenic TCRs T58 and D115, compared to transduced PBL, the cells were co-cultured with target cells loaded with titrated amounts of YMD peptide (Figure 4.38c). As target cells K562 transduced with HLA-A2 and CD86 were used (K562_A2_CD86). IFN-γ release indicated activation of these cells and served as a measure to determine the antigen concentration required for half-maximal response (EC50), corresponding to measured functional avidity of the transduced T cells.

Peptide concentrations resulting in half-maximal IFN-γ release (EC50) were comparable in all three recipient cells (Figure 4.38c). All T58-transduced cells exhibited more than 10-fold higher functional avidity compared to the corresponding cells expressing TCR D115. EC50 for cells expressing T58 was calculated to be induced at peptide concentrations of nearly 10^{-8} M. In contrast, D115-transduced cells reached EC50 only at peptide concentrations ranging from 6.5 - 6.8 x 10^{-6} M. This demonstrated that the generated TCR-deficient CD3-Chimera expressing T cell clones, CD8$^+$_001 and CD8$^+$_002, could exhibit peptide sensitivities comparable to PBL when expressing the same transgenic TCR. Therefore, the sensitive parameter "functional avidity" did not change, which demonstrated that these TCR-deficient T cell clones can serve as a valid test system to evaluate functional avidity conferred to T cells by transgenic TCRs.

5   Discussion

The aim of this thesis included the generation of universal recipient cells that could be used as a test system for the high-throughput functional characterization of transgenic TCRs. These universal recipient cells should carry certain characteristics in order to qualify as a suitable TCR test system. First, the cells should proliferate to high cell numbers independent of the endogenous TCR via engagement of an introduced chimeric construct, e.g. a CAR. Second, expression of the endogenous TCR should be prevented by gene knockout to enable expression and testing of transgenic TCRs in these cells without dominant negative effects of the endogenous TCR or possible TCR mispairing. Third, the generated TCR-deficient cells should exhibit all effector functions required for a physiological read-out of specificity, killing capacity and functional avidity mediated by the transgenic TCR. To date, bulk PBL, comprising a diverse mixture of different lymphocyte subsets, are commonly used as TCR recipient cells. To avoid the introduction of unknown variables into experiments based on heterogenous reactivity profiles of PBL, universal recipient cells were generated from individual T cell clones. Using selected T cell clones, it was first determined whether proliferation of T cell clones could be induced by engagement of an introduced CAR construct independent of the endogenous TCR. For these experiments well-characterized CAR constructs recognizing the CEA antigen were utilized and allowed the establishment of a stimulation procedure suitable for expansion of individual T cell clones independent of subset origin. Once proliferation could be induced sufficiently in individual T cell clones, the endogenous TCR was targeted for knockout using the TALEN technology. Initial poor survival of TCR-deficient T cell clones via CEA-CAR engagement led to the generation of new chimeric constructs that should better promote proliferation of T cell clones in the absence of the endogenous TCR. These included a CD19-CAR construct published by Hudececk *et al.* and a CD3-Chimera construct that should mediate activation of T cells via binding of mitotic antibodies recognizing CD3. Using these chimeric constructs, a new high-throughput strategy could be developed that allowed the immediate identification of TCR-deficient T cell clones that could be expanded via engagement of CD19-CAR or CD3-Chimera, respectively. The procedure included analysis of mutations introduced by TALEN-mediated targeting of the TCR α and β chains using NGS, which allowed the confirmation of the TCR knockout status on mRNA level for each individual T cell clone. This process contributed to the characterization of candidate universal recipient cells and enabled the preferential selection of TCR-deficient T cell clones exhibiting a knockout of both TCR chains. Based on this screening procedure, candidate universal recipient cells were selected and investigated for effector functions upon introduction of transgenic TCRs. The steps and experimental procedures contributing to the generation of universal recipient cells are discussed in detail below.

5.1 T cell stimulation via chimeric antigen receptors (CARs)

The *in vitro* expansion of bulk PBL through CAR engagement has been investigated previously and resulted in cell numbers comparable to physiological TCR stimulation (Maher *et al.*, 2002; Finney, Akbar and Alastair, 2004). However, whether proliferation of individual T cell clones could be induced through CAR engagement sufficiently to be of use as an *in vitro* test system has not been shown before. Additionally, since CAR constructs were generally designed to mediate tumor cell killing rather than T cell expansion, the CAR domain structure best suited for physiological expansion of T cell clones *in vitro* had to be determined. Several clinical studies also demonstrated the importance of CAR-induced T cell proliferation for clinical benefit and led to the generation of second and third generation CARs comprising additional co-stimulatory domains to promote activation and persistence of T cells *in vivo* (Sadelain, Brentjens and Rivière, 2013). To investigate proliferation of T cell clones upon CAR engagement *in vitro*, an established CD4$^+$ T cell clone, Clone 234, was used as a first test system. Clone 234 was transduced with either CEA-CAR_CD4 or CEA-CAR_CD8, respectively, and could be successfully enriched via FACS (Figure 4.2a). Stable expression of the respective CAR construct was observed over a period of 42 days and was independent of TCR- or CAR-specific activation of the transduced T cells (Figure 4.2b). However, median FI values indicated that expression levels of CEA-CAR_CD4 were generally higher compared to CEA-CAR_CD8. No downregulation of either construct could be observed independent of the type of stimulation. When comparing X-fold expansion of the same cells over 42 days, it became apparent that proliferation rates of cells stimulated via CAR engagement were around 3-fold lower than for cells that were activated via the endogenous TCR (Figure 4.3). In this initial expansion period, the same stimulation conditions were used for both types of activation, which included 1 x 10^6 T cells per 24-well in co-culture with 0.3 x 10^6 irradiated TCR or CAR target cells, respectively. The low expansion rates of cells stimulated via CAR could be overcome by increasing the amount of CEA antigen present during activation. When E:T ratios were greater than 1:5 for CAR-specific activation, proliferation rates comparable to native TCR engagement could be reached (Figure 4.4b). While direct comparison of CAR- and TCR-mediated activation has been difficult due to their differences in antigen recognition and general structure, the TCR complex has been shown to be more sensitive compared to CARs that require higher amounts of antigen for activation of T cells (Harris and Kranz, 2016). Recently, a system has been developed by Stone *et al.* that allowed direct comparison by using the analog of a scFv, which comprised a single chain TCRVβ-TCRVα fragment, combined with typical CAR signaling domains (Stone *et al.*, 2014). However, also in this system, CAR constructs were 10 – 100-fold less sensitive than TCRs recognizing the same peptide-MHC complex, which indicated that signaling kinetics through the native TCR complex are more efficient (Harris *et al.*, 2017). Therefore, increasing antigen density is a sensible

measure to achieve comparable activation rates for T cells stimulated via CAR or TCR, respectively. While this might reveal limitations for the use of CARs in cancer immunotherapy, increasing the numbers of CAR target cells is feasible for the use in an *in vitro* test system where the introduced CAR is supposed to mediate proliferation of T cells rather than killing of tumor cells. In this context, high antigen density in combination with the presence of co-stimulatory molecules on B cells might contribute to the clinical efficacy of CD19-CARs observed in patients suffering from B cell malignancies (Kalos *et al.*, 2011; Porter *et al.*, 2011). Together, these results indicated that appropriate antigen density might have to be determined empirically for each CAR construct dependent on specificity and affinity of the scFv as well as intracellular signaling domains.

While both CEA-CAR constructs mediated proliferation of Clone 234, CEA-CAR_CD8 engagement did not result in IFN-γ release. In contrast, binding of CEA antigen by CEA-CAR_CD4 led to IFN-γ release, which increased proportionally to the numbers of target cells and peaked at an E:T ratio of 1:4 (Figure 4.4a). This demonstrated that secretion of IFN-γ does not necessarily correlate with induction of proliferation in individual T cell clones. Both CAR constructs carry the same α-CEA scFv, but differ in the composition of their signaling domains (Figure 4.1). While CEA-CAR_CD4 comprised a 4-1BB singling domain coupled to a CD4 transmembrane domain, CEA-CAR_CD8 contained a CD28 transmembrane and signaling domain. This showed that in the established CD4$^+$ T cell clone, which secrets IFN-γ in response to its native antigen recognized by the TCR, the CD28 co-stimulatory domain present in the CEA-CAR_CD8 could not mediate the same type of activation. These results are in contrast to previous observations, where engagement of CD28-containing CARs induced IFN-γ release in CD4$^+$ as well as CD8$^+$ T cells (Hombach and Abken, 2011). However, these experiments were performed in heterogenous bulk sorted CD4$^+$ and CD8$^+$ T cells, respectively, which showed that individual T cell clones may exhibit different effector functions in the presence of distinct signaling domains.

5.2   Knockout of the endogenous TCR in CAR-transduced T cells

Once proliferation of the T cell clone could be achieved by CAR engagement, the next step comprised the knockout of the endogenous TCR. For this, TALEN pairs as well as CRISPR gRNA have been designed to target the same region of exon 1 of the *TRAC* or *TRBC* locus, respectively (Figure 4.5). Unmodified Clone 234 served as a model system to assess knockout efficiency in isolated T cell clones utilizing either CRISPR/Cas9 or TALEN methods (Figure 4.6a). Introduction of TALEN pairs targeting the respective TCR chains resulted in TCR knockout rates of 14.5% for *TRAC* and 20.3% for *TRBC* locus*,* as monitored by loss of CD3

expression 7 days after transfection. Comparable or higher knockout rates have been reported in primary human T cells utilizing overlapping target regions and introduction of TALEN pairs in the form of ivt-RNA (Berdien *et al.*, 2014; Poirot *et al.*, 2015). Recently, a study by Knipping *et al.* could demonstrate up to 81% TALEN-mediated TCR knockout rate, while CRISPR/Cas9 introduction resulted only in up to 20% CD3-negative T cells (Knipping *et al.*, 2017). Although higher knockout rates could be achieved by using nuclease-protected modified CRISPR gRNAs, poor gene-editing rates were observed when gRNA produced by *in vitro* transcription in the laboratory was introduced (Osborn *et al.*, 2016). No detectable knockout of either TCR chain was observed when utilizing the CRISPR/Cas9 system in Clone 234. For these experiments CRISPR gRNA was also generated by *in vitro* transcription, which might explain the unsuccessful targeting of the endogenous TCR due to premature degradation of the gRNA. Since knockout of the TCR α and β chains could be achieved by TALEN pairs, ivt-RNA generated from these constructs was used for all subsequent knockout experiments. To our knowledge this represented the first TCR knockout performed in an individual T cell clone rather than in bulk populations of primary human T cells. Comparable knockout rates could also be detected in Clone 234 transduced with the respective CAR constructs (Figure 4.6b). Enrichment of TCR-deficient cells via bead-bound α-CD3 antibody yielded 97% CD3-negative cells, which simultaneously expressed the introduced CEA-CAR. This represented an easy and fast method for isolation of TCR-knockout cells that left the cells of interest untouched by utilizing a negative isolation strategy. Using the established expansion protocol, the enriched CEA-CAR-positive cells were stimulated by co-culturing them at an E:T ratio of 1:6 with irradiated CAR target cells (Figure 4.6c). However, expansion of the TCR-deficient CAR-expressing T cells could not be observed. To exclude the possibility that the failed expansion of TCR-negative cells via CAR engagement might be due the nature of the used model system, Clone 234, a new strategy was developed that would allow the testing of various individual T cell clones.

5.3   Improved strategy for selection of CAR[+] T cell clones

The improved strategy comprised the transduction of bulk PBL followed by subsequent single cell cloning to enable the identification of T cell clones that showed superior proliferative capacity when activated via CAR engagement (Figure 4.7). Utilizing this strategy, 40 well-expanding T cell clones could be isolated that were characterized for CAR expression and IFN-γ release upon co-culture with CAR target cells (Figure 4.9). As observed before, expression levels of CEA-CAR_CD4 were higher compared to CEA-CAR_CD8 as reflected by measured median FI values detected in flow cytometry. This was observed in CD4^{+} as well as CD8^{+} T cell clones, which demonstrated that CAR expression levels were independent of the

T cell subset. While almost all T cell clones transduced with CEA-CAR_CD4 were able to secret high amounts of IFN-γ upon encounter with LS174T tumor cells, half of the CEA-CAR_CD8-expressing T cells clones showed very low IFN-γ release. As observed before for Clone 234, IFN-γ release did not always correlate with T cell expansion. This observation is relevant for the use of the CAR construct in immunotherapy, as autocrine IFN-γ release by T cells has been shown to enhance target cell killing (Bhat *et al.*, 2017). Therefore, functionality of the CAR construct could not be unambiguously proven by IFN-γ secretion and would have to be evaluated based on proliferative capacity upon engagement of the CAR.

Up to this point, expansion of T cells from a single T cell clone was performed utilizing the mitogen PHA in the stimulation mix, which triggers T cell division by crosslinking carbohydrates on cell surface receptors, including the TCR (Chilson, Boylston and Crumpton, 1984). Since the specificity of TCRs present on individual T cell clones derived from PBL was unknown, PHA served to mimic TCR-specific T cell activation. Utilizing this expansion method, the number of well-proliferating CEA-CAR_CD4-expressing T cell clones (n = 31) was much higher than T cell clones transduced with CEA-CAR_CD8 (n = 9). This was observed for PBL derived from two donors in two independent experiments (not shown). In particular, a large number of CD4$^+$ T cell clones expressing CEA-CAR_CD4 exhibited fast expansion rates, while this was not necessarily the case for CEA-CAR_CD8-transduced CD4$^+$ T cell clones. However, the number of well proliferating CD8$^+$ T cell clones was comparable when transduced with either of the CAR constructs. These observations would suggest that T cells, in particular CD4$^+$ T cells, expressing 4-1BB-comprising CAR constructs have a proliferative advantage even in the absence of CAR-specific activation. This antigen-independent increased proliferative capacity of T cells has also been observed for α-CD19 CARs carrying the 4-1BB signaling domain and was contributed to tonic signaling due to the continuous presence of a 4-1BB domain on the cell surface (Milone *et al.*, 2009).

To examine proliferative capacity of the T cell clones upon CAR engagement, four representative T cell clones from each approach were selected for further evaluation. CAR-driven proliferation was monitored after incubation with CEA-expressing CAR target cells and compared to expansion via a PHA-containing stimulation mix that was used for initial expansion of the individual T cell clones. CellTrace Violet staining allowed the monitoring of cell division 3 and 7 days after TCR or CAR-specific activation, respectively (Figure 4.10). While T cells stimulated via CAR engagement showed higher proliferation rates 3 days after co-culture with CAR target cells, expansion was comparable after 7 days independent of the type of stimulation. This was further confirmed by fold expansion 11 days after activation demonstrating that engagement of the introduced CAR construct could induce maximal proliferation rates comparable to standard activation via PHA, which was termed TCR

stimulation (Figure 4.11a). However, while all T cell clones could be expanded via CAR engagement, CEA-CAR_CD4 transduced cells showed up to 20-fold expansion compared to CEA-CAR_CD8-expressing cells, which exhibited a maximal 10-fold expansion rate. This supports the hypothesis that 4-1BB-containing CAR constructs promote T cell proliferation better than CARs carrying CD28 signaling domains. Additionally, expansion rates of CD4$^+$ T cell clones was slightly higher compared to CD8$^+$ T cell clones transduced with the same CAR construct. However, as observed before, T cell proliferation did not correlate with IFN-γ release observed upon CAR engagement (Figure 4.11b). All T cell clones showed antigen-specific secretion of IFN-γ to varying degrees, demonstrating that the transduced CAR constructs were present on the cell surface and specifically recognized the CEA antigen. While T cell clones stimulated via PHA exhibited much higher antigen-specific IFN-γ release compared to cells activated via CAR engagement, expansion rates were comparable. This suggests different activation states of the respective T cell clones dependent on TCR or CAR engagement 11 days after stimulation. For stimulation via TCR, it has been shown that the activation threshold shifts to lower antigen concentrations with the duration of the last antigen encounter (Hesse *et al.*, 2001). Similar effects might be seen for CAR engagement, where T cell clones stimulated via PHA were more responsive to CEA antigen, which they did not encounter in the previous stimulation cycle.

These experiments clearly demonstrated that CD4$^+$ as well as CD8$^+$ T cell clones could be expanded via CAR engagement with proliferation rates comparable to standard T cell expansion protocols *in vitro*. However, after knockout of the endogenous TCR, the CAR-expressing T cell clones could not be expanded via CAR engagement and did not survive the expansion period (Figure 4.12). This was observed in two independent experiments regardless of T cell subset affiliation and transduced CAR construct. Expansion of TCR-knockout T cells via CAR engagement has not been shown on a single cell level yet, therefore it can not be excluded that intrinsic mechanisms connected to signaling and regulation of the CAR constructs were responsible for the failed expansion. Additionally, most of the studies regarding CAR functionality in T cells were performed utilizing cells that still did express the endogenous TCR (Milone *et al.*, 2009; Hombach and Abken, 2011; Hudecek *et al.*, 2015; Sommermeyer *et al.*, 2015). However, recent publications could show that αCD19-CAR integration into the *TRAC* locus of PBL is feasible to generate CAR-expressing T cells that lack the endogenous TCR and do not exhibit impairment of proliferation or functionality (Eyquem *et al.*, 2017; MacLeod *et al.*, 2017). Both approaches utilized CAR constructs recognizing CD19, which is highly expressed on B cells that naturally interact with T cells. Based on these observations, the failed expansion of TCR-deficient T cell clones via CEA-CARs might be attributed to CEA-positive target cells (LS174T) used in the experiments. CEA is a glycoprotein associated with cell adhesion, which is normally only expressed during fetal development and

serves as a marker for colorectal cancer in adults (Duffy, 2001). While the restricted expression of CEA on tumors makes it a suitable target for cancer immunotherapy, available CEA-expressing cell lines are consequently adherent tumor cell lines, like LS174T. Due to their growth behavior and potential expression of inhibitory molecules characteristic for tumor cells, these adherent tumor cells might not be favorable for the purpose of T cell expansion from low cell numbers. Nevertheless, proliferation could be induced in isolated CEA-CAR-expressing T cell clones in the presence of LS174T tumor cells from cell numbers as low as 1×10^5 (Figure 4.10). However, the low number of TALEN-modified T cells that were isolated after electroporation might be affected more drastically by the unfavorable culture conditions produced by LS174T cells. In order to test this hypothesis, new chimeric constructs were generated that would allow the activation of modified T cell clones in the presence of LCL, which are rich in co-stimulatory molecules and should therefore create a more favorable environment for T cell expansion.

5.4 Process improvements

To improve the survival of TCR-deficient T cell clones after the TCR knockout has been performed utilizing the TALEN technology, two new constructs were generated that were used for T cell expansion in the absence of the endogenous TCR. These included a previously published CD19-CAR as well as a newly developed chimeric construct, termed CD3-Chimera. Additionally, the phenotype of T cell clones expanded via CAR engagement was evaluated to determine if a given T cell subset would exhibit superior proliferative capacity when stimulated independent of the endogenous TCR. These cells could serve as a basis for universal recipient cells and would allow a pre-selection for T cell clones exhibiting desired characteristics for prolonged *in vitro* expansion. Based on results obtained with the newly generated CD19-CAR and CD3-Chimera construct, a new high-throughput strategy for the generation of universal recipient cells was established that allowed immediate identification of suitable TCR-deficient T cell clones and shortened the *in vitro* expansion period.

5.4.1 Expansion of molecular toolbox

The CD19-CAR was generated based on the structure published by Hudecek *et al.* and comprised a CD28 transmembrane domain followed by a 4-1BB signaling domain, which should support T cell survival and expansion as demonstrated in clinical studies and *in vitro* analyses (Milone *et al.*, 2009; Porter *et al.*, 2011; Hudecek *et al.*, 2015). Successful transduction could be monitored by eGFP expression and the functionality of the CAR construct was confirmed by IFN-γ release upon co-culture with CD19-expressing LCL (Figure

4.14a, b). Initial expansion of CD19-CAR-expressing single cell clones demonstrated that proliferation rates comparable to activation via the TCR complex could be achieved in CD4$^+$ as well as CD8$^+$ T cell clones when exposed to CD19-positive B cell lines (Figure 4.14c). This demonstrated that the CD19-CAR construct was able to support expansion of individual T cell clones like the CEA-CAR constructs used previously.

The CD3-Chimera construct was designed based on crystal structures that demonstrated native folding of CD3$\gamma\epsilon$ and CD3$\delta\epsilon$ dimeric ectodomains in complex with bound α-CD3 antibodies recognizing the CD3ϵ subunit (Arnett, Harrison and Wiley, 2004; Kjer-Nielsen *et al.*, 2004). Another study by Law *et al.* additionally showed that CD3 δ and ϵ subunits could be expressed as a soluble scF to generate epitopes recognizable by mitotic α-CD3 antibodies (Law *et al.*, 2002). Based on these data, a scFv fragment was designed that linked the CD3δ to the CD3ϵ ectodomain via a flexible (Gly$_4$Ser)$_3$ linker. To avoid oligomerization and disulfide scrambling, the conserved stalk domains were not included in the construct (Kim *et al.*, 2000; Sun *et al.*, 2001; Law *et al.*, 2002). Instead, the CD8α hinge region was fused to a CD28 transmembrane region to enable expression of a monomeric unpaired protein on the plasma membrane. To provide signaling that would mimic the physiological activation through the TCR complex, the CD3ζ domain was added to the intracellular part of the chimeric protein (Figure 4.15). In contrast to conventional CAR constructs that were designed for tumor cell killing through recognition of a specific antigen, the CD3-Chimera does not bind any target and should therefore abolish the risk of off-target recognition. The proposed mode of action includes the activation of TCR-deficient T cells via binding of mitotic α-CD3 antibodies to the CD3-Chimera construct analogous to standard unspecific *in vitro* expansion of T cells. To enable physiological T cell proliferation, co-stimulation by engagement of CD28 has to be provided in the form of α-CD28 antibodies or by natural binding of CD80 and CD86 molecules present on antigen presenting cells. Since T cells endogenously express CD3 on the cell surface, the functionality of this chimeric construct could only be evaluated in TCR-deficient T cells after the knockout of the endogenous TCR. However, expression and native folding could be tested in the TCR-deficient T cell lymphoma cell line Jurakt-76 (Figure 4.17). These cells have lost their ability to provide basic T cell effector functions and do not express endogenous CD3 (Heemskerk *et al.*, 2007; Bürdek, 2009). After transduction of Jurkat-76 cells with the chimeric construct, CD3-Chimera expressing cells could be detected by α-CD3 antibody staining, which demonstrated native folding based on recognition of the α-CD3 epitope usually present in endogenously expressed CD3. Isolated single cell clones transduced with CD3-Chimera showed that expression levels could vary between individual clones. While some clones exhibited high expression levels reflected by distinct CD3-positive populations, others showed just small shifts compared to the negative control, which suggested low expression levels.

Differences in the levels of the CD3-Chimera construct expression might result from different copy numbers present in the individual host genomes or respective integration sites of these randomly integrating retroviral vectors. Dependent on target loci, the integrated provirus can be subject to transcriptional silencing, which has been associated with mechanisms like DNA methylation or histone modification (Swindle and Klug, 2002; Ellis, 2005). Compared to α-CD3 staining, eGFP expression levels also varied in individual clones, but were much lower as reflected by low median FI values. Even though the P2A element coupling CD3-Chimera and eGFP should ensure equimolar expression levels, it has been shown that protein expression can be decreased at the second gene position compared to the first gene position in bicistronic constructs, probably due to discontinued translation (Osborn *et al.*, 2005; Liu *et al.*, 2017). Nevertheless, eGFP could be still used as a marker to identify high-expressing CD3-Chimera cells. In summary, the results demonstrated that the designed CD3-Chimera construct was folded correctly and expressed on the cell surface of TCR-deficient Jurkat-76 cells, even though expression levels could vary between individual clones.

5.4.2   Phenotypic evaluation of CAR-transduced T cells

To evaluate whether certain T cell subsets exhibit proliferative advantages *in vitro*, CAR-expressing CD4$^+$ and CD8$^+$ T cell clones showing either low or high proliferation rates, respectively, were analyzed for their phenotypes (Figure 4.18). According to common T cell markers, all T cell clones were characterized as effector memory T cells exhibiting a CD4$^+$/CD8$^+$ CD45RA$^-$ CD62L$^-$ CD95$^+$ phenotype. All isolated T cell clones showed the same phenotype after several weeks of *in vitro* culture. This is consistent with observations of *in vitro* cultured PBL derived from different T cell subsets and probably reflects the principle of T cell differentiation upon repeated activation in the presence of IL-2 (Foster *et al.*, 2008; Gattinoni, Klebanoff and Restifo, 2012; Schmueck-Henneresse *et al.*, 2017).

It has been shown that transgenic TCR- or CAR-transduced T cells derived from the central memory compartment exhibited better proliferative capacity, effector function and persistence *in vivo* compared to cells derived from the effector compartment (Berger *et al.*, 2008; Gattinoni *et al.*, 2011; Graef *et al.*, 2014; Sommermeyer *et al.*, 2015). However, whether this superior expansion and prolonged survival would also be observed for T cell clones originating from the central-memory subset after prolonged culture *in vitro* has not been investigated yet. Since these properties would be essential when generating universal recipient T cells, the proliferative capacity of CD19-CAR-expanded T cell clones derived from distinct T cell subsets was evaluated. Based on previous observations, the phenotype of T cells after several weeks in culture allowed no conclusion concerning the T cell subset from which they originated. Therefore, the CD19-CAR transduced PBL were labeled with α-CD45RA and α-CD62L

antibodies at the time of sorting, which enabled their classification into distinct T cell subsets retrospectively by analyzing index sort data acquired by the BD FACSDiva™ Software (BD Bioscience). The majority of CD4$^+$ and CD8$^+$ CAR-transduced T cell clones that expanded 14 days after FACS were derived from the naïve or central-memory compartment, which simply reflected the mean T cell subset distribution in two donors (Figure 4.19a). To further evaluate the impact of T cell compartment origin on proliferation, 48 selected single cell clones were expanded via CAR engagement and classified as excellent, good or poor expanding T cell clones, respectively, 28 days after sorting (Figure 4.19b). In all three groups, the majority of the cells were derived either from the naïve or central-memory subset independent of their proliferation rate. Additionally, T cell clones originating from the effector-memory or effector compartments also exhibited good or excellent expansion rates, respectively, while frequencies were comparable to poorly proliferating cells. If T cell clones derived from the central-memory subset would show superior proliferation rates *in vitro*, as observed for *in vivo* experiments, it would have been expected to find fewer cells derived from the effector-memory or effector compartments exhibiting good or excellent expansion rates. Therefore, no correlation could be observed between T cell subset origin and proliferative capacity *in vitro*. The distribution of T cell compartment descent in the three expansion categories simply mirrored the percentages already observed at the time of sorting. The experimental procedure additionally revealed that only 12% and 21% of the selected T cell clones exhibited excellent or good expansion rates, respectively. However, the majority of the cells could not be expanded to suffcent numbers, rendering them unsuitable for use in an *in vitro* test system. This demonstrated that the fraction of cells exhibiting superior proliferative capacity is rather low and could not be identified based on T cell subset origin. Whether other factors, like telomer length, metabolism or alternative signal transduction due to the presence of the CAR, might contribute to better survival *in vitro* needs to be evaluated. To avoid exclusion of potentially suitable T cell clones for generation of universal recipient cells, bulk PBL were used for further experiments without focusing on a certain T cell subset as starting material.

5.4.3   New strategy for the generation of universal recipient cells

The collective results obtained from experiments performed with CAR-transduced T cell clones enabled the setup of expansion procedures for stimulation via CAR engagement independent of the endogenous TCR and served as a preliminary proof of principle. However, they also revealed shortcomings of the procedure that needed to be resolved to successfully generate universal recipient T cells. This included the failed expansion of CEA-CAR-transduced T cells from small cell numbers after electroporation with TALEN pairs. Based on the assumption that the nature of the CEA-CAR target cells might create an unfavorable environment for T cell

expansion, this should be circumvented by utilizing the newly generated CAR constructs, CD19-CAR and CD3-Chimera, which mediate activation of T cells in the presence of LCL equipped with co-stimulatory molecules. Another factor that could impact T cell clone survival is repeated clonal expansion required to (I) identify T cell clones exhibiting superior proliferative capacity upon CAR-specific stimulation and to (II) subsequently determine the TCR knockout status of CAR-expressing T cell clones. The requirement of expanding selected recipient cells from a single T cell clone twice could substantially prolong the *in vitro* culture period and probably considerably shortens the life span of the isolated T cells. However, determining the TCR knockout status is imperative in order to create a fully characterized and reproducible test system for the direct comparison of transgenic TCRs. Recent studies published by various groups predominately focused on disruption of the *TRAC* locus in bulk PBL to avoid expression of the endogenous TCR in CAR-engineered T cells for cancer therapy (Poirot *et al.*, 2015; Eyquem *et al.*, 2017; MacLeod *et al.*, 2017; Ren *et al.*, 2017). In these studies, CARs rather than a transgenic TCR were introduced in the generated TCR-deficient cells to redirect T cell specificity. Therefore, the risk of TCR mispairing could be neglected and targeting only one TCR chain was sufficient to prevent expression of the endogenous TCR. However, when introducing a transgenic TCR in universal recipient cells for functional characterization, a knockout of both TCR chains is needed in order to avoid the risk of TCR chain mispairing. This entails that two separate gene segments (*TRAC* and *TRBC*) had to be targeted in a single cell simultaneously rather than sequentially to circumvent an additional round of clonal expansion.

In order to shorten the *in vitro* culture period and avoid repeated clonal expansion, a new strategy was developed, which would generate T cell clones that could be directly selected for essential criteria characterizing desired universal recipient cells. These criteria included: (I) knockout of the endogenous TCR, which could be monitored by loss of CD3 expression and (II) high expansion rates via CAR engagement in the absence of the endogenous TCR. To achieve an early selection of T cells clones exhibiting these criteria, the strategy was modified to allow simultaneous TCR targeting and CAR introduction in one stimulation cycle (Figure 4.20). The generated T cell clones could immediately be screened for TCR knockout and CAR expression by antibody staining and subsequent expansion of the sorted cells enabled the direct identification of T cell clones exhibiting the ability to proliferate solely via CAR engagement. The process was integrated into the automated workflow platform EVO200 to allow the high-throughput screening of various candidate T cell clones displaying the required criteria to become universal recipient cells (Figure 4.21). In order to genetically modify candidate T cell clones only once at the beginning of the procedure, the constant regions of both TCR chains (*TRAC* and *TRBC*) were targeted simultaneously by introducing both TALEN pairs targeting the TCR α and β chain, respectively. Utilizing this strategy, the generated T cell clones would only need to be expanded once from a clonal level, which simultaneously ensures

that the expanded T cells derived from a single T cell clone all have the same modifications in *TRAC* and *TRBC* gene segments. However, while ensuring that all descendants of selected T cell clones exhibit the same genotype, targeting both TCR chains at the same time also implies that the TCR knockout status of individual T cell clones had to be determined at a later time point. Depending on TALEN activity, the resulting T cell clones could comprise one of three possible knockout states: (I) knockout of both TCR chains (α + β KO), (II) knockout of only the TCR α chain (α KO) or (III) knockout of only the TCR β chain (β KO). Because cells comprising any possible knockout status would exhibit the same CD3-negative phenotype, the successful targeting of either TCR chain could only be determined by DNA sequencing. Therefore, a high-throughput NGS procedure was developed for the determination of the TCR knockout status that allowed the identification of unique mutations in *TRAC* and *TRBC* loci of each individual T cell clone (Figure 4.26). This enabled a detailed analysis of the modifications introduced by targeting the respective TCR chains utilizing TALEN pairs. In contrast, the analysis of TCR knockout in bulk T cell populations can not be performed on a single cell level and rather represent a quantification of the general knockout efficiency. Generally, the T7 endonuclease assay is used to detect mutations in the *TRAC* and *TRBC* loci of mixed PBL, which is based on the preference of T7 endonuclease to cleave heteroduplex DNA (Osborn *et al.*, 2016; Knipping *et al.*, 2017). Subsequent topo cloning of PCR fragments followed by sequencing can only give a general overview over mutations that occurred. Additionally, when targeting both loci simultaneously, identification of T cells comprising a knockout of both TCR chains is not feasible with this method. For this reason, Berdien *et al.* developed a strategy that would allow the sequential targeting of respective loci, while a successful knockout is monitored via CD3-staining. In this protocol TCR α-deficient T cells are transduced with transgenic TCR α chain, which enables enrichment due to re-expression of CD3 on the cell surface, followed by subsequent TCR β knockout and introduction of the transgenic TCR β chain (Berdien *et al.*, 2014). While this ensures the generation of T cells expressing the transgenic TCR that carries a knockout of both TCR chains, the procedure has to be repeated for each transgenic TCR. This should be circumvented by generating universal recipient cells that proliferate independently of TCR expression and that are ready-to-use for the introduction of various transgenic TCRs.

5.5 Characterization of TCR-deficient T cell clones

In order to serve as a suitable test system for transgenic TCRs, TCR-deficient universal recipient cells that proliferate to high cell numbers upon CAR engagement have to exhibit all effector functions required for a physiological read-out. This implies that antigen specificity, killing capacity and functional avidity of universal recipient cells has to be redirected by the

introduced transgenic TCR. Several candidate universal recipient cells either expressing the CD19-CAR or CD3-Chimera construct, respectively, were evaluated for their capacity to display effector functions conferred to the cells by transgenic TCRs.

5.5.1 CD19-CAR

Utilizing the CD19-CAR construct, the new high-throughput approach for the generation and identification of suitable universal recipient cells could be successfully implemented (Figure 4.21). The enrichment of $\alpha\beta$ T cells prior to introduction of TALENs and transduction of the CD19-CAR ensured that no other cell types, like $\gamma\delta$ T cells, present in bulk PBL would be included in the procedure (Figure 4.22). The simultaneous TCR knockout and CD19-CAR introduction could be monitored in subsequent flow cytometric analysis. Utilizing the sorting strategy described in Figure 4.23a, T cell clones exhibiting the desired phenotype could be single-cell sorted to allow clonal expansion of T cell clones that can proliferate upon interaction with CAR target cells, independent of the endogenous TCR. Screening of the expanded single cell clones, utilizing flow cytometry in combination with HTS, demonstrated that the new high-throughput strategy resulted in the isolation of high numbers of T cell clones that comprised TCR knockout cells while expressing the introduced CAR (Figure 4.24). 7% of the T cell clones did exhibited no, 15% only incomplete TCR knockout and were mistakenly sorted utilizing the described strategy. These cells were transduced with the CD19-CAR and could therefore proliferate in the presence of CAR target cells. While the presence of the CD19-CAR could only be monitored via eGFP expression from a bicistronic construct that sometimes results in lower expression of the second gene, it is assumed that actual CD19-CAR expression was higher than reflected by detection of eGFP (Osborn *et al.*, 2005; Liu *et al.*, 2017). Numerous T cell clones (n = 158), exhibiting the desired phenotype while showing good proliferative capacity, were selected for NGS analysis. After excluding some datasets due to low read count, the majority of the cells exhibited a knockout of the TCR α or β chain, respectively. While single-chain knockouts were prominent, only nine T cell clones could be identified that showed successful targeting of both TCR chains. This indicated that the efficiency for targeting both TCR chains simultaneously is much lower compared to targeting each TCR chain separately, where knockout rates of up to 20% could be achieved (Figure 4.6). This might be due to the fact that for a double knockout to occur, four relatively large ivt-RNAs (ca. 2.8 kb), coding for the two TALEN pairs, have to enter the cell simultaneously. While all TALEN ivt-RNAs have been mixed prior to electroporation, allowing a homogenous distribution, four TALEN ivt-RNAs might border on nucleotide levels toxic for the electroporated cells, thereby reducing the number of cells that survive the procedure. In total, 20 T cell clones were selected for further analysis, which included the nine T cell clones exhibiting the knockout of both TCR

chains and 11 T cell cones that comprised either the knockout of the TCR α or β chain, respectively. One CD4⁺ T cell clone transduced with the CD19-CAR, that lacked any modification of the *TRAC* or *TRBC* locus, was also included as a control to identify possible effects on proliferation when the endogenous TCR is absent in CAR-transduced cells. While ten CD4⁺ and ten CD8⁺ T cell clones were selected to monitor expansion over a 56-day period, only six CD4⁺ T cell clones proliferated sufficiently to be of use for an *in vitro* test system (Figure 4.30). The other 12 T cell clones, which included all the isolated CD8⁺ T cell clones, did not survive the expansion period. This poor survival of CD8⁺ T cell clones *in vitro* is also a concern when isolating tumor-specific cytotoxic T cells for use in immunotherapy and the reason why strategies for fast identification of suitable CD8⁺ T cell clones and the rapid isolation of the corresponding TCR sequences have been developed (Wilde, Sommermeyer, *et al.*, 2012; Dössinger *et al.*, 2013; Simon *et al.*, 2014). Additionally, better expansion of CD4⁺ bulk PBL, transduced with an CD19-CAR, compared to CD8⁺ PBL has also been observed by Sommermeyer *et al.* (Sommermeyer *et al.*, 2015). This effect might be pronounced on a clonal level and might explain why isolated CD4⁺ T cell clones show better survival compared to CD8⁺ T cell clones *in vitro*.

A summary of the knockout status for the seven T cell clones exhibiting the highest proliferation rates is shown in Table 4.1. Clone CD4⁺_50 served as a control to validate the NGS results and carried no modification of either TCR chain. The other clones contained either mutations in both TCR chains or only in the *TRBC* locus, respectively. The two T cell clones CD4⁺_74 and CD4⁺_17 exhibited the best expansion rates via CAR engagement, comparable to the control CD4⁺_50, while carrying mutations in both TCR chains. This indicated that the lack of the endogenous TCR did not have a negative impact on proliferation, although proliferation rates of individual T cell clones could vary (Figure 4.30).

All T cell clones, except for the control CD4⁺_50, exhibited the desired CD3-negative phenotype, demonstrating the absence of the endogenous TCR from the cell surface, while still expressing the co-receptor CD4 or CD8, respectively (Figure 4.31). Knockout of the endogenous TCR did not have any effect on other cell surface markers characterizing the T cell clones CD4⁺_74, CD4⁺_24, CD4⁺_17 and CD8⁺_62 as effector-memory T cells, as observed before for *in vitro* cultured T cells (Figure 4.32). However, the T cell clones CD4⁺_54 and CD4⁺_46 expressed CD45RA, categorizing them as terminally differentiated effector T cells. Interestingly, clone CD4⁺_54 additionally expressed CD62L at low levels, which is normally expressed on naive or central-memory T cells (Golubovskaya and Wu, 2016). However, there is evidence for heterogeneity of CD62L expression among the effector-memory CD4⁺ T cell compartment (Sallusto *et al.*, 1999; Ahmadzadeh, Hussain and Farber, 2001). While low CD62L expression has been shown to indicate high proliferative capacity,

resembling effector cells; high CD62L expression was indicative for resting memory T cells exhibiting lower proliferative capacity (Sallusto *et al.*, 1999; Ahmadzadeh, Hussain and Farber, 2001). Since the described cells have been cultured *in vitro* over multiple simulation cycles, it is not clear to which extent T cell compartment affiliation is accurate and representative for T cell effector function.

In order to evaluate the effector functions of these TCR-deficient T cell clones, a well-characterized TCR recognizing the NY-ESO-1$_{157-165}$ peptide (SLLMWITQC; HLA-A2-restricted) was introduced into four selected T cell clones. Staining of the specific TCR-Vβ chain in combination with CD3 demonstrated simultaneous expression of the transgenic TCR and re-expression of endogenous CD3 on the cell surface of the transduced T cell clones (Figure 4.33c). The specificity of all four T cell clones could be redirected by the transgenic TCR, which was reflected by specific IFN-γ release upon co-culture with NY-ESO-1-expressing Mel624.38 tumor cells (Figure 4.33b). Co-culture with CD19-expressing LCL served as a positive control to measure IFN-γ secretion induced by CAR-specific activation. All T cell clones, except for clone CD4$^+$_17, showed recognition of CD19-CAR target cells reflected by release of high amounts of IFN-γ. Clone CD4$^+$_17 did not secret IFN-γ upon co-culture with CD19-positive LCL, even though the T cell clone could be successfully expanded utilizing the same target cells. This phenomenon has already been observed in the established CD4$^+$ T cell clone, Clone 234, transduced with CEA-CAR_CD8, which did not release IFN-γ upon encounter of CAR target cells while the same cells induced proliferation via the transduced CAR (Figure 4.4). In both cases, recognition of antigen presented by MHC molecules via the TCR resulted in high amounts of IFN-γ secretion. While these CD4$^+$ T cell clones are generally able to produce IFN-γ, activation via the CAR construct might not result in IFN-γ transcription due to altered signal transduction. IFN-γ secretion is normally induced by binding of the master regulator for Th1 differentiation, T-bet, to the IFN-γ promoter site. T-bet, in turn, is induced by TCR engagement or cytokine-mediated signaling (Placek *et al.*, 2009; Lai *et al.*, 2011; Zhu *et al.*, 2012). Even though the absence of IFN-γ secretion upon CAR engagement has not been reported before, this phenomenon might not be detectable in bulk PBL. However, the results obtained here for individual T cell clones suggest that signal transduction via CAR engagement, independent of the intrinsic CAR-signaling domains, might be altered for distinct CD4$^+$ T cells without affecting proliferative capacity of these cells. Since CARs are artificially assembled receptors that mediate T cell activation via mechanisms yet to be determined, alterations of the signaling pathways associated with proliferation and effector function might occur (Harris and Kranz, 2016).

It has been demonstrated that the effector functions, including tumor cell killing and cytokine secretion, can be transferred to recipient cells by an introduced transgenic TCR (Wilde *et al.*,

2009; Wilde, Sommermeyer, *et al.*, 2012). While this was reflected by specific IFN-γ release of all four NY-ESO TCR-expressing T cell clones, only two of the T cell clones could be redirected by the NY-ESO TCR to target NY-ESO-1-positive tumor cells. T cell clone CD4+_17, specifically killed NY-ESO-1-expressing tumor cells, while not inhibiting the outgrowth of NY-ESO-1-negative 647-V cells (Figure 4.33a). This was also observed for T cell clone CD4+_74, whose killing capacity was even higher, reflected by faster decay in Mel624.38 cell count. However, T cell clones CD4+_54 and CD4+_46, which specifically produced IFN-γ in response to NY-ESO-1-expressing tumor cells and CAR target cells, were not able to inhibit outgrowth of NY-ESO-1-positive tumor cells. These T cell clones differed from cytolytic CD4+ T cell clones regarding their phenotype, which was characterized by expression of CD45RA in both T cell clones and additional CD62L expression in clone CD4+_54 (Figure 4.32). However, whether expression of these cell surface markers might indicate reduced killing capacity is not clear. The different killing capacities observed for CD4+ T cell clones transduced with the same NY-ESO TCR indicated that the introduced transgenic TCR could not redirect the effector functions of all T cell clones sufficiently. However, in contrast to previous studies, effector functions mediated by a MHC class I-restricted TCR were tested not in CD8+ T cells, but in CD4+ T cell clones. CD4+ T cells are generally known to help mediate adaptive immune responses rather than exhibiting specific killing capacity. However, a CD4+ T cell subset with cytotoxic activity has been observed, that targets tumor cells in an MHC class II-restricted manner. While this subset has been thought to be an artifact of long-term *in vitro* culture, increasing evidence demonstrated their importance in antiviral and anti-tumor immunity *in vivo* (Takeuchi and Saito, 2017). Whether MHC class II-restricted TCRs derived from these cytotoxic CD4+ T cells can transfer killing capacity to all CD4+ T cells when transgenically expressed is not clear. However, the fact that the transgenic NY-ESO TCR could confer killing capacity only to some CD4+ T cell clones might suggest intrinsic lineage-dependent transcriptional programs that can not be changed by introduction of transgenic TCRs. Therefore, NY-ESO TCR-transduced T cell clones exhibiting cytolytic activity might derive from CD4+ T cell clones that already possessed cytolytic capacities prior to introduction of the transgenic TCR.

Since no CD8 co-receptor is present in these CD4+ T cells, the transgenic NY-ESO-1-specific TCR has to mediate antigen recognition in a co-receptor independent manner. The co-receptors CD4 and CD8 augment the sensitivity and reactivity of T cells to cognate peptide-MHC complexes by stabilizing the interaction and recruitment of Lck to the TCR complex (Veillette *et al.*, 1989). However, it has been shown that the extent of co-receptor dependency is inversely correlated to affinity of TCR s to peptide-MHC complexes (Holler and Kranz, 2003; Laugel *et al.*, 2007; Artyomov *et al.*, 2010). TCRs exhibiting high affinity to peptide-MHC complexes, are less or non-dependent on the presence of CD8 co-receptor, while TCRs exhibiting affinities typical for syngeneic interactions require CD8 co-stimulation (Munz *et al.*,

1999; Wilde *et al.*, 2009). This demonstrated that the generated recipient cells can be used to test co-receptor dependency of transgenic TCRs. For clinical application, transgenic TCRs showing no dependency on the CD8 co-receptor could broaden the spectrum of reactive T cells in a non-enriched clinical PBL product because the transgenic TCR would be functional in CD4$^+$ as well as CD8$^+$ T cells.

The results demonstrated that two of the CD19-CAR-expressing CD4$^+$ T cell clones, CD4$^+$_74 and CD4$^+$_17, can be used as suitable test system for MHC class-I transgenic TCRs that do not show co-receptor dependency. The two T cell clones carry mutations in both TCR chains preventing the expression of an endogenous TCR. Therefore, transgenic TCR expression can be tested in these recipient cells without the risk of TCR mispairing or negative influences originating from dominant endogenous TCR expression. This enables the validation of correct assembly and expression of transgenic TCR constructs that have been reconstructed from isolated TCR sequences *in silico.* Additionally, isolated transgenic candidate TCRs, derived from cytotoxic CD8$^+$ T cells, can be evaluated for co-receptor dependency in these CD4$^+$ T cell clones. Transgenic TCRs that can transfer effector functions without requirement for the CD8 co-receptor, can be characterized for specificity and killing capacity in the generated TCR-deficient CD4$^+$ T cell clones.

5.5.2   CD3-Chimera

Activation of T cells transduced with the CD3-Chimera construct was mediated by binding of the α-CD3 antibody to the chimeric construct in presence of co-stimulation provided by LCL and feeder cells. Utilizing the new strategy comprising simultaneous knockout and transduction of the construct, only a small number of T cell clones could be isolated compared to the CD19-CAR approach. While this low recovery could be due to ineffective activation mediated via the CD3-Chimera, another likely explanation is based on the low transduction rate observed in Figure 4.23. In contrast to the CD19-CAR construct, the sorting strategy comprised the gating on T cells exhibiting lack of TCR$\alpha\beta$ expression while α-CD3 antibody should bind to the CD3-Chimera construct. However, less than 1% of the T cells showed the desired phenotype and expressed eGFP, that indicated a successful transduction with the CD3-Chimera construct. While the TCR knockout efficiency mediated by TALEN pairs was sufficient to generate nearly 30% TCR-negative T cells, the transduction procedure needs optimization to obtain higher transduction rates and increase the yield of TCR-deficient CD3-Chimera-expressing T cell clones.

The two T cell clones, CD8$^+$_001 and CD8$^+$_002, that could be expanded over the 56-day expansion period exhibited high proliferation rates, which were comparable or even higher

than the positive control CD4$^+$_50 (Figure 4.34a). In contrast to the CD19-CAR approach, where only CD4$^+$ T cell clones could be expanded, the two CD3-Chimera-transduced T cell clones were both derived from the CD8 compartment. The high 40 – 50-fold expansion could only be observed when OKT-3 was present in the stimulation-mix (Figure 4.34b). This demonstrated that proliferation in these TCR-deficient T cell clones had to be induced by binding of OKT-3 antibody to the introduced CD3-Chimera construct. Cells that were stimulated without the addition of OKT-3 antibody exhibited highly reduced proliferation rates with only 9-fold expansion 10 days after activation. This moderate proliferation of T cells mediated only via CD28 engagement in the presence of IL-2 has been observed previously and was attributed to a possible mechanism for memory T cell homeostasis in the absence of antigen (Flynn and Müllbacher, 1997; Siefken *et al.*, 1998). In another study, activation of TCR-negative PBL utilizing CD3/CD28 beads resulted in only 5-fold expansion due to lack of TCR expression, whereas the low proliferation rates observed were also attributed to CD28 co-stimulation (Berdien *et al.*, 2014; Osborn *et al.*, 2016). Taken together, these results allowed the conclusion that the observed high expansion rates of CD3-Chimera-transduced T cell clones, lacking endogenous TCR expression, was mediated by binding of OKT-3 antibody to the CD3-Chimera construct.

According to results obtained from NGS analysis, clone CD8$^+$_001 displayed mutations in the TCR α chain, while CD8$^+$_002 contained modifications in the TCR β chain (Table 4.2). In both cases, base deletions in the TCR constant region resulted in a frame-shift mutation that introduced a pre-mature stop codon in the amino acid sequence, thereby preventing cell surface expression. This was consistent with the observed TCR$\alpha\beta$-negative phenotype (Figure 4.35a). However, while both T cell clones expressed eGFP, indicating successful transduction of CD3-Chimera construct, the construct could not be detected using α-CD3 antibody. The utilized α-CD3 antibody was derived from clone UCHT-1, which is described to bind the CD3ε subunit present in the CD3-Chimera construct (Arnett, Harrison and Wiley, 2004). To exclude that this α-CD3 antibody used for detection might be responsible for the unsuccessful staining of the CD3-Chimera construct, the staining was repeated using an antibody derived from clone OKT-3 (Figure 4.35b). As demonstrated in Figure 4.34b, this mitotic α-CD3 antibody was successfully used for expansion of TCR-deficient T cell clones and should therefore bind the CD3-Chimera construct. However, the CD3-Chimera construct could not be detected with either α-CD3 antibody, independent of the hybridoma from which they were derived. This was a surprising observation, since the CD3-Chimera construct could be successfully detected in transduced Jurkat-76 utilizing the same antibodies, even though expression levels varied in different clones (Figure 4.17). In transduced Jurkat-76, low CD3-Chimera expression was connected to equally low eGFP expression. However, this could not be observed in the two

TCR-deficient T cell clones, that exhibited a distinct eGFP-positive population while the CD3-Chimera could not be detected using the same α-CD3 antibody concentrations. Increasing the α-CD3 antibody concentration 5-fold resulted in a small positive shift of the CD8$^+$_002 population compared to the negative control (Figure 4.35c). This positive shift was also observed in CD3-expressing T cells used as positive control, which could be expected when exposing cells positive for the CD3 antigen to higher antibody concentrations. While this might indicate the presence of low of CD3-Chimera expression on the cell surface of transduced T cell clones, no distinct CD3-positive cell population could be observed. Whether CD3-Chimera expression was too low for detection or the construct assumed a conformation on the cell surface that did not allow binding of α-CD3 antibody conjugated to fluorophores will need to be investigated in further experiments. However, more CD3-Chimera-expressing T cell clones need to be isolated in order to detect possible differences in cell surface expression levels already observed in Jurkat-76 clones. Additionally, the domain structure of the CD3-Chimera construct could be re-evaluated to determine whether the use of different hinge or transmembrane domains, like a IgG4-hinge or CD8 transmembrane domain, might improve expression levels. Unfortunately, Western blot analysis to determine expression of the construct on a protein level could not be performed due to the presence of the endogenous CD3 complex in T cells. Nevertheless, functionality and therefore binding of the structural epitope of mitotic OKT-3 antibody could be demonstrated by high expansion rates of the CD3-Chimera-transduced T cell clones activated in the presence of OKT-3 antibody (Figure 4.34). Phenotypically, the two T cell clones resembled T cells of the effector-memory compartment, as previously observed for *in vitro* cultured T cell clones (Figure 4.36).

While these CD3-Chimera-transduced T cell clones exhibited high proliferation rates in the absence of the endogenous TCR, their suitability as an *in vitro* test system had to be evaluated based on effector functions mediated by introduced transgenic TCRs. For this, two well characterized TCRs, T58 and D115, recognizing the same tyrosinase$_{369-377}$ peptide (YMDGTMSQV; YMD) presented by HLA-A2 were transduced into the T cell clones CD8$^+$_001 and CD8$^+$_002. While T58 is characterized as a TCR conferring high functional avidity in a transgenic setting, PBL expressing transgenic D115 showed lower functional avidity to the same target (Wilde *et al.*, 2009). This difference in functional avidity allowed to estimate the sensitivity of the generated *in vitro* test system. By comparing killing capacity, IFN-γ secretion and functional avidity of the transduced T cell clones to bulk PBL expressing the transgenic TCRs, representing the standard test system, it could be evaluated whether effector functions conferred by the transgenic TCRs are adequately reflected in the generated universal recipient cells.

Both T cell clones, CD8$^+$_001 and CD8$^+$_002, transduced either with T58 or D115, specifically recognized and killed the tumor cells, while untransduced control cells did not inhibit outgrowth of Mel624.38 cells (Figure 4.37). Additionally, T58- and D115-transduced cells did not target tyrosinase-negative A375 tumor cells, indicating high specificity mediated by the transgenic TCRs. This demonstrated that both T cell clones could be successfully redirected by the introduced TCRs and displayed effector functions required to mediate target cell killing. While in CD3-Chimera-transduced T cell clones both TCRs eradicated tumor cells to a comparable level, D115-transduced PBL exhibited lower killing capacity compared to T58-expressing PBL. These observations were also reflected by specific IFN-γ release of transduced T cell clones and PBL when co-cultured with tyrosinase-positive tumor cells (Figure 4.38b). The T cell clones, CD8$^+$_001 and CD8$^+$_002, transduced with either TCR and T58-expressing PBL, that showed high tumor cell killing, secreted IFN-γ at the same level as the PMA/ionomycin control, that served as a measure for maximal T cell activation. In contrast, D115-transduced PBL released reduced amounts of IFN-γ when co-cultured with Mel624.38 tumor cells compared to the PMA/ionomycin positive control. This reduced IFN-γ secretion and killing capacity of PBL transduced with D115 TCR might be attributed to lower functional avidity compared to T58-transduced PBL. In turn, this would also suggest that the generated CD3-Chimera-expressing T cell clones lacked sensitivity to reflect different functional avidities conferred by the two TCRs. However, when functional avidity was determined by exposure to graded amounts of peptides, universal recipient cells expressing either T58 or D115 exhibited different functional avidities dependent on the transgenic TCR present in the cells (Figure 4.38c). While T cells transduced with T58 were more sensitive and released half-maximal amount of IFN-γ at a peptide concentration of 10^{-8} M, D115-expressing cells required higher amounts of antigen to reach EC50. These results were comparable to the functional avidity measured in PBL transduced with the same TCRs and in accordance with previous observations by Wilde *et al.* when autologous PBL were used for peptide presentation (Wilde *et al.*, 2009). Therefore, even though tumor cell recognition of CD3-Chimera-expressing T cell clones was comparable when mediated by T58 and D115 TCR, sensitivity for tyrosinase$_{369-377}$ peptide reflected functional avidity of PBL transduced with the same TCRs.

Unlike PBL transduced with the transgenic TCRs, D115-transduced T cell clones eradicated tyrosinase-positive tumor cells as efficiently as T58-expressing T cell clones. However, the generated universal recipient cells expressing the transgenic TCRs, T58 and D115, exhibited the expected sensitivity to tyrosinase$_{369-377}$ peptide. Therefore, the differences in tumor cell killing could not be attributed to altered functional avidity mediated by transgenic TCR-expressing universal recipient cells. However, the observed increased killing capacity of D115-transdcued T cell clones might correlate with transgenic TCR expression levels in the respective recipient cells (Figure 4.38a). In both TCR-deficient T cell clones, CD8$^+$_001 and

CD8$^+$_002, expression of the specific TCR-Vβ chain and binding of YMD-tetramer correlated with re-expression of endogenous CD3, which could not be detected in untransduced cells. Introduction of TCR D115 resulted in both T cell clones in distinct CD3$^+$YMD-tertramer$^+$ cell populations, which indicated the expression of only one functional TCR on the cell surface. In contrast, PBL transduced with D115 showed nearly 97% TCR-Vβ-positive cells, while less than 40% of the cells specifically bound the YMD-tetramer. This indicated that expression of a functional transgenic D115 TCR was reduced in PBL compared to the generated universal recipient cells. The reduced expression of functional transgenic D115 TCR can be attributed to the presence of various endogenous TCRs in bulk PBL, which increase the risk of TCR mispairing and might compete with the transgenic TCR for CD3 molecules required for cell surface expression (Ahmadi *et al.*, 2013). In contrast, the generated universal recipient cells lack a functional endogenous TCR that could sequester the CD3 complex. This indicated that the increased cell surface expression of functional transgenic D115 TCR was responsible for the increased killing capacity of D115-transduced universal recipient cells.

For T58-transduced PBL, the killing capacity was comparable to universal recipient cells expressing the transgenic T58 TCR (Figure 4.37). This efficient control of tumor cell growth by T58-transduced PBL was observed despite low specific YMD-tetramer binding, which suggested that less than 50% of the PBL expressed of functional transgenic T58 TCRs (Figure 4.38a). This allows the assumption that TCRs conferring high functional avidity, can counteract lower cell surface expression by exhibiting higher sensitivity for the specific peptide. Therefore, T58-transduced PBL showing high functional avidity could mediate adequate tumor cell killing despite lower cell surface expression of functional T58 transgenic TCRs.

The generated universal recipient cells exhibited high expression levels of the introduced transgenic TCRs and showed the expected functionality (Figure 4.37, Figure 4.38). Unlike in transduced PBL, high expression levels of functional transgenic TCRs could be demonstrated by specific binding to the YMD-tetramer complex. However, in T cell clone CD8$^+$_002 transduced with T58 two distinct CD3$^+$TCR-Vβ$^+$ and CD3$^+$YMD-tetramer$^+$ cell populations could be detected by flow cytometric analysis (Figure 4.38a). The two cell populations might indicate high and low expression levels of the introduced transgenic TCR or potential mispairing of transgenic TCR β chain and endogenous TCR α chain. While both CD3-Chimera-expressing T cell clones carry a knockout of one of the endogenous TCR chains (CD8$^+$_001: TCR α knockout; CD8$^+$_002: TCR β knockout) resulting in the TCR-negative phenotype, the respective second TCR chain was not targeted by the TALEN pairs (Table 4.2). Therefore, the respective endogenous TCR chain comprising the wildtype sequence could potentially pair with introduced transgenic TCR chains. This emphasizes that in order to abolish the risk of TCR mispairing completely, both TCR chains need to be targeted in recipient cells. To achieve

this, additional universal recipient cells have to be generated that carry a knockout of both the endogenous TCR α and β chain. Alternatively, the respective second wildtype TCR chain could be targeted for knockout in the generated T cell clones CD8$^+$_001 and CD8$^+$_002 to accomplish a complete knockout of the endogenous TCR. However, clonal expansion from a single cell level would be required to detect a successful targeting of the second TCR chain, which would considerably shorten the life span of the isolated T cells. Even though the generated universal recipient cells carry only a knockout of one TCR chain, no functional endogenous TCR is present in these cells that could influence experimental read-out through dominant negative effects. Additionally, based on the absence of a functional endogenous TCR, competition for CD3 molecules should be reduced, therefore supporting cell surface expression of transgenic TCRs (Ahmadi *et al.*, 2013).

The functional experiments demonstrated that the generated universal recipient cells served as a sensitive and reliable test system to evaluate functional avidity conferred to T cells by transgenic TCRs. While the universal recipient cells displayed different sensitivities to antigen dependent on the transgenic TCR, high expression of functional TCRs on the cell surface could overcome the higher activation threshold of D115-transduced cells and allowed effective tumor cell killing comparable to T58-expressing T cells. Modification of the TCR constant regions to achieve preferential pairing has so far been a promising measure to improve transgenic TCR expression and prevent TCR mispairing (Sommermeyer and Uckert, 2010). However, complete knockout of the endogenous TCR would entirely abolish the risk of off-target toxicity mediated by mispairing and allow effective redirection of T cell specificity by solitary expression of the introduced transgenic TCR. Berdien *et al.* proposed a process that would allow the successive knockout of TCR chains while gradually introducing respective transgenic chains by lentiviral transduction (Berdien *et al.*, 2014). However, recent studies demonstrated the benefits of integrating CARs into the *TRAC* locus, thereby placing them under the transcriptional control of endogenous regulatory elements (Eyquem *et al.*, 2017; MacLeod *et al.*, 2017). Therefore, in order to achieve effective physiological reprogramming of T cells, the ideal solution would entail the replacement of endogenous TCR chains by targeting the respective transgenic TCR chains to the native TCR locus. Results obtained with TCR T58 and D115 in this thesis suggest that knockout of endogenous TCRs in clinical products T cell products might open the door for clinical use of TCRs conferring lower functional avidity, that exhibit optimal safety profiles.

The generated universal recipient cells represent the first reproducible test system that allows the direct comparison of transgenic TCRs in a T cell without potential negative interfering factors often observed when PBL are used as recipient cells. The absence of an endogenous functional TCR in universal recipient cells reduces the risk of introducing unspecific

background into complex cellular assays. This unspecific background predominately originates from dominant negative effects of endogenously expressed TCRs of unknown specificity. Without an endogenous functional TCR present, competition of transgenic and endogenous TCR is reduced and high transgenic TCR expression levels can be reached. As observed for the transgenic D115 TCR that confers lower functional avidity to recipient cells, knockout of at least one TCR chain resulted in control of tumor cell growth comparable to high avidity TCR T58 (Figure 4.37), which could not be observed in bulk PBL. Due to the negative effects of endogenous TCRs, the TCR D115 would have been excluded as a potential candidate for clinical application. However, by using universal recipient cells, also transgenic TCRs with high antigen specificity that exhibit impaired killing capacity only in the presence of endogenous TCRs can be identified. With the new gene editing techniques available, also these transgenic TCR could be of potential clinical benefit, when endogenous TCR expression is abolished. Therefore, utilizing universal recipient cells that lack a functional endogenous TCR opens the possibility to evaluate actual effector functions transferred to recipient cells solely by the transgenic TCR independent of interfering factors that are introduced by donor PBL. This is particularly important for safety-relevant assays, since decreasing unknown variables in the test system helps to unambiguously determine off-target or on-target/off-tumor recognition mediated by the candidate transgenic TCR.

6   Conclusions & Outlook

Based on results obtained from experiments with isolated T cell clones expressing CEA-CARs, a new strategy could be developed that allowed the identification and isolation of TCR-deficient T cell clones that can be expanded solely via engagement of the introduced chimeric construct. Simultaneous knockout of the endogenous TCR and introduction of the chimeric construct provided a fast selection method for T cell clones that could proliferate in the absence of the endogenous TCR and reduced the *in vitro* expansion period considerably. High-throughput screening of T cell clones in combination with modified NGS protocols enabled an early determination of the knockout status for individual T cell clones, which could be selected for further evaluation of effector functions required for physiological read-out after introduction of candidate transgenic TCRs. Utilizing a CD19-CAR, high expansion rates for CD4$^+$ T cell clones could be achieved that exhibited knockout of either one or both TCR chains. Introduction of a NY-ESO-1-specific TCR in these cells resulted in high expression levels of the transgenic TCR without impairment mediated by endogenous TCR chains. While IFN-γ release could be used as a measure to determine transgenic TCR specificity in all selected T cell clones, only two CD4$^+$ T cells exhibited cytolytic activity and could serve as a test system for killing capacity. Due to the absence of CD8 in these T cells, only MHC class I restricted TCRs showing co-receptor independent activation can be evaluated. However, this opens the possibility to use these universal recipient cells to test for co-receptor dependency of transgenic TCRs. Since antigen-recognition of CD8-dependent TCRs would not result in activation of the recipient cells, effector functions should be restored when CD8 is provided simultaneously. Additionally, the generated universal recipient cells provide an ideal environment for evaluating correct expression and multimer-binding of *in silico* reconstructed transgenic TCRs in absence of endogenous TCR chains. This can be helpful when identified tumor-specific cytotoxic T cell clones express two productive alpha chains of which only one mediates the desired specificity; this has been estimated to occur at a frequency as high as 20% (Malissen *et al.*, 1992; Piper, Litwin and Mehr, 1999). In contrast to the CD19-CAR approach, only a small number of T cell clones could be isolated that could be expanded utilizing OKT-3 antibody for the engagement of the designed CD3-Chimera construct in TCR-deficient T cell clones. However, two well-proliferating T cell clones could be identified that were derived from the CD8$^+$ T cell compartment carrying either a knockout of the TCR α or β chain, respectively. Both T cell clones exhibited high proliferation rates in the absence of the endogenous TCR, which was mediated by binding of mitogenic OKT-3 antibody to its structural epitope. While correct folding and surface expression of CD3-Chimera could be demonstrated in Jurkat-76 cells, expression of the construct by binding of fluorophore-labeled antibodies has yet to be unambiguously determined in TCR-deficient T cell clones. The generated universal recipient cells exhibited all effector functions required to mediate tumor cell killing directed by the introduced transgenic

tyrosinase-specific TCRs, T58 and D115. While both TCRs recognize the same tyrosinase$_{369\text{-}377}$ peptide in the context of HLA-A2, PBL transduced with T58 show higher functional avidity than D115-transduced PBL (Wilde *et al.*, 2009). This difference in peptide sensitivity could be successfully reproduced in the isolated T cell clones, demonstrating that the generated recipient cells allow the direct comparison and evaluation of different TCRs recognizing the same target. In contrast to PBL expressing various endogenous TCRs of unknown specificities, universal recipient cells enabled the testing and characterization of transgenic TCRs without the risk of introducing unspecific background into complex cellular assays. In case of the transgenic D115 TCR, that exhibits lower sensitivity to the target peptide, the absence of a functional endogenous TCR allowed expression of transgenic TCR that resulted in improved tumor cell recognition and killing. This indicated that the generated universal recipient cells represent a sensitive test system that allows the identification of effector functions that are transferred to recipient cells solely by the transgenic TCR when potential influencing factors are diminished.

Therefore, the generated universal recipient cells lacking the endogenous TCR represent the first stable and physiological test system for *in vitro* efficacy and safety testing of transgenic TCRs. TCR-independent proliferation via engagement of the introduced chimeric construct allows expansion of the TCR-deficient T cells to sufficient numbers to serve as ready-to-use recipients for the introduction of various transgenic TCRs. Testing of different transgenic TCRs in the same defined universal recipient cells enables the reproducible and direct comparison regarding transgenic expression, specificity and functionality. This reproducibility is especially important when comparing different TCRs recognizing the same target to identify the most potent candidate. In contrast, unknown specificities of endogenously expressed TCRs and diverse effector functions of bulk PBL can vary in each donor and interfere with functional read-outs and make interpretation of experimental results difficult.

By utilizing universal recipient cells as a standardized test system, these unknown influences could be circumvented to allow the unbiased identification of transgenic TCRs. Based on the developed high-throughput strategy, additional CD4$^+$ and CD8$^+$ universal recipient cells could be generated that would carrying a knockout of both TCR chains and proliferate upon engagement of the same chimeric construct. In contrast to the CD19-CAR, the CD3-Chimera construct does not show any target recognition and therefore reduces the risk of background reactivity mediated mediated by the recipient cells in cellular assays. Characterization of this chimeric protein has to be improved to enable the isolation of larger numbers of T cell clones. However, the principle of activating TCR-deficient T cells solely via OKT-3 binding and CD28 engagement, e.g. by using CD3/CD28 beads, opens new possibilities for the generation of universal recipient cells for clinical use. Since generating individual clinical products from cells

derived from critically ill cancer patients, usually pre-treated with chemotherapy can be challenging regarding both the production process and logistics, establishing "off-the-shelf" biobanks with genetically modified T cells from healthy third-party donors represents a promising alternative for the future of adoptive T cell therapy (Poirot *et al.*, 2015; Torikai and Cooper, 2016). Even though CRISPR/Cas9 mediated knockout of endogenous HLA class I molecules by targeting β-microglobulin could abolish the requirement for HLA-matched donors, an area of possible concern is the *in vivo* targeting of HLA-deficient cells by the patients' NK cells specialized in detecting HLA-downregulation (Ren *et al.*, 2017). The described "off-the-shelf" approaches are designed for TCR-knockout T cells expressing predominantly a CD19-CAR for the treatment of B cell malignancies. Since TCR mispairing is not a concern in CAR-T cell therapy, the knockout of one TCR chain is sufficient to abolish TCR expression and avoid off-target toxicities mediated through the endogenous TCR. It has been demonstrated that introducing the CD19-CAR into the *TRAC* locus achieves both TCR knockout and CD19-CAR expression in a single step and can thereby reduce production steps for genetically modified T cells (Eyquem *et al.*, 2017; MacLeod *et al.*, 2017). However, to avoid mispairing and dominant negative effects of endogenous TCRs in adoptive T cell therapy utilizing transgenic TCRs both endogenous TCR chains would have to be targeted in donor T cells. This could be achieved either by sequential knockout of the respective TCR chains as described by Berdien *et al.* or by directed knockin of transgenic TCR chains in the respective native TCR loci mediated by TALEN pairs or CRISPR/Cas9 introduction together with template DNA coding for transgenic TCR chains. Although both TCR chains could be targeted with these methods, just as for proposed "off-the-shelf" CAR-based approaches, the clinical cell products would require the repeated individual preparation for each transgenic TCR that would be used in clinical application. To avoid this, a biobank from various allogenic donors could be generated that comprises T cells exhibiting a complete knockout of the endogenous TCR. These prepared TCR-deficient T cells could then be selected based on HLA-match with the patient and modified to express the required transgenic TCR designed for the respective indication. This would enable a fast generation of clinical products for each patient based on allogenic T cells from healthy donors that could be validated in advance for safety. By TALEN- or CRISPR/Cas9-mediated knockin of reporter proteins, like the fluorescence proteins GFP or mCherry, into the *TRAC* and *TRBC* locus, respectively, T cells comprising a knockout of both TCR chains could be easily enriched by FACS. The critical point would be to enable T cell activation and proliferation in the absence of the endogenous TCR to allow subsequent introduction of transgenic TCRs. For this, much like for universal recipient cells for *in vitro* testing, the cells could be equipped with a construct similar to the CD3-Chimera. While the construct could be used for *ex vivo* expansion, it would not be required once the transgenic TCR is introduced. However, since the construct does not recognize any target and therefore

does not show off-target recognition, it should not negatively influence effector function of genetically modified T cells. Additionally, *in vivo* activation via the CD3-Chimera should not occur due to the lack of mitotic α-CD3 antibodies. TCR-deficient CD3-Chimera-expressing universal recipient cells activated via e.g. CD3/CD28 beads could then again be modified to express the desired transgenic TCR by utilizing TALEN- or CRISPR/Cas9-mediated knockin of transgenic TCR chains. While this method would abolish the requirement for retroviral transduction, it would also allow the introduction of the transgenic TCRs into their respective natural loci under the control of endogenous regulatory elements. Additionally, successful introduction of transgenic TCRs could be easily monitored by expression of the transgenic TCR and simultaneous loss of the respective fluorescence proteins. Therefore, the designed CD3-Chimera construct could serve as a basis for generating biobanks of universal recipient cells for clinical applications that lack the endogenous TCR and can be activated via engagement of the chimeric construct and CD28 by α-CD3 and α-CD28 antibodies, respectively. These ready-to-use recipient cells could then be utilized for the fast and virus-free generation of tumor-specific T cell products for the treatment of cancer patients.

7 Abbreviations

%	Percent
°C	Degree Celsius
A	Adenine
aa	Amino acid
AmpR	Ampicillin resistance gene
APC	Antigen presenting cell
ATP	Adenosine triphosphate
bp	Base pair
BSA	Bovine serum albumin
C	Cytosine
CAR	Chimerica antigen receptor
CD	Cluster of differentiation
cDNA	Complementary DNA
CMV	Cytomegalovirus
CMV	Human cytomegalovirus
CO2	Carbondioxide
CRISPR	Clustered regularly-interspaced short palindromic repeats
CTL	Cytotoxic T lymphocites
d	Day
DMEM	Dulbecco´s Modified Eagle Medium
DMSO	Dimethylsulfoxide
DNA	Desoxyribonucleic acid
dNTPs	deoxy nuleoside triphosphates
EBV	Epstein-Barr virus
EDTA	Ethylenediaminetetraacetic acid
EF1A	Elongation factor 1A
eGFP	enhanced green fluorescence protein
EP	Electroporation
EtBr	Ethidium bromide
FACS	Fluorescence activated cell sorter
FCS	Fetal calf serum
FCS	Furin cleavage site
FCS	Fetal calf serum
FITC	Fluorescein isothiocyanate
g	Gramme
g	Gravitational acceleration

G	Guanine
GTP	Guanosine triphosphate
Gy	Gray
h	Hour
H2O	Water
HEK	Human embryonic kidney
HLA	Human leukocyte antigen
HR	Homologous recombination
HS	Human Serum
IFN	Interferon
IL	Interleukin
ivt-RNA	in vitro transcribed RNA
kb	Kilobase
L	Liter
LB	Lysogenic broth
LTR	Long terminal repeats
M	Molar
MCS	Multiple cloning site
mg	Milligramme
MHC	Major histocompatibility complex
min	Minute
MIT	Medigene immunotherapies
mL	Milliliter
MoMuLV	Moloney murine leukemia virus
MPSV	Myeloproliferative sarcoma virus
mRNA	messenger RNA
ms	Millisecond
NaCl	Sodium chloride
NaOH	Sodium hydroxide
ng	Nanogramme
NHEJ	Non-homologous end joining
nm	Nanometer
O2	Oxygen
P2A	porcine teschovirus-1 2A "self-cleaving" protein
PB	Pacific Blue
PBL	Peripheral blood lymphocytes
PBMC	Peripheral blood mononuclear cells

PBS	Phosphate buffered saline
PCR	Polymerase chain reaction
PE	Phycoerythrin
PerCP	Peridinin chlorophyll protein
PFA	Paraformaldehyde
pH	potentia hydrogenii
RNA	Ribonucleic acid
rpm	Rounds per minute
RT	Room temperature
RVD	Repeat-variable di-residue
s	Second
scFv	Single chain variable fragment
SDS	Sodiumdodecylsulfate
SIN	self-inactivating
SSA	Single strand annealing
T	Thymine
TAA	Tumor associated antigen
TAE	Tris-acetate-EDTA
TALEN	Transcription activator-like effector nuclease
TCR	T cell receptor
Th	T helper cells
TM	Transmembrane domain
TNF	Tumor necrosis factor
TRA locus	TCR α locus
TRB locus	TCR β locus
U	Unit
UTR	Untranslated region
UV	Ultraviolett
V	Volt
WPRE	Woodchuck hepatitis virus posttranscriptional regulatory element short version (overlap between the WPRE elements used in MMLV and HIV based vectors)
ZNF	Zinc finger nuclease
µg	Microgramme
µL	Microliter

8   References

Abbey, J. L. and O'Neill, H. C. (2008) 'Expression of T-cell receptor genes during early T-cell development.', *Immunology and cell biology*, 86(2), pp. 166–74.

Agarwala, R. *et al.* (2016) 'Database resources of the National Center for Biotechnology Information', *Nucleic Acids Research*, 44(D1), pp. D7–D19.

Ahmadi, M. *et al.* (2013) 'CD3 limits the efficacy of TCR gene therapy in vivo CD3 limits the efficacy of TCR gene therapy in vivo', *Blood*, 118(13), pp. 3528–3537.

Ahmadzadeh, M., Hussain, S. F. and Farber, D. L. (2001) 'Heterogeneity of the memory CD4 T cell response: persisting effectors and resting memory T cells.', *The Journal of immunology*, 166(2), pp. 926–35.

Ahmed, R. and Gray, D. (1996) 'Immunological Memory and Protective Immunity: Understanding Their Relation', *Science*, 272(5258), pp. 54–60.

Allison, T. J. and Garboczi, D. N. (2002) 'Structure of γδ T cell receptors and their recognition of non-peptide antigens', *Molecular Immunology*, 38(14), pp. 1051–1061.

Altman, J. *et al.* (1996) 'Phenotypic analysis of antigen-specific T lymphocytes', *Science*, 274(5284), pp. 94–96.

Arnett, K. L., Harrison, S. C. and Wiley, D. C. (2004) 'Crystal structure of a human CD3-epsilon/delta dimer in complex with a UCHT1 single-chain antibody fragment.', *Proceedings of the National Academy of Sciences of the United States of America*, 101(46), pp. 16268–16273.

Artyomov, M. N. *et al.* (2010) 'CD4 and CD8 binding to MHC molecules primarily acts to enhance Lck delivery', *Proceedings of the National Academy of Sciences*, 107(39), pp. 16916–16921.

Barrangou, R. *et al.* (2007) 'CRISPR Provides Aquired Resistance Against Viruses in Prokaryotes.' *Science*, 315(5819), pp. 1709-12.

Barrangou, R. and Marraffini, L. A. (2014) 'CRISPR-Cas Systems : Prokaryotes Upgrade to Adaptive Immunity', *Molecular Cell.*, 54(2), pp. 234–244.

Bassing, C. H., Swat, W. and Alt, F. W. (2002) 'The mechanism and regulation of chromosomal V(D)J recombination', *Cell*, 109(2 SUPPL. 1), pp. 45–55.

Baylis, F. and McLeod, M. (2017) 'First-In-Human Phase 1 CRISPR Gene Editing Cancer Trials: Are We Ready?', *Current Gene Therapy*, 17, pp. 309–319.

Bendle, G. M. *et al.* (2010) 'Lethal graft-versus-host disease in mouse models of T cell receptor gene therapy', *Nature Medicine*, 16(5), pp. 565–570.

Berdien, B. *et al.* (2014) 'TALEN-mediated editing of endogenous T-cell receptors facilitates efficient reprogramming of T lymphocytes by lentiviral gene transfer', *Gene Therapy,* 21, pp. 539–548.

Berger, C. *et al.* (2008) 'Adoptive transfer of effector CD8+ T cells derived from central memory cells establishes persistent T cell memory in primates', *Journal of Clinical Investigation*, 118(1), pp. 294–305.

Bhat, P. *et al.* (2017) 'Interferon-γ derived from cytotoxic lymphocytes directly enhances their motility and cytotoxicity', *Cell Death and Disease,* 8(6), e2836.

Birnbaum, M. E. *et al.* (2014) 'Molecular architecture of the αβ T cell receptor–CD3 complex', *Proceedings of the National Academy of Sciences*, 111(49), pp. 17576–17581.

Bitinaite, J. *et al.* (1998) 'FokI dimerization is required for DNA cleavage.', *Proceedings of the National Academy of Sciences of the United States of America*, 95(18), pp. 10570–5.

Blankenstein, T. *et al.* (2015) 'Targeting cancer-specific mutations by T cell receptor gene therapy', *Current Opinion in Immunology*, 33, pp. 112–119.

Boch, J. *et al.* (2009) 'Breaking the code of DNA binding specificity of TAL-type III effectors.', *Science*, 326(5959), pp. 1509–12.

Boch, J. (2011) 'TALEs of genome targeting.', *Nature biotechnology*, 29(2), 135–136.

Boch, J. and Bonas, U. (2010) 'Xanthomonas AvrBs3 family-type III effectors: discovery and function.', *Annual review of phytopathology*, 48, pp. 419–36.

Bogdanove, A. J. and Voytas, D. F. (2011) 'TAL effectors: customizable proteins for DNA targeting.', *Science*, 333(6051), pp. 1843–6.

Bolotin, D. A. *et al.* (2012) 'Next generation sequencing for TCR repertoire profiling: Platform-specific features and correction algorithms', *European Journal of Immunology*, 42(11), pp. 3073–3083.

Bolotin, D. A. *et al.* (2013) 'MiTCR: Software for T-cell receptor sequencing data analysis', *Nature Methods*, 10(9), pp. 813–814.

Bonini, C. and Mondino, A. (2015) 'Adoptive T-cell therapy for cancer: The era of engineered T cells', *European Journal of Immunology*, 45(9), pp. 2457–2469.

Boon, T. *et al.* (1994) 'Genes Coding for Tumor-specific Rejection Antigens', *Cold Spring Harbor Symposia on Quantitative Biology* , 59 , pp. 617–622.

Borgulya, P. *et al.* (1992) 'Exclusion and inclusion of alpha and beta T cell receptor alleles', *Cell*, 69(3), pp. 529–37.

Brameshuber, M. *et al.* (2018) 'Monomeric TCRs drive T cell antigen recognition', *Nature Immunology*, 19(5), 487-496.

Bürdek, M. (2009) 'Generierung WT1-spezifischer T-Zellen und Selektion spezifischer T-Zellrezeptoren mittels transgener Expression in Jurkat-T-Zellen', *Dissertation,* LMU Muenchen.

Burnet, M. (1957) 'Cancer; a biological approach. I. The processes of control.', *British medical journal*, 1(5022), pp. 779–86.

Call, M. E. *et al.* (2002) 'The Organizing Principle in the Formation of the T Cell Receptor-CD3 Complex', *Cell*, 111(7), pp. 967–979.

Call, M. E. and Wucherpfennig, K. W. (2007) 'Common themes in the assembly and architecture of activating immune receptors.', *Nature Reviews Immunology*, 7(11), pp. 841–850.

Cameron, B. J. *et al.* (2013) 'Identification of a Titin-Derived HLA-A1 – Presented Peptide as a Cross-Reactive Target for Engineered MAGE A3 – Directed T Cells', *Science Translational Medicine*, 5(197), pp. 197ra103.

Carpenter, A. C. and Bosselut, R. (2010) 'Decision checkpoints in the thymus.', *Nature immunology*, 11(8), pp. 666–73.

Caruso, H. G. *et al.* (2015) 'Tuning sensitivity of CAR to EGFR density limits recognition of normal tissue while maintaining potent antitumor activity', *Cancer Research*, 75(17), pp. 3505–3518.

Cermak, T. *et al.* (2011) 'Efficient design and assembly of custom TALEN and other TAL effector-based constructs for DNA targeting.', *Nucleic acids research*, 39(12), p. e82.

Chenchik, A. *et al.* (1996) 'Full-length cDNA cloning and determination of mRNA 5' and 3' ends by amplification of adaptor-ligated cDNA.', *BioTechniques*, 21(3), pp. 526–534.

Chilson, O. P., Boylston, a W. and Crumpton, M. J. (1984) 'Phaseolus vulgaris phytohaemagglutinin (PHA) binds to the human T lymphocyte antigen receptor.', *The EMBO journal*, 3(13), pp. 3239–3245.

Chmielewski, M. *et al.* (2004) 'T Cell Activation by Antibody-Like Immunoreceptors : Increase in Affinity of the Single-Chain Fragment Domain above Threshold Does Not Increase T Cell Activation against.' *The Journal of Immunology*, 173(12), pp. 7647-7663.

Christian, M. *et al.* (2010) 'Targeting DNA double-strand breaks with TAL effector nucleases.', *Genetics*, 186(2), pp. 757–61.

Cong, L. *et al.* (2013) 'Multiplex Genome Engineering Using CRISPR/Cas Systems', *Science*, 339(6121), p. 819 LP – 823.

Coulie, P. G. *et al.* (2014) 'Tumour antigens recognized by T lymphocytes: at the core of cancer immunotherapy', *Nature Reviews Cancer*, 14(2), pp. 135–146.

Curtsinger, J. M. *et al.* (1999) 'Inflammatory cytokines provide a third signal for activation of naive CD4+ and CD8+ T cells.', *Journal of immunology*, 162(6), pp. 3256–62.

Dagdas, Y. S. *et al.* (2017) 'A conformational checkpoint between DNA binding and cleavage by CRISPR-Cas9', *Science Advances*, 3(8), eaao0027.

Dal Porto, J. M. *et al.* (2004) 'B cell antigen receptor signaling 101', *Molecular Immunology*, 41(6-7), pp. 599–613.

Davis, M. M. and Bjorkman, P. J. (1988) 'T-cell antigen receptor genes and T-cell recognition', *Nature*, 334(6181), pp. 395–402.

Deltcheva, E. *et al.* (2011) 'CRISPR RNA maturation by trans-encoded small RNA and host factor RNase III', *Nature*, 471(7340), pp. 602–607.

Deng, D. *et al.* (2012) 'Structural basis for sequence-specific recognition of DNA by TAL effectors.', *Science*, 335(6069), pp. 720–3.

Dössinger, G. *et al.* (2013) 'MHC Multimer-Guided and Cell Culture-Independent Isolation of Functional T Cell Receptors from Single Cells Facilitates TCR Identification for Immunotherapy', *PLoS one*, 8(4), e61384.

Doyle, E. L. *et al.* (2012) 'TAL Effector-Nucleotide Targeter (TALE-NT) 2.0: tools for TAL effector design and target prediction.', *Nucleic acids research*, 40(Web Server issue), pp. W117–22.

Dudley, M. E. *et al.* (2005) 'Adoptive Cell Transfer Therapy Following Non-Myeloablative but Lymphodepleting Chemotherapy for the Treatment of Patients With Refractory Metastatic Melanoma', *Journal of Clinical Oncology* , 23 (10), pp. 2346–2357.

Dudley, M. E. and Rosenberg, S. a (2003) 'Adoptive-cell-transfer therapy for the treatment of patients with cancer.', *Nature reviews. Cancer*, 3(9), pp. 666–75.

Duffy, M. J. (2001) 'Carcinoembryonic antigen as a marker for colorectal cancer: Is it clinically useful?', *Clinical Chemistry*, 47(4), pp. 624–630.

Dunbar, C. E. *et al.* (2018) 'Gene therapy comes of age', *Science*, 359(6372), eaan4672.

Dunn, G. P. *et al.* (2004) 'The Immunobiology of Cancer Immunosurveillance and Immunoediting', *Immunity*, 21(2), pp. 137–148.

Duong, C. P. M. *et al.* (2015) 'Cancer immunotherapy utilizing gene-modified T cells: From the bench to the clinic', *Molecular Immunology*, 67(2 Pt. A), pp. 46–57.

Ellis, J. (2005) 'Silencing and Variegation of Gammaretrovirus and Lentivirus Vectors', *Human Gene Therapy*, 16(11), pp. 1241–1246.

Engels, B. *et al.* (2003) 'Retroviral vectors for high-level transgene expression in T lymphocytes.', *Human gene therapy*, 14(12), pp. 1155–68.

Engler, C. *et al.* (2009) 'Golden Gate Shuffling: A One-Pot DNA Shuffling Method Based on Type IIs Restriction Enzymes', *PLoS one.*, 4(5), p. e5553.

Exley, M., Terhorst, C. and Wileman, T. (1991) 'Structure, assembly and intracellular transport of the T cell receptor for antigen.', *Seminars in immunology*, 3(5), pp. 283–297.

Eyquem, J. *et al.* (2017) 'Targeting a CAR to the TRAC locus with CRISPR/Cas9 enhances tumour rejection', *Nature*, 543(7643), pp. 113–117.

Fehling, H. J. and Boehmer, H. Von (1997) 'Early αβ T cell development in the thymus of normal and genetically altered mice', *Current Opinion in Immunology*, 9(2), pp. 263–275.

Finney, H. M., Akbar, A. N. and Alastair, D. G. (2004) 'Activation of Resting Human Primary T Cells with Chimeric Receptors: Costimulation from CD28, Inducible Costimulator, CD134, and CD137 in Series with Signals from the TCR zeta Chain', *The Journal of Immunology,* 172(1)104-113.

Flynn, K. and Müllbacher, A. (1997) 'The generation of memory antigen-specific cytotoxic T cell responses by CD28/CD80 interactions in the absence of antigen', *European Journal of Immunology*, 27(2), pp. 456–462.

Foster, A. E. *et al.* (2008) 'Human CD62L- memory T cells are less responsive to alloantigen stimulation than CD62L+ naive T cells : potential for adoptive immunotherapy and allodepletion. *Blood*, 104(8), pp. 2403-2409.

Gaj, T., Gersbach, C. a and Barbas, C. F. (2013) 'ZFN, TALEN, and CRISPR/Cas-based methods for genome engineering.', *Trends in biotechnology*, 31(7), pp. 397–405.

Garcia, K. C. *et al.* (1996) 'An alphabeta T cell receptor structure at 2.5 A and its orientation in the TCR-MHC complex.', *Science*, 274(5285), pp. 209–19.

Gasiunas, G. *et al.* (2012) 'Cas9-crRNA ribonucleoprotein complex mediates specific DNA cleavage for adaptive immunity in bacteria', *Proceedings of the National Academy of Sciences*, 109(39), pp. E2579–E2586.

Gattinoni, L. *et al.* (2011) 'A human memory T cell subset with stem cell-like properties', *Nature Medicine*, 17(10), pp. 1290–1297.

Gattinoni, L., Klebanoff, C. a and Restifo, N. P. (2012) 'Paths to stemness: building the ultimate antitumour T cell.', *Nature reviews. Cancer*, 12(10), pp. 671–84.

Germain, R. N. (1994) 'MHC-dependent antigen processing and peptide presentation: providing ligands for T lymphocyte activation.', *Cell*, 76(2), pp. 287–99.

Gill, S., Maus, M. V and Porter, D. L. (2016) 'Chimeric antigen receptor T cell therapy : 25 years in the making', *Blood Reviews*, 30(3), pp. 157–167.

Golubovskaya, V. and Wu, L. (2016) 'Different subsets of T cells, memory, effector functions, and CAR-T immunotherapy', *Cancers*, 8(3), p. 36.

Gong, M. C. *et al.* (1999) 'Cancer Patient T Cells Genetically Targeted to Prostate-Specific Membrane Antigen Specifically Lyse Prostate Cancer Cells and Release Cytokines in Response to Prostate-Specific Membrane Antigen', *Neoplasia*, 1(2), pp. 123–127.

Graef, P. *et al.* (2014) 'Serial Transfer of Single-Cell-Derived Immunocompetence Reveals Stemness of CD8+ Central Memory T Cells', *Immunity*, 41(1), pp. 116–126.

Gross, G., Waks, T. and Eshhar, Z. (1989) 'Expression of immunoglobulin-T-cell receptor chimeric molecules as functional receptors with antibody-type specificity.', *Proceedings of the National Academy of Sciences*, 86(24), pp. 10024–10028.

Gu, W. G. (2015) 'Genome editing-based HIV therapies', *Trends in Biotechnology*, 33(3), pp. 172–179.

Harris, D. T. *et al.* (2017) 'Comparison of T Cell Activities Mediated by Human TCRs and CARs That Use the Same Recognition Domains', *The Journal of Immunology*, 200(3), pp. 1088-1100

Harris, D. T. and Kranz, D. M. (2016) 'Adoptive T Cell Therapies : A Comparison of T Cell Receptors and Chimeric Antigen Receptors', *Trends in Pharmacological Sciences*, 37(3), pp. 220–230.

Harty, J. T., Tvinnereim, A. R. and White, D. W. (2000) 'CD8+ T Cell Effector Mechanisms in Reistance To Infection', *Annual Reviews of Immunology*, 18(1), pp. 275–308.

Hashimoto, S. *et al.* (1991) 'Mechanism of Calcium Ionophore and Phorbol Ester-Induced T-cell Activation: Accessory Cell Requirement for T-cell Activation', *Scandinavian Journal of Immunology*, 33(4), pp. 393–403.

Haute, L. Van *et al.* (2013) 'Knockout mice created by TALEN- mediated gene targeting', *Nature Biotechnology,* 31(1), pp. 23–24.

Heemskerk, B., Kvistborg, P. and Schumacher, T. N. M. (2013) 'The cancer antigenome', *The EMBO Journal*, 32(2), pp. 194–203.

Heemskerk, M. H. M. *et al.* (2003) 'Redirection of antileukemic reactivity of peripheral T lymphocytes using gene transfer of minor histocompatibility antigen HA-2-specific T-cell receptor complexes expressing a conserved alpha joining region', *Blood*, 102(10), pp. 3530–3540.

Heemskerk, M. H. M. *et al.* (2007) 'Efficiency of T-cell receptor expression in dual-specific T cells is controlled by the intrinsic qualities of the TCR chains within the TCR-CD3 complex', *Blood*, 109(1), pp. 235–243.

Heemskerk, M. H. M. (2010) 'T-cell receptor gene transfer for the treatment of leukemia and other tumors', *Haematologica*, 95(1), pp. 15–19.

Herbers, K., Conrads-Strauch, J. and Bonas, U. (1992) 'Race-specificity of plant resistance to bacterial spot disease determined by repetitive motifs in a bacterial avirulence protein', *Nature*, 356(6365), pp. 172–174.

Hesse, M. D. *et al.* (2001) 'A T Cell Clone's Avidity Is a Function of Its Activation State', *The Journal of Immunology*, 167(3), p. 1353–1361.

Ho, W. Y. *et al.* (2006) 'In vitro methods for generating CD8+T-cell clones for immunotherapy from the naïve repertoire', *Journal of Immunological Methods*, 310(1-2), pp. 40–52.

Holler, P. D. and Kranz, D. M. (2003) 'Quantitative analysis of the contribution of TCR/pepMHC affinity and CD8 to T cell activation', *Immunity*, 18(2), pp. 255–264.

Hombach, a. *et al.* (2001) 'Tumor-Specific T Cell Activation by Recombinant Immunoreceptors: CD3 Signaling and CD28 Costimulation Are Simultaneously Required for Efficient IL-2 Secretion and Can Be Integrated Into One Combined CD28/CD3 Signaling Receptor Molecule', *The Journal of Immunology*, 167(11), pp. 6123–6131.

Hombach, A. a and Abken, H. (2011) 'Costimulation by chimeric antigen receptors revisited the T cell antitumor response benefits from combined CD28-OX40 signalling.', *International journal of cancer*, 129(12), pp. 2935–44.

Hsu, P. D., Lander, E. S. and Zhang, F. (2014) 'Development and applications of CRISPR-Cas9 for genome engineering', *Cell*, 157(6), pp. 1262–1278.

Huang, P. *et al.* (2011) 'Heritable gene targeting in zebrafish using customized TALENs.', *Nature biotechnology*, 29(8), pp. 699–700.

Hudecek, M. *et al.* (2013) 'Receptor affinity and extracellular domain modifications affect tumor recognition by ROR1-specific chimeric antigen receptor T cells.', *Clinical cancer research : an official journal of the American Association for Cancer Research*, 19(12), pp. 3153–64.

Hudecek, M. *et al.* (2015) 'The Nonsignaling Extracellular Spacer Domain of Chimeric Antigen Receptors Is Decisive for In Vivo Antitumor Activity', *Cancer Immunology Research*, 3(2), pp. 125–135.

Imai, C. *et al.* (2004) 'Chimeric receptors with 4-1BB signaling capacity provoke potent cytotoxicity against acute lymphoblastic leukemia', *Leukemia*, 18(4), pp. 676–684.

Jackson, S. A. *et al.* (2017) 'CRISPR-Cas: Adapting to change', *Science*, 356(6333), eaal5056.

Jackson, S. P. (2002) 'Sensing and repairing DNA double-strand breaks.', *Carcinogenesis*, 23(5), pp. 687–96.

Jiang, F. and Doudna, J. A. (2017) 'CRISPR – Cas9 Structures and Mechanisms', *Annu.Rev.Biophys*, 46(March), pp. 505–529.

Jiang, W. *et al.* (2013) 'RNA-guided editing of bacterial genomes using CRISPR-Cas systems', *Nature Biotechnology*, 31(3), pp. 233–239.

Jinek, M. *et al.* (2012) 'A Programmable Dual-RNA – Guided DNA Endonuclease in Adaptive Bacterial Immunity', *Science*, 337(6096), pp. 816–822.

Jinek, M. *et al.* (2014) 'Structures of Cas9 endonucleases reveal RNA-mediated conformational activation', *Science*, 343(6176), p. 1247997.

Johnson, L. A. *et al.* (2009) 'Gene therapy with human and mouse T-cell receptors mediates cancer regression and targets normal tissues expressing cognate antigen', *Blood*, 114 (3), pp. 535–546.

Jung, D. and Alt, F. W. (2004) 'Unraveling V(D)J Recombination: Insights into Gene Regulation', *Cell*, 116(2), pp. 299–311.

Kalos, M. *et al.* (2011) 'T cells with chimeric antigen receptors have potent antitumor effects and can establish memory in patients with advanced leukemia.', *Science translational medicine*, 3(95), 95ra73.

Kannan, A. *et al.* (2012) 'Signal Transduction via the T cell Antigen Receptor in naïve and effector/memory T cells', *The international journal of biochemistry & cell biology*, 44(12), pp. 2129–2134.

Kay, S. *et al.* (2007) 'A Bacterial Effector Acts as a Plant Transcription Factor and Induces a Cell Size Regulator', *Science*, 318 (5850), pp. 648–651.

Kim, K. S. *et al.* (2000) 'Heterodimeric CD3epsilongamma extracellular domain fragments: production, purification and structural analysis.', *Journal of molecular biology*, 302(4), pp. 899–916.

Kjer-Nielsen, L. *et al.* (2004) 'Crystal structure of the human T cell receptor CD3 epsilon gamma heterodimer complexed to the therapeutic mAb OKT3.', *Proceedings of the National Academy of Sciences of the United States of America*, 101(20), pp. 7675–80.

Klein, L. *et al.* (2014) 'Positive and negative selection of the T cell repertoire: what thymocytes see (and don't see).', *Nature reviews. Immunology*, 14(6), pp. 377–91.

Knipping, F. *et al.* (2017) 'Genome-wide specificity of highly efficient TALEN and CRISPR/Cas9 for T cell receptor modification', *Molecular Therapy - Methods & Clinical Development*, 4(January), pp. 213–224.

Kuball, J. *et al.* (2007) 'Facilitating matched pairing and expression of TCR chains introduced into human T cells', *Blood*, 109(6), pp. 2331–2338.

Lai, W. *et al.* (2011) 'Transcriptional Control of Rapid Recall by Memory CD4 T Cells', *The Journal of Immunology*, 187(1), pp. 133–140.

Laugel, B. *et al.* (2007) 'Different T cell receptor affinity thresholds and CD8 coreceptor dependence govern cytotoxic T lymphocyte activation and tetramer binding properties.', *The Journal of biological chemistry*, 282(33), pp. 23799–810.

Law, C.-L. *et al.* (2002) 'Expression and characterization of recombinant soluble human CD3 molecules: presentation of antigenic epitopes defined on the native TCR-CD3 complex.', *International immunology*, 14(4), pp. 389–400.

Lefranc, M. P. *et al.* (2015) 'IMGT®, the international ImMunoGeneTics information system® 25 years on', *Nucleic Acids Research*, 43(D1), pp. D413–D422.

Li, T. *et al.* (2011) 'Modularly assembled designer TAL effector nucleases for targeted gene knockout and gene replacement in eukaryotes.', *Nucleic acids research*, 39(14), pp. 6315–25.

Lim, W. A. and June, C. H. (2017) 'The Principles of Engineering Immune Cells to Treat Cancer', *Cell*, 168(4), pp. 724–740.

Liu, Z. *et al.* (2017) 'Systematic comparison of 2A peptides for cloning multi-genes in a polycistronic vector', *Scientific Reports*, 7(1), p. 2193.

Longinotti, G. (2018) 'Isolation and characterization of a TCR specific for a new unconventional NY-ESO-1 epitope.' *Dissertation in preparation*, LMU Muenchen.

Love, P. E. and Hayes, S. M. (2010) 'ITAM-mediated Signaling by the T-Cell Antigen Receptor', *Cold Spring Harbor Perspectives in Biology*, 2(6), p. a002485.

Lozzio, C. and Lozzio, B. (1975) 'Human chronic myelogenous leukemia cell-line with positive Philadelphia chromosome.', *Blood*, 45(3), pp. 321–334.

Lugli, E. *et al.* (2012) 'Identification, isolation and in vitro expansion of human and nonhuman primate T stem cell memory cells', *Nature Protocols*, 8(1), pp. 33–42.

MacLeod, D. T. *et al.* (2017) 'Integration of a CD19 CAR into the TCR Alpha Chain Locus Streamlines Production of Allogeneic Gene-Edited CAR T Cells', *Molecular Therapy*, 25(4), pp. 1–13.

Maher, J. *et al.* (2002) 'Human T-lymphocyte cytotoxicity and proliferation directed by a single chimeric TCRζ/CD28 receptor', *Nature Biotechnology*, 20(1), pp. 70–75.

Mali, P. *et al.* (2013) 'RNA-Guided Human Genome Engineering via Cas9', *Science*, 339(6121), p. 823LP–826.

Malissen, B. and Bongrand, P. (2015) 'Early T Cell Activation: Integrating Biochemical, Structural, and Biophysical Cues', *Annual Review of Immunology*, 33(1), pp. 539–561.

Malissen, M. *et al.* (1988) 'A T cell clone expresses two T cell receptor alpha genes but uses one alpha beta heterodimer for allorecognition and self MHC-restricted antigen recognition.', *Cell*, 55(1), pp. 49–59.

Malissen, M. *et al.* (1992) 'Regulation of TCR α and β gene allelic exclusion during T-cell development', *Immunology Today*, 13(8), pp. 315–322.

Maus, M. V. and June, C. H. (2016) 'Making better chimeric antigen receptors for adoptive T-cell therapy', *Clinical Cancer Research*, 22(8), pp. 1875–1884.

Miller, J. C. *et al.* (2011) 'A TALE nuclease architecture for efficient genome editing.', *Nature biotechnology*, 29(2), pp. 143–8.

Miller, J. F. A. P. and Sadelain, M. (2015) 'The journey from discoveries in fundamental immunology to cancer immunotherapy', *Cancer Cell*, 27(4), pp. 439–449.

Milone, M. C. *et al.* (2009) 'Chimeric receptors containing CD137 signal transduction domains mediate enhanced survival of T cells and increased antileukemic efficacy in vivo', *Molecular Therapy: the journal of the American Society of Gene Therapy,* 17(8), pp. 1453–1464.

Mojica, F. J. M. *et al.* (2009) 'Short motif sequences determine the targets of the prokaryotic CRISPR defence system', *Microbiology*, 155(3), pp. 733–740.

Mojica, F. J. M. and Montoliu, L. (2016) 'On the Origin of CRISPR-Cas Technology : From Prokaryotes to Mammals', *Trends in Microbiology*, 24(10), pp. 811–820.

Montagna, D. *et al.* (2001) 'Ex vivo priming for long-term maintenance of antileukemia human cytotoxic T cells suggests a general procedure for adoptive immunotherapy', *Blood*, 98(12), pp. 3359–3366.

Morbitzer, R. *et al.* (2011) 'Assembly of custom TALE-type DNA binding domains by modular cloning', *Nucleic Acids Research* , 39(13), pp. 5790–5799.

Morgan, R. a *et al.* (2006) 'Cancer regression in patients after transfer of genetically engineered lymphocytes.', *Science*, 314(5796), pp. 126–9.

Morgan, R. A. *et al.* (2010) 'Case report of a serious adverse event following the administration of t cells transduced with a chimeric antigen receptor recognizing ERBB2', *Molecular Therapy: the journal of the American Society of Gene Therapy*, 18(4), pp. 843–851.

Morgan, R. A. *et al.* (2013) 'Cancer Regression and Neurological Toxicity Following anti-MAGE-A3 TCR gene therapy', *Journal of Immunotherapy*, 36(2), pp. 133–151.

Moscou, M. J. and Bogdanove, A. J. (2009) 'A Simple Cipher Governs DNA Recognition by TAL Effectors', *Science* , 326 (5959), p. 1501.

Mullis, K. *et al.* (1986) 'Specific Enzymatic Amplification of DNA In Vitro: The Polymerase Chain Reaction', *Cold Spring Harbor Symposia on Quantitative Biology* , 51(Pt 1) , pp. 263–273.

Munz, C. *et al.* (1999) 'Alloreactivity as a source of high avidity peptide-specific human CTL', *The Journal of Immunol*ogy, 162(1), pp. 25–34.

Mussolino, C. *et al.* (2011) 'A novel TALE nuclease scaffold enables high genome editing activity in combination with low toxicity.', *Nucleic acids research*, 39(21), pp. 9283–93.

Natarajan, A. *et al.* (2016) 'Structural Model of the Extracellular Assembly of the TCR-CD3 Complex', *Cell Reports*, 14(12), pp. 2833–2845.

Nishimasu, H. *et al.* (2014) 'Crystal structure of Cas9 in complex with guide RNA and target DNA', *Cell*, 156(5), pp. 935–949.

Nishimasu, H. and Nureki, O. (2017) 'Structures and mechanisms of CRISPR RNA-guided effector nucleases', *Current Opinion in Structural Biology*, 43, pp. 68–78.

Obenaus, M. *et al.* (2015) 'Identification of human T-cell receptors with optimal affinity to cancer antigens using antigen-negative humanized mice.', *Nature biotechnology*, 33(4), pp. 402–7.

Osborn, M. J. *et al.* (2005) 'A picornaviral 2A-like sequence-based tricistronic vector allowing for high-level therapeutic gene expression coupled to a dual-reporter system', *Molecular therapy : the journal of the American Society of Gene Therapy*, 12(3), pp. 569–574.

Osborn, M. J. *et al.* (2016) 'Evaluation of TCR gene editing achieved by TALENs, CRISPR/Cas9, and megaTAL nucleases', *Molecular Therapy. the journal of the American Society of Gene Therapy*, 24(3), pp. 570–581.

Padovan, E. *et al.* (1993) 'Expression of two T cell receptor α chains: dual receptor T cells', *Science*, 262(5132), pp. 422–24.

Paez-Espino, D. *et al.* (2013) 'Strong bias in the bacterial CRISPR elements that confer immunity to phage', *Nature Communications*, 4, 1430.

Petrie, H. T. *et al.* (1993) 'Multiple Rearrangements in T Cell Receptor alpha Chain Genes Maximize the Production of useful Thymocytes', *Journal of Experimental Medicine*, 178(2), pp. 615–622.

Ping, Y., Liu, C. and Zhang, Y. (2017) 'T-cell receptor-engineered T cells for cancer treatment: current status and future directions', *Protein & Cell*, 9(3), pp. 254–266.

Pingoud, A. and Wende, W. (2011) 'Generation of Novel Nucleases with Extended Specificity by Rational and Combinatorial Strategies', *ChemBioChem*, 12, pp. 1495–1500.

Piper, H., Litwin, S. and Mehr, R. (1999) 'Models for antigen receptor gene rearrangement. II. Multiple rearrangement in the TCR: allelic exclusion or inclusion?', *The Journal of Immunol*ogy, 163(4), pp. 1799–1808.

Placek, K. *et al.* (2009) 'Integration of distinct intracellular signaling pathways at distal regulatory elements directs T-bet expression in human CD4+ T cells.', *The Journal of immunology*, 183(12), pp. 7743–7751.

Poirot, L. *et al.* (2015) 'Multiplex genome edited T-cell manufacturing platform for "off-the-shelf" adoptive T-cell immunotherapies.', *Cancer research,* 75(18), pp. 3853-64.

Porter, D. L. *et al.* (2011) 'Chimeric Antigen Receptor–Modified T Cells in Chronic Lymphoid Leukemia', *New England Journal of Medicine*, 365(8), pp. 725–733.

Pryshchep, S. *et al.* (2014) 'Accumulation of Serial Forces on TCR and CD8 Frequently Applied by Agonist Antigenic Peptides Embedded in MHC Molecules Triggers Calcium in T Cells', *The Journal of Immunology*, 193(1), pp. 68–76.

Qasim, W. *et al.* (2017) 'Molecular remission of infant B-ALL after infusion of universal TALEN gene-edited CAR T cells', *Science Translational Medicine*, 9(374), pp. 1–9.

Ramos, C. a, Savoldo, B. and Dotti, G. (2014) 'CD19-CAR trials.', *Cancer journal*, 20(2), pp. 112–8.

Raulet, D. *et al.* (1985) 'Developmental regulation of T-cell receptor gene expression', *Nature,* 314, pp. 103-107.

Ren, J. *et al.* (2017) 'Multiplex Genome Editing to Generate Universal CAR T Cells Resistant to PD1 Inhibition', *Clinical Cancer Research*, 23(9), pp. 2255–2266.

Restifo, N. P., Dudley, M. E. and Rosenberg, S. a (2012) 'Adoptive immunotherapy for cancer: harnessing the T cell response.', *Nature reviews. Immunology*, 12(4), pp. 269–81.

Restifo, N. P. and Gattinoni, L. (2013) 'Lineage relationship of effector and memory T cells.', *Current opinion in immunology*, 25(5), pp. 556–63.

Riddell, S. R. and Greenberg, P. D. (1990) 'The use of anti-CD3 and anti-CD28 monoclonal antibodies to clone and expand human antigen-specific T cells', *Journal of Immunological Methods*, 128(2), pp. 189–201.

Rivoltini, L. *et al.* (1995) 'Quantitative Correlation between HLA Class I AlÃ-ele Expression and Recognition of Melanoma Cells by Antigen-specific Cytotoxic T Lymphocytes', *Cancer research*, 55, pp. 3149–3157.

Rosati, E. *et al.* (2017) 'Overview of methodologies for T-cell receptor repertoire analysis', *BMC Biotechnology*, 17(1), p. 61.

Rosenberg, S. A. *et al.* (2011) 'Durable complete responses in heavily pretreated patients with metastatic melanoma using T-cell transfer immunotherapy', *Clinical Cancer Research*, 17(13), pp. 4550–4557. doi: 10.1158/1078-0432.CCR-11-0116.

Rosenberg, S. A., Spiess, P. and Lafreniere, R. (1986) 'A new approach to the adoptive immunotherapy of cancer with tumor-infiltrating lymphocytes', *Science* , 233 (4770), pp. 1318–1321.

Sadelain, M., Brentjens, R. and Rivière, I. (2009) 'The promise and potential pitfalls of chimeric antigen receptors', *Current Opinion in Immunology*, 21(2), pp. 215–223.

Sadelain, M., Brentjens, R. and Rivière, I. (2013) 'The basic principles of chimeric antigen receptor design.', *Cancer discovery*, 3(4), pp. 388–98.

Sailer, N. (2013) 'Targeting the Human T Cell Receptor with TAL Effector Nucleases in Herpesvirus saimiri Transformed T Cells.' *Master Thesis,* Ludwig-Maximilians-Universität München, Department of biochemistry.

Sallusto, F. *et al.* (1999) 'Two subsets of memory T lymphocytes with distinct homing potential and effector functions', *Nature*, 401(6754), pp. 708–712.

Sander, J. D. *et al.* (2011) 'Targeted gene disruption in somatic zebrafish cells using engineered TALENs.', *Nature biotechnology*, 29(8), pp. 697–8.

Sander, J. D. and Joung, J. K. (2014) 'CRISPR-Cas systems for editing, regulating and targeting genomes', *Nature Biotechnology*, 32(4), pp. 347–350.

Sanjana, N. E. *et al.* (2012) 'A transcription activator-like effector toolbox for genome engineering.', *Nature protocols*, 7(1), pp. 171–92.

Schatz, D. G. and Ji, Y. (2011) 'Recombination centres and the orchestration of V(D)J recombination', *Nature Reviews Immunology*, 11(4), pp. 251–263.

Schmueck-Henneresse, M. *et al.* (2017) 'Comprehensive Approach for Identifying the T Cell Subset Origin of CD3 and CD28 Antibody–Activated Chimeric Antigen Receptor–Modified T Cells', *The Journal of Immunology*, 199(1), pp. 348-362.

Schreiber, R. D., Old, L. J. and Smyth, M. J. (2011) 'Cancer Immunoediting: Integrating Immunity's Roles in Cancer Suppression and Promotion', *Science*, 331(6024), pp. 1565–1570.

Sebestyen, Z. *et al.* (2008) 'Human TCR That Incorporate CD3 Induce Highly Preferred Pairing between TCR and Chains following Gene Transfer', *The Journal of Immunology*, 180(11), pp. 7736–7746.

Seder, R. A. and Ahmed, R. (2003) 'Similarities and differences in CD4+ and CD8+ effector and memory T cell generation', *Nature Immunology*, 4(9), pp. 835–842.

Shim, G. *et al.* (2017) 'Therapeutic gene editing: Delivery and regulatory perspectives', *Acta Pharmacologica Sinica*, 38(6), pp. 738–753.

Siefken, R. *et al.* (1998) 'A CD28-associated signaling pathway leading to cytokine gene transcription and T cell proliferation without TCR engagement', *The Journal of Immunology*, 161(4), pp. 1645–1651.

Sievers, F. *et al.* (2011) 'Fast, scalable generation of high-quality protein multiple sequence alignments using Clustal Omega', *Molecular Systems Biology*, 7, p. 539.

Simon, P. *et al.* (2014) 'Functional TCR Retrieval from Single Antigen-Specific Human T Cells Reveals Multiple Novel Epitopes', *Cancer Immology Reasearch,* 2(12), pp. 1230–1244.

Singer, A., Adoro, S. and Park, J. H. (2008) 'Lineage fate and intense debate: Myths, models and mechanisms of CD4- versus CD8-lineage choice', *Nature Reviews Immunology*, 8(10), pp. 788–801.

Smith-Garvin, J. E., Koretzky, G. a and Jordan, M. S. (2009) 'T cell activation.', *Annual review of immunology*, 27, pp. 591–619.

Sommermeyer, D. *et al.* (2015) 'Chimeric antigen receptor-modified T cells derived from defined CD8+ and CD4+ subsets confer superior antitumor reactivity in vivo', *Leukemia*, 30(2), pp. 492–500.

Sommermeyer, D. and Uckert, W. (2010) 'Minimal amino acid exchange in human TCR constant regions fosters improved function of TCR gene-modified T cells.', *The Journal of immunology*, 184(11), pp. 6223–31.

Srivastava, S. and Riddell, S. R. (2015) 'Engineering CAR-T cells : Design concepts', *Trends in Immunology*, 36(8), pp. 494–502.

Starr, T. K., Jameson, S. C. and Hogquist, K. a (2003) 'Positive and negative selection of T cells.', *Annual review of immunology*, 21, pp. 139–76.

Stone, J. D. *et al.* (2014) 'A novel T cell receptor single-chain signaling complex mediates antigen-specific T cell activity and tumor control', *Cancer Immunology, Immunotherapy*, 63(11), pp. 1163–1176.

Sun, Z. Y. J. *et al.* (2001) 'Mechanisms contributing to T cell receptor signaling and assembly revealed by the solution structure of an ectodomain fragment of the CD3εγ heterodimer', *Cell*, 105(7), pp. 913–923.

Swindle, C. S. and Klug, C. a (2002) 'Mechanisms that regulate silencing of gene expression from retroviral vectors.', *Journal of hematotherapy & stem cell research*, 11(3), pp. 449–456.

Takeuchi, A. and Saito, T. (2017) 'CD4 CTL, a cytotoxic subset of CD4+T cells, their differentiation and function', *Frontiers in Immunology*, 8, p. 194.

Tang, X.-Y. *et al.* (2016) 'Third-generation CD28/4-1BB chimeric antigen receptor T cells for chemotherapy relapsed or refractory acute lymphoblastic leukaemia: a non-randomised, open-label phase I trial protocol', *BMJ Open*, 6(12), p. e013904.

Tesson, L. *et al.* (2011) 'Knockout rats generated by embryo microinjection of TALENS.', *Nature biotechnology*, 29(8), pp. 695–6.

Tieleman, D. P. (2004) 'The molecular basis of electroporation.', *BMC biochemistry*, 5, p. 10.

Till, B. G. *et al.* (2012) 'CD20-specific adoptive immunotherapy for lymphoma using a chimeric antigen receptor with both CD28 and 4-1BB domains : pilot clinical trial results', *Blood*, 119(17), pp. 3940–3951.

Torikai, H. and Cooper, L. J. N. (2016) 'Translational Implications For Off-the-Shelf Immune Cells Expressing Chimeric Antigen Receptors.', *Molecular therapy : the journal of the American Society of Gene Therapy*, 24(7), pp. 1178–1186.

Turatti, F. *et al.* (2007) 'Redirected activity of human antitumor chimeric immune receptors is governed by antigen and receptor expression levels and affinity of interaction', *The Journal of Immunotherapy*, 30(7), pp. 684–693.

Veillette, A. *et al.* (1989) 'Engagement of CD4 and CD8 expressed on immature thymocytes induces activation of intracellular tyrosine phosphorylation pathways', *The Journal of Experimental Medicine*, 170(5), pp. 1671–1680.

Viganò, S. *et al.* (2012) 'Functional avidity: A measure to predict the efficacy of effector T cells?', *Clinical and Developmental Immunology*, 2012, 153863.

Wang, X. *et al.* (2011) 'A transgene-encoded cell surface polypeptide for selection, in vivo tracking, and ablation of engineered cells', *Blood*, 118(5), pp. 1255–1263.

Van Wauwe, J. P., De Mey, J. R. and Goossens, J. G. (1980) 'OKT3: a monoclonal anti-human T lymphocyte antibody with potent mitogenic properties.', *The Journal of Immunology*, 124(6), pp. 2708–2713.

Wiedenheft, B., Sternberg, S. H. and Doudna, J. A. (2012) 'RNA-guided genetic silencing systems in bacteria and archaea', *Nature,* 482(7385), pp. 331-8.

Wilde, S. *et al.* (2009) 'Dendritic cells pulsed with RNA encoding allogeneic MHC and antigen induce T cells with superior antitumor activity and higher TCR functional avidity.', *Blood*, 114(10), pp. 2131–9.

Wilde, S., Geiger, C., *et al.* (2012) 'Generation of allo-restricted peptide-specific T cells using RNA-pulsed dendritic cells', *OncoImmunology*, 1(2), pp. 129–140.

Wilde, S., Sommermeyer, D., *et al.* (2012) 'Human antitumor CD8+ T cells producing Th1 polycytokines show superior antigen sensitivity and tumor recognition.', *The Journal of immunology*, 189(2), pp. 598–605.

Wood, A. J. *et al.* (2011) 'Targeted genome editing across species using ZFNs and TALENs.', *Science*, 333(6040), p. 307.

Xiao, Y. *et al.* (2017) 'How type II CRISPR-Cas establish immunity through Cas1-Cas2-mediated spacer integration', *Nature*, 550(7674), pp. 137–141.

Xu-Monette, Z. Y. *et al.* (2017) 'PD-1/PD-L1 blockade: Have we found the key to unleash the antitumor immune response?', *Frontiers in Immunology*, 8, p. 1597.

Yang, J. C. (2015) 'Toxicities Associated with Adoptive T-Cell Transfer for Cancer', *Cancer journal*, 21(6), pp. 506–509.

Zhang, F. *et al.* (2011) 'Efficient construction of sequence-specific TAL effectors for modulating mammalian transcription', *Nature biotechnology,* 29(2), pp. 149–153.

Zhong, S. *et al.* (2013) 'T-cell receptor affinity and avidity defines antitumor response and autoimmunity in T-cell immunotherapy', *Proceedings of the National Academy of Sciences*, 110(17), pp. 6973–6978.

Zhu, J. *et al.* (2012) 'The Transcription Factor T-bet Is Induced by Multiple Pathways and Prevents an Endogenous Th2 Cell Program during Th1 Cell Responses', *Immunity*, 37(4), pp. 660–673.

Zhu, J. and Paul, W. E. (2010) 'Heterogeneity and plasticity of T helper cells.', *Cell research*, 20(1), pp. 4–12.

9   Acknowledgements

Over the past years many people have contributed to the success of this thesis.

First, I want to express my sincere gratitude to my supervisor Prof. Dr. Dolores J. Schendel, who gave me the opportunity to work on my PhD thesis. I want to thank her for introducing me to the interesting field of T cell biology, for her continuous support and her scientific advice over the past years.

My sincere thanks also goes to Prof. Dr. Horst Domdey, who agreed to be my internal supervisor at the faculty for chemistry and pharmacy at the LMU. I am very grateful for his support.

I would particularly like to thank my direct supervisor in the lab, Dr. Christian Ellinger, for his professional guidance, his constant support and his scientific advice. I am really grateful for the many fruitful scientific discussions that helped shape the outline of this PhD thesis.

I also would like to thank all my colleagues for their continuous support during the last years. Special thanks goes to Dr. Slavoljub Milošević and his team, Tatjana Ott, Tanja Lange and Veronika Redai, for the support with the modification of the NGS procedure and the automatization of the process. Without their help, screening and picking of thousands of T cell clones would have not been possible. I also want to thank Dr. Slavoljub Milošević for the helpful scientific discussions and his scientific input. Special thank you also to Anja Moesch for helping me perform the bioinformatic analysis of the NGS data.

I thank Prof. Dr. Hinrich Abken for kindly providing the CEA-CAR constructs that were very useful for the setup of the initial process.

Finally, I want to thank my friends and family for their continuous support. Special thanks to my boyfriend Ferdinand (Jaquetón) for his patience, his loving support and for always putting a smile on my face no matter how hard the day was. Last, but not least, I want to thank my parents for always being there for me and for teaching me to work hard for the things I want to achieve. Without their support, I would not be where I am today.